



Libraries and Learning Services

# University of Auckland Research Repository, ResearchSpace

## Copyright Statement

The digital copy of this thesis is protected by the Copyright Act 1994 (New Zealand).

This thesis may be consulted by you, provided you comply with the provisions of the Act and the following conditions of use:

- Any use you make of these documents or images must be for research or private study purposes only, and you may not make them available to any other person.
- Authors control the copyright of their thesis. You will recognize the author's right to be identified as the author of this thesis, and due acknowledgement will be made to the author where appropriate.
- You will obtain the author's permission before publishing any material from their thesis.

## General copyright and disclaimer

In addition to the above conditions, authors give their consent for the digital copy of their work to be used subject to the conditions specified on the [Library Thesis Consent Form](#) and [Deposit Licence](#).

Approaches to Describe and Quantify  
Uncertainty in Bio-physical Agricultural  
Computer Simulation Models

Esther Meenken

A thesis submitted in partial fulfilment of the requirements for the degree of

Doctor of Philosophy in Statistics

University of Auckland

2016



# Abstract

The objective was to explore the *definition, sources, quantification, and management* of uncertainty in bio-physical agricultural deterministic computer simulation models (crop models). One aim was to provide recommendations from a formalised statistical viewpoint on management of uncertainty for a small pool of crop model researchers in New Zealand. These researchers face unique issues with models that describe temperate, island-based conditions. An equally important goal was to identify ways to provide predictions complete with uncertainty bounds beyond those offered by sensitivity analysis. Given these objectives, my focus was on a single model. Section I proposes an uncertainty evaluation (UE) framework to explore how the combined components of a crop model contribute to the overall output uncertainty. Tools to curate information, diagnose the most important sources of uncertainty, and identify UE objectives have been developed. The framework links qualitative and quantitative analysis through a review of techniques for generating and analysing data from such models. Although many elements considered appear in the literature, amalgamation into a united framework is an original contribution. In Section II a detailed description of a case-study model that simulates wheat development is provided. This model provides a concrete foundation by which to demonstrate the UE framework, and illustrates the nature of crop models as constructs upon which mechanistic understanding of real-world systems continues to develop. A theoretical addition to a recent model that combines physiological and genetic characteristics of wheat is proposed based on laboratory based experimental work, reducing structural uncertainty. Finally, Section III is centred on the analysis of simulated data. In particular, it addressed the desire to provide credible intervals for state-space model estimates. This was achieved through fitting a probabilistic Bayesian hierarchical model with MCMC, a general form of data assimilation that recursively updates state predictions based on available data. Credible bounds of both an observed and a latent state variable were estimated for the case-study model. Finally, I summarise how these three sections tie together to resolve research objectives. I discuss the benefits of this research, recommendations and limitations, and propose directions for future work.



# Acknowledgements

I would like to express my gratitude to my supervisor Professor Chris Triggs for academic and technical guidance. Given that this PhD program was completed off-campus, I am particularly grateful to Chris for keeping every interaction, and the project overall, focussed and moving forward.

I am grateful to my supervisor Doctor Hamish Brown for providing the opportunity to undertake this project and for supporting the proposal leading to this work. In addition, I am appreciative of the grounding in the principles of wheat physiology and modelling he provided. I am grateful for guidance on scope and direction to help keep the thesis cohesive and on track.

I want to thank my husband Graeme Muir for his constant belief in me and interest in my work. His encouragement has helped to keep me going when it was difficult to see the light at the end of the tunnel. I have enjoyed musing over knotty problems and philosophical tangents with him.

I am grateful to colleagues both past and present at Plant and Food Research who became involved at different stages of this project. In particular, I would like to mention Pete Jamieson and Derek Wilson for managerial and conceptual support leading to successful funding of this project. I would like to thank Edmar Teixeira for his interest in discussing ideas for evaluating uncertainty in crop models, and for feedback when structuring the associated paper. I am grateful to Ian Brooking for donating wisdom based on a huge amount of experience in wheat physiology when we were planning experiments and interpreting results; and Merle Forbes for keeping an eye on me as I ventured from my desk and into the glasshouse and the lab, and for assistance with primordia dissection work. Thanks also to Sarah Sinton for collecting the data used in the Bayesian data assimilation section of this thesis. Thanks to Catherine Langford, Naomi Shaw, Rob Zyskowski, Amber Parker and Yohei Mikawa for proof-reading various parts of this thesis. Finally, I acknowledge and thank the New Zealand Institute for Plant & Food Research for providing funding for fees, travel, materials and my salary through the completion of this PhD program.



# Table of Contents

1.	Motivation, Outline and Research Justification.....	1
1.1	Research Motivation .....	1
1.2	Outline .....	4
1.3	How the Research Fits In .....	6
1.4	Summary .....	7
	Section I - An Uncertainty Evaluation Framework.....	9
2.	Setting the Scene.....	11
2.1	Executive Summary .....	11
2.2	Introduction to Computer Simulation Models .....	11
2.3	Terminology .....	15
2.4	Bio-physical Agricultural Computer Simulation Models .....	16
2.5	State-space Modelling, Probability and Data.....	19
2.6	Bayesian Data Analysis .....	22
2.7	Putting It All Together.....	25
2.8	Summary .....	27
3.	Uncertainty Evaluation Framework.....	29
3.1	Executive Summary .....	29
3.2	A State-space Framework .....	29
3.3	Framework for Robust Computer Simulation Model UE .....	36
3.4	Summary .....	45
4.	UE Techniques.....	47
4.1	Executive Summary .....	47
4.2	Introduction .....	47



4.3	Sampling: Design of computer experiments to generate output data.....	48
4.4	Analysis/Summary of Simulated Data .....	52
4.5	Summary .....	63
Section II - SIRIUS: A Model for Wheat Development.....		65
5.	Scientific modelling of wheat flowering time physiology .....	67
5.1	Executive Summary .....	67
5.2	Introduction .....	67
5.3	Biological Motivation: Estimate Flowering Time in Wheat .....	68
5.4	The Physiology of Leaf Development in Wheat .....	70
5.5	Overview of the History of Modelling in Wheat.....	81
5.6	SIRIUS in the Spotlight.....	85
5.7	Conclusion.....	95
6.	Historical Data Analysis .....	97
6.1	Executive Summary .....	97
6.2	Photoperiod Response .....	97
6.3	Prediction of Leaf Appearance in Wheat: A Question of Temperature .	105
6.4	Remaining Papers .....	112
6.5	Summary .....	113
7.	A model as a live framework for research .....	115
7.1	Executive Summary .....	115
7.2	Introduction .....	115
7.3	Benefits of Deeper Sowing .....	118
7.4	Experiments .....	119
7.5	Materials and Methods.....	120

7.6	Results.....	123
7.7	Discussion.....	127
7.8	Summary .....	131
Section III Performance Statistics.....		133
8.	UE Framework and Sensitivity Analysis.....	135
8.1	Executive Summary .....	135
8.2	Application of the UE Framework.....	135
8.3	Sensitivity Analysis of the Input Parameters .....	140
9.	SIRIUS implemented as a State-Space model via MCMC .....	149
9.1	Executive Summary .....	149
9.2	Introduction .....	149
9.3	Formulation of the Model via Bayes Theorem.....	150
9.4	Practical Implementation .....	153
9.5	Results of UE.....	163
9.6	Diagnostics .....	170
9.7	Alternative Formulations .....	171
9.8	Estimation of Uncertainty in a Latent Variable. ....	171
9.9	Summary .....	173
10.	Uncertainty estimation for latent state variables.....	175
10.1	Executive Summary .....	175
10.2	A Mixture Distribution to Reduce Uncertainty for a Latent Variable...176	
10.3	Sensitivity Analysis of Latent State Equations.....	201
10.4	Summary .....	204
Section IV Conclusion .....		207

11. Conclusion .....	207
11.1 Introduction .....	207
11.2 What Was Done .....	208
11.3 The Pathway.....	212
11.4 Key Outcomes - UE Framework .....	213
11.5 Key Outcomes - Bayesian Data Assimilation.....	214
11.6 Further Work and Limitations of the Research.....	214
11.7 Conclusion.....	215
Appendices .....	217
A1: GenStat Code for Photoperiod response analysis as described in Chapter Six	217
A2: Genstat code for Leaf Appearance in response to temperature as described in Chapter Six .....	234
A3: Genstat wrap-around code for Bayesian Data Assimilation model described in Chapter Nine.....	238
A4: GenStat Code for mixing algorithms described in Chapter Ten.....	241
A5: Diagnostics for Model c described in Chapter Nine .....	244
A6: Conference Posters.....	249
Bibliography .....	251

# Table of Figures

Figure 1: Schematic of dissertation.....	3
Figure 2: Simplified schematic of phases of a computer simulation model's life..	37
Figure 3: Seven steps for computer simulation model UE.....	38
Figure 4: Schematic of the model building process. ....	39
Figure 5: Classification of commonly used sampling techniques.....	44
Figure 6: Classification of commonly used analysis techniques for calibration and sensitivity analysis. ....	45
Figure 7: A view of data assimilation (adjusted from Lewis et al. (2006)) .....	58
Figure 8: Effect of increasing photoperiod on the FLN the plant will target for plants with high (black line) medium (green line) and low (red line) photoperiod sensitivity. ....	86
Figure 9: The calculation of daily vernalisation for a theoretical cultivar as modelled in SIRIUS. The x-axis represents daily mean temperature and the y-axis represents daily vernalisation increment at that temperature for a theoretical cultivar.....	88
Figure 10: Relationships between FLN in Rongotea wheat and daylength at a) Haun stage 1.5, b) FLP, c) FLP+2, d) FLP+4. Dates imply whether <i>PP</i> is increasing or decreasing at the time of sowing. Black filled in circles denote average values and red crosses denote replicated data points.....	100
Figure 11: Relationships between FLN in Batten wheat and daylength at a) Haun stage 1.5, b) FLP, c) FLP+2, d) FLP+4. Dates imply whether <i>PP</i> is increasing or	

decreasing at the time of sowing. Black filled in circles denote average values and red crosses denote replicated data points. ....101

Figure 12: Relationships between FLN in Otane wheat and daylength at a) Haun stage 1.5, b) FLP, c) FLP+2, d) FLP+4. Dates imply whether *PP* is increasing or decreasing at the time of sowing. Black filled in circles denote average values and red crosses denote replicated data points. ....102

Figure 13: Relationships between FLN in CRSW6 wheat and daylength at a) Haun stage 1.5, c) FLP, c) FLP+2, d) FLP+4. Dates imply whether *PP* is increasing or decreasing at the time of sowing. Black filled in circles denote average values and red crosses denote replicated data points.....103

Figure 14: Relationship between leaf appearance in Avalon wheat and thermal time accumulation from seedling emergence, calculated from a) air temperature only, and b) near surface soil temperature until leaf 10, then air temperature. ..108

Figure 15: Comparison of leaf appearance predictions by the four models with observations for 4 sowing dates. Figures recomputed based on un-replicated data.....109

Figure 16: Deviations of predicted from observed leaf number for each observation of ligule appearance for 4 models at each sowing date. Mean bias indicated on each frame. Lines are used to join points for easier viewing.....111

Figure 17: Sequence of development of primordia in *TT* and their relationship to Haun stage. ....117

Figure 18: Effect of Cultivar and Sow depth on back-transformed FLN counts. Bars represent back-transformed 95% confidence intervals.....125

Figure 19: Wheat plants in Trial One at the flag leaf stage. ....126

Figure 20: Suggested interactions of Vrn1, Vrn2, and Vrn3 at different phases of phenological development modified from those proposed by Brown, Jamieson et al. (2013) for spring wheat. ....	131
Figure 21: Suggested differential relative expression of Vrn1, Vrn2, and Vrn3, including vernalisation target for early (Petri dish) and late (deep sown) <i>PP</i> perception after imbibition. ....	131
Figure 22: $S_i$ + remainder and $T_i$ for theoretical spring varieties. ....	146
Figure 23: Mean temperature for the three years under study. ....	147
Figure 24: $fln$ ( $y$ -axis) for sowing day averaged over year ( $x$ -axis). Red lines represent $lmin = 5$ , black lines represent $lmin = 9$ . Triangle symbols represent $ps = 0.70$ . Circle symbols represent $ps = 0.01$ . ....	147
Figure 25: Bayesian graphical model; double edges link to logical nodes, single edges link to stochastic nodes, ovals denote variables and boxes denote constants. Here blue denotes observed data, green state variables, orange input parameters, and black recursive priors. ....	158
Figure 26: Bayesian model for SIRIUS. ....	159
Figure 27: Hierarchical Model Code for day $t$ . ....	161
Figure 28: Data file for day $t = 45$ ....	162
Figure 29: Effect of number of observations on estimation and range of number of leaves through time for Otane. i. Model a, ii. Model b, and iii. Model c. Shading represents 95% credible intervals. Dashed line indicates the process model, solid line indicates the filtered estimate from the BHM, dotted lines indicate observed data. ....	166

Figure 30: Effect of adjusting prior for  $lmin$  on estimation and range of number of leaves through time for Otane. i. Model d, ii. Model e, and iii. Model f. Shading represents 95% credible intervals. Dashed line indicates the process model, solid line indicates the filtered estimate from the BHM, dotted lines indicate observed data.....167

Figure 31: Effect of  $bp$  on estimation and range of number of leaves through time for Otane. i. Model p, ii. Model b, and iii. Model k. Shading represents 95% credible intervals. Dashed line indicates the process model, solid line indicates the filtered estimate from the BHM, dotted lines indicate observed data.....168

Figure 32: Effect of low  $bp$  and # observations on estimation and range of number of leaves through time for Otane. i. Model p, and ii. Model o. Shading represents 95% credible intervals. Dashed line indicates the process model, solid line indicates the filtered estimate from the BHM, dotted lines indicate observed data. ....169

Figure 33: Effect of high minimum leaf number and number of observations on estimation and range of number of leaves through time for Otane. i. Model r, and ii. Model q. Shading represents 95% credible intervals. Dashed line indicates the process model, solid line indicates the filtered estimate from the BHM, dotted lines indicate observed data. ....170

Figure 34: Posterior density for  $ln_t$  where  $t = 1, 5, 10,$  and  $45$  from left to right based on model t. ....172

Figure 35: Posterior density for  $fln_t$  where  $t = 1, 5, 10,$  and  $45$  from left to right based on model t. ....172

Figure 36: a) Estimated values and credible intervals for  $ln_t$  (black line, dark grey range) and  $fln_t$  (red line, light grey range). b) Densities of  $ln$  and  $fln$  at  $t = 45$  based on 10,000 realisations.....173

Figure 37: Shape of Mixture density for  $fln_t$  where  $t = 1, 3, \dots, 31$ . Frames ordered row 1, 1-4 from left to right, row 2, 5-8 from left to right and so on. Model with Gamma ( $fln_{t-1}, 1$ ) prior for  $fln_t$ . .....189

Figure 38: Contour density plot of the model realisations for  $fln$  and  $ln$  on day 18. x-axis =  $fln_{18}$  and y-axis =  $ln_{18}$ . .....190

Figure 39: Estimated credible intervals for  $fln_t$  and  $ln_t$  based on several different prior distribution for  $fln_t$  for models *i.* without and *ii.* with incorporation of the mixing algorithm. Solid black line indicates the posterior estimate for  $fln_{t-1}$ , with light grey polygon indicating its credible intervals after mixture. In *iii.* the solid black line indicates posterior estimate for  $ln_{t-1}$ , with light grey polygon indicating its credible intervals.....192

Figure 40: Density for  $\tau$  based on several prior distributions for  $fln_t$  for (left) predicted at  $day = alpha$  and (right) smoothed at  $day = t = 35$ .....200

Figure 41: Jittering model code. ....202

Figure 42: Diagnostics for  $mu.fln_t$  where  $t = 1, 2, 5, 10, 30$  and  $50$ .....245

Figure 43: Diagnostics for  $phyllochron_t$  where  $t = 1, 2, 5, 10, 30$  and  $50$ .....246

Figure 44: Diagnostics for  $primordia_t$  where  $t = 1, 2, 5, 10, 30$  and  $50$  .....247

Figure 45: Diagnostics for  $fln_t$  where  $t = 1, 2, 5, 10, 30$  and  $50$ .....248





# Glossary of Crop Physiology Terms

Apical Meristem	A meristem at the tip of a plant shoot or root that causes the shoot or root to increase in length.
Anthesis	The action or period of opening of a flower.
Crop Physiology	Complementary studies of plants growing singly and in stands, with emphasis being placed on the major crops (wheat, rice, maize, barley, soybean and some pasture grasses).
Determinate	Leaf production by a stem ceases once spikelet initiation has begun.
Development	The sequential production, differentiation, expansion and loss of the structural units of a plant.
Facultative	Occurring optionally in response to circumstance rather than by nature.
Flag Leaf	The uppermost leaf on a fertilised stem; the leaf immediately below the flowers or seed head.
Final Leaf	See Flag leaf.
Genotype	The genetic constitution of a cell, an organism or an individual.
Growth	Increase in plant or crop dry weight, the net result of acquisition and loss of resources.
Haun Stage	Number of fully developed leaves.
Intercepted Radiation	Amount of available solar radiation intercepted by the crop.
Internode	Stem between nodes.

Lateral Shoot	Shoots originating from vegetative buds in the axis of leaves or from the nodes of stems.
Leaf axis	The lower surface of a lateral organ such as a leaf or petal.
Meristem	A localised group of actively dividing cells from which the permanent tissue systems are derived.
Node	Primordia locations.
Phenology	The physical constitution of an organism as determined by the interaction of its genetic components and environment.
Photoperiod	The period of daylight in every 24 hours.
Phyllochron	The interval between the appearance of successive leaves.
Plastochron	The interval between the appearance of successive organs.
Plant Physiology	A sub-discipline of botany concerned with fundamental processes such as photosynthesis of plants.
Primordium	The earliest detectable stage of a plant organ.
Spikelet	Modules of the ear, each generating several florets which, upon fertilisation, become grains.
Senescence	The onset and duration of the derogation of a plant or plant organ eventually leading to its death.
Thermal Time	Integral of time of environmental temperature above a base temperature. In practice a daily mean of maximum and minimum temperatures is normally used.
Vegetative Development	Stem and leaf development, in contrast to flower and seed (reproductive) development.

Vegetative Stage	The developmental stage prior to the appearance of fruiting structures.
Vernalisation	The cooling of seed and plant during germination and development in order to accelerate flowering.



This form is to accompany the submission of any PhD that contains research reported in published or unpublished co-authored work. **Please include one copy of this form for each co-authored work.** Completed forms should be included in all copies of your thesis submitted for examination and library deposit (including digital deposit), following your thesis Acknowledgements.

Please indicate the chapter/section/pages of this thesis that are extracted from a co-authored work and give the title and publication details or details of submission of the co-authored work.

Chapters One, Two and Three (Section One)

Nature of contribution by PhD candidate

First author. Tables, literature review, framework and figures. Discussions with co-authors to improve framework, structure and target audience.

Extent of contribution by PhD candidate (%)

90%




## CO-AUTHORS

Name	Nature of Contribution
Edmar Teixeira	Expert advice concerning targeting review/UA framework paper/sounding board for development.
Chris Triggs	Supervisor. Specialised discussion concerning formalisation and target audience
Hamish Brown	Supervisor. Specialised discussion concerning formalisation and target audience

## Certification by Co-Authors

The undersigned hereby certify that:

- ❖ the above statement correctly reflects the nature and extent of the PhD candidate's contribution to this work, and the nature of the contribution of each of the co-authors; and
- ❖ in cases where the PhD candidate was the lead author of the work that the candidate wrote the text.

Name	Signature	Date
Chris Triggs		14/10/2015
Hamish Brown		6/10/2015
Edmar Teixeira		7/10/2015
		<a href="#">Click here</a>
		<a href="#">Click here</a>
		<a href="#">Click here</a>



# Chapter One: Motivation, Outline, and Research Justification

## 1.1 Research Motivation

Bio-physical agricultural models are used to inform and support farm-level decision making, agronomic research, breeding strategies, and government policy (Rosenzweig et al. 2013). Colloquially known as crop models, they are simplified mathematical representations of physiological and physical processes that occur in plants and soils in response to environmental and management drivers. Crop model applications include the areas of food security and climate change impact and adaptation assessments (Boote et al. 1996; Sinclair and Seligman 2000; Jamieson et al. 2007; Cooper et al. 2009; Hochman et al. 2009; Bezlepkina et al. 2010; Teixeira et al. 2011; Teixeira et al. 2013; Holzworth et al. 2014).

Although crop models are mathematically deterministic, there are many possible sources of uncertainty that can contribute to overall model uncertainty. Recently, there has been increasing recognition in the agricultural (and wider) modelling community that the impact of uncertainty on crop model results needs to be considered (Hammer et al. 2002; O'Hagan 2008; Rotter et al. 2011; O'Hagan 2012; Rosenzweig et al. 2013; Wallach et al. 2014; Holzkämper et al. 2015; Uusitalo et al. 2015). The New Zealand Institute of Plant & Food Research Limited has therefore funded this PhD research project to describe and quantify uncertainty in crop models to help grow institute capability in this area.

The development of methods to evaluate uncertainty in deterministic models is an active area of research both within and outside of the agricultural sector, and many approaches have been proposed including multi-model ensembles (Ewert



et al. 2009; Asseng et al. 2013; Bassu et al. 2014), sensitivity analysis (Saltelli et al. 2000; Teixeira et al. 2015) and emulators (O'Hagan 2006; Stanfill et al. 2014). However, the large number of methodological options for model uncertainty evaluation (UE) makes it difficult to identify the most fit-for-purpose technique(s).

The objective of this PhD dissertation is therefore to explore the *definition, sources, quantification, and management* of uncertainty in bio-physical agricultural deterministic computer simulation models.

The body of this dissertation consists of three sections, each with a clear independent focus that ties back to the overall objective. Section I proposes a framework by which to *manage* uncertainty in bio-physical agricultural computer simulation models. Section II explores the conceptualisation, experimental and coding stages of building a bio-physical agricultural model. A single model is used as a case study throughout. A gap in current physiological understanding of the model is identified, and further experimental work to investigate this gap is described. Section III utilises the case study model described in Section II to demonstrate uncertainty evaluation through sensitivity analysis. It exploits data that updates through time and expert opinion to *quantify* uncertainty in a non-normal, non-linear context for observable and latent variables. A visual representation of the framework for this thesis can be seen in Figure 1.

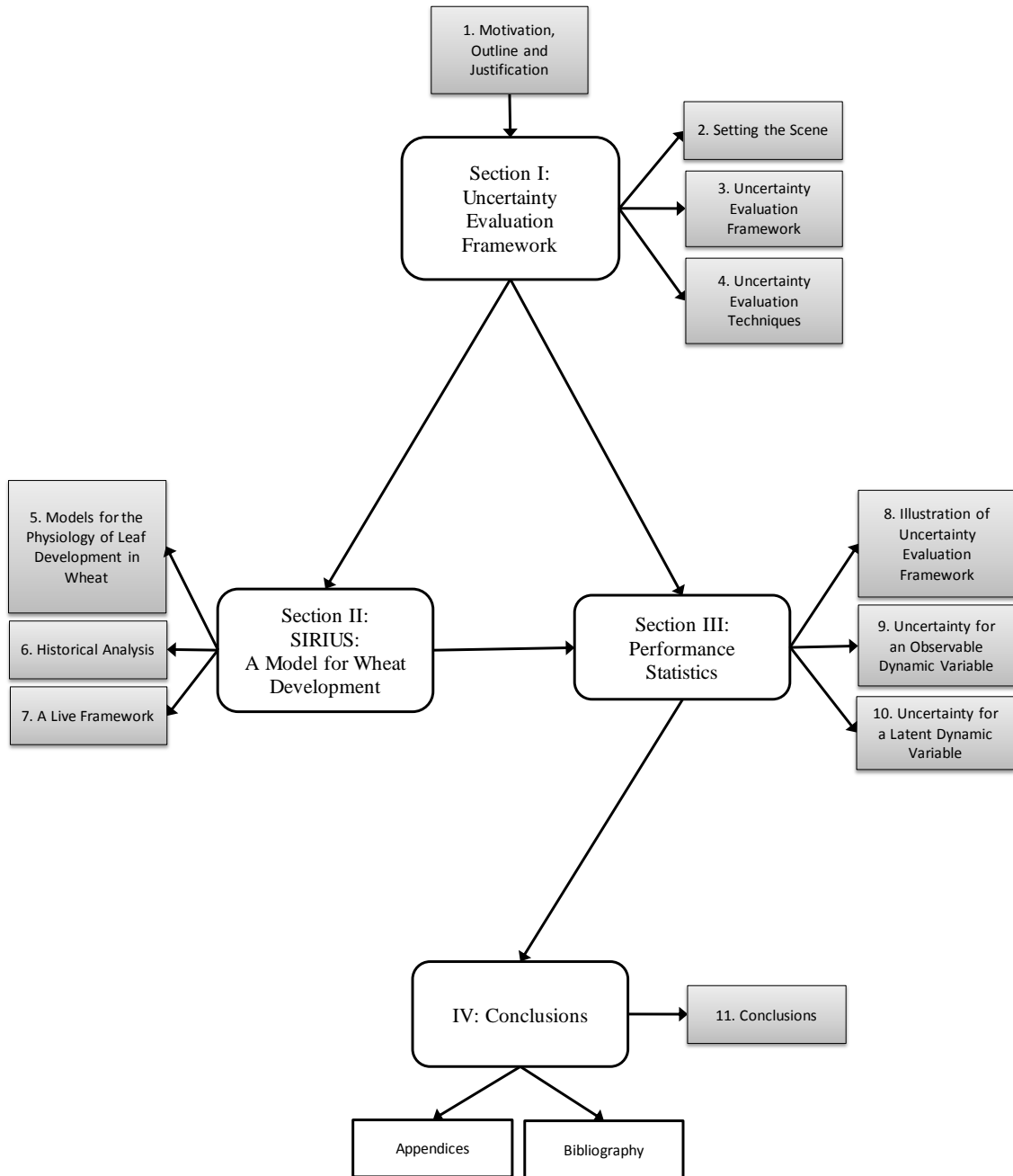


**Figure 1: Schematic of dissertation.**

## 1.2 Outline

### 1.2.1 Section I – An Uncertainty Evaluation Framework

A deterministic computer simulation model is defined by a series of equations, decisions, and input information that aims to characterise a real world process. In Chapter Two I introduce and define computer simulation models, and the impact of uncertainty on their use. The unambiguous state-space structure upon which the remainder of the thesis is based is also described in this chapter.

Those who rely on models increasingly wish to know how much they can trust their outputs, and the development of tools for evaluation uncertainty in deterministic models is an active area of research both within and outside of the agricultural sector. Different disciplines focus on different areas as deemed most appropriate to handle the types and sources of uncertainty of primary concern in each area. The agricultural sector has not been left behind, with an increasing number of research efforts being focussed on UE of computer simulation models. However the large number of methodological options makes it difficult to identify the most appropriate technique(s) for a given situation. With time, the methodologies will likely begin to become more unified (Strogatz 2014). There seems to have been a shift in recent years from optimisation of a model by finding a single set of input parameters that best match the data, to exploration of possible outcomes and a more holistic evaluation of different sources of uncertainty. This fundamentally requires an understanding of the sources and types of uncertainty in their model. An Uncertainty Evaluation (UE) framework to explore the *definition* and *sources* of uncertainty in a computer simulation model is therefore proposed in Chapter Three. Tools to help to curate information, to diagnose the most important sources of uncertainty, and to identify uncertainty evaluation objectives have been developed. Finally, Chapter

Four reviews a suite of techniques for the quantification of uncertainty, and links these techniques to the Uncertainty Evaluation (UE) framework proposed in Chapter Three. Together, Chapters Two, Three and Four provide a conceptual system to *manage* uncertainty in computer simulation models.

This framework can be used to ensure that whenever an evaluation of model uncertainty is carried out, a consistent structure to summarise and document the results can be expected.

## 1.2.2 Section II – Case Study: SIRIUS - A Bio-Physical Agricultural Model

A case-study model is introduced to provide a concrete foundation by which to demonstrate the uncertainty evaluation framework. It also illustrates the nature of crop models as constructs upon which researchers continue to develop mechanistic understanding of real-world systems. The wheat development sub-model SIRIUS (Brooking et al. 1995; Jamieson et al. 1995a; Jamieson et al. 1995b; Brooking 1996; Brooking and Jamieson 2002; Jamieson et al. 2007; Jamieson et al. 2008) was selected as the case-study for this project because of its importance as a physiological developmental model, and its accessibility as a major tool within The New Zealand Institute for Plant & Food Research Limited (PFR), by whom this project is funded. Research building upon this model is on-going within PFR (Brown et al. 2013), as part of this project, and also externally (He et al. 2012). As such, in the final Chapter of Section II, I describe lab-based experimental work that assesses the physiological development of wheat prior to emergence. I propose a new, theoretical addition to a recent model that combines physiological and genetic characteristics of wheat such that the function of vernalisation genes in spring wheat varieties prior to exposure to light is more complex than previously supposed.

### 1.2.3 Section III – Computation of Performance Statistics

The research focus for the final Section will be on computing performance statistics for the case study model SIRIUS. SIRIUS, like many agricultural models, is a process based, time-step model. Importantly, the simulated data are non-Normal and non-linear. In Chapter Eight, the UE framework is illustrated and a traditional sensitivity analysis for spring and winter varieties of wheat is carried out. Conclusions are compared and contrasted with those found by a recent paper by He et al. (2012). In Chapter Nine, a Bayesian hierarchical model fitted in a state-space framework is implemented to take advantage of data that has been collected through time. This approach allows quantification of input parameters, expert opinion and observed data in a unified setting. It provides filtered estimates of the state variable (Leaf Number) that updates through time in response to observed data. These estimates are presented with the usual performance statistics that are available when fitting a Bayesian hierarchical model. Probabilistic sensitivity analysis of input parameters is carried out within this framework. In Chapter Ten, the flexibility of the framework is demonstrated in two ways. First, it is extended to estimate uncertainty for a latent dynamic (updates through time) state variable. Second a probabilistic sensitivity analysis of structural uncertainty (state equations) is carried out. This last analysis reflects recent uncertainty research directions (Strong et al. 2012).

## 1.3 How the Research Fits In

Research into model uncertainty evaluation in the US, Europe, and even Australia may not provide all the desired outcomes for New Zealand specific conditions. In the agricultural sector, particularly in the EU region, multi-model ensemble techniques to assess uncertainty have been of particular interest to researchers. However, in New Zealand, agricultural systems are subject to

unique environmental conditions, and our smaller population means a smaller number of researchers usually dictate a smaller pool of appropriate models to which to apply such methods. Further, this approach does not naturally facilitate continued learning about the model and the system's mechanisms. For these reasons, my particular focus is upon improved understanding of uncertainty in a single dynamic model.

A detailed description of a wheat development model used as a case-study throughout this thesis is provided. Many agricultural models are process based, time-step models. These models can be evaluated through data assimilation techniques if appropriate data is available. This can be an invaluable tool to assess uncertainty, not only at the end, but also through time to confirm that the conceptual understanding of the updating process is accurate. This is extremely important because if we wish to forecast into unknown scenarios (i.e. under climate change research situations, for example), then a higher degree of certainty in the accuracy of latent processes is an obvious requirement.

## 1.4 Summary

The purpose of this first Chapter was to provide the research motivation, outline, and justification. This dissertation is set up in three main sections that will be explored and then tied together in the concluding chapter. Themes have been introduced relating to model uncertainty, particularly in the context of crop models in New Zealand. There is a case-study model that has been selected to allow a detailed description of the scientific approach to building and using such a model; and to allow uncertainty evaluation to be carefully studied and illustrated. Section I next consists of three chapters that jointly present the UE framework based on a state-space structure and including a review of UE techniques considered most pertinent to crop model UE.



# Section I – An Uncertainty Evaluation framework

This Section provides a detailed discussion of UE for computer simulation models. This includes an introduction to and definition of computer simulation models, and the impact of uncertainty in their use (Chapter Two). Once the state-space framework has been defined, this is further extended to describe how (in general) a deterministic model might fit within a Bayesian Hierarchical Model framework. As such, some background is provided to Bayesian Data Analysis. In Chapter Three, the UE framework is proposed. This requires clear definition of the components of a computer simulation model, and how uncertainty in model outputs may be traced back to one or more of these components. A seven-step UE framework, complete with tools to curate information, diagnose uncertainty and set analysis objectives based on available information is then laid out. Finally, in Chapter Four, steps six and seven from the UE framework are linked to current, quantitative approaches described in the literature for sampling from and analysing output data from the model. This allows the research contribution of the UE framework Section to be placed within the current themes in the literature relating to uncertainty analysis. This Section therefore provides the tools by which to *define, compartmentalise* (based on the sources of uncertainty) and *manage* uncertainty in computer simulation models. Tools to *quantify* uncertainty are also introduced, but will be expanded upon in Section III.





# Chapter Two: Setting the Scene

## 2.1 Executive Summary

In Chapter Two computer simulation models are introduced, particularly in the context of agricultural research and development. The effect of uncertainty on the use of these models was discussed in terms of the disciplines historical and current approaches to management. A state-space framework is proposed to help combine deterministic models, probability, and data in a Bayesian setting. This state-space framework allows the types of uncertainty that can be introduced by each model component in Chapter Three.

## 2.2 Introduction to Computer Simulation Models

### 2.2.1 Models

Models are a symbolic, simplified abstract representation of an object or system, and modelling is a typical human way of thinking about the world around them. There are few, if any, limits on what can be modelled, and definitions include conceptual, verbal, mathematical, physical or empirical models (Williams et al. 2002). Any idea, or 'theory' is essentially a conceptual model, and all other models arise from that initial idea. For example, Neyman (1957) stated that 'scientific theories are no more than models of natural phenomena'; Hawking (1988) that 'A theory is just a model of the universe...'; and Hillborn and Mangel (1997) that 'One can think of hypotheses and models in a hierarchic fashion with models simply being a more specific version of a hypothesis'.

The invention of deliberately oversimplified theories is one of the major techniques of science (Williams et al. 2002), and today, carefully developed system-specific mathematical deterministic models are common. This type of

model is utilised across almost all areas of scientific discovery including engineering, meteorology, hydrology, medicine, oceanography, and agriculture. A computer simulation model is the implementation in code of such a mathematical description of a real world process.

### 2.2.2 Computer Simulation Models

Bayarri et al. (2009) defined a computer simulation model as ‘a computational representation of a complex real-world process’. They further comment that ‘a computer simulation model is usually developed to approximately describe and allow direct simulation of the real-world process’. Although often denoted a simulator in the literature (O'Hagan 2006), this is not common in the agricultural modelling literature, so the terms ‘computer simulation model’, ‘crop model’ and ‘model’ to denote a bio-physical agricultural computer simulation model will be used throughout this dissertation. In the context of the Bayesian model described in this Chapter and implemented in Chapter Nine the term ‘state model’ is used to differentiate between the data and parameter models. When referring to a conceptual or mathematical representation that has not yet been implemented into code the term model is retained.

A computer simulation model is defined by a series of equations, decisions and input information that aims to characterise a real world process (Saltelli et al. 2000; McFarland 2008). When run, the outputs of a computer simulation model are a simplified prediction of the real world phenomena. Often these models are dynamic and update through time whilst responding to environmental information such as rainfall or nutrient management input. An important characteristic is that although outputs are deterministic function of the inputs, in practice the computer simulation model can be sufficiently complex that the outcome cannot be known prior to simulation (Kennedy and O'Hagan 2001).

### 2.2.3 The Empirical Foundation of Computer Simulation Models

The scientific method is a procedure that characterises modern scientific research. It consists of systematic observation, measurement, experiment; and the formulation, testing, and modification of hypotheses (Simpson and Weiner 1989). A central concept is that all evidence must be dependent on observed evidence (Skinner 1956; Popper 1959, 1972). Thus an empirical model is one that describes a system that is amenable to experimentation by the collection of empirical data (Williams et al. 2002). Although computer simulation models that represent detailed scientific understanding of real-world systems are called deterministic models rather than empirical models, the distinction is rather artificial because nearly all process models contain equations whose forms or coefficients are empirically determined (Sinclair and Muchow 2001; O'Hagan 2006).

### 2.2.4 Use of Computer Simulation Models

Deterministic models are often used as a research tool to investigate how a specific set of mechanisms (system) work together (Williams et al. 2002), and to test innovative hypotheses to help understand specific aspects of a system e.g. Jamieson and Munro (1999), Sinclair and Seligman (2000). An example of this is a recent paper by Brown et al. (2012b), who used the crop model APSIM (Holzworth et al. 2014) to characterise the developmental phenotype of different wheat varieties. Computer simulation models are also used to understand and predict the outcomes of complex processes, and for many kinds of decision and policy making (Boote et al. 1996). For example, some ways in which this can be implemented are suggested by Trucano et al. (2006):

- Simulating an experiment without knowledge of its results or prior to its execution can save money and time,

- Making scientific judgements about phenomena that cannot currently be studied experimentally,
- Using computation to extrapolate existing understanding into experimentally unexplored regions.

Models are a vital part of research and development. However, as famously stated by Box (1976) ‘all models are wrong, but some are useful’. For computer simulation models, this is because there are important sources of uncertainty and inaccuracy in the input parameters, data, and model structure (Montanari et al. 2009). Those who rely on computer simulation models increasingly wish to know how much they can trust their outputs (O'Hagan 2008), and this requires an evaluation of the sources and types of uncertainty.

### 2.2.5 Uncertainty in Computer Simulation Models

The approaches chosen to describe the uncertainty in a given model depend on specific properties of that model, and any attempt to parameterise uncertainty cannot be general or universal. Thus, the evaluation of uncertainty in a computer simulation is an exploration that will be specific not only to the model but to the environment or scenario for which it is to be used (McFarland 2008). Research into evaluating computer simulation model uncertainty is very topical across many research areas, and as a consequence it is not straightforward to definitively designate a single set of procedures for UE; rather, a selection of techniques best suited to each situation (e.g. type of model, data, model's life stage) is more likely to be useful. There are widely accepted norms in the uncertainty literature in around terminology. Sources and types of uncertainty in computer simulation models, and a framework to evaluate these are more fully discussed in Chapters Three and Four.

## 2.3 Terminology

There are widely accepted norms in the uncertainty literature in around terminology. Some of these are not consistent across disciplines, so some terms are defined here.

### 2.3.1 Calibration and History Matching

Kennedy and O'Hagan (2001) defined calibration as 'the process of fitting the model to the observed data by adjusting the parameters,... typically affected by *ad hoc* fitting... and after calibration the model is used...to predict the future behaviour of the system'. In the oil and gas industry, when reservoir models are used to simulate values and then compare them with historical data, the term 'history matching' is commonly used as in González-Rodríguez et al. (2005), Gharib Shirangi (2014): 'The history matching problem consists in adjusting a set of parameters,...in order to match the data obtained with the computer simulation model to the actual production data in the reservoir'. The term calibration will be used in this dissertation to describe any activities where the model is challenged in some way with observed data.

### 2.3.2 Equifinality

In the oil and gas industry it is generally recognised that calibration is a non-unique problem, i.e. that multiple combinations of input parameters can result in an equally-good history match (Streamsim Technologies 1999-2014). In hydrological modelling this phenomenon is termed 'equifinality' (Beven and Binley 1992) and recently in the literature efforts in calibration/history matching have begun to emphasise exploration rather identification of the single best combination of parameters which minimise the total error between observed data

and simulated data, leading toward more of a focus on uncertainty quantification and decision making (Streamsim Technologies 1999-2014).

### 2.3.3 Sensitivity Analysis

Sensitivity Analysis refers to exploration of the effect of changes in input parameters, input data or model structure on the outcomes  $y$ . This approach is an exploration of the model, and does not relate model behaviour in relation to calibration data.

## 2.4 Bio-physical Agricultural Computer Simulation Models

### 2.4.1 Background

Bio-physical agricultural models are made up of a set of processes that jointly describe a larger, real-world system. They are simplified mathematical representations of physiological and physical processes that occur in plants (e.g. leaf appearance rates) and soils (e.g. mineralisation of N) in response to environmental (e.g. temperature) and management (e.g. sowing dates) drivers. They will often be dynamic; that is, simulation is based on a set of decisions and steps to be taken at each time step based on environmental inputs such a mean daily temperature.

The process of building agricultural models involves an iterative process of fitting a model and improving knowledge through further experimentation. In one sense, we can think of deterministic model building as a tool that helps iteratively define the question or hypothesis. A historical feature of crop models is the lack of holistic management of uncertainty, and the development of tools to evaluate uncertainty in deterministic agricultural models is an active area of research as discussed in the next section.

## 2.4.2 Uncertainty in Agricultural Computer Simulation Models

In 1994 a special symposium was held at the annual meetings of the American Society of Agronomy in Seattle on 14 November 1994. This symposium was entitled 'Use and Abuse of Crop Simulation Models', and four papers resulting from this symposium were published in volume 88(5) of the Agronomy Journal in 1996. These papers, together with some others, resulted in the following discussion points in the agricultural computer simulation modelling literature.

1. Since a whole model is a set of processes, or hypotheses, they inherently cannot be easily tested in the sense normally accepted as good scientific method (Pease and Bull 1992; Oreskes et al. 1994). They contain a set of hypotheses that can only be rigorously tested with measurements that describe the performance of the crop over a wide range of environments. Such information is rarely available (Monteith 1996).
2. To address this, modellers have adopted the words *validation*, *calibration*, and *verification* for the process of comparison of the output of a model with a new dataset, comparison between competing models, and objective assessment (Passioura 1996; Sinclair and Seligman 2000). However, care is needed as these tools are not as powerful a tool as hypothesis testing as they are an attempt to show the model (or hypothesis) is correct.
3. Further, much of the validation practices were based on the assumption that the data used for validation represented the truth. The natural variability contained within data was enough that failing to recognise sources of variability due to experimental and observation error meant a reduction in ability to assess bias, accuracy or range of models (Sinclair and Seligman 1996).
4. An assumption in many crop modelling efforts was that scientific rigour could be ensured by expressing processes only in basic physical, chemical



and physiological terms; with crops being modelled as deterministic, continuous systems (Sinclair and Seligman 1996). In reality the development is a complex combination of deterministic and stochastic processes (Sinclair and Muchow 2001).

These discussion points resulted in the following set of seven outcomes which indicate uncertainty estimation may help facilitate progress:

1. The primary value of the model is to force logical, quantitative thinking about the variables and processes that influence the performance of the organisms of interest (Innis et al. 1980),
2. Models can justifiably be viewed as heuristic tools to aid our interpretation of reality (Wullschleger et al. 1994; Sinclair and Seligman 1996),
3. The limits of crop models as surrogates for reality should be recognised and accepted as inevitable consequences of simplification (Sinclair and Seligman 1996),
4. Research should be more than refitting a model to some new data (Sinclair and Seligman 2000; Rotter et al. 2011),
5. Models have a continuing role to support scientific investigation, facilitate decision making by crop managers, and to aid in education (Hammer et al. 2002),
6. Models are a prime contributor in understanding and advancing the genetic regulation of plant performance and plant improvement (Hammer et al. 2002; Brown et al. 2013),<sup>1</sup>

---

<sup>1</sup> Chapter 6

7. And of particular consequence for this project; uncertainty estimation, particularly under changing climate conditions, is an important consideration (Rotter et al. 2011).

The use of agricultural simulation models as research tools, crop system management and policy analysis tools are more valuable and defensible if tempered by recognition of uncertainty. This is reflected in current research. The discipline of agricultural modelling as a global discipline in the past several years has had an increasing focus on UE of computer simulation models. Areas of note include uncertainty in climate change (Clifford et al. 2013; Teixeira et al. 2015), multi-model ensemble forecasting (Ewert et al. 2009; Asseng et al. 2013; Bassu et al. 2014), emulators (Stanfill et al. 2014) and sensitivity analysis e.g. (Cichota et al. 2013).

## 2.5 State-space Modelling, Probability and Data

### 2.5.1 State-space Framework

Agricultural bio-physical computer simulation models often simulate processes through time (i.e. they are dynamic). This type of deterministic dynamic system is often represented as a state-space model e.g. (Spiegelhalter and Best 2002). Here, the *state* of a system is defined by a set of *state* variables, or collectively as the *state process*. In general, state variables may be physical variables defined at specific locations in physical space. Any system whose state changes with time over a state space according to a fixed rule is a dynamic system. The evolution of the system through *state space* is often called a *trajectory*. If the current state of the system uniquely determines the future states (perhaps with a first order Markov

property<sup>2</sup>), the system is referred to as a *deterministic dynamic system*. The *transition* function describes the behaviour of the state process as time evolves (Candy 2009; Cressie and Wikle 2011). *State equations* are therefore defined as a set of difference equations. A difference equation is defined as a set of formulas that together express the values of all variables at the next step in terms of the values at the current step (Lorenz and Emanuel 1998). Difference equations determine the transition function at each time step based on the state at the previous step such that each term of the sequence is defined as a function of the previous terms of the sequence (Gonze 2012):

$$X_n = f(X_{n-1}, X_{n-2}, \dots, X_0)$$

This formulation highlights the need to conceptually separate state equations (including the empirically determined coefficients for state processes) from input parameters<sup>3</sup>. This may not be an obvious step for some modellers, and selection separation of the two may not always be simple. A framework to help compartmentalise and frame an agricultural deterministic model in a state-space setting is provided in the Chapter Three.

## 2.5.2 Probability

It is not always obvious how real world processes or mechanisms can be directly incorporated with traditional statistical approaches, which can unfortunately lead to an understanding of the science being pushed into the background.

---

<sup>2</sup> A process has the Markov property if the conditional probability distribution of future states of the process depends only on the present state.

<sup>3</sup> The term input parameter is defined in the Chapter Three.

However, since our knowledge is rarely complete, approaches that allow some incorporation of probabilistic effects can provide insight that would otherwise be impossible (Portier 2001; Williams et al. 2002; Greene 2005; Cressie and Wikle 2011). Probability can add objectivity and rigour to what is at times essentially a subjective ‘best guess’ about a real world system. An ideal model could be one that both recognises the dynamic scientific aspects of the phenomenon under study, and allows uncertainties to be expressed through statistical probabilities (Giorlami 1997; Cressie and Wikle 2011)<sup>4</sup>. Bayesian approaches provide a relatively straightforward pathway to allow this. Bayesian analysis allows the quantification of all kinds of uncertainty, whether aleatory or epistemic, through probabilities (O’Hagan 2006). Information about parameters can be either expressed as a prior distribution, or derived as a posterior distribution given a synthesis of available data. Here, multiple sources of evidence can be differentially weighted according to their assumed quality (Spiegelhalter and Best 2002).

### 2.5.3 Data

Data is the best guide to the unknown. It follows that the most appropriate methods to explore uncertainty in computer simulation models should utilise data wherever practicable. An obvious limitation is that, at best, observation data is only available up until the present time. Careful consideration of data, probability and the model in an integrated manner is required to best evaluate computer simulation model uncertainty. I agree with the opinion of Cressie and

---

<sup>4</sup> This is not a new idea; Laplace and many of his contemporaries believed that determinism and probability can be reconciled to create a greater whole. (Stigler 1986)

Wikle (2011) that a Bayesian analysis approach is the best paradigm to date in which to achieve this goal.

## 2.6 Bayesian Data Analysis

### 2.6.1 Bayes Theorem

Bayesian inference is a very powerful tool for quantifying uncertainty when using observed data for parameter estimation. Bayesian analysis begins with what is known as a ‘prior’ distribution for uncertain parameters  $\lambda^5$ , denoted by its probability  $P$ , that is,  $P(\lambda)$ . Knowledge about the uncertain parameters is then updated by observations,  $C^6$ , to arrive at the ‘posterior’ distribution for  $\lambda$ , given  $C$ . This is expressed formally through Bayes theorem:

$$P(\lambda|C) = \frac{P(\lambda)P(C|\lambda)}{P(C)}$$

The probability of the observed data given the parameters,  $P(C|\lambda)$ , is the likelihood. Bayes theorem specifies that the posterior distribution of  $\lambda$  is proportional to the prior times the likelihood, since the denominator acts to normalise the posterior distribution so that it totals unity. The primary difficulty with Bayesian analysis lies in evaluating the denominator and in most situations numerical methods will be needed. The numerical integration technique known as Markov Chain Monte Carlo (MCMC) sampling is the most widespread approach (McFarland 2008).

---

<sup>5</sup> The Greek symbol  $\lambda$  is used here as the more commonly used  $\theta$  is utilised later in a more specific context. This usage of  $\lambda$  is restricted to this general overview of Bayesian modelling.

<sup>6</sup>  $C$  denotes ‘calibration data’ as distinct from input environmental data. This is discussed in detail in Chapter Three.

## 2.6.2 The Prior Distribution

In Bayesian analysis, the prior distribution  $P(\lambda)$  is a representation of all the knowledge and information about the unknowns, before accounting for the observed data  $C$ . It is possible to use a prior distribution that represents a large amount of prior information thus dominating the effect of observed data. However logical choices also exist for prior distributions that capture the idea of a lack of prior information (McFarland 2008).

## 2.6.3 Elicitation

Elicitation is the term used to describe the process of extracting expert knowledge about an uncertain quantity. Elicited information has a particular role in forming the prior distribution for Bayesian data analysis. This is particularly (though not solely) relevant for quantifying input parameter uncertainty in the absence of data. There has been a considerable amount of research aimed at toward establishing robust methods for elicitation e.g. O'Hagan (2006). The basic idea was described as follows by Strong (2012):

There are four roles, the *decision maker* (the individual who requires the probability distribution for the purposes of making some decision), the *expert* (the individual deemed to have useful subject matter knowledge), the *statistician* (an individual that can provide basic knowledge of probability and validate results) and the *facilitator* (manages the dialogue with the expert). Several steps are involved in the process:

1. Identify uncertain quantities,
2. Recruit expert,
3. Explain process and train expert in basic probability,

4. Expert makes a series of statements about the unknown quantity or quantities, that reveal aspects of their underlying subjective distribution,
5. Facilitator or statistician fits a probability distribution to these summaries,
6. This is refined until the expert is confident that it reflects their judgements through an iterative process of feedback and checking the elicited distribution.

#### 2.6.4 Markov Chain Monte Carlo (MCMC)

Markov Chain Monte Carlo (MCMC) is a numerical simulation method that is often used in Bayesian analysis to construct the posterior distribution when no analytical expression of  $P(\lambda | C)$  is available. It works by drawing values of  $\lambda$  from approximate distributions and then correcting those draws to better approximate the target posterior distribution, thus generating random samples from the target distribution, such that at each step of the process we expect to draw from a distribution that becomes closer and closer to  $P(\lambda | C)$ . For a wide class of problems this appears to be the easiest way to get reliable results. The key to Markov chain simulation is to create a Markov process whose stationary distribution is the specified  $P(\lambda | C)$  and run the simulation long enough that the distribution of the current draws is close enough to this stationary distribution. Convergence should always be checked by investigating trace plots, posterior densities for each node, and autocorrelation plots (Gelman et al. 2006). Two widely used Markov chain simulation algorithms are the Gibbs Sampler and the Metropolis Hastings algorithm. The Gibbs sampler is the simplest of the Markov chain simulation algorithms, and is the first choice for conditionally conjugate models. The Metropolis algorithm can be used for models that are not

conditionally conjugate; for example if some of the conditional posterior distributions in a model can be sampled from directly, and some cannot, then the parameters can be updated one at a time using the appropriate method. This type of approach is implemented in WinBUGS, the software used in this project (Spiegelhalter et al. 2004).

## 2.7 Putting It All Together

By unifying the ideas described in Sections 2.4 - 2.6 an agricultural computer simulation model can be set in a Bayesian state-space framework. This approach takes the conditional probabilities inherent in Bayesian hierarchical models (Carlin and Louis 2000; Gelman et al. 2006), and incorporates the ability to update (filter) state predictions using recursive Bayesian model properties. It independently allows the incorporation of a probability distribution function describing input parameter uncertainty when appropriate, perturbation of structural state equations if desired and up-to-date information from data when available (Cressie and Wikle 2011).

The joint probability distribution function (pdf) of all the quantities in the model (i.e. the state model, and expert prior knowledge of input parameters) results from multiplying together the conditional pdf's to provide an estimate of the process under study at time  $t$  based on all of the data available at that time (Gordon et al. 1993; Higdon 2007; Candy 2009; Vrugt et al. 2009a; Vrugt et al. 2009b; Cressie and Wikle 2011; Murray 2013).

A general solution that updates Bayes rule to allow inclusion of the state evolution model is provided by Berliner (1996), Candy (2009), and Cressie and Wikle (2011). This solution also allows the posterior at day  $t = 1$  to become the prior at day  $t = 2$ . The hierarchical state-space framework uses an order one Markov assumption, and is referred to by Cressie and Wikle (2011), (Chapter 7)



as a dynamic spatio-temporal model (DSTM), and by Candy (2009), (Chapter 2) as a sequential Bayesian filtering processor. The filter allows an enhanced signal with associated performance statistics to be estimated.

It is helpful to follow the terminology of Cressie and Wikle (2011) to help incorporate the state equations into the Bayesian framework. Instead of 'likelihood', 'prior' and 'posterior' we will use 'data model' ( $C$ ), 'input parameter model' ( $\theta$ ) and 'filtering model' (defined fully below). In addition, the 'state evolution model', or 'state model' ( $Z$ ) enables the entrance of the mathematical model. The hierarchical structure of the model is given here:

- The data model  $C|Z, \theta$  is what is most likely to be true given conditional dependency upon the crop model in addition to the standard dependency upon the parameter model. An important feature of this framework is the lack of requirement for either linearity or normality in the data model.
- The state model  $Z|\theta$  is represented by a series of unobserved/hidden or latent variables that are inferred through analysing the mathematical equations that describe the underlying scientific process of interest and are conditionally dependent on the parameters. A first order Markov model in time is assumed.
- The input parameter model  $\theta$  contains the parameters which are each described by a prior distribution usually represented by expert opinion or by independent 'non-informative' priors. The sequential estimation procedure additionally allows the prior at time  $t$  to be represented by the posterior pdf at time  $t-1$ .
- The general form of the joint filtering model is then:

$$P(Z_t, \theta | C_{1:t}) \propto P(C_t | Z_t, \theta) P(Z_t | C_{1:t-1}, \theta) P(\theta)$$

This is derived in the context of the case-study model SIRIUS in Chapter Nine.

## 2.8 Summary

This Chapter introduced and defined computer simulation models, particularly in the context of agricultural research and development. One thread explored the concerns of the discipline as a whole that there is a need to properly estimate uncertainty in model outputs. This is becoming an important theme in agricultural research literature. The effect of uncertainty on the use of these models was then discussed in terms of the discipline's historical and current approaches to management of uncertainty. The concept of a state-space framework was introduced and will be adopted to help combine deterministic models, probability, and data in a Bayesian setting. It allows the uncertainty inherent in the deterministic model estimates at each step to be carried forward through time, thereby combining what happened in the past with observed data and expert opinion in a seamless package. The next Chapter will build on these tools to carefully describe the types and sources of uncertainty in a computer model, and develop a UE framework to manage uncertainty in a methodical manner.



# Chapter Three: Uncertainty Evaluation

## Framework

### 3.1 Executive Summary

In order to utilise the tools described in the previous chapter, a clear compartmentalisation of the model into its components is necessary. Once this has been achieved, allocating the types and sources of uncertainty (whether epistemic or aleatory) to each component should be far more straightforward. For this, the state-space structure,  $\mathbf{r} = f(\mathbf{ME}, \boldsymbol{\theta}, \mathbf{E}_t, \mathbf{C}_t, \varepsilon)$  is defined such that the real world  $\mathbf{r}$  is predicted to behave as a function  $f$  of the model's state equations,  $\mathbf{ME}$ , input parameters  $\boldsymbol{\theta}$ , calibration and environmental data  $\mathbf{C}_t$  and  $\mathbf{E}_t$ , and residual stochasticity  $\varepsilon$ . Based on this state-space structure, tools to help curate information, to diagnose the most important sources of uncertainty, and to identify UE objectives have been developed. This clear UE framework will help save time and resources, and add confidence in conclusions by ensuring that no available resources are overlooked but are rather utilised as well as possible.

### 3.2 A State-space Framework

#### 3.2.1 Components of a Computer Simulation Model

Many bio-physical agricultural and agro-ecosystem computer simulation models are dynamic in nature. It is useful to adopt a state-space framework and follow the notation of authors such as Gordon et al. (1993) and Cressie and Wikle (2011) to compartmentalise the model. Each component defined in this Section can introduce uncertainty in the computer simulation model, and this is discussed in detail with respect to SIRIUS in Section III. Notation is used such that bold font indicates a vector and non-bold a single variable.

### 3.2.1.1 Input Parameters

Input parameters are denoted  $\theta$ .  $\theta$  represents independent input information that does not change during the sequential updating process of a dynamic computer simulation model. Examples of input parameters in an agricultural setting could be soil type, cultivar or other 'scenario' indicators as discussed by Teixeira et al. (2015) and Holzkämper et al. (2015).

### 3.2.1.2 State Equations

The model's state equations  $ME$  jointly define the processes that make up the model. The model outputs are then a function  $f$  of all the model components. State equations represent either experimentally derived relationships or theoretical constructs. State equations are mathematical equations that describe the underlying scientific processes of the model. Although the coefficients of these equations may have been derived via a calibration process during the model building phase (O'Hagan 2006), these coefficients and the equations to which they relate are distinct from the input parameters as they are usually constant for all scenarios under which the model might be expected to simulate crop responses. For example, the thermal-time calculation used to drive phenological development of lucerne (Teixeira et al. 2009) or the vernalisation requirement for wheat (Brooking 1996).

### 3.2.1.3 Observation Data

Data which are observed are denoted  $D_t$ . The subscript  $t$  identifies individual points at the time step the dynamic computer simulation model operates on (e.g. week/day/hour). Observation data may be present at each time point  $t$ , only at selected time points, or on some more or less precise scale. The notation  $t$  will be used to signify values that will update in some way related to the computer

simulation model's time step.  $\mathbf{D}_t$  is decomposed into  $\mathbf{D}_t = \begin{pmatrix} \mathbf{C}_t \\ \mathbf{E}_t \end{pmatrix}$  where  $\mathbf{C}_t$  represents response or calibration data (possibly for multiple variables and/or scenarios hence the vector notation). This could also be available only as a single  $C$  e.g. yield at the end of the simulation process for a selection of scenarios or  $C$  for a single scenario. Similarly,  $\mathbf{E}_t$  represents updating environmental or managerial inputs such as rainfall, irrigation, or temperature.

#### 3.2.1.4 State Variables

State variables,  $\mathbf{Z}_t$ , as defined in the previous chapter, are the value of each state equation at each time-step  $t$  given the input parameters  $\theta$  and the environmental input data  $\mathbf{E}_t$ . An important corollary of the structure of the model being allowed to depend upon theoretical constructs is that some components of  $\mathbf{Z}_t$  may be latent, or unable to be observed in practice.

### 3.2.2 Notation

Computer simulation models are built for many different purposes and have many forms, but a generic model can be formally represented as the functional relationship:

$$\mathbf{y} = f(\mathbf{x}) \tag{1}$$

where  $\mathbf{x}$  is a vector of inputs and  $\mathbf{y}$  a vector of outputs. The model structure  $f(\bullet)$  specifies (mathematically or computationally) how the characteristics of  $\mathbf{y}$  are determined by those of  $\mathbf{x}$ . It specifies a formal statement of assumptions about the real world process (McKay and Morrison 1997). Strong (2012) additionally

identified an extra discrepancy term  $\delta$  as a linear, additive term to quantify the effect of structural error<sup>1</sup> on the model's ability to predict the true, unknown target quantity  $r : r = f(\mathbf{x}) + \delta$ . I extend this to include instead a general term  $\xi$  that does not assume either linearity or additivity, and is used to 'catch' any form of uncertainty that cannot be otherwise allocated (i.e as discussed in Section III). Then:

$$r = f(\mathbf{x}, \xi) \quad (2)$$

I do take some liberties with the notation here, of  $f$  in particular by changing it to some function (or model form) that describes the real world based on inputs and noise. But I am not aiming to change the process model itself. Rather I would like to propose an alternate way of describing the model that directly defines each of the *types* of components that are likely to appear in a crop model. This is the beginning of a refinement process that will result in a more detailed expression of how the model represents the real world.

Now, the possible inputs of the model  $\mathbf{x}$  have been partitioned into input parameters  $\theta$  and input environmental data  $\mathbf{E}_t$ . Then it is possible to define:

$$r = f(\theta, \mathbf{E}_t, \xi) \quad (3)$$

Note that state equations have not been incorporated in this formal representation. The form of the model  $f$  is used instead, as it includes not only the equations in the model, but also their interactions. If  $f$  is restricted to apply only

---

<sup>1</sup> Structural and other components of uncertainty in computer simulation model outputs  $\mathbf{y}$  are discussed in Section III.

to the form of the model and not to the individual state equations it would then be equally correct to define a more complete state-space framework:

$$\mathbf{r} = f(\mathbf{ME}, \boldsymbol{\theta}, \mathbf{E}_t, \boldsymbol{\xi}) \quad (4)$$

Finally,  $\boldsymbol{\xi}$  is further decomposed to allow for the uncertainty associated with observed calibration data  $\mathbf{C}_t$ , separately from the remaining unidentified uncertainty to define:

$$\mathbf{r} = f(\mathbf{ME}, \boldsymbol{\theta}, \mathbf{E}_t, \mathbf{C}_t, \boldsymbol{\varepsilon}) \quad (5)$$

Here in this final refinement  $f$  is defined as the way in which these components together can describe the real world, which I have called *model form*.

In the next Section sources of uncertainty in computer simulation models are described, and allocated to one of the three components on the right hand side of the simple representation in equation (5).

### 3.2.3 Types and Sources of Uncertainty and Their Allocation to Model Components

Computer simulation models represent detailed scientific understanding of real-world systems. Although a vital part of research and development, they are simplifications of reality and hence imperfect. Imperfections may arise to epistemic uncertainty, or the lack of exact knowledge (Refsgaard et al. 2007). Imperfections can also arise because of random variation of a real world process (aleatory uncertainty). The types and sources of uncertainty in computer simulation models have been discussed extensively in the literature (O'Hagan et al. 1999; Kennedy and O'Hagan 2001; Katz 2002; Spiegelhalter and Best 2002; O'Hagan 2006; Cressie and Wikle 2011; Gupta et al. 2012). Epistemic and aleatory



sources of uncertainty are aligned with model components next and in Table 1. Elements of equation (5) are **red** to help identify where the source of each type of uncertainty is allocated.

### 3.2.3.1 Epistemic Uncertainty

Input parameter uncertainty  $r = f(\mathbf{ME}, \boldsymbol{\theta}, \mathbf{E}_t, \mathbf{C}_t, \varepsilon)$  is also known as ‘state of the world’ uncertainty. It refers to uncertainty about the appropriate values to describe the scenario to be modelled.

Data uncertainty  $r = f(\mathbf{ME}, \boldsymbol{\theta}, \mathbf{E}_t, \mathbf{C}_t, \varepsilon)$  may enter due to bias or scaling/aggregation. Scaling/aggregation uncertainty refers to situations in which the model is used on a scale different from that on which it was developed to operate. This is sometimes known as change of support (Katz 2002; Cressie and Wikle 2011). Bias occurs when the model is used on a scale different from which it was developed to operate. Calibration data,  $r = f(\mathbf{ME}, \boldsymbol{\theta}, \mathbf{E}_t, \mathbf{C}_t, \varepsilon)$ , is used when calibrating or updating predictions with actual observations. Environmental input data,  $r = f(\mathbf{ME}, \boldsymbol{\theta}, \mathbf{E}_t, \mathbf{C}_t, \varepsilon)$ , is used directly to inform state equations and can introduce uncertainty both as set of imperfectly measured observations, but also in a similar way to input parameters.

Structural uncertainty,  $r = f(\mathbf{ME}, \boldsymbol{\theta}, \mathbf{E}_t, \mathbf{C}_t, \varepsilon)$ , is also known as model inadequacy (Gupta et al. 2012), state equation uncertainty, or ‘ignorance’. It refers to our basic lack of knowledge concerning the structure of the model relative to the processes they represent. This may be in the nature of the state equations  $r = f(\mathbf{ME}, \boldsymbol{\theta}, \mathbf{E}_t, \mathbf{C}_t, \varepsilon)$ , or the more inclusive model form  $r = f(\mathbf{ME}, \boldsymbol{\theta}, \mathbf{E}_t, \mathbf{C}_t, \varepsilon)$ . The obvious symptom is the difference between the true mean value of the real world process and the model output at the true values of the input data and parameters.

An additional source of uncertainty that must be discussed is code uncertainty which arises when the response surface of model outputs is sampled (Kennedy and O'Hagan 2001). This type of uncertainty is only briefly touched on through this dissertation and sits outside the UE framework proposed here as it describes uncertainty from the truth of the model as opposed to truth of the real system. There exists situations in which a particularly large or complex model is difficult to evaluate due to the length of time taken to run a single simulation. In these situations an emulator approach can be used to predict how a computer simulation model (computer simulation model) might be expected to behave, based on a small number of actual runs of the computer simulation model. Estimates of the 'code' uncertainty around the computer simulation model expected values can then be obtained (Kennedy and O'Hagan 2001).

### 3.2.3.2 Aleatory Uncertainty

Aleatory uncertainty  $r = f(ME, \theta, E_r, C_r, \epsilon)$  is usually thought of as an intrinsic, stochastic, random variation of a real world process even when the conditions are fully specified. The true process  $r$  is then defined as the mean value averaged over this intrinsic variation. It will only be able to be quantified as an aspect of the residual uncertainty in observed calibration.

### 3.2.4 Consolidation of Sources of Uncertainty

The information provided in Section 3.2 is summarised in Table 1, where the model form is expanded to include additional components as the type of uncertainty associated with that component is introduced.

**Table 1: Sources of uncertainty.**

Source of uncertainty	Notation
Aleatory uncertainty	$r = f(x, \varepsilon)$
Input parameter uncertainty	$r = f(\boldsymbol{\theta}, \mathbf{E}_t, \varepsilon)$
Environmental data uncertainty	$r = f(\boldsymbol{\theta}, \mathbf{E}_t, \varepsilon)$
Calibration data uncertainty	$r = f(\boldsymbol{\theta}, \mathbf{E}_t, \mathbf{C}_t, \varepsilon)$
Model form uncertainty	$r = f(\mathbf{ME}, \boldsymbol{\theta}, \mathbf{E}_t, \mathbf{C}_t, \varepsilon)$
State-equation uncertainty	$r = f(\mathbf{ME}, \boldsymbol{\theta}, \mathbf{E}_t, \mathbf{C}_t, \varepsilon)$

This clear partitioning of the components of the model is an important step for any UE of a computer simulation model. As pointed out by Gupta et al. (2012), the separation of errors into their source components is often difficult, particularly if the models are nonlinear and different sources of errors may interact. This is true both across different types of uncertainty (e.g. structural vs. input parameter) and within types (e.g. which input parameter has the greatest influence on the output). However, it is important in understanding where the greatest sources of uncertainties reside (Brown and Heuvelink, 2005). Although some of the partitions discussed in this Section may seem somewhat artificial, they are necessary to enable the objectives of the UE to be stated without confusion.

### 3.3 Framework for Robust Computer Simulation Model UE

I will use the term ‘model uncertainty evaluation’ or ‘uncertainty evaluation’ (UE) to refer to exploration of any of the sources of uncertainty described in this section. Note that specific subsets of these have their own name that is ubiquitous across the literature; for example *sensitivity analysis* usually refers to exploration of the effect of changes in input parameters and data  $\boldsymbol{\theta}$ ,  $\mathbf{E}_t$  on the model outcomes  $\mathbf{y}$ .

### 3.3.1 The Life of a Computer Simulation Model

One thing to consider when approaching an UE of a crop model is the phases of model development and use. The model's life is usually a continuum of phases starting with conceptualisation and implementation in code (Model Building), testing (Model Assessment) and use (Model Application). However, model building and assessment are not often considered 'complete', and adjustments are made as understanding of the system changes. It may be useful to conceptualise a simplified schematic of the life of a model as shown in Figure 2 below. Explicit identification of the model phase during UE process is necessary when defining the objective of the UE to help identify the most appropriate UE techniques.

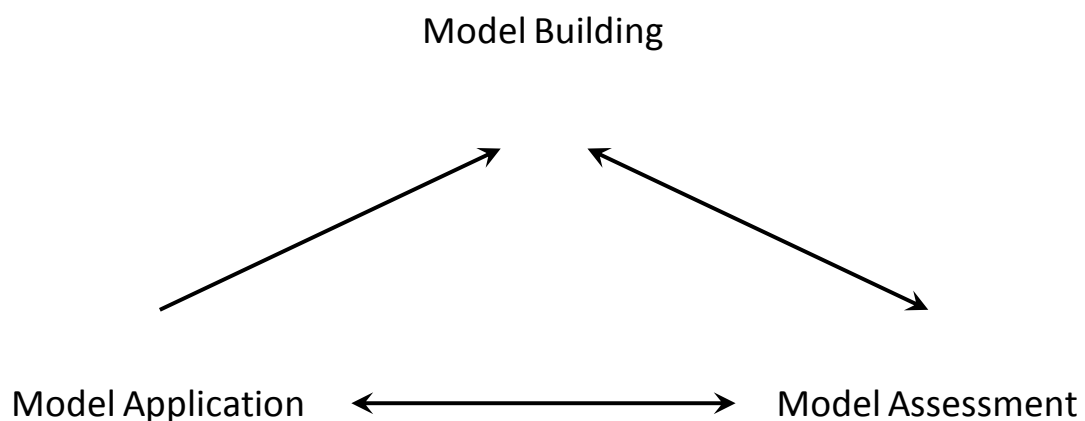


**Figure 2: Simplified schematic of phases of a computer simulation model's life.**

### 3.3.2 Outline of a Robust UE

Several sampling and analysis techniques are reviewed in the next Chapter. Whilst many are complementary, not all will be suitable for all applications. The choice of which techniques to utilise is dependent upon what resources are

available and the objectives (see Section 3.3.2.5) of the UE. Figure 3 outlines seven steps that, if followed, can help ensure a robust UE of a model. Figure 3 is not dissimilar to the framework put forward by Refsgaard et al. (2006). Each step in this outline is expanded upon in Sections 3.3.2.1 – 3.3.2.7. A clear UE framework will help save time and resources by ensuring that no available resources are overlooked but are utilised as well as possible. This will ensure that time spent back-tracking and re-doing simulations is minimised. The framework is illustrated for the case-study model in Chapter Eight.

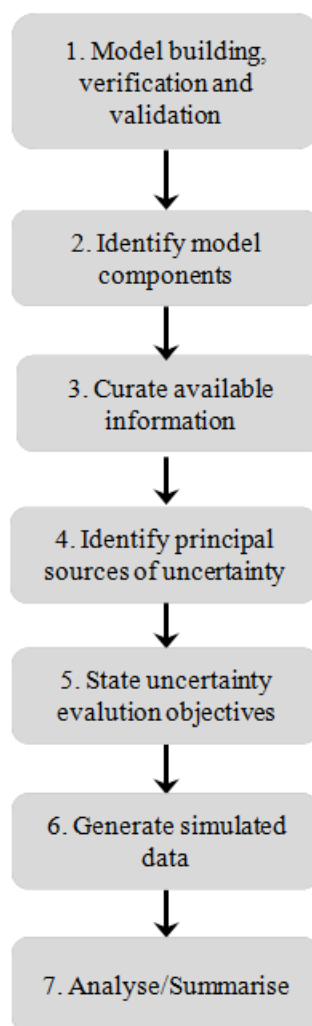


**Figure 3: Seven steps for computer simulation model UE.**

### 3.3.2.1 Step 1: Verify and Validate the Model

Figure 4 displays the iterative process that is central to computer simulation model building. As with any modelling exercise, it begins with an observation, from which hypotheses are derived, and then implemented in code. The joint processes of verification and validation, which are integral components of model building, are defined below.

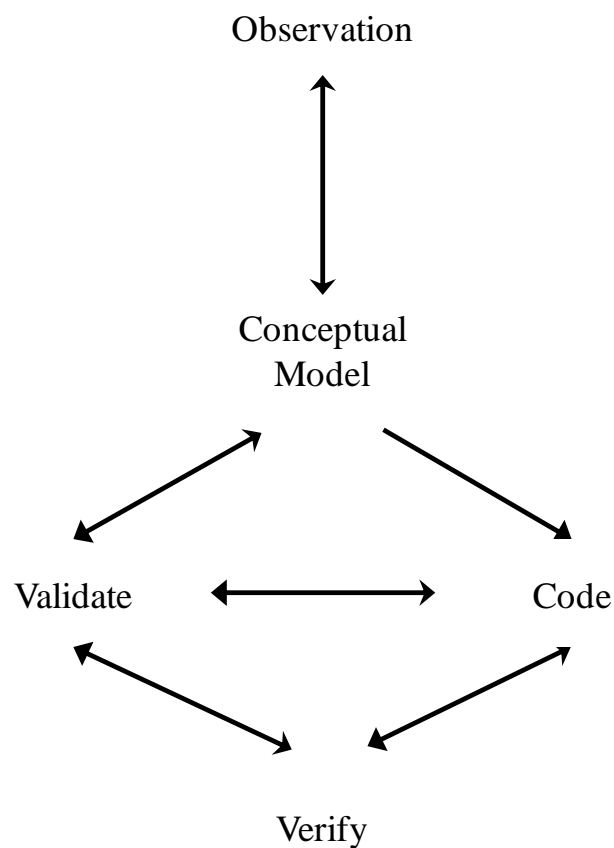


**Figure 4: Schematic of the model building process.**

Verification is defined as the process of determining whether the model implemented in computer code accurately represents the algorithms that were intended (Carson 2002; Trucano et al. 2006). Since verification is usually considered a part of the minimum standard for the coding process it will not be

discussed further in this paper. Validation is more complex, with authors such as Oberkampf and Roy (2010) pointing out that different communities view validation from different perspectives. One such perspective is that validation is defined as ‘quantification of the accuracy of the computer simulation model’s results by comparing outputs with experimental data’. Another, that validation is ‘determination of whether the estimated accuracy of the computer simulation model results satisfies some specified accuracy requirements’. In the first case some experimental data is required, whereas in the second it is not necessarily expected. However, as long as the process of validation is kept conceptually as ‘confirmation of being fit for purpose’ then I enjoy the definition of Sargent (2005), ‘Validation is the process of determining the degree to which a simulation model and its associated data are an accurate representation of the real world from the perspective of its intended uses’. Techniques for model UE during the validation stage are discussed in greater detail in the next Chapter.

### 3.3.2.2 Step 2: Identify Components of the Model

Each component of the model defined in Equation 5 should be able to be assigned to one of the columns in Table 2. If not, another column should be added to allow for other types of components.

### 3.3.2.3 Step 3: Curate Available Information

Data, expert opinion, phase of the computer simulation model’s life, model components, sources of uncertainty, and other relevant information can be identified in Table 3. Extra rows should be added as required for each individual component; e.g. if there are 10 state equations then there should be 10 rows in the first segment. If the computer simulation model is too large to easily enable this process a first step should be to identify which sub-component of the model structure is to be evaluated.

**Table 2: Model component matrix.**

Input Parameter	Observation Variable		Structural Uncertainty		State Variable
	Calibration Variable	Environmental Variable	Model Form	State Equation	
$r = f(ME, \theta, E_v, C_v, \varepsilon)$	$r = f(ME, \theta, E_v, C_v, \varepsilon)$	$r = f(ME, \theta, E_v, C_v, \varepsilon)$	$r = f(ME, \theta, E_v, C_v, \varepsilon)$	$r = f(ME, \theta, E_v, C_v, \varepsilon)$	$Z_t - NA$

**Table 3: Model information matrix (adjusted from (Refsgaard et al. 2007)).**

Context	Notation	Data	Expert opinion	Other
Structural Uncertainty	$r = f(ME, \theta, E_v, C_v, \varepsilon)$			
Model Inputs	$r = f(ME, \theta, E_v, C_v, \varepsilon)$			
Aleatory Uncertainty or biased/scaled/aggregated observed data	$r = f(ME, \theta, E_v, C_v, \varepsilon)$			



#### 3.3.2.4 Step 4: Identify Principal Sources of Uncertainty in the Model

Given the components identified in Steps 2 and 3 (Figure 3), assess which of the sources of information are likely to be of primary importance.

#### 3.3.2.5 Step 5: State Objectives of Evaluation

Any attempt to parameterise uncertainty cannot be general or universal; rather, it is an exploration that will be specific not only to the model but to the environment/scenario for which it is to be used (McFarland 2008). In most situations a selection of techniques will be likely to be helpful and should be combined to provide a heuristic view of the model; hence our use of the term ‘uncertainty evaluation’. Which techniques will prove most insightful will vary depending on the phase of the computer simulation model’s life (Figure 2) that is under study. Further, during computer simulation model building, assumptions and simplifications are made. The techniques chosen to describe the uncertainty in a given model depend on specific properties of that model (Wallach et al. 2014) and these include:

- Principal sources of uncertainty for that particular model,
- Assumptions made during the model building process,
- What information (data, expert opinion) is available.

The key to any computer simulation model UE is to clearly state the objective of the analysis, allowing for the information and other resources available as summarised in Tables 1-3. Once the objectives have been written down, sampling and analysis can begin.

### 3.3.2.6 Step 6: Generate Simulation Data

Acquiring an appropriate sample of simulated data from the model is an important aspect of UE. A selection of sampling techniques to explore structural, input parameter, or environmental data uncertainty is shown in Figure 5. And discussed in greater detail in Section 4.3. Simulated data provides information about how the computer simulation model responds to complex combinations of inputs, and is not synonymous with real-world, observed data. Simulation data generated from a computer simulation model using a technique such as those described in the next Chapter can be used either to explore  $y = f(\mathbf{ME}, \boldsymbol{\theta}, \mathbf{E}_t)$  (sensitivity analysis) or  $\mathbf{r} = f(\mathbf{ME}, \boldsymbol{\theta}, \mathbf{E}_t, \mathbf{C}_t, \varepsilon)$  (calibration) (see Figure 6). The difference lies in whether there is real-world data  $\mathbf{C}_t$  available to provide information about  $\mathbf{r}$ , and hence  $\varepsilon$ .

Given a large amount of time and computer resources for a particular problem, the ideal approach to data generation would be to sample evenly over all possible combinations of parameter values. However, this is usually impractical or even impossible, and the objective is therefore to reduce computational load whilst ensuring an appropriate representation of the response surface is obtained. The objectives of the evaluation defined in the previous step should help guide the sampling technique taken.

The technique used to generate data from the computer simulation model will strongly influence the direction of the analysis toward evaluating uncertainty either due to input parameters or to structural uncertainty. Some techniques will allow more options than others, however. These and others will be discussed in Chapter Four. Note that these techniques would usually not apply to calibration data uncertainty since the nature of the data will pre-determine the scenario to be simulated. An exception is a well-known approach known as Generalised

Likelihood Uncertainty Estimation (GLUE) that is discussed in more detail in the following chapter. In general, simulated data arising from any of the sampling techniques could be used for most analysis techniques described in Chapter Four. An exception is the analysis technique for code uncertainty that arises from a Gaussian Process (GP) emulator sample, as discussed in the following Chapter.

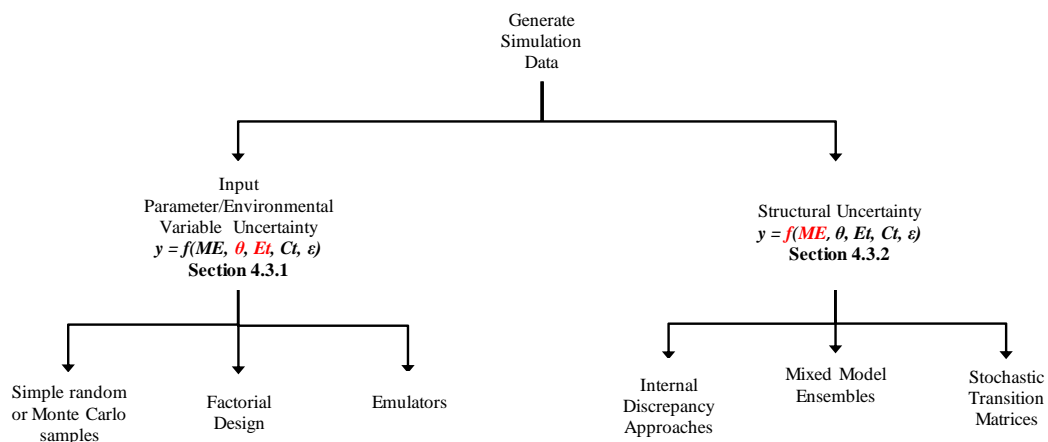


**Figure 5: Classification of commonly used sampling techniques.**

### 3.3.2.7 Step 7: Analyse/Summarise data

Once the simulation data has been generated, analysis and summary of the information can begin. Depending on the objectives defined in step 5 (Section 3.3.2.5), the data will be analysed either to identify areas in need of further research (computer simulation model assessment), or to predict or smooth with confidence ranges representing the desired sources of information (computer simulation model application).

Figure 6 shows a possible classification of UE techniques in this phase. Some techniques based on real-world observation data (calibration) or not (sensitivity analysis) are shown as also described in Section 4.4.

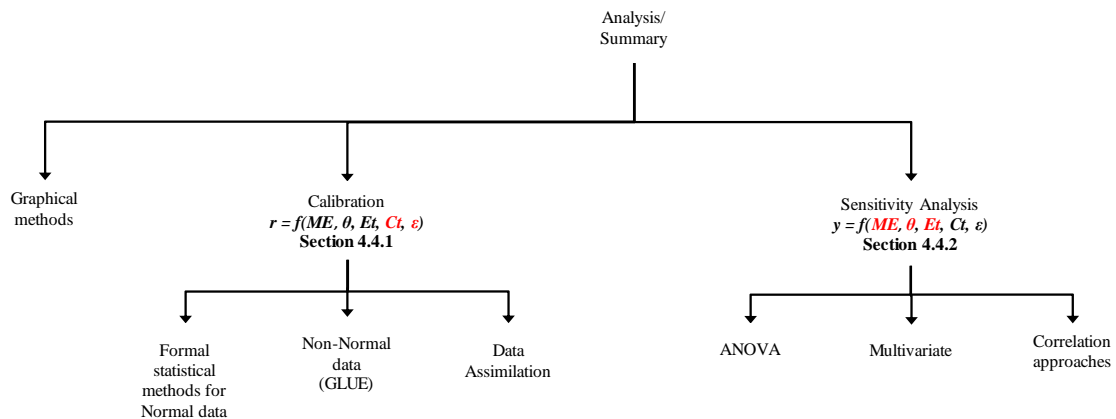


**Figure 6: Classification of commonly used analysis techniques for calibration and sensitivity analysis.**

### 3.3.2.8 Calibration Data Collection

This dissertation does not explore methods for collecting observational data  $\mathbf{D}_k$ . If this is desired and/or possible, interested readers may find many introductory statistical texts for optimal data collection in many fields of research. An important feature of such real-world calibration data is that it is often difficult or impossible to obtain for many possible computer simulation scenarios. For obvious reasons in these situations only simulation data can be obtained, and are analysed via Sensitivity Analysis. The elicitation of expert opinion has been discussed by authors such as Refsgaard et al. (2007) and O'Hagan (2012) and is described in Chapter Two.

## 3.4 Summary

The UE framework proposed is one of the most important contributions of this project to the agricultural modelling community. This Chapter built on the state-space structure provided in Chapter Two to introduce the notion that that a

complete specification of each model component with respect to how it may introduce uncertainty into model predictions is vital. Here, compartmentalising each model component and curating information related to that component makes it easier to diagnose how such uncertainty might be introduced. The UE framework then naturally moves forward to allow analysis objectives to be clearly proposed (or reframed if already stated) based on what information is available, what tools and techniques are suitable and which sources of uncertainty are likely to be most important. The UE framework adds confidence to conclusions by ensuring that available information is not overlooked, but rather is utilised as well as possible. By providing concrete tools and guidelines for uncertainty management, it places uncertainty assessment on a robust and unified footing. This will ensure that time spent back-tracking and re-doing simulations is minimised, saving time and resources. In the next Chapter the most appropriate technique(s) to resolve the UE objectives identified through the framework is (are) reviewed. Approaches to both sample from and analyse data thus obtained from a computer simulation model are linked to the UE framework via a review of uncertainty assessment methods.

# Chapter Four: UE Techniques

## 4.1 Executive Summary

This Chapter is a literature review of techniques for identifying and quantifying uncertainty in computer simulation models. Besides the Introduction and a brief discussion of some common terminology, it is divided into two main sections which describe Sampling and Analysis/Summary techniques. Each Section follows the notation introduced in Chapter Three, filling in the details of the UE framework proposed. The framework therefore directly links qualitative and quantitative analysis through a review of classical and modern techniques for generating and analysing data from such simulation models. Insights are expected to provide guidelines for the identification of most suitable methodological approaches to explore the uncertainty inherent in different aspects of crop models.

## 4.2 Introduction

There are many techniques in the literature that provide insight into computer simulation model uncertainty. Some may be preferred by certain research disciplines, types of models, or intended model usage. For this reason a broad overview of classes of exploration for different types and sources of uncertainty at each stage of model building and evaluation is helpful. A detailed description of a selection of techniques will be provided. Given the topical and wide-ranging nature of this subject, this review is not intended to be exhaustive. Rather, it aims to provide insight into the classes of technique available, specifically those considered to be of particular value to the agricultural modelling community.

## 4.3 Sampling: Design of computer experiments to generate output data

### 4.3.1 Generation of Data to Represent Input Parameter and Input

Data uncertainty  $r = f(\mathbf{ME}, \boldsymbol{\theta}, \mathbf{E}_i, \mathbf{C}_i, \varepsilon)$

#### 4.3.1.1 Simple and Monte Carlo Sampling

Since there are usually many possible values of varying levels of plausibility (Helton 1997) for the input parameters  $\boldsymbol{\theta}$ , uncertainty in  $\boldsymbol{\theta}$  can be characterised by assigning a distribution probability distribution function (pdf) to the parameters, thus defining a sampling space that is practically reasonable. These pdfs characterise a degree of knowledge with respect to where the appropriate input to use in the analysis is located, and this translates confidence about the appropriate values of the distribution of outcomes  $\mathbf{y}$ . Helton and Davis (2000) suggest that it is usually most helpful to elicit expert opinion to characterise the distributions of  $\boldsymbol{\theta}$ . The process of expert elicitation is discussed by O'Hagan and Oakley (2004) and Strong (2012) amongst others. One straightforward approach is then to use simple random sampling from the appropriate range, or Monte Carlo sampling to simulate the pdf of the input parameters. The same concepts can apply to simulate input data  $\mathbf{E}_i$ , if desired.

#### 4.3.1.2 Factorial Experiments

The well-known principles of experimental design (Fisher 1926; Cochran and Cox 1957; Mead 1988) can be readily extended to computer simulation experiments by selecting the combinations of factor values that will be simulated (Sacks et al. 1989) based on the pdfs described above. Factorial and fractional factorial experiments can be used when there are relatively few factors or variates that can be summarised by a manageable number of sensible factor levels. Analysis of the

data is straightforward using ANOVA like decompositions, and can help identify less important parameters, so that they can be set to their nominal values and other terms more fully explored. It can also identify interactions between variables (Santner et al. 2003).

The lack of random error in deterministic computer experiments leads to a number of differences from the traditional design of experiments. The absence of random error ensures that the complexity of the computer code is not disguised, and the adequacy of a response-surface model fitted to the observed computer data is determined solely by systematic bias. There is no need for blocking, and the concepts of experimental units, replication and randomisation are irrelevant (Sacks et al. 1989).

#### 4.3.1.3 Gaussian Process Emulators

The sampling techniques described above usually demand a very large number of model runs, and when a single model run takes several minutes or more, these methods quickly become impractical. One way to reduce the CPU load in the optimisation is to use response surfaces as proxies to the true model response. This results in a statistical representation of the computer simulation model, often called a Gaussian process emulator. It is analogous to regression modelling or multivariate neural networks, but more flexible, accurate, and efficient than these methods in challenging problems where there is limited information about the computer simulation model. A full mathematical treatment of this technique is available (Kennedy and O'Hagan 2001; Oakley and O'Hagan 2002; Oakley and O'Hagan 2004). A tutorial is given by O'Hagan (2006).

The use of Gaussian process emulators has been a very large area of research across many disciplines, both extending the methodologies via research in



different areas of mathematical complexity (Oakley and O'Hagan 2004; Bhattacharya 2007; Rougier 2008; Conti and O'Hagan 2010; Johnson et al. 2011; Wilkinson et al. 2011) and across a wide range of biological, medical, oceanographic, climate, economic and engineering applications (O'Hagan et al. 2001; Stevens et al. 2003; O'Hagan et al. 2005; Kennedy et al. 2006; Rougier et al. 2009; Becker et al. 2011; Fricker et al. 2011; Hall et al. 2011; O'Hagan 2012; Strong et al. 2012; Cripps et al. 2013).

#### 4.3.1.4 Other Input Parameter Sampling Plans

When there are many input variables that may interact to form complex response surfaces, the choice of inputs that will adequately describe the simulation space is less straightforward. There had been a large amount of research in this area, and texts by Santner et al. (2003) and Saltelli et al. (2000) provide summaries of these. If two or more input variables are correlated then it is necessary that the appropriate correlation structure be incorporated into the sample if meaningful results are to be obtained in subsequent analyses (Iman and Davenport 1982; Jacques et al. 2006; Da Veiga et al. 2009).

#### 4.3.2 Generation of Data to Represent Structural Uncertainty

$$\mathbf{r} = f(\mathbf{ME}, \boldsymbol{\theta}, \mathbf{E}_i, \mathbf{C}_i, \varepsilon)$$

##### 4.3.2.1 Internal Discrepancy Approach

This technique, put forward by Strong et al. (2012), is based on specifying a distribution for the model structural error. There is no attempt to make assessments about the adequacy of the model structure in relation to alternative structures as in ensemble methods (discussed next); instead what is assessed is how large an error might be due to the structure of a single model. The method requires the ability to decompose the model into 'sub-functions'. Where there is

thought to be potential structural error, a discrepancy term is introduced. The key idea is that in some applications it is easier to make judgements about internal discrepancies than about the external discrepancy which results from inadequacies throughout the whole model (Strong 2012; Strong et al. 2012; Strong and Oakley 2014). Strong et al. (2012) introduced this technique for simple discrete sub-functions; however, in a more complex (e.g. dynamic) case, we may want to introduce discrepancies at each time step, most likely leading to a correlated structure. This idea was explored in a state-space context by Strong and Oakley (2014). A similar idea has been explored in the context of multiple models by Goldstein and Rougier (2009).

#### 4.3.2.2 Ensemble Methods

Also known as model averaging, a multi-model ensemble (MME) is usually defined as a technique that incorporates outputs across more than one model. In this technique the predictions or probability statements of a number of plausible models are averaged, with weights based either on some measure of model adequacy or some measure of the probability that the model is true (Draper 1995; Kadane and Lazar 2004; Strong et al. 2012; Strong and Oakley 2014). By incorporating the views of many research groups/scientists and experts, the structural effects are said to be better described than if only one model is used (Gal et al. 2014). Model averaging is a well-documented technique (Rougier 1996; Kalnay 2003; Raftery et al. 2005) and has been adopted in much agricultural simulation work (Van Ittersum et al. 2008; Ewert et al. 2009; Asseng et al. 2013; Bassu et al. 2014; Martre et al. 2015). Both frequentist and Bayesian approaches to model averaging can be used to allocate weights to the outputs from different models based on data (Bernardo and Smith 1994; Claeskens and Hjort 2008; Montgomery et al. 2012).

This technique has also been applied in the hydrological modelling area (Hsu et al. 2009; Rings et al. 2012). Here Clark et al. (2008) attempted to quantify the uncertainty in model structure by using a method, 'Framework for Understanding Structural Errors' (FUSE). This technique constructs many unique model structures by combining components from a smaller number of parent models.

#### 4.3.2.3 Transition Matrix Probabilities

A very common implementation is to incorporate stochasticity within the transition matrices of a state space model, e.g. as described by Spiegelhalter and Best (2002) for a discrete state-space medical cost-effectiveness model.

### 4.4 Analysis/Summary of Simulated Data

The techniques discussed in Section 4.3 can often be applied at any of the phases of model development (Figure 2). However, some are more commonly used earlier or later in the process, for example, calibration techniques are often related to the model building phase, whereas sensitivity analyses are more often related to the model assessment phase. Both techniques may be helpful in the model application phase, depending upon the objective of the application. As with any statistical analysis, exploratory data analysis (EDA) is an important step to help understand patterns in the data. Problems with linearity and monotonicity can be identified and help guide selection of appropriate analysis techniques. The generation of scatterplots is the simplest sensitivity analysis technique (Helton and Davis 2000). A scatterplot matrix helps to identify correlations between multiple input parameters. The parallel coordinates plot is a way of visualising multivariate data (Wegman 1990; Cressie and Wikle 2011) that is very popular for sensitivity analysis (Saltelli et al. 2000; Kurowicka and Cooke 2006). In these references it is referred to as a *cobweb plot*. Visually, the vertical axes are placed in

parallel in some predetermined order. Each component of a given multivariate observation is plotted on its respective axis. Then a piecewise straight line is drawn between corresponding values on each axis. The use of colour can very much enhance the interpretability of the plot.

#### 4.4.1 Calibration – Techniques to Assess How Well the Computer Simulation Model Behaves in Relation to Observed Data

$$r = f(\mathbf{ME}, \boldsymbol{\theta}, \mathbf{E}_i, \mathbf{C}_i, \varepsilon).$$

##### 4.4.1.1 Formal Statistical Methods for Normal Data

Tools commonly used to explore the goodness of fit of the simulated data to observed data (Smith et al. 1997; Kobayashi and Salam 2000; Gauch et al. 2003) are described next. These methods are usually an important part of the model building phase (Figure 2).

The total difference between the simulated and measured values can be assessed by the root mean square error: RMSE:

$$RMSE = \sqrt{\frac{\sum_{i=1}^n (O_i - P_i)^2}{n}}$$

Where  $i = 1, 2, \dots, n$ .  $P_i$  represents a simulated value,  $O_i$  an observed value and  $\bar{O}$  the mean of the observed values. This value is often used to compare competing models.

The mean bias in the total difference between simulations and measurements is determined by:

$$Bias = \frac{\sum_{i=1}^n (O_i - P_i)}{n}$$

The modelling efficiency, EF, provides a comparison of the efficiency of the chosen model to the efficiency of describing the data as the mean of the observations, i.e.:

$$EF = \frac{\sum_{i=1}^n (O_i - \bar{O})^2 - \sum_{i=1}^n (P_i - O_i)^2}{\sum_{i=1}^n (O_i - \bar{O})^2} = 1 - \frac{\sum_{i=1}^n (P_i - O_i)^2}{\sum_{i=1}^n (O_i - \bar{O})^2}$$

Values for EF can be positive or negative with a maximum value of 1. A positive value indicates that the simulated values describe the trend in the measured data better than the mean of the observations. A negative value indicates that the simulated values describe the data less well than the mean of the observations.

Pearson's correlation coefficient, denoted  $r$ , is useful to assess how well the shape of the simulation data matches the shape of the measured data (e.g. is the relationship approximately linear). This value will be between 0 and 1, with one indicating perfect correlation.

$$r = \frac{\text{cov}(O, P)}{\sqrt{\text{var}(O) \text{var}(P)}} = \frac{\sum_{i=1}^n (O_i - \bar{O})(P_i - \bar{P})}{\sqrt{\sum_{i=1}^n (O_i - \bar{O})^2} \sqrt{\sum_{i=1}^n (P_i - \bar{P})^2}}$$

The square of the correlation coefficient, often known as the coefficient of determination, or  $R^2$ , is defined as the proportion of the total variation in the observed data that is explained by the data fitted by the model, and gives a

measure of how well the regression line approximates the real data points. It is a statistic that gives some information about the goodness of fit of the model.

Finally, simple least squares regression modelling testing the following hypotheses will help describe straight-line departures from the 1:1 line using F-statistics to test the following four hypotheses:

1.  $P = O$ : The relationship between the predicted and observed values and the 1:1 line,
2.  $P = \alpha + O$ : The relationship between the predicted and observed values and the 1:1 line with a constant adjustment  $\alpha$  upward or downward,
3.  $P = \beta O$ : The relationship between the predicted and observed values converge to the origin, but depart from the 1:1 line,
4.  $P = \alpha + \beta O$ : The relationship between the predicted and observed values diverge from the origin and the 1:1 line.

Taken together, RMSE, Bias, EF,  $r$ ,  $R^2$ , and linear regression can help explore the model more thoroughly than one measure alone.

#### 4.4.1.2 Calibration for Output Data Not Assumed to be Normally Distributed

There are situations in which the data are correlated, non-stationary or non-Gaussian. Researchers publishing in the area of hydrological models in particular have explored formal (Kavetski et al. 2002; Kavetski et al. 2006; Kuczera et al. 2006; Montanari and Grossi 2008; Thyer et al. 2009; Renard et al. 2010; Schoups and Vrugt 2010) and informal statistical techniques when normality assumptions about residuals may be inappropriate. One well-known informal method was put forward by Beven and Binley (1992), with further work done by Beven and Freer (2001) and Beven (2006). The methodology, called

Generalised Likelihood Uncertainty Estimation (GLUE) has been extremely popular [the 1992 paper has received greater than 1,000 citations e.g. (Blazkova and Beven 2009; Juston et al. 2010)]. The methodology works as follows:

1. Sample from the space of each input parameter to generate a model scenario,
2. Fit the model using the scenario,
3. Use the resulting simulated data to assess how well the model fits against some observed data using a pre-selected rule,
4. Accept or reject that scenario,
5. Uncertainty bounds are set at the desired percentage of the accepted models.

Authors including Pappenberger (2006) and Stedinger et al. (2008) appraised the method, discovering that the prediction limits derived from GLUE can be significantly different from prediction limits derived from correct classical and widely accepted statistical methods. It has been suggested that this approach needs to be used with great care; and further that there is a need for a standardised set of terms as to what is actually meant by 'uncertainty' in cases such as these (Montanari 2007). Some (Vrugt et al. 2003; Blasone et al. 2008; Vrugt et al. 2008) have put forward algorithms that place the sampling methodology on a more statistically grounded framework using adaptive MCMC sampling. Formal and informal likelihood techniques have been compared by Vrugt et al. (2009b), who found that the formal and informal approaches have more common ground than would perhaps be expected that the on-going debate between the two would suggest.

I have seen this approach used to help identify suitable parameter combinations when observations were not available, and I do believe that this method has a

place when the elicitation of prior distributions is truly not possible; however, in general a more statistically robust approach such as the method used in Chapter Nine of this thesis is preferable.

#### 4.4.1.3 Data Assimilation

Data assimilation is the process by which observations are incorporated into the estimates from a computer simulation model, using all available information for optimal prediction. It is distinct from calibration techniques discussed so far in that it makes use of observed data as it becomes available through time. Data assimilation is based on a two-step process and depends on a state-space model formulation, the forecast step, and the update (filtering) step. Figure 7 provides a view of data assimilation (Lewis et al. 2006) that shows how the state evolution model, observations, and input parameters are unified to provide filtered estimates that can be used to explore model sensitivity, uncertainty, and predictability. Some well-known examples of data assimilation techniques are described next.

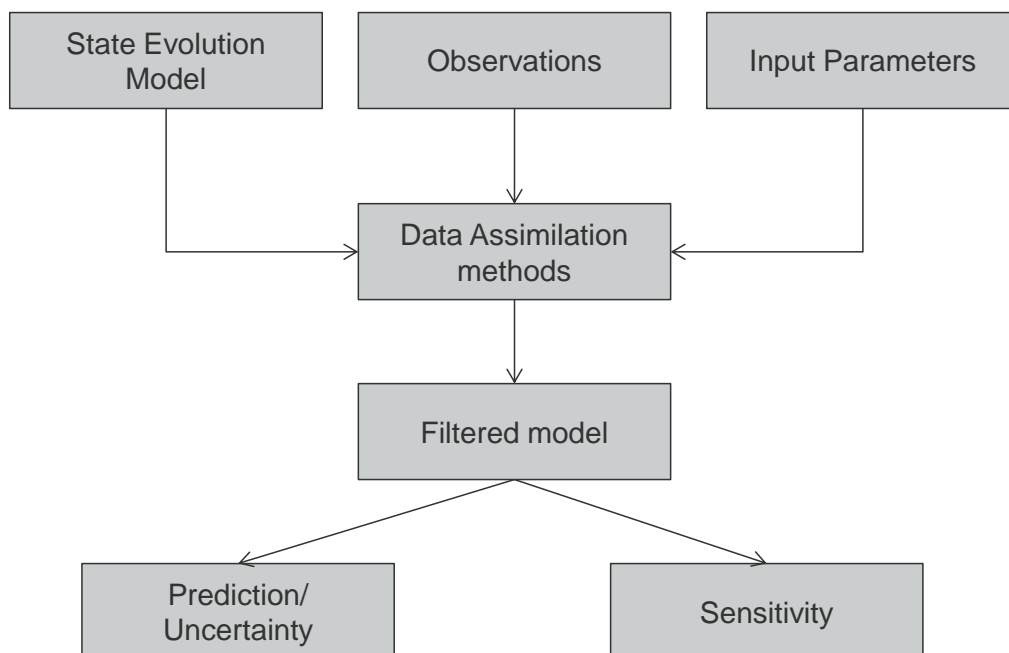




**Figure 7: A view of data assimilation (adjusted from Lewis et al. (2006))<sup>1</sup>**

### **Bayesian Data Assimilation**

The Bayesian data assimilation approach takes the conditional probabilities inherent in Bayesian hierarchical models (Carlin and Louis 2000; Gelman et al. 2006) and incorporates the ability to update (filter) state predictions using recursive Bayesian model properties. It is the best paradigm to date in which to partition variability and quantify input parameter, data and structural uncertainty (Cressie and Wikle 2011). The joint pdf of all the quantities in the model (e.g. the state model, and expert prior knowledge of input parameters) results from multiplying together the conditional pdfs to provide an estimate of the process under study at time  $t$  based on all of the data available at that time (Gordon et al. 1993; Higdon 2007; Candy 2009; Vrugt et al. 2009a; Vrugt et al. 2009b; Cressie and Wikle 2011; Murray 2013). This technique allows an enhanced, dynamic signal with associated performance statistics to be estimated. Such an approach is implemented in Chapter Nine of this dissertation.

### **Kalman Filter**

The Kalman Filter is the most well-known of all the Bayesian data assimilation techniques. It is optimal in the very specific case that assumes normality in the noise component of the model outputs and the observation data. There are many books and tutorials describing the Kalman Filter (Thacker and Lacey 1996; Lewis et al. 2006).

---

<sup>1</sup> reproduced by permission of Cambridge University Press

The Kalman filter uses a series of (noisy) measurements observed over time to produce updated estimates of state variables. Use of the Kalman filter requires the same matrices need to be specified as discussed in Section II with regards to the state-space model framework:  $\mathbf{Z}_t$ , the state-transition model;  $\mathbf{H}_t$ , the observation model.  $\mathbf{CovP}_t$  is defined as the covariance of the process noise and  $\mathbf{CovObs}_t$ , the covariance of the observation noise. Sometimes

$\mathbf{B}_t$ , the control-input model for each time-step,  $t$ , may also included, but has not been here. Therefore, the linear form of the Kalman filter model assumes the true state  $\mathbf{t}$  at time  $t$  evolves from the state at  $(t-1)$  according to the **state equation**:

$$\mathbf{r}_t = \mathbf{Z}_t \mathbf{r}_{t-1} + \mathbf{w}_t$$

Where  $\mathbf{Z}_t$  is the state transition model which is applied to the previous state  $\mathbf{r}_{t-1}$  with  $\mathbf{w}_t$  being the additive, linear process noise which is assumed to be drawn from a zero mean multivariate normal distribution with covariance  $\mathbf{CovP}_t$ .

$$\mathbf{w}_t \sim N(\mathbf{0}, \mathbf{CovP}_t)$$

It is not possible to directly observe the true state vector  $\mathbf{r}_t$ . At time  $t$  an observation (or measurement)  $\mathbf{C}_t$  of the true state  $\mathbf{r}_t$  is made according to the **observation equation**:

$$\mathbf{C}_t = \mathbf{H}_t \mathbf{r}_t + \mathbf{v}_t$$

Where  $\mathbf{H}_t$  is the observation model which maps the true state space into the observed space and  $\mathbf{v}_t$  is the additive, linear observation noise which is assumed to be zero mean Gaussian noise with covariance  $\mathbf{CovObs}_t$ .

$$\mathbf{v}_t \sim N(\mathbf{0}, \mathbf{CovObs}_t)$$

## Extended and Ensemble Kalman Filter

These techniques are extensions to when the linearity requirement of the Kalman Filter cannot be met (Evensen 2007; Fowler 2012).

## Particle Filter

Non-Bayesian Particle filters (also known as Sequential Monte Carlo (SMC)) can help with problems that do not fit into the framework required for a Kalman Filter. Particle filters use a grid-based approach, and work by propagating and updating a set of random samples (particles) to approximate the required continuous probabilistic distribution. The state-space model can be non-linear and the initial state and noise distributions can take any form required (Arulampalam et al. 2002; Künsch 2013).

## Bayesian Model with Particle Filter

Bulygina and Gupta (2009) used a Bayesian data assimilation approach to directly construct the form of the input parameters, outputs, and state variables such that they are statistically consistent with data measurements of the system, and then incorporated the method of particle filtering to construct efficient estimates of the pdfs of the internal model structure.

### 4.4.2 Sensitivity Analysis - Techniques to Explore the Impact of Changes to Structure, Input Parameters, or Environmental Input Variables $r = f(\mathbf{ME}, \boldsymbol{\theta}, \mathbf{E}_t, \mathbf{C}_t, \varepsilon)$

Sensitivity Analysis (SA) assumes the form of the model as defined by the state equations is adequate (Saltelli et al. 2000). SA, like calibration techniques, is dependent on the generation of a reliable simulated data set. It relies on tools such design and analysis of computer experiments, multivariate analysis

techniques, partitioning of variance, and other useful tools (Chatfield and Collins 1980; Sacks et al. 1989; Koehler and Owen 1996; Krzanowski 2000; Saltelli et al. 2000; Santner et al. 2003; Cacuci et al. 2005; Kurowicka and Cooke 2006; Saltelli et al. 2006). Although usually considered to be related to input parameters  $\theta$ , or data  $E_i$ , the process variables  $Z_i$  may themselves exhibit random variability, so model structure can itself be considered as an unknown state of the world and be a subject of probabilistic sensitivity analysis (Spiegelhalter and Best 2002; Strong et al. 2012; Strong and Oakley 2014).

#### 4.4.2.1 Variance Decomposition

Variance based methods are a particularly useful class of sensitivity analysis techniques. Sensitivity indices (for input parameters for example) are based on an ANOVA type decomposition (Welch et al. 1992) of the function  $f(\theta)$  and sensitivity and total sensitivity indices of each term can be studied to assess the sensitivity of the output to individual variables or combinations of variables, even when the effects are not linear (Santner et al. 2003; Wallach et al. 2014). This is a large area of research that is still very active e.g. (Prieur 2014), so a very brief overview follows (Saltelli et al. 2000). The variance decomposition is the same as that for standard Design of Experiments if orthogonal (e.g. statistically independent) inputs (Archer et al. 1997), and has many of the same strengths. The use of variance as an indicator of importance for input factors also underlies regression based methods, and these techniques are useful for situations with non-linearity and or non-monotonicity in  $f(\theta)$ . In contrast, the correlation ratio (McKay 1995) and importance measures (Hora and Iman 1986), are simple tools based on conditional variance of model outputs that describe uncertainty using probability distributions. None of these analyses are appropriate when inputs are not independent and orthogonal.

#### 4.4.2.2 Correlation Based Methods

Linear and nonlinear least-squares regression are other common tools to analyse simulated data in practice. However, there are some fairly stringent assumptions (Trucano et al. 2006) usual to analyses assuming the normal distribution. There are many standard statistical texts that provide detailed descriptions of these methods (Draper and Smith 1981). Saltelli et al. (2000) is an excellent resource.

#### 4.4.2.3 Multivariate Statistics

Multivariate approaches can be helpful to summarise, reduce dimensions, and describe complex interactions between many inputs. There are many resources available on multivariate data analysis approaches, (Chatfield and Collins 1980; Krzanowski 2000; Harding and Payne 2011).

#### 4.4.2.4 Analysis Allowing for Code Uncertainty

The techniques outlined above are used in calibrating parameters of models, taking into account uncertainty in the observation data but assuming no uncertainty in the model itself (structural uncertainty). Formal Bayesian statistical methods that address code uncertainty, rather, describe the relationship between the observations  $z_i$ , the true process  $\zeta(\bullet)$ , and the computer model output  $\eta(\bullet)$ :  $z_i = \zeta(\mathbf{x}_i) + e_i = \rho\eta(\mathbf{x}_i, \theta) + \delta(\mathbf{x}_i) + e_i$  (Kennedy and O'Hagan 2001). Here,  $e_i$  is the observation error for the  $i$ th observation,  $\rho$  is an unknown regression parameter and  $\delta(\mathbf{x}_i)$  is a model inadequacy function (as discussed in Section 2) that is *independent* of the code output.  $\theta$  represents input parameters and  $\mathbf{x}_i$  input data. Here, the error term  $e_i$  is assumed to be normally distributed without systematic error, and the constant regression parameter  $\rho$

implies that the underlying observation process  $\delta(x_i) + e_i$  is stationary, which may be unrealistic in some applications (Trucano et al. 2006; McFarland 2008).

## 4.5 Summary

Managing uncertainty in computer models is very topical. This is evidenced by the very wide range of techniques that have been proposed in the literature (particularly in the past 15 years) to describe and quantify uncertainty. In fact, there are methods by which each type of uncertainty discussed in Chapter Three can be quantified. As such, the UE framework developed in this Section is conceptually aligned with existing model assessment technology.

There are many excellent resources that discuss and describe the different types of uncertainty, and others describe the conceptualisation of time-step models in a state-space structure. Others again put forward plans and frameworks for UE. However, as far as I could ascertain, none explicitly combined all three aspects of model UE. In the three chapters that make up Section I, an existing framework has been built upon existing work to propose a framework that explicitly describes and allocates each type of uncertainty within a state-space structure. The structure is used to curate available information *prior* to diagnosing principal sources of uncertainty and setting or adjusting analysis objectives. That's why the framework proposed in this section, particularly the compartmentalisation of types and sources of uncertainty, is one of the most exciting outcomes of this project.

The next Section focuses on introducing and describing the developmental sub-model of the wheat model SIRIUS. SIRIUS is the basis for the applied, practical components of this dissertation.



## Section II – SIRIUS: A Model for Wheat Development

In the previous section, A UE framework was proposed for computer simulation models. The detailed information required to properly implement the framework requires knowledge not only of how a model is constructed, but also of the scientific understanding upon which it is based. In order to illustrate the framework for a case-study model therefore, it is useful to provide a detailed description of a particular model. The model selected as the case study for this dissertation is a sub-model of the wheat development model SIRIUS. This model was selected as it is of direct relevance to on-going work within PFR, and is still a globally influential research tool. SIRIUS was based upon pre-existing models that were built on historical, scientific understanding about growth and development processes that control wheat response to temperature and photoperiod. SIRIUS built upon and fine-tuned these characterisations to create a new paradigm of model that is based on physiological mechanisms that well describe observed experimental data. In Chapter Five the phenological and physiological scientific background to the wheat development model SIRIUS is introduced. In Chapter Six, data used to characterise several of the key mechanisms incorporated into SIRIUS is re-analysed to describe possible sources of uncertainty. Finally, crop models often act as constructs upon which researchers may continue to develop mechanistic understanding of real world systems. They can help identify biological processes that are not accurately understood. In Chapter Seven a potential source of structural uncertainty is identified and experimental work carried out to assess its impact.





# Chapter Five: Scientific Modelling of Wheat Flowering Time Physiology

## 5.1 Executive Summary

The objective of this Chapter is to provide a description of the deterministic leaf development sub-model implemented within the SIRIUS wheat model (Jamieson et al. 1998a). It includes a biological motivation for the model, an overview of the scientific principles of the crop physiology, and brief journey through the research and development of wheat development models in the past five decades. Key concepts and terminology are defined, and finally, the case study model SIRIUS is defined and described.

## 5.2 Introduction

Building mechanistic and developmental models is an important technique in agricultural research. They provide a framework for the integration of current physiological understanding; and tools for identification of gaps in understanding. They are also valuable tools for estimating real world outcomes from hypothetical scenarios and provide the basis of practical decision support systems in horticulture and agriculture (Holzworth et al. 2014). The science of crop modelling is to understand and quantify the responses of different physiological processes in arable crops to the environment (e.g. climate, soil) and management (e.g. irrigation, fertiliser) and the interaction of different processes within the system. Crop physiologists study the behaviour of system components separately, and then integrate these mechanisms into a crop model. These models can then be used to predict crop behaviour by inputting any required scenario (environmental and management conditions). The need to develop models that accurately simulate crop development has spurred much of our current

understanding of physiological mechanisms. The case study model for this dissertation simulates the leaf development of wheat. Section 5.3 provides a biological motivation for the case-study model selected. Section 5.4 describes the current scientific understanding that underpins this phase of wheat development. Section 5.5 provides a history of model construction over the past five decades ending in a detailed description of SIRIUS.

### 5.3 Biological Motivation: Estimate Flowering Time in Wheat

Wheat (*Triticum aestivum* L.) is the second most important crop in the world; after maize, but before rice and potatoes. Wheat development can be divided into five phases as follows:

1. Sowing – emergence,
2. Leaf Development from emergence to flag leaf (vegetative phase),
3. Flag leaf – anthesis,
4. Anthesis – start grain fill,
5. Start grain fill to end grain fill (Grain filling).

Studies have shown that wheat phenology and physiology, in particular anthesis (flowering) date, is the main determinant of genetic adaptation to the environment (Law and Worland 1997; Iwaki et al. 2001; Snape et al. 2001; Goldringer et al. 2006). This is because the timing of anthesis in wheat strongly influences its yield, as it determines the environmental conditions experienced by the plant during grain-filling (Jamieson et al. 1998b). In wheat, as in most plants, progress toward flowering is chronologically accelerated by increased temperature (Porter and Gawith 1999). That is, physical development of each

plant organ (e.g. tillers, leaves, or spikelets), or progress to consecutive development stages can be related to accumulated thermal-time<sup>1</sup> (Miglietta 1989; Jamieson et al. 1995a; Robertson et al. 1996). During the vegetative phase (leaf development), wheat can also have facultative (optional) responses to photoperiod and cool weather conditions with longer photoperiod and/or exposure to cool temperatures inducing an advance in flowering (Hay and Kirby 1991). The cool temperature response is known as vernalisation and is described in greater detail in Section 5.4.12. Genetics influence these responses with varietal variation in the sensitivity to photoperiod and the extent of vernalisation responses (Syme 1973; Halloran 1975; van Beem et al. 2005; Trevaskis et al. 2007a; Distelfeld et al. 2009a; Eagles et al. 2010; Yang et al. 2011). As anthesis occurs a fixed (for each cultivar) thermal time interval after the emergence of the flag leaf ligule, understanding the developmental processes that control the rate of leaf development and the final number of leaves is vital to predicting the timing of anthesis (Jamieson et al. 1995b; Hay and Porter 2006). For this reason the focus throughout most of this dissertation is the leaf development phase. The exception is Chapter Seven, which focusses on the phase from sowing to emergence. Section 5.4 next describes the current understanding of the biology of leaf development in wheat from emergence until flag leaf.

---

<sup>1</sup> As defined in the glossary, daily thermal time is defined as the integral of time of environmental temperature above a base temperature. In practice a daily mean of maximum and minimum temperatures is normally used. Accumulated thermal time is the sum of daily thermal times from the day of sowing. Thermal time is discussed in more detail in Section 5.4.6

## 5.4 The Physiology of Leaf Development in Wheat

### 5.4.1 Physiology

All physiological science (Crop, Plant, Cell, and Molecular) aims to understand the effects of both environment and genetics on plant form and function. The distinction between these disciplines is the scale at which the study focuses. Crop physiology integrates ideas from plant, cell, and molecular physiology to explain crop scale responses in the field.

### 5.4.2 Phenology

Phenology relates to plant development, describing the occurrence of sequential events (vegetative and reproductive) that can be observed in the plant's life cycle. The primary requirement for the adaptation of a crop in a particular area is that its phenology fits the environment. Therefore the phenology of a crop must allow it to flower and complete the formation of viable autonomous reproductive organs when environmental conditions are suitable.

### 5.4.3 Development

It is important to note that development and growth are two separate processes. Development is the sequential production, differentiation, expansion and loss of the structural units of the plant. Temperature is the primary controller of the rate of development (Chujo 1966a), but photoperiod<sup>2</sup> has a modulating influence in many cases.

---

<sup>2</sup> Described in Section 5.4.11

#### 5.4.4 Growth

Growth refers to increase in crop dry weight, the net result of acquisition and loss of resources. Photosynthetic assimilation is the primary element of growth and is primarily driven by the total amount of intercepted radiation. Growing a crop is an exercise in energy transformation, in which intercepted solar radiation is converted to more useful forms of chemical potential energy (crop dry matter) and partitioned into harvested crop organs. This transformation involves three processes in sequence beginning with the interception of incident solar radiation by the crop's canopy (leaves), followed by conversion of the intercepted radiant energy to chemical potential energy (photosynthesis producing dry matter) which is then partitioned between leaves, stems, roots, and reproductive organs.

#### 5.4.5 Adaptive Fitness

The success of a wheat crop depends on the fit of its genetic characteristics to the environment in which it is grown. There is a remarkable degree of adaptation of modern wheat varieties to climate and management, with the result that crops sown several months apart can converge to give anthesis dates spanning a few days. This results in different varieties having effectively the same grain-filling period and harvest date (Hay and Porter 2006). This fine tuning of the crop to its environment is a consequence of interactions among plant mechanisms in response to different environmental signals (Hay and Kirby 1991; Hay 1999). These behaviours are controlled within each genotype by a unique combination of photoperiod, vernalisation, and other temperature dependent responses. A crop with appropriate vernalisation and photoperiod responsiveness will flower at a time that is appropriate for the environment in which it is grown. This is referred to as adaptive fitness. A variety that flowers too early or too late may experience environmental conditions which cause it to perform poorly. For

example, it may flower in a period of cold weather increasing the chance of frost damage. This plant would then be considered to be poorly adapted to the specific environment.

#### 5.4.6 Thermal Time

Temperature determines the rates of most developmental processes. The use of thermal time is central to the study of crop development (Hay and Porter 2006). Each developmental process in each cultivar<sup>3</sup> has an individual relationship with temperature (Porter and Gawith 1999). Thermal time is a commonly used term that is defined as the integral over time of environmental temperature above a base temperature. This base temperature represents that at which the rate of the process falls to zero. In practice a daily mean of maximum and minimum temperatures is normally used, although hourly data enables more accurate calculations of thermal time if available (Sharma and D'Antuono 2011). The practice of using a daily mean of maximum and minimum temperatures has been shown by these authors to result in an important source of scaling/aggregation uncertainty.

#### 5.4.7 Minimum and Maximum Leaf Number

Each wheat cultivar has an inherent minimum and maximum number of leaves that it may produce. Once the maximum leaf number is reached, flowering will almost always occur. Similarly, a plant will never flower before its minimum leaf number is reached, even in the most favourable of conditions. Any vernalisation

---

<sup>3</sup> A plant variety that has been produced in cultivation by selective breeding.

and photoperiod responses will act to decrease the final leaf number within these boundaries.

#### 5.4.8 Phyllochron

The phyllochron is the thermal time accumulation required for a full leaf to develop. Each leaf developed may also be called a *Haun* stage (Haun 1973); e.g. a wheat plant with 6 and one half fully emerged leaves is at Haun stage 6.5. Phyllochron usually increases with Haun stage, depending only on the temperature of the apical meristem and the current number of leaves. It is independent of photoperiod (Jamieson et al. 1995a). In contrast to Sharma and D'Antuono (2011), evidence was also given that only mean daily temperatures are required to calculate leaf appearance rates.

#### 5.4.9 Primordia

Primordia are undifferentiated organs on the apex of the mainstem which may develop to become leaves or spikelets. The embryo of a wheat grain has usually produced 2-3 primordia (see Figure 17 in Chapter Seven) when the mother plant is ready for harvest.

#### 5.4.10 Plastochron

The plastochron is the thermal time taken for individual primordia to develop. Within the range of conditions experienced in temperate areas, primordia initiation is assumed to be dependent solely upon temperature (Brooking et al. 1995). Accurate simulation requires correct measurement of the temperature experienced by the apical meristem. It is common to use air temperature as a temperature input even when the apical meristem (the temperature sensitive growing tip) is underground. However, the difference between air and soil



temperature is often too large for accurate simulation, particularly in the warmer months (Jamieson et al. 1995b; Jamieson et al. 2008).

## 5.4.11 Photoperiod Sensitivity

### 5.4.11.1 Definition and Effect of Photoperiod Independent of Vernalisation

Photoperiod, the number of hours of daylight in a day, can influence the final leaf number in wheat. A plant can only respond to photoperiod once its vernalisation requirement is met, and different cultivars vary in the extent of their response to photoperiod. The adaptive response delays flowering in short photoperiods, ensuring that flowering will occur when environmental conditions are more favourable for crop development. The first step in understanding the mechanisms driving final leaf number is to describe and parameterise the photoperiod response independent of any vernalisation response, e.g. for vernalisation insensitive (spring) varieties. This was done by Brooking et al. (1995), who described the nature and timing of the day length response to final leaf number for several different spring wheat cultivars and sow dates. They included information about when the plant is sensitive to photoperiod, differences in responses between genotypes, and how photoperiod affects development progress.

### 5.4.11.2 Inductive Conditions

Essentially, inductive conditions are a set of conditions that will guarantee triggering the switch from vegetative to floral development. The term inductive refers to whether or not the wheat plant is able to respond to photoperiod, i.e. is exposed to appropriately warm temperatures, is emerged, and is fully vernalised. It is suggested that, unlike rice and maize, exposure of the first green leaf to light sets in train the photoperiodic reactions leading to floral initiation without a

juvenile phase (Gott et al. 1955; Cooper 1956; Kiniry et al. 1983; Collinson et al. 1992; Ellis et al. 1992). This progresses as shown in Figure 17 and described in Section 7.2.1 in Chapter Seven.

#### 5.4.11.3 Wave of Commitment

An early hypothesis by Miglietta (1991b) assumed that crops responded to day length immediately after emergence; determining which primordium would be the first spikelet and thus fixing the final leaf number. Brooking et al. (1995) pointed out that this would lead to the same response if the crop emerged to decreasing day length, which does not occur. Rather, in spring wheat, the first spikelet primordium is not committed to its ultimate fate until sometime after it has formed. This work is explored in detail in Chapter Six, Section 6.2. If the plant emerges at a time when photoperiod is not inductive, the plant must commit to a final leaf number at some point during its development, switching from a vegetative to a reproductive state. Slafer and Rawson (1994b) showed that the rate of change of day length had no influence on final leaf number independent of the effects of day length. Hence, commitment to final leaf number must occur at some fixed thermal time during spikelet development. In fact, depending on the cultivar, the plant can display photoperiod sensitivity until terminal spikelet formation. For four cultivars, Brooking et al. (1995) showed that the final commitment to final leaf number occurred at different developmental stages in different genotypes. In two of the four cultivars analysed, final leaf number was controlled by the day length midway through spikelet initiation. In the third and fourth cultivars, the day lengths at the beginning and end respectively of spikelet initiation were the controlling factors. Thus the final leaf primordia may not commit until many plastochrons after it is formed, depending on cultivar. This is shown in greater detail in Chapter Six, Section 6.2.

There is assumed to be a fixed relationship between the rate of appearance of leaves and leaf primordia (Kirby 1990; Brooking et al. 1995) (Figure 17). This is not true between leaf and spikelet primordia appearance. When apical meristem development is plotted against the appearance of leaves in inductive conditions, then leaf primordia appear at a slower rate than spikelet primordia. In non-inductive conditions, the first few spikelet primordia may be produced at the same rate as leaf primordia (Delecolle et al. 1989; Brooking et al. 1995). It seems likely, then, that the rate at which primordia are initiated changes at around the time the first primordium commits to becoming a spikelet in inductive conditions. At this stage, however, older (uncommitted) primordia can still become either spikelets or leaves, so that a 'wave of commitment' of primordia that occurs after the initiation of the terminal spikelet is still somewhat sensitive to photoperiod (Brooking et al. 1995). This enables the plant to reflect abrupt changes in day length (Brooking et al. 1995).

In summary, primordia will continue to develop and commit to becoming leaves until the (genotype specific) photoperiod signals are received to commit to a final leaf number. During this time, some primordia will have committed to becoming spikelets, changing the rate of emergence of primordia. However, this in itself will not impact on the final leaf number. Once final leaf number is fixed, all primordia between the first committed spikelet and last committed leaf will rapidly commit to becoming either leaves or spikelets, generating the 'wave of commitment'. A photoperiod response is not present in all wheat genotypes, and it may be influenced by a vernalisation requirement in winter genotypes as described in the next section. Interactions between daylength and temperature responses must therefore occur because temperature will determine the time at which plants set the final leaf number, and hence the daylength to which they

will be exposed at the time. Variations between cultivars are caused by variations in phyllochron; hence cultivars with shorter phyllochrons will flower earlier.

## 5.4.12 Vernalisation

### 5.4.12.1 Introduction

Vernalisation is a less well understood process than photoperiod response. The consequences and importance of vernalisation, and early approaches to understanding its mechanism are described. These, however, failed to differentiate between the mechanisms of vernalisation and vegetative development. In 1995, a developmental framework was proposed that sets the scene for modelling the effect of vernalisation independently of vegetative development. (Jamieson et al. 1995b; Robertson et al. 1996; Jamieson et al. 1998a).

### 5.4.12.2 Brief Outline of Vernalisation in Wheat

The vernalisation response is an accumulating period of time at appropriately low temperatures. Chourd (1960) defined vernalisation as a preparatory process to flowering. The major effect of vernalisation is to shorten the duration of the phase of leaf primordia production (Griffiths et al. 1985) by a chilling treatment. The vernalisation response is important in adapting the plant to the environment in which it is grown so it can make the best use of the seasonal opportunities for growth and avoid adverse climatic factors (Levitt 1948; Gott et al. 1955; Aitken 1961; Tottman 1987).

This requirement for cold temperatures that advance flowering, and consequently decrease final leaf number, is what separates spring and winter wheat varieties. Only winter genotypes of wheat demonstrate a vernalisation response, with spring varieties having a low final leaf number regardless of the

temperature. Although winter wheat plants subjected to cold temperatures when young will flower sooner than non-vernalised plants, non-vernalised plants will eventually flower without exposure to low temperatures (Ahrens and Loomis 1963; Chujo 1966a) so vernalisation response is said to be facultative.

The final number of leaves the plant will develop starts at the maximum final leaf number and reduces in proportion to the extent of vernalisation saturation. Vernalisation continues independent of other developmental events during the vegetative phase until the 6th Haun stage (Gott 1957). A consequence of the combination of temperature responses of vernalisation and primordium production is that plants vernalised at the warm end of the range of vernalising temperatures will set more leaves and need more thermal time to reach anthesis than those vernalised at the cool end (Jamieson et al. 1998a). This is due to a slower progress toward vernalisation at higher temperatures (Reinink et al. 1986; Kirby 1992; Brooking 1996). The vernalisation response is said to be 'saturated' when the lowest possible total leaf number at anthesis (minimum final leaf number) is obtained (Brooking 1996).

#### 5.4.12.3 A Mechanism for Vernalisation

As stated previously, vernalisation and vegetative development occur concurrently. Some early approaches to understanding the response of wheat were based only on the consequence of vernalisation (Hansel 1953). That is, the progress to anthesis rather than the process of vernalisation in itself. This led to difficulties in separating the effect of vernalisation and development (Chujo 1966a; Brooking 1996), since the morphological effect of vernalisation was not visible until floral initiation had begun (Chourd 1960).

To properly understand the relationship between temperature and vernalisation, information is required to monitor vernalisation progress prior to flowering, and take account of both the extent and consequences of continued vegetative development during vernalisation (Brooking 1996).

Brooking (1996) suggested a methodology to pinpoint the time of vernalisation saturation through differentiating between the vernalisation and vegetative development mechanisms. This methodology was based on existing data resulting from experimental work that was originally used to relate wheat morphology and phenology (Kirby 1974; Hay and Kemp 1990; Hay and Kirby 1991; Hay and Kemp 1992). In contrast, Brooking (1996) aimed to define developmental aspects of the temperature response of the vernalisation process in wheat. Since leaf and spikelet initiation are sequential processes, and leaf primordia appear at a slower rate than spikelet primordia (Kirby 1990), it is possible to detect even quite subtle changes in the timing of the transition from vegetative to reproductive stages under inductive conditions prior to actual flowering (Brooking 1996). Brooking's mechanism is described next.

As discussed above, spring genotypes that emerge into fully inductive conditions are almost immediately transferred to a reproductive stage. For winter genotypes, vernalisation continues until the vernalisation requirement is saturated or the current number of primordia equals the maximum final leaf number<sup>4</sup>. When one of these two conditions is met, vernalisation ceases and the plant becomes responsive to photoperiod. This pattern of apical development in vernalisation sensitive genotypes suggests a juvenile stage which progressively

---

<sup>4</sup> The mechanism for calculating attainable final leaf number is given in 5.6.4.

decreases as vernalisation proceeds (Brooking 1996). Brooking described two possible outcomes in terms of behaviour of primordia once the vernalisation requirement is saturated. These outcomes are mainly driven by temperature during vernalisation. There are two options; either, apical development is inhibited either by low temperature or lack of moisture. This means the apical meristem only has its original 2-3 primordia when the vernalisation requirement is saturated. Thus, once inductive conditions are reached, vegetative development needs to continue to reach the minimal leaf number prior to emergence. In this case there would be no juvenile stage, and plant behaviour after emergence would be identical to that of a spring genotype. Alternatively, apical development is not inhibited during vernalisation. Vernalisation is not complete on emergence, so leaf primordia continue to be initiated (juvenile stage). When inductive conditions are reached all further primordia will be spikelets. (i.e. transition immediately to the reproductive state).

This developmental interpretation maintains the focus clearly on the transition of the apical meristem from a vegetative to a reproductive state, based on the transition from leaf to spikelet primordia production (indicated by the increased rate of primordia initiation). This transition is the first measurable developmental event in the 'acceleration of the ability to flower', and occurs rapidly after perception of the photoperiodic signal in vernalisation-insensitive genotypes. By equating the vernalisation response with the progressive reduction of a juvenile phase, the time taken to reach the point of saturation at a given treatment temperature can then be used as measure of the rate of vernalisation per se at that temperature (Brooking 1996). That is, the change in the rate of primordia production immediately indicates that vernalisation is saturated in inductive conditions, as is also discussed in Section 5.4.11.2.

### 5.4.13 Joint Effect of Photoperiod and Vernalisation on Final Leaf Number

The processes of apical development (in response to photoperiod and thermal time), vernalisation and frost tolerance are associated in a complex manner, and it is likely that they will not be thoroughly unravelled until the molecular basis of each is understood (Brooking 1996; Robertson et al. 1996; Brooking and Jamieson 2002). Controlled environment experiments have established that there is interaction between vernalisation and photoperiod in relation to the number of leaves and time to flowering (Krekule 1987). More recent work (Brown et al. 2012a; Brown et al. 2013) for example, link phenotypic information with genetic characteristics of cultivars. These characteristics are discussed in greater detail in Chapter Seven. The genes coding for vernalisation and photoperiod response indicate a wide variety of responses to temperature and photoperiod representing the many phenotypes of wheat that are fit for a variety of environmental conditions.

## 5.5 Overview of the History of Modelling in Wheat

Failure to predict anthesis date correctly is a major cause of simulation models giving incorrect predictions of yield (Porter et al. 1993), which impacts all areas in which such models are being used. Models that realistically represent the processes that cause variation in the time to flower are necessary for the accurate prediction of crop behaviour in different situations and to serve as a framework to integrate and develop understanding of these processes. Although crop models cannot be a complete surrogate for reality, they can be of great value when used as research tools and aids to reasoning about the functioning and response of crop system (Sinclair and Seligman 1996). They are also important as crop system management and policy analysis tools (Boote et al. 1996). Three



types of models in use today are those based on empirical representations of wheat phenological stages; AFRC2 (Porter et al. 1982; Weir et al. 1984; Porter 1993; Jamieson et al. 1998b; Hay and Porter 2006), physiological mechanisms underlying phenological development, e.g. SIRIUS (Jamieson et al. 1998a), and a combination of physiological and molecular mechanisms controlling wheat phenology (Brown et al. 2013). I briefly describe the shift from phenological to mechanistic modelling and recent developments toward an integrated physiological/molecular framework next.

#### 5.5.1.1 Empirical Modelling of Wheat Phenology (the AFRC2 model)

The focus of research for AFRC2 is the empirical quantification of developmental phases in wheat. Practical agronomists resolved the problem of describing the dynamics of development using a Decimal Code system for 'development stages' (Table 4). These stages are readily observed in the field without the need to bring plants back to the laboratory for dissection. Many investigations and crop simulation models are based on this method of phasic development stages. These phenological phases, however, are only empirically connected to development processes, and as such the models were not necessarily easily generalised to new temperature or photoperiod conditions. An alternative, mechanistic modelling approach was proposed to address underlying driving processes. This is described in the next section.

**Table 4: Primary and secondary stages used in the Decimal Code for the description of the development of wheat (Tottman 1987)<sup>5</sup>.**

<b>0</b>	<b>Germination</b>	<b>3</b>	<b>Stem extension</b>
1	water absorption	30	pseudostem extension
.		31	first node detectable
.		.	
.		.	
07-09	coleoptile above ground	.	
		36	sixth node detectable
<b>1</b>	<b>Seedling growth</b>	37-39	flag leaf visible
10	first leaf through coleoptile		
11	first leaf emerged (ligule visible)	<b>4</b>	<b>Ear in 'boot'</b>
12	2-3 leaves emerged	49	tip of ear visible
.			
.		<b>5</b>	<b>Ear emergence</b>
.			
18	8 leaves emerged	<b>6</b>	<b>Anthesis</b>
19	9 or more leaves emerged		
		<b>7</b>	<b>Milk Development</b>
<b>2</b>	<b>Tillering</b>		
20	main shoot only	<b>8</b>	<b>Dough Development</b>
21	main shoot and 1 tiller		
.		<b>9</b>	<b>Ripening</b>
.			
.			
29	main shoot and 9 or more tillers		

#### 5.5.1.2 Physiological Modelling of Wheat Phenology (the SIRIUS model)

Although prediction using the traditional phasic methodology does work for carefully calibrated models, it provides little insight to how different responses to vernalisation and day length occur in different varieties. According to Jamieson et al. (1998b) there are two main principles that a developmental wheat modelling approach requires to be successful. First, the timing of the

<sup>5</sup> Reproduced in part with permission from the British Crop Production Council

intermediate observable phenological events must be associated with true changes in development. Second, the duration of the phases between such events must be predictable. In fact, the timing of phenological events is not always closely linked to developmental change; rather, they are events associated with early development of the ear, and not relevant to calculating timing of anthesis. Therefore, the traditional model does not adhere to these expectations. The alternate mechanistically based framework offered by SIRIUS provides the basis for making sense of the diversity of responses in wheat.

This is achieved by assessing the appearance of primordia on the apical meristem and their differentiation into leaves or spikelets (Jamieson et al. 1998b). That is, most developmental events until anthesis can be related to the number and rate of appearance of main stem leaves (Hay and Kirby 1991; Miglietta 1991a; Jamieson et al. 1995a). The rate at which leaves appear in relation to temperature is called the phyllochron, and can be determined for each cultivar regardless of other environmental conditions. However, the total number of leaf primordia developed in the apical meristem is set during the vegetative phase in response to vernalisation and photoperiod conditions. Different wheat varieties will differentially commit to a final number of leaves depending upon their physiological response to environmental conditions. Understanding these responses is vital for accurate description of crop environmental responses (Robertson et al. 1996).

This new direction of research and modelling emphasises the importance of final leaf number and its dependence on genotype specific photoperiod and vernalisation requirements (Hay and Porter 2006). There are a suite of critical papers for this shift in emphasis to understanding the mechanisms driving final leaf number (Brooking et al. 1995; Jamieson et al. 1995b; Brooking 1996; Jamieson

et al. 1996; Brooking and Jamieson 2002; Jamieson et al. 2008). A mechanistic model for wheat development based on this research followed soon after in the wheat model SIRIUS (Jamieson et al. 1998a).

### 5.5.1.3 An Integrated Physiological/Molecular Framework

Recently Brown et al. (2013) integrated the physiological constructs of APSIM (Holzworth et al. 2014) with molecular models of wheat development, creating a new paradigm for agricultural modelling. Relating the genetic information to physiological mechanisms can add insight to wheat development, as described in Chapter Seven. This model was fundamental in interpreting experimental results from Chapter Seven of this dissertation, demonstrating how model development as a research tool represents a living and changing framework to support scientific discovery.

## 5.6 SIRIUS in the Spotlight

The information in 5.6 regarding the components in the model is summarised in Table 5. This table includes the components type, label, and unit type. It also provides default, minimum, and maximum values where applicable. The provenance of this information is unpublished PFR wheat cultivar data. This is the first location in which the notation is formally defined for model components in SIRIUS. Here, observed environmental data used within the model is capitalised and italicised, e.g. photoperiod is denoted  $PP_t$  (Table 5). Although not included as a model component, this is the appropriate time to also define to notation for observed calibration data. Such observed variables shall be denoted as capitalised, but not italicised. That is, observed leaf number on day  $t$  will be  $LN_t$  and observed final leaf number will be  $FLN_t$  (Table 5).

### 5.6.1 Modelling of Apical Meristem Temperature

Based on the work of Brooking et al. (1995) described in Section 6.3.3, calculations to adjust air temperature during the first stages of development were suggested for future versions of the model, but are not incorporated in the model under study for this dissertation. This is therefore another known source of uncertainty.

### 5.6.2 Graphical Conceptualisation of how the Photoperiod Response is Modelled in SIRIUS

Figure 8 shows the final leaf number the plant will achieve with increasing photoperiod for three theoretical cultivars as modelled in SIRIUS (Jamieson et al. 1998a)

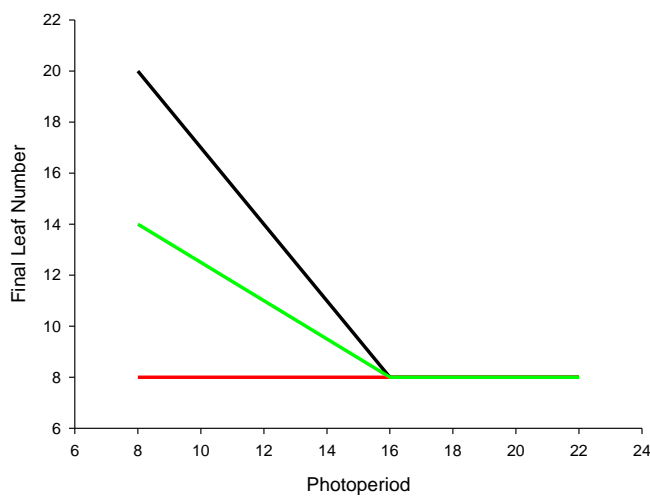


**Figure 8: Effect of increasing photoperiod on the FLN the plant will target for plants with high (black line) medium (green line) and low (red line) photoperiod sensitivity.**

### 5.6.3 Conceptualisation of how the Vernalisation Response is Modelled in SIRIUS via a Vernalisation Index.

Brooking et al. (1996) showed that vernalisation rate increases between -1 and 8 °C, and with no reduction in FLN at 16 °C (Figure 9). Robertson et al. (1996) implemented this mechanism in SIRIUS (see Section 5.6.4) and tested it experimentally. They used this knowledge, and that from research described above, to develop a predictive model around the explicit modelling of the effect of vernalisation on final leaf number under a range of low temperature and plant age treatments. This allowed improved models that incorporate concurrent vegetative development and vernalisation responses, leading in turn to better predictions of final leaf number. It was also shown that vernalisation temperatures (Figure 9) are cultivar-specific (Robertson et al. 1996). Genotypic differences are likely to be important particularly when low temperatures are intermittent and/or warmer temperatures are prevalent; but minimal when vernalisation is saturated before emergence. This model calculates an index from 0 to 1, where 0 indicates a completely unvernalsed plant and 1 a plant where the vernalisation requirement is saturated.

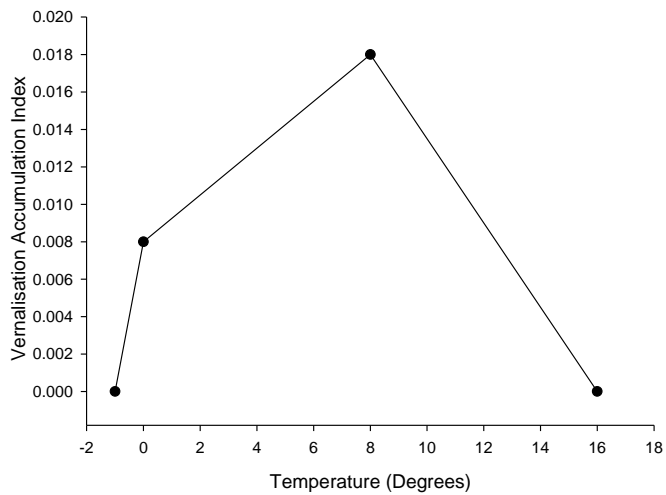


**Figure 9: The calculation of daily vernalisation for a theoretical cultivar as modelled in SIRIUS. The x-axis represents daily mean temperature and the y-axis represents daily vernalisation increment at that temperature for a theoretical cultivar.**

Observations of the leaf and primordia number on the apical meristem can be used to predict final leaf number for winter wheat varieties regardless of sowing date or location (Baker and Gallagher 1983a, b). Explicit modelling of the effect of vernalisation on final leaf number provides a more robust and physiologically sound prediction of flowering time than the timing of developmental effects as in the traditional model (Brooking 1996; Robertson et al. 1996). Jamieson et al. (1998b) furthered the work of Robertson et al. (1996) on the developmental model by using simulations to understand and explain development through this framework.

#### 5.6.4 State equations and the form of the model $y = f(\mathbf{ME}, \theta, E_t)$

SIRIUS simulates the development of a wheat plant as described above. Within SIRIUS, the variations associated with vernalisation requirement and daylength sensitivity are described mechanistically in terms of primordium initiation, leaf

production and final main-stem leaf number as described earlier in this chapter. The leaf production phase from emergence to flag leaf integrates the effects of thermal time, vernalisation and photoperiod. The equations describing this process as implemented in SIRIUS are summarised below following He et al. (2012). All model components and parameters are summarised in Table 5.

The vegetative phase is based on two independently controlled processes, leaf development, and process defining the determination of the final number of leaves that will be produced on the apical meristem. Accumulated thermal time since emergence ( $TT$ ) is calculated with a base temperature of 0 degrees C (He et al. 2012).

Leaf production follows a segmented linear model in thermal time (Boone et al. 1990; Jamieson et al. 1995a; Slafer and Rawson 1997):

$$ln_t = \min \left( fln_{t-1} \frac{T_t}{\text{phyllchron}_t} + ln_{t-1} \right)$$

Here,  $t$  represents a time step. The inverse of the rate of leaf emergence is known as the *phyllchron*, but the first two leaves appear more rapidly than the next six, and then leaf appearance slows again for the subsequent leaves independently of the total number of leaves produced. A varietal parameter known as base phyllchron ( $bp$ ) is defined. This is the rate of leaf development at leaves 2 - 8. *phyllchron<sub>t</sub>* is then defined (Jamieson et al. 1995a):

$$\text{phyllchron}_t = r * bp$$

$$\text{Where } r = \begin{cases} 0.75 & \text{if } ln_{t-1} \leq 2 \\ 1 & \text{if } 2 < ln_{t-1} \leq 8 \\ 1.3 & \text{if } ln_{t-1} > 8 \end{cases}$$



The time-step nature of the model is clear here in that the calculation of *phyllochron<sub>t</sub>* requires information about yesterday's leaf number. Differences in phyllochron for different sowing dates is likely to be due to difference in air and soil temperature experience at the apical meristem (Vincour and Ritchie 2001; Jamieson et al. 2008). The phyllochron from Haun stages 2-8, *bp*, is therefore a single varietal parameter as long as the difference in air and soil temperature are appropriately accounted for.

At any time during vegetative development apical meristem primordia number (*primordia*) is calculated through a simple metric relationship with leaf number (Kirby 1990) under the assumption that the apical meristem contains four primordia at emergence and that they accumulate at twice the rate of leaf emergence (Brooking et al. 1995; Jamieson et al. 1998a).

$$primordia_t = pe + pn * ln_t$$

Concomitant processes governing apical progress toward a reproductive state and defining *fln* (e.g. vernalisation and photoperiod responses) are modelled sequentially. Vernalisation commences once the seed has imbibed water. The daily vernalisation increment *vinc<sub>t</sub>* increases at a constant rate *vai* with daily mean temperature *T<sub>t</sub>* from its value *vbee* at the minimum vernalising temperature *tmin* to a maximum for an intermediate temperature *tint*. Above this the vernalisation increment reduces to zero at the maximum vernalising temperature *tmax* (He et al. 2012):

$$vinc = \begin{cases} (vai_t * T_t) + vbee_t & \text{if } tmin \leq T_t \leq tint \\ ((vai_t * tint) + vbee_t) * \frac{tmax - T_t}{tmax - tint} & \text{if } tint \leq T_t \leq tmax \\ 0 & \text{if } tmin > T_t \text{ or } T_t > tmax \end{cases}$$

Where  $vai$  and  $vbee$  are varietal vernalisation response parameters. Thus the progress toward full vernalisation ( $vi$ ) is simulated over time:

$$vi_t = r$$

$$\text{Where } r = \begin{cases} 1 & \text{if } vinc_t + vi_{t-1} > 1 \\ vinc_t + vi_{t-1} & \text{otherwise} \end{cases}$$

Two varietal parameters define the minimum ( $lmin$ ) and maximum ( $lmax$ ) number of leaves that can emerge on the main-stem. The model assumes that plants start their life with a high potential leaf number  $flna_t$  (set at  $lmax$ ) which decreases with vernalisation progress (He et al. 2012).

$$flna_t = lmax - (lmax - lmin) * vi$$

Vernalisation is complete when one of three conditions is met. Either  $vi$  has reached a value of 1,  $flna_t$  has reached a value that equal  $lmin$ , or  $flna_t$  has reduced to  $primordia_t$ . These primordia are all assumed to produce leaves.

Based on this information, then the model assumes that the minimum  $fln_t$  that the plant will reach *on the current day* is given by:

$$fln_t = \begin{cases} fln_{t-1} & \text{if } vi_t = 1, \text{ or } flna_t < primordia_t, \text{ or } flna_t \geq lmin \\ lmin & \text{if } vi_t < 1, \text{ and if } primordia_t \leq lmin \\ primordia_t & \text{otherwise} \end{cases}$$

This state equation acts within the model to ensure that the FLN will never be less than is possible; e.g. the maximum of  $primordia_t$  or  $lmin$ .

For winter wheat, the crop responds to photoperiod ( $PP$ ) only once vernalisation is complete. Spring wheat responds to  $PP$  since emergence for a spring cultivar as they do not require vernalisation. If  $PP$  of the day when vernalisation is completed exceeds a given value ( $ppsat$ ), then the fln target  $flnt$  is set to the value calculated at the end of the vernalisation routine (Brooking et al. 1995).

$$flnt_t = lmin + (ps * (ppsat - PP_t) * s)$$

Where  $s = \begin{cases} 1 & \text{if } PP_t \leq ppsat \\ 0 & \text{otherwise} \end{cases}$

Here,  $ps$  represents a varietal parameter defining the daylength response as a linear function of photoperiod.

The estimated final leaf number  $flnt_t$  is then given by

$$fln_t = \begin{cases} flnv_t & \text{if } vi_t < 1 \\ \min(flnt_t, primordia_t) & \text{if } primordia_t < flnt_t + pe \\ fln_{t-1} & \text{otherwise} \end{cases}$$

The default values for the state equation coefficients are shown in Table 5. These are values that are not expected to change when simulating new scenarios using the model. They are set empirically during model building and are considered to be part of the model structure.

#### 5.6.5 Input Parameters $y = f(ME, \theta, E_t)$

Scalar cultivar specific parameters do not update as the model progresses, but are rather constants that are estimated through experimentation. They include base phyllochron ( $bp$ ), minimum ( $lmin$ ) and maximum ( $lmax$ ) number of leaves,

saturation photoperiod ( $pps_{sat}$ ), response to photoperiod ( $ps$ ), and vernalisation requirements (Brooking 1996).

#### 5.6.6 Environmental Data $y = f(\mathbf{ME}, \boldsymbol{\theta}, \mathbf{E}_t)$

Environmental input data is dependent on factors external to and driving the crop responses. Daily temperature is measured, and as such is subject to uncertainty. SIRIUS uses minimum and maximum daily temperature to calculate the daily mean ( $T$ ) and thus the accumulated thermal time ( $TT$ ) that is used to drive both vegetative and reproductive development. These parameters take the form of updating vectors. Location information provides photoperiod, which is also an updating vector with a starting value on the sowing date.

#### 5.6.7 State Variables $\mathbf{y} = f(\mathbf{ME}, \boldsymbol{\theta}, \mathbf{E}_t)$

State variables represent a vector of states at each time-step  $t$  as calculated by the state equations. Each state variable excepting  $ln_t$  is treated as an unobservable latent variable throughout the day-to-day simulation of the wheat plant development. At the completion of the vegetative development phase, the state variable  $fln_t$  is observable once the onset of spikelets is seen.

**Table 5: Model component summary.**

Component Type	Parameter	Description	Value			Unit
			Default in SIRIUS	Min	Max	
State equation	$ln_t$	leaf number on day $t$	-	-	-	leaf
	$phyllochron_t$	rate of leaf development on day $t$	-	-	-	leaf/day
	$primordia_t$	number of organs on day $t$	-	-	-	primordia/day
	$vinc_t$	amount of vernalisation achieved on day $t$	-	-	-	vernalisation/day
	$vi_t$	accumulated vernalisation achieved on day $t$	-	-	-	total vernalisation
	$flnv_t$	the minimum fln possible to be achieved on day $t$ based on the vernalisation index	-	-	-	leaf
	$fna_t$	the minimum fln possible to be achieved on day $t$ if no vernalisation has occurred	-	-	-	leaf
	$fnt_t$	adjustment of fln possible to be attained for photoperiod on day $t$	-	-	-	leaf
	$fln_t$	the fln estimated on day $t$	-	-	-	leaf
State equation coefficients	$pe$	primordia in grain at imbibition	2	-	-	primordia
	$pn$	primordia per mainstem leaf	2	-	-	primordia
	$tmin$	minimum temperature for vernalisation to occur	0	-	-	°C
	$tmax$	maximum temperature for vernalisation to occur	18	-	-	°C
	$tint$	intermediate temperature for vernalisation to occur	8	-	-	°C
	$ppsatsat$	saturation photoperiod	16	-	-	hour
Input parameters	$lmin$	minimum leaf number	6	1	11	leaf
	$lmax$	maximum leaf number	18	11	28	leaf
	$bp$	base phyllochron	100	90	110	°C day
	$vai$	vernalisation rate in response to temperature	0.001	0	0.01	1/°C day
	$vbee$	vernalisation rate at temperature equal to $tmin$	0.01	0	2	1/day
	$ps$	leaf production in response to daylength	0.15	0	3	leaf/hour
Environmental Variables	$T_t$	mean daily temperature	-	-	-	°C
	$TT_t$	accumulated thermal time	-	-	-	°C day
	$PP_t$	photoperiod	-	-	-	hour
Observed Variables	$LN_t$	accumulated number of leaves	-	-	-	-
	$FLN_t$	final number of leaves	-	-	-	-

## 5.7 Conclusion

Mechanistic and developmental models represent a framework for the integration of current understanding; and acting as research tools to help identify gaps in scientific knowledge. They also provide the basis of practical decision support systems in horticulture and agriculture. This Chapter described a particular model that simulates the developmental behaviour of a wheat plant during its vegetative stage prior to anthesis. This developmental sub-model of SIRIUS is used for illustrating and implementing UE tools in the remainder of this dissertation. In Chapter Six next, historical data is used to understand mechanisms driving responses to cold temperature and photoperiod is re-analysed to explore potential sources of structural uncertainty in SIRIUS.



# Chapter Six: Historical Data Analysis

## 6.1 Executive Summary

The objective of this Chapter is to carry out an analysis of the methodology used to develop the processes which make up the leaf development sub-model of SIRIUS. Using historical data the steps taken to conceptualise and build the computer simulation model will be replicated. Hypotheses from a selection of papers that describe the key processes (e.g. photoperiod response, thermal accumulation, and vernalisation response) contained within the model will be retested. Some sources of uncertainty that can be investigated with a view to quantifying and managing their impact on final predictions in later chapters will be identified.

## 6.2 Photoperiod Response

### 6.2.1 Introduction

Prior to 1995, it had been established that most developmental events until anthesis were related to the appearance of main-stem leaves, and that vernalisation and photoperiod influences the time of flowering by their effect on the final leaf number (FLN) on the main-stem (Miglietta 1989; Kirby 1990; Hay and Kirby 1991; Miglietta 1991a) The objective of Brooking et al. (1995) was to define the nature and timing of the daylength response that determines final leaf number, and whether there is any variation in the timing of the response.

### 6.2.2 Materials and Methods Following Brooking et al. 1995

All analyses were repeated within GenStat v. 14 (VSN\_International 2013). GenStat code for photoperiod response analyses is provided in Appendix A1. The analysis was carried out on data collected at Palmerston North, New



Zealand. Six sowings of wheat were made to cover a range of increasing and decreasing daylengths at anthesis: 2 June, 24 July, 18 September and 25 November 1989, then 21 February and 5 April 1990. Eleven wheat cultivars were included in the original trial, with a range of sensitivities to both daylength and vernalisation. For the paper, only data for spring wheat varieties was used (Otane, Rongotea, Batten and CRSW6). The experiment was a randomised split plot design with sowing dates as main plots and cultivars as split plots, with 3 replicates. At 10 – 15 day intervals throughout the season, five plants per cultivar, per replicate were harvested and the number of fully developed leaves (e.g. Haun stages) were determined (Haun 1973). The plants were then dissected and the number of primordia counted, cumulative from leaf 1. The final number of main-stem leaves was determined at flag leaf emergence as the mean number of leaves per main-stem (Brooking et al. 1995).

To determine the time at which plants responded to daylength to fix FLN, the latter was plotted against daylength at either emergence, at Haun stage 1.5 (chosen because at that time there will be seven leaf primordia, the minimum number of leaves likely to be set (Figure 17)) at time of initiation of the final leaf primordium (FLP), or at Haun leaf intervals from FLP (FLP+n, where *n* is the number of leaves past FLP). The day of occurrence of these events was determined by linear interpolation between measurements (Brooking et al. 1995).

### 6.2.3 Results Following Brooking et al. 1995

The assumption upon which this mechanism is based is that when the relationship between FLN and daylength is linear and without hysteresis, the correct timing of the response to daylength has been established. The form of the response is then similar to that observed in controlled environments with constant daylengths (Levy and Peterson 1972). This is the simplest hypothesis,

and means that the plants are responding to an immediate stimulus (daylength). In two of the four cultivars, final commitment of the last leaf primordium was controlled by the day-length midway through spikelet initiation (Rongotea, Batten; Figure 10 & Figure 11). In the third and fourth cultivars, the daylengths at the beginning and end respectively of the spikelet initiation phase were the controlling factors (Otane, CRSW6; Figure 12 & Figure 13). Only Otane showed evidence of a saturation response to daylength, e.g. a daylength beyond which FLN is no longer reduced (Brooking et al. 1995). These visual findings are confirmed by fitted models (Table 6) where the higher  $R^2$  values are one indication of how well the daylength at each stage of development is related to FLN.

The results suggest that cultivars differ in the timing of their response of final leaf number to daylength, as well as in the magnitude of their response (Brooking et al. 1995). These differences are adaptations of different cultivars that will aid their fitness to different environments. My results vary slightly from those in the paper as my calculations were all based on the data at the experimental unit level rather than treatment averages as in the paper.

A procedure can be developed that periodically samples the daylength and sign of its rate of change, and can be used iteratively to improve on estimate of FLN, in concert with calculations of the current Haun stage. Thus the number of leaf primordia can be calculated simultaneously and the FLN fixed when the appropriate stage has been reached. The procedure used in SIRIUS is discussed and implemented by Brooking et al. (1995). The parameters used in the model are found via linear regression of best fit for each cultivar (as shown in **red** in Table 6)

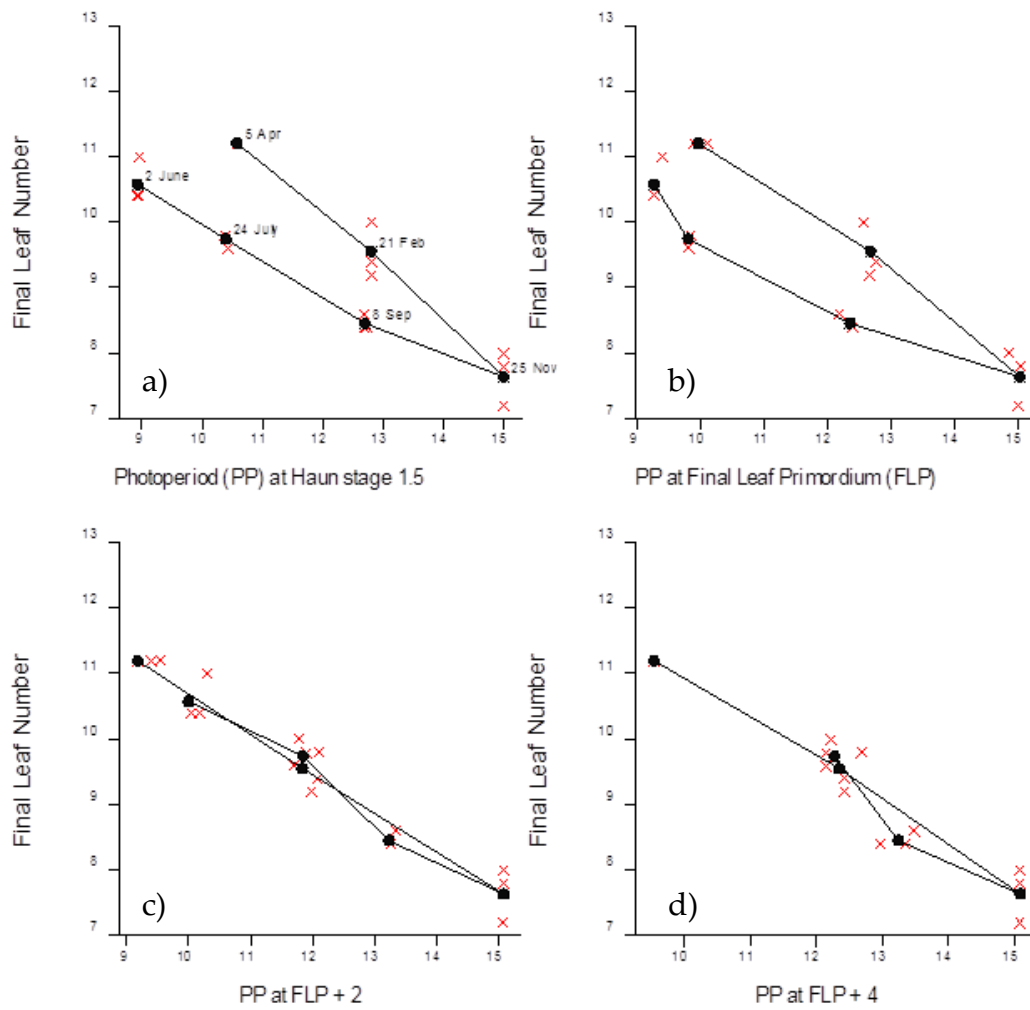


**Figure 10: Relationships between FLN in Rongotea wheat and daylength at a) Haun stage 1.5, b) FLP, c) FLP+2, d) FLP+4. Dates imply whether *PP* is increasing or decreasing at the time of sowing. Black filled in circles denote average values and red crosses denote replicated data points.**

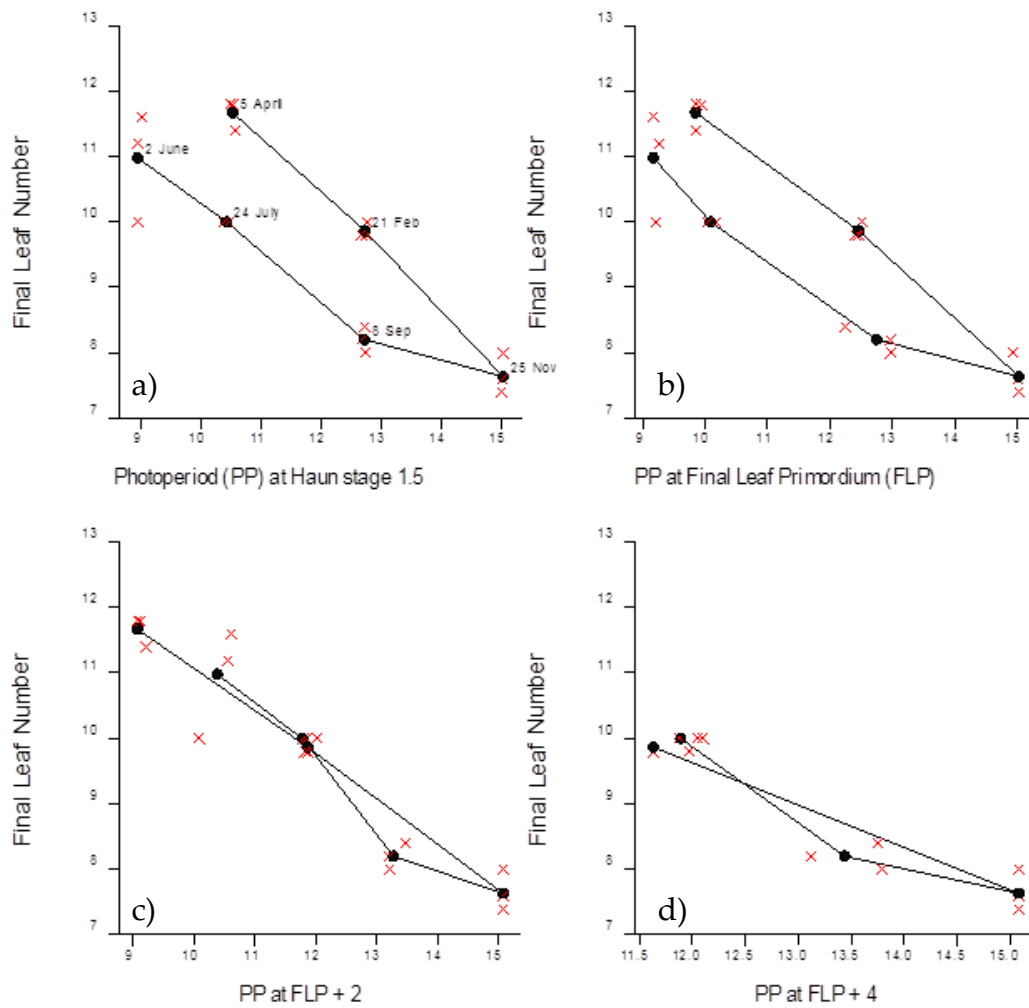


**Figure 11: Relationships between FLN in Batten wheat and daylength at a) Haun stage 1.5, b) FLP, c) FLP+2, d) FLP+4. Dates imply whether *PP* is increasing or decreasing at the time of sowing. Black filled in circles denote average values and red crosses denote replicated data points.**

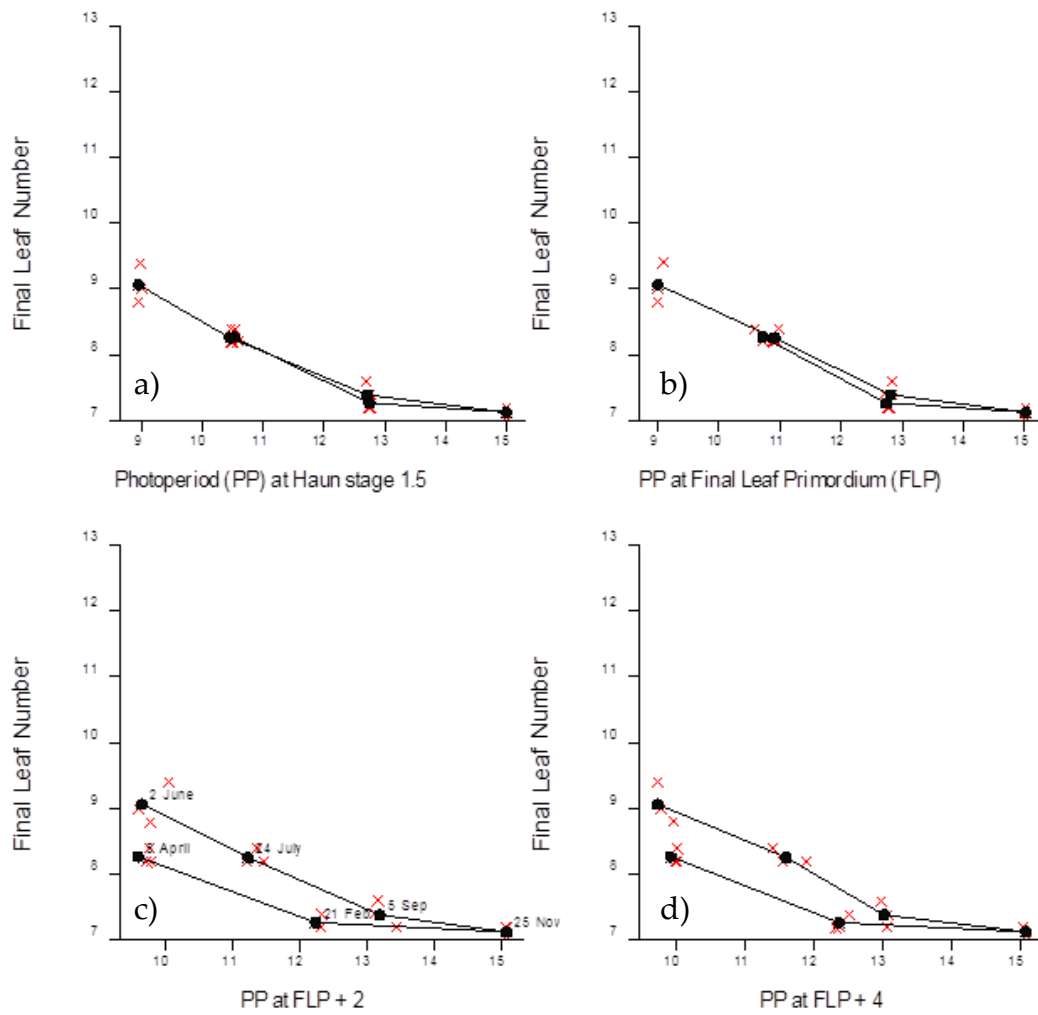


**Figure 12: Relationships between FLN in Otane wheat and daylength at a) Haun stage 1.5, b) FLP, c) FLP+2, d) FLP+4. Dates imply whether *PP* is increasing or decreasing at the time of sowing. Black filled in circles denote average values and red crosses denote replicated data points.**

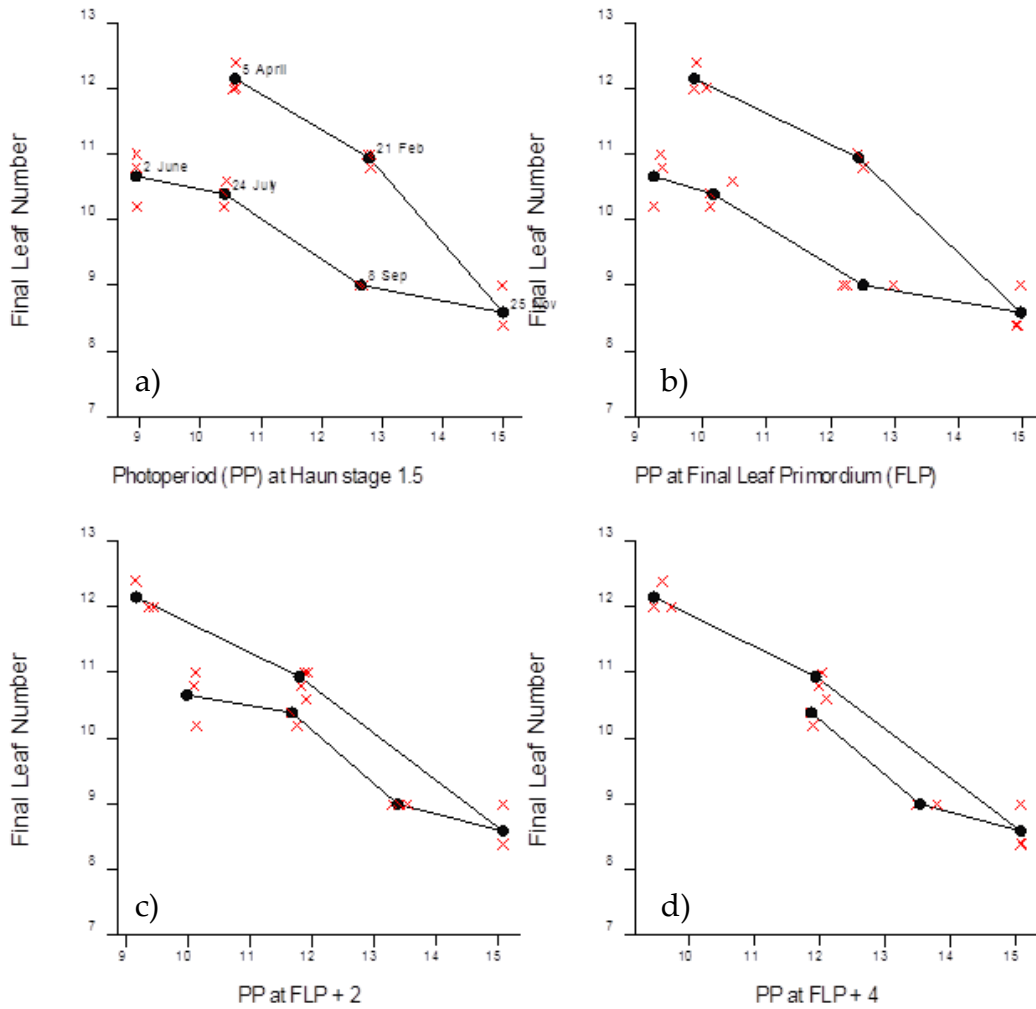


**Figure 13: Relationships between FLN in CRSW6 wheat and daylength at a) Haun stage 1.5, c) FLP, c) FLP+2, d) FLP+4. Dates imply whether *PP* is increasing or decreasing at the time of sowing. Black filled in circles denote average values and red crosses denote replicated data points.**

**Table 6: Percentage variance accounted for (R-sq), parameter estimates, and s.e.'s for linear regression models of FLN on daylength at four stages of development (no data excluded).**

Genotype	Developmental stage	R-sq	Constant	s.e.	Slope	s.e.
Otane	Haun 1.5	85.5	11.8	0.39	-0.33	0.033
Otane	FLP	<b>86.8</b>	<b>12.2</b>	<b>0.14</b>	<b>-0.36</b>	<b>0.012</b>
Otane	FLP + 2	69.2	11.7	0.22	-0.32	0.019
Otane	FLP+4	71.7	12.0	0.22	-0.35	0.019
Rongotea	Haun 1.5	69.9	15.6	0.97	-0.52	0.082
Rongotea	FLP	68.6	15.5	0.33	-0.51	0.029
Rongotea	FLP + 2	<b>93.9</b>	<b>17.1</b>	<b>0.16</b>	<b>-0.63</b>	<b>0.013</b>
Rongotea	FLP+4	89.3	17.8	0.30	-0.68	0.024
Batten	Haun 1.5	66.1	16.8	1.23	-0.60	0.103
Batten	FLP	75.1	17.1	0.37	-0.63	0.032
Batten	FLP + 2	<b>88.7</b>	<b>18.4</b>	<b>0.27</b>	<b>-0.72</b>	<b>0.023</b>
Batten	FLP+4	89.4	18.7	0.38	-0.75	0.029
CRSW6	Haun 1.5	39.0	15.0	1.37	-0.40	0.115
CRSW6	FLP	47.1	15.6	0.48	-0.45	0.042
CRSW6	FLP + 2	82.1	17.2	0.28	-0.58	0.024
CRSW6	FLP+4	<b>92.7</b>	<b>18.8</b>	<b>0.23</b>	<b>-0.69</b>	<b>0.019</b>

#### 6.2.4 Uncertainty Inference

The method used for obtaining overall averages affects the final relationships. The numbers found in my reproduction were a little different, although overall trends appear to be similar. One reason for this may be variation in the point at which replicate values were averaged. There is a good estimate of the variation associated with parameter estimations resulting from this trial as data arises from a replicated, designed experimental trial. This is an area that can help guide understanding of prior distributions.

## 6.3 Prediction of Leaf Appearance in Wheat: A Question of Temperature

### 6.3.1 Introduction

As discussed in the previous chapter, most developmental actions depend on temperature. This includes the rate of leaf development. However, historically, it had been noted that the rate of leaf development in response to *air* temperature was not consistent between autumn and spring sowings. This variation had been attributed to a preconditioning response in the plant, possibly dependent on whether the daylength was increasing or decreasing (Cao and Moss 1991). However, in the context of the state-space computer model, the plant is only aware of daylength today; it does not remember the daylength yesterday as would be necessary for this mechanism to be true. Jamieson et al. (1995) hypothesised a more simple solution to the observed differential behaviour as follows: Experiments characterising the phyllochron were based on recorded air temperature, however, early in the plant's development, when the apical meristem is still underneath or close to the surface of the soil, this may not realistically represent the temperature that the apical meristem is experiencing. These authors believed that the large seasonal variation in the differences between soil and air temperature fostered the incorrect belief that the daylength had an effect. They suggested that there is a consistent response to thermal time, but that the temperature used to characterise the phyllochron must accurately represent what the plant is actually experiencing.

### 6.3.2 Materials and Methods Following Jamieson, Brooking et al. (1995)

The hypothesis was tested using plant developmental data from Palmerston North in the North Island of New Zealand and Lincoln in the South Island of



New Zealand. Soil and Canopy temperatures were simulated by SIRIUS, based on its calculation of LAI and the crop and soil surface energy budget. Code is shown in Appendix A2.

#### 6.3.2.1 Data

**Data set 1:** The data from Palmerston North was the result of a ‘developmental’ trial carried out in 1984 with 4 sowing dates (11 May, 1 June, 21 September, 2 November). Each sowing date was randomly assigned to a large plot. Three to five plants were destructively sampled and mean tips present at each occasion were used for analysis. The trial used a single wheat cultivar, Avalon. Air temperature was recorded hourly and used to calculate accumulated thermal time. Soil temperature was measured by a single thermistor that spent 265 days in the Sowing 1 plot, then moved to the newly sown Sowing 3 plot, and finally to the bare Sowing 4 plot from a partial canopy in Sowing 3.

**Data set 2:** The data from Lincoln was available only in summary format. The experiment was carried out in 1984 with 4 sowing dates (4 May, 13 June, 1 August, 12 September). Soil and canopy temperature was simulated as described next.

#### 6.3.2.2 Models for Simulations

Four competing hypothetical models to describe the relationship between thermal time and development were tested. Agreement between measured and simulated values was quantified using root mean square deviations (RMSDs). The phyllochron for the first three models was based on later results presented in the paper; it is as follows: base 0 °C, 75 °C days from Haun stage 0-2, 100 °C days from Haun stages 208, thereafter 130 °C days. The models are:

1. Based on air temperature,
2. Based on soil temperature and then on canopy temperature from a fixed Haun stage,
3. Based on air temperature adjusted by a factor related to rate of change of daylength at emergence (Baker et al. 1980; Bindi et al. 1995),
4. Based on air temperature and a phyllochron which increased by 3% for each new leaf (Miglietta 1991a).

### 6.3.3 Results Following Jamieson et al (1995)

#### 6.3.3.1 Measurements

There was evidence of a difference in the nonlinear spline for the rate of leaf appearance in response to air temperature for the autumn and spring sown wheat crops ( $p < 0.001$ ) (Figure 14a). However, this dichotomy disappears if soil temperature is used to predict Haun Stage until 10 leaves have appeared with season either as a main effect ( $p = 0.782$ ) or interacting with the spline term ( $p = 0.897$ ) (Jamieson et al. 1995a) (Figure 14b).

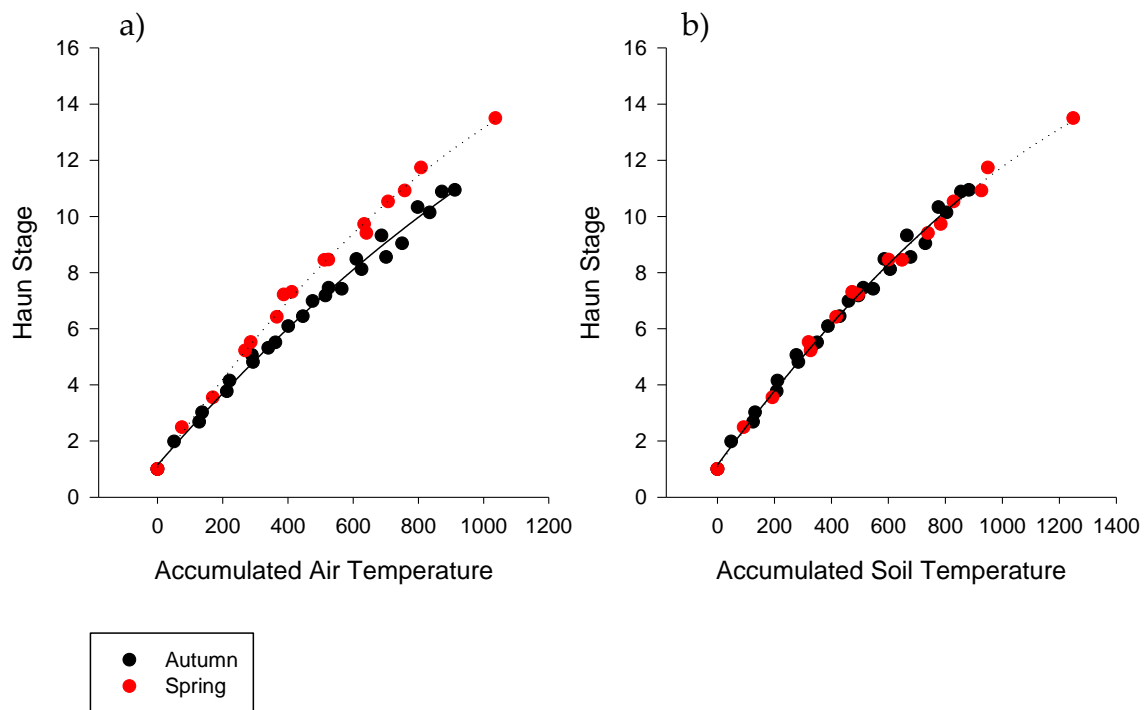


**Figure 14: Relationship between leaf appearance in Avalon wheat and thermal time accumulation from seedling emergence, calculated from a) air temperature only, and b) near surface soil temperature until leaf 10, then air temperature.**

### 6.3.3.2 Simulations

Based on the Lincoln data set, Model 2 was the most consistent predictor of leaf appearance (Table 7, Figure 15). Air temperature (Model 1) provided accurate predictions for only the two later sowings, and the general fit was improved only slightly by adjusting the temperature for the rate of change of daylength at emergence (Model 3). The Miglietta model (4) predicted leaf appearance slightly less well than Model 2.

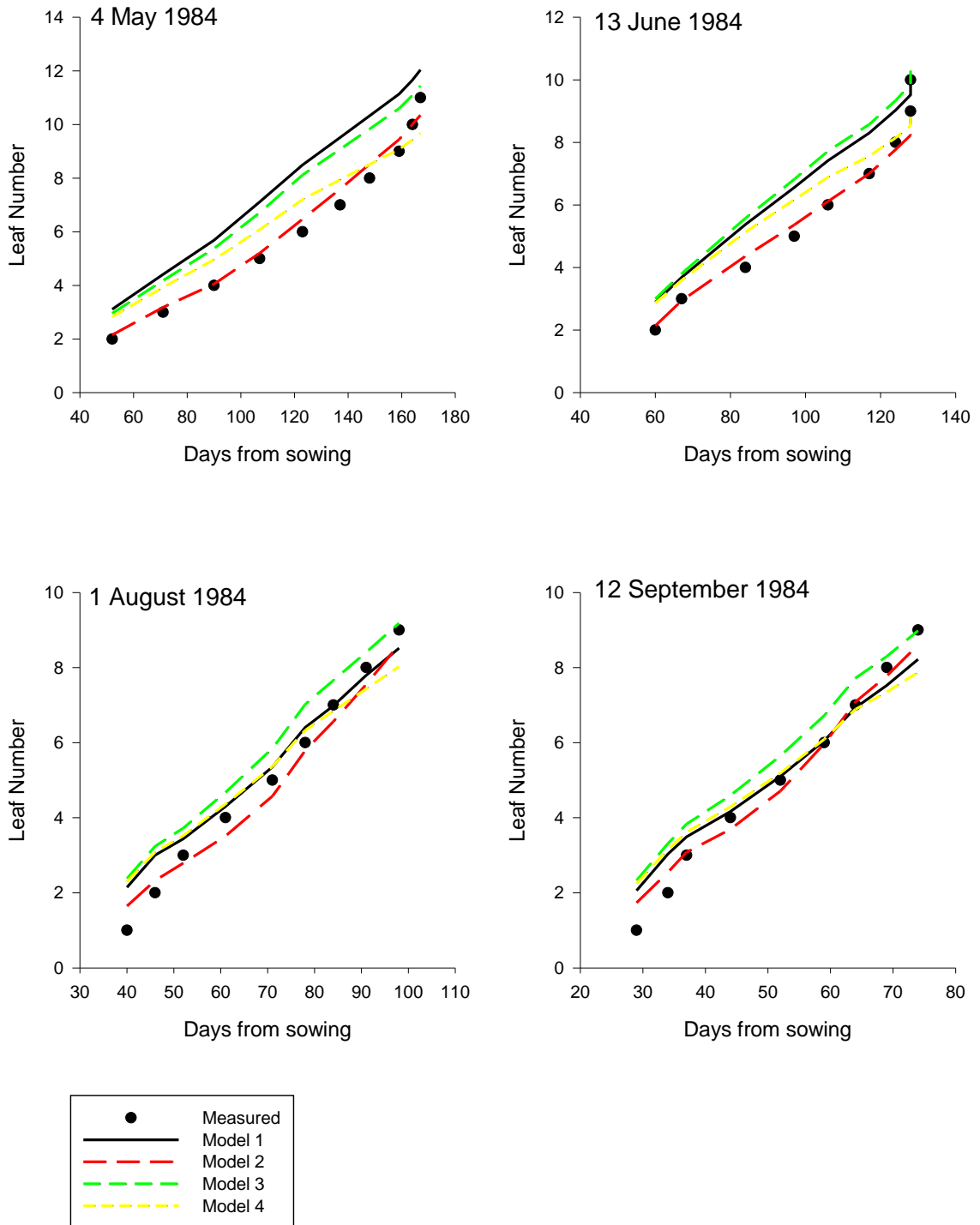


**Figure 15: Comparison of leaf appearance predictions by the four models with observations for 4 sowing dates. Figures recomputed based on un-replicated data.**

**Table 7: RMSE deviations of predicted from observed leaf number at each observation date for calculations based on the four models.**

Sowdate	Model 1	Model 2	Model 3	Model 4
4-May-84	1.92	0.40	1.53	0.91
13-Jun-84	1.09	0.52	1.32	0.85
1-Aug-84	0.59	0.42	0.87	0.73
12-Sep-84	0.61	0.37	0.82	0.75

The influence of bias in the overall RMSE, compared to variation around the mean of each model (compare Table 7 with Table 8) was not the same. Models 1 and 3 had particular problems with bias error. This can be seen more clearly in Figure 16.

**Table 8: RMSE about the mean bias error for each model**

Sowdate	Model 1	Model 2	Model 3	Model 4
4-May-84	1.12	0.74	0.77	0.87
13-Jun-84	1.10	0.52	1.33	0.86
1-Aug-84	0.88	1.29	0.44	1.06
12-Sep-84	0.60	0.49	0.55	0.74

The variation of the difference between observed and predicted leaf appearance was different for each model (Figure 16). The general pattern of prediction – early prediction of early leaves and late prediction of late leaves – appears to support other data in the literature which suggests a change in phyllochron with leaf number (Jamieson et al. 1995a) as implemented in SIRIUS. This is addressed in other papers.

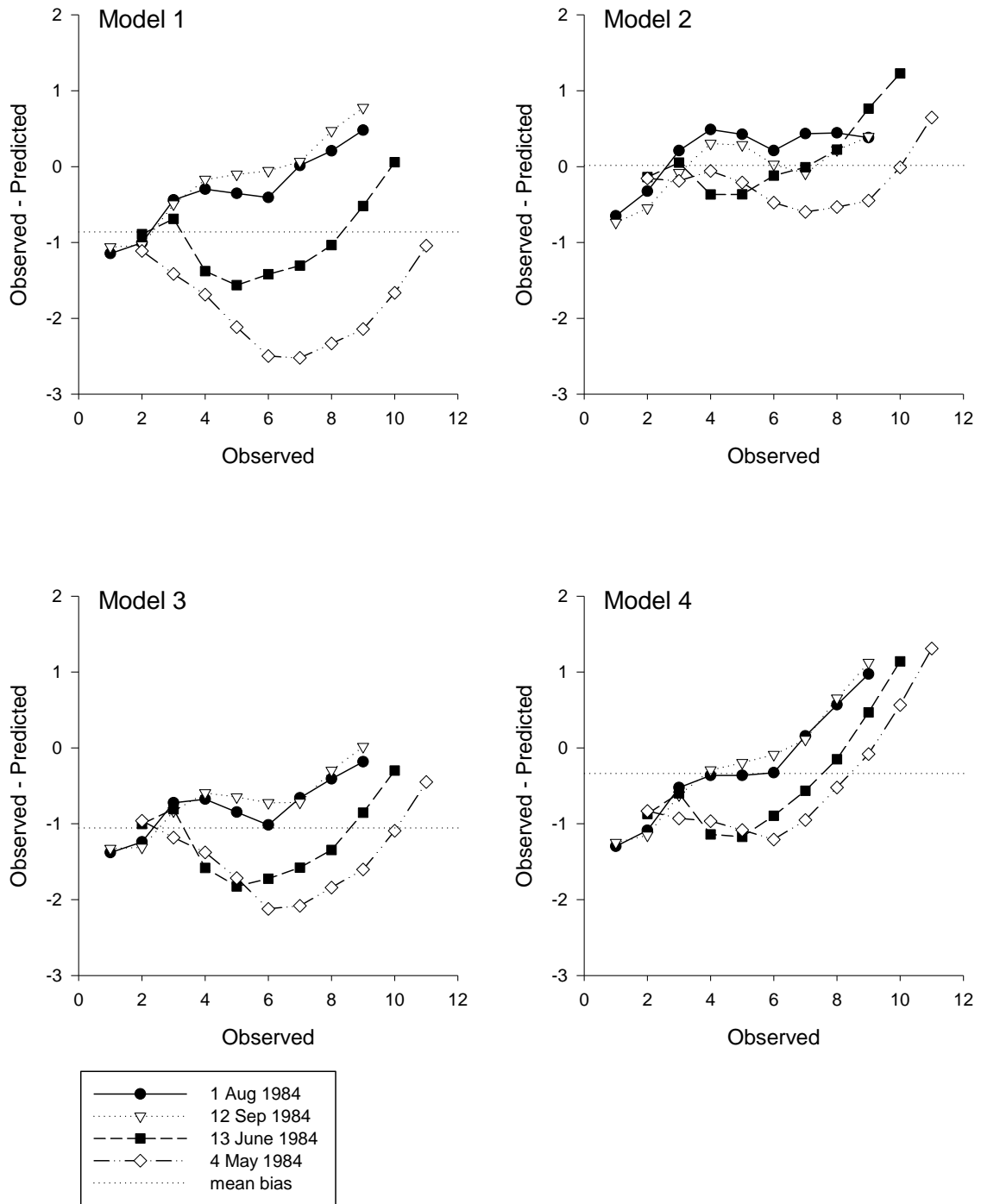


Figure 16: Deviations of predicted from observed leaf number for each observation of ligule appearance for 4 models at each sowing date. Mean bias indicated on each frame. Lines are used to join points for easier viewing.

### 6.3.4 Uncertainty Inference

The objective of the work of Jamieson, Brooking et al. (1995) was to provide a new, improved, and more parsimonious mechanism for phyllochron. However, even the seemingly most appropriate mechanism from a set of four (Model 2) showed an indication of bias that, whilst possibly corrected post-hoc, could be the result of an incorrectly specified mechanism (that phyllochron remains constant; in fact SIRIUS no longer assumes this). This possibility of an incorrectly specified developmental mechanism is an example of model structural uncertainty.

## 6.4 Remaining Papers

“Temperature Response of Vernalization in Wheat: Modelling the Effect on the Final Number of Mainstem Leaves” (Robertson et al. 1996). It was not possible to work with the historical data from this paper as it was stored on floppy disks and have unfortunately become corrupted with age.

“Making sense of wheat development: A critique of methodology”, (Jamieson et al. 1998b). This paper presents the 8 hypotheses of wheat development, focusing on the importance of Final Leaf Number, on which the SIRIUS sub-model is based. It is thus a description and comparison of this model to the old methodologies and models based on other hypotheses or the division of development into phenological phases between observable states of the apical meristem; it does not suggest new mechanisms which could propagate uncertainty through the model. As such re-assessment of historical data or simulation results from this paper is not useful.

“Temperature and photoperiod response of vernalisation in near-isogenic lines of wheat” (Brooking and Jamieson 2002). The experimental work was not based on replicated data, indicating that re-assessment will not provide additional

information in terms of uncertainty estimates associated with the vernalisation parameters obtained.

## 6.5 Summary

Re-analysis of historical data enabled a re-enactment of the processes taken to build the crop model SIRIUS. This process helps identify and understand sources of uncertainty and assumptions made while building the model. The inclusion of data driven processes in models indicates that some level of uncertainty is sure to be present, whether due to bias, scaling/aggregation, or aleatory uncertainty. However, the presence of such data can also help guide prior distributions when fitting models to quantify uncertainty. This will be described and discussed in more detail in Section III. The next Chapter explores identification of sources of structural uncertainty introduced by misspecification of a biological process.





# Chapter Seven: A Model as a Live Framework for Research

## 7.1 Executive Summary

Besides being tools for research into novel situations, crop models act as constructs upon which researchers continue to develop mechanistic understanding of real world systems. An important aspect of UE is therefore to identify biological processes that are not accurately represented in the model. One biological process that was identified as not being experimentally confirmed during model building of SIRIUS is the development of the wheat plant prior to emergence and exposure to daylight. This Chapter therefore describes experimental work exploring the effect of sowing depth on minimum leaf number in spring wheat cultivars. It illustrates the effectiveness of a crop model as a live framework for research and development. Results indicate that the developmental process implemented in SIRIUS prior to emergence is in fact erroneous, and suggest a more complex alternate hypothesis based on molecular interactions between vernalisation genes *Vrn1*, 2 and 3 is likely.

## 7.2 Introduction

The final number of leaves (FLN) attained by a wheat plant is an important property that determines the timing of anthesis (Hay and Porter 2006). This can influence timing of when the plant become reproductive, and hence have a major impact on yield. For example, in Australia, delays in sowing (and hence in timing of anthesis in inductive photoperiods) can represent substantial yield losses of between 7 and 17% per week (Rebetzke et al. 2007) and in Japan around 20% per week (Tanio and Kato 2007).

Current phenological models describing progress toward anthesis focus on mechanisms that occur during the vegetative stage between emergence and flag leaf (FL) appearance. Developmental progress in the period between imbibition and emergence is modelled as a constant relationship between organ (primordia) numbers and accumulated thermal time ( $TT$ ) (Brooking et al. 1995). This Chapter aims to determine the extent of uncertainty that is introduced to the modelling of FLN by assuming this constant developmental progress prior to emergence.

### 7.2.1 Recap of Key Principles of Wheat Development Between Emergence and Anthesis Under Phenological Model SIRIUS

The process based, phenological development mechanisms incorporated into the wheat model SIRIUS (Jamieson et al. 1998b) provide a link between vegetative development (leaf appearance) and the switch to reproductive development. Key phases of development in a wheat plant include a) imbibition, when the grain perceives moisture, begins to develop primordia and the apex extends, b) emergence, when the plant first perceives light, c) vernalisation saturation, when winter varieties are able to respond to photoperiod, d) floral initiation, or reproductive commitment, when the plant switches from vegetative to reproductive development, and e) terminal spikelet, the final organ to be initiated prior to the biomass sequestration phase.

The development of primordia in thermal time ( $TT$ ) as conceptualised in SIRIUS for spring wheat varieties is shown in Figure 17<sup>1</sup>. Spring wheat varieties are traditionally defined as those that do not require a period of cold temperatures of

---

<sup>1</sup> The scale on the x-axis between -1 and 0 represents the period after imbibition but prior to apex emergence when additional primordia have begun to develop but the apex has not yet begun to extend the first leaf.

around 0-10°C (vernalisation) to flower. After emergence, the plastochron (time taken for a primordium to develop) is closely linked to the phyllochron (time taken for a leaf to develop) and the general rule of thumb is that there are two plastochrons to one phyllochron. Therefore, since the phyllochron up until the 2<sup>nd</sup> Haun stage (Haun 1973) is approximately 120 degree days, the plastochron prior to emergence and during the first two Haun stages should be approximately 60 degree days. At emergence, most spring wheat cultivars require around 1-2 Haun Stages (~240 accumulated degree days) before they become able to respond to photoperiod (Brooking et al. 1995). If the photoperiod (*PP*) at this stage is saturating (approximately 16 hours), then the conditions are said to be fully inductive and the plant sets FLN at the number of primordia developed at that time (usually 6-8). At the same time, the plant commits to becoming reproductive (Brooking and Jamieson 2002).

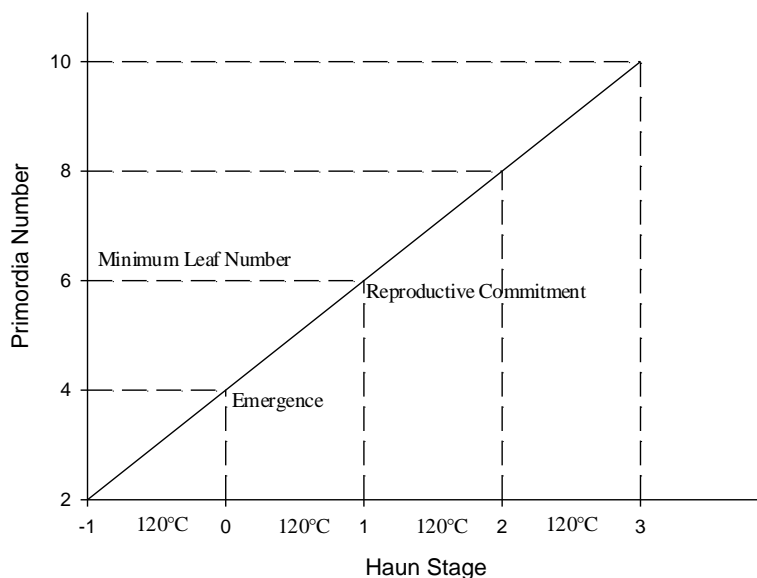


**Figure 17: Sequence of development of primordia in *TT* and their relationship to Haun stage.**

### 7.2.2 Wheat Development Prior to Emergence

In SIRIUS, developmental progress in the period between imbibition and emergence is modelled as a direct, constant relationship between primordia numbers and accumulated  $TT$  (Brooking et al. 1995). The number of primordia at emergence (PAE) is fixed at a constant value of four (Figure 17). It is made up of two primordia which are present on the main-stem in the seed, and a further two primordia that are initiated between germination and emergence, assuming one phyllochron from imbibition to emergence. This is appropriate for a sowing depth of approximately 5 cm (Kirby et al. 1987; Kirby 1993; Hay and Porter 2006). Since the SIRIUS mechanism requires that primordia number (PN) increase in time, it can be hypothesised that deeper sowings will give later emergence, implying that more primordia would be accumulated at the time of emergence, with an accompanying increase in PAE. PN will then increase at  $2 \cdot LN$  from emergence until commitment. Assuming long days, the plant will set its FLN based on PN at at  $\sim 240$  degree days after emergence (as seen in Figure 17), and this number will be greater if the plant was sown deeper and took longer to emerge. Thus deeper sowing would cause a higher FLN.

In order to determine the extent of uncertainty that is introduced by assuming PAE is constant, the effect of sowing depth on a) FLN, b) the number of primordia present at emergence, and c) timing of emergence will be explored.

### 7.3 Benefits of Deeper Sowing

The literature in the area of phenological responses to environmental conditions and managerial decisions in the phase between imbibition and emergence indicates that there is some developmental (including FLN) and yield impact with increasing sowing depth, particularly at depths greater than 10 cm (Photiades and Hadjichristodoulou 1984; Kirby 1993). However it is not clear

how the timing of exposure to environmental drivers, photoperiod (*PP*) in particular, affects FLN in spring wheat varieties.

The possibility of increasing sowing depth may be of interest particularly under environmental conditions (e.g. especially dry or hot) where a deeper sowing depth may increase access to moisture and cooler conditions (Photiades and Hadjichristodoulou 1984; Mahdi et al. 1998; Rebetzke et al. 2007). For example, Mahdi et al. (1998) found that the establishment of plants sown at 3, 9, and 12 cm was poorer than those sown at 6 cm. However, the success rate of implementing deep sowing management approaches has had mixed results; whilst there is evidence that genotypic increases in coleoptile length improves establishment and yield parameters (Liang and Richards 1994; Rebetzke et al. 2007), other studies have found with some cultivars that increasing depth leads to less successful establishment and viability, leading to reduced yield (Jong and Best 1979; Photiades and Hadjichristodoulou 1984; Kirby 1993; Cussans et al. 1996; Mahdi et al. 1998). These results indicate that if sowing depth is to be explored, careful selection for cultivars genetically capable of emerging from greater depths is required.

## 7.4 Experiments

The following hypotheses were tested in a set of three glasshouse based trials:

1. Does sowing depth affect FLN in spring wheat varieties?

If yes, then it is necessary to confirm development is progressing as expected:

2. Does later light perception lead to greater numbers of primordia?

Finally:

3. Given expected development in response to *TT* prior to *PP* perception (emergence) occurs, does extended development time prior to *PP* perception increase or decrease FLN?

## 7.5 Materials and Methods

### 7.5.1 Pilot: Genetic Ability to Emerge From Deep Sowing in Six Spring Wheat Varieties.

First a selection of suitable cultivars and sowing depth for each trial was identified in a pilot study. The pilot trial investigated three depths (5.0, 10.0, 15.0 cm) with only 1 replicate pot sown with 15 grains for each cultivar. The six cultivars were 'Otane', 'Kohika', 'Torlesse', 'Spring Batten', 'Morph', and 'Monad'. Glasshouse lighting was set to a photoperiod of 16 hours, so that all seedlings emerged into fully inductive conditions. The mean temperature in this glasshouse was 22°C for all trials. The results recorded from this trial were simply the number of seedlings that emerged in each pot.

### 7.5.2 Trial one: Does sowing Depth Affect FLN in Spring Wheat Varieties?

The fully replicated trial was set up in a 6 x 6 resolvable Latinised block design (Harshbarger and Davis 1952), in both directions, with 6 cultivar x 2 sow depth factorial treatment structure. The trial was carried out with 16 hour *PP* with lights when necessary to extend the natural daylength. This trial was established in January 2011. Each pair of blocks of six units in both directions comprised a full set of the 12 treatments. Cultivars were limited to spring wheat varieties. The six cultivars were 'Otane', 'Kohika', 'Torlesse', 'Batten', 'Monad', and 'Morph'. The two sow depths were 5.0 and 0.5 cm since a pilot trial showed most cultivars

(excepting Batten Spring) were unable to emerge at 10cm or deeper. Fifteen grains were sown in each pot.

Glasshouse lighting was set to a photoperiod of 16 hours, so that all seedlings emerged into fully inductive conditions. Temperature is not reported as it affects rate of development (Slafer and Rawson 1995), but not the FLN. For this reason, variation in temperature conditions for seedlings emerging later or with higher minimum leaf numbers according to cultivar specific characteristics should not directly affect the FLN. FLN was counted when fully visible on 22 April for all cultivars excepting Morph, which did not complete the vegetative phase until 1.5 weeks after the other cultivars. This cultivar was excluded from further analysis.

### 7.5.3 Trial two: Does Later Light Perception Halt Primordia Development?

Trial two focussed on whether it was possible to differentiate the number of primordia present in the apex at the expected time at which it became able to perceive light. This aims to confirm the current understanding represented in SIRIUS that development in response to *TT* begins immediately after imbibition has occurred, prior to emergence. Two treatments widely separated in expected time of light perception were established with seeds from one treatment sown at 10cm depth and seeds from the other treatment germinated on a Petri dish under full light. Each pot was established with 20 grains (to allow for an expected emergence rate of 60%), and the Petri dish with 8 grains. The trial was established in July 2013 in an incubator under continuous light on constant 22 degree temperature. The lights provided both warm and cool lights to ensure all wavelengths were available. To confirm that light was not perceived earlier through the incomplete blocking effect of soil, a third treatment was established at a later date but in the same incubator where the deep sown treatment was



germinated in soil at a depth of 10 cm and grown to 1-2 cm emerged coleoptile in a light tight box. The time required for this treatment to reach the appropriate stage was established prior to establishment of experimental units. Replicate pots were established at consecutive time intervals on Mondays and Thursdays to ensure sufficient time was available for dissection. A single spring wheat cultivar, Spring Batten, was selected for this study as it was shown in the pilot study that this cultivar had a consistent rate of 20% successful emergence from a 10cm sowing depth. Further, this cultivar is known to have a low amount of Vrn2 expression (pers. comm. Hamish Brown). As soon as 1 - 2 cm of coleoptile was visible, it was dissected and the number of primordia counted following (Kirby and Appleyard 1981) using a Leica NZ12 stereo microscope.

#### 7.5.4 Trial three: Does Number of Primordia Present at the Time of First Light Perception Affect FLN?

Trial three aimed to relate the results from trial two in terms of primordia number at emergence to FLN (and hence anthesis). Thus, the same three treatments, widely separated in expected time of light perception and allowing for fully and partially dark conditions for seeds sown at 10cm depth were established with seeds from two treatments sown at 10cm depth either under full light or full dark conditions, and seeds from the other treatment germinated on a Petri dish under full light. Each pot was established with 20 grains, and the Petri dish with 8 grains. The trial was established in September 2013 in the incubator under constant 22 degree temperature. The size of the incubator meant that each replicate was established one after another, and when germinated/emerged with visible coleoptile length of 1-2 cm the pots containing the deep sown seeds were moved straight to the glasshouse and the seedlings germinated on the Petri dish were carefully planted just below the surface and then moved to the same glasshouse conditions as in previous trials. The dark treatment was then

established for rep 1, and transferred at the appropriate time, and so on for each replicate. The pots in the glasshouse were laid out in a 2x6 row-column design. FLN was counted when fully visible.

### 7.5.5 Statistical Analysis

Average counts from each pot from trial one were analysed by a hierarchical generalised linear model (Lee et al. 2006). The fixed effects were modelled as having a Poisson distribution with a log link. The Latinised row column structure of the resolvable block design was modelled as random effects with a Gamma distribution and a log link. Diagnostic tests and predicted values were obtained.

The hierarchical structure of trial three in terms of glasshouse row and column layout was explored and fitted with a Generalised Linear Mixed Model (Schall 1991). There was no evidence of a significant amount of spatial variability so the final model was a simple Generalized Linear Model assuming the Poisson distribution and using a log link. The dispersion parameter was 0.017. The difference between dark and light deep sown FLNs once the Petri dish was accounted for was assessed through partitioning the sums of squares to obtain orthogonal contrasts. The data modelled was the average FLN count for each pot.

## 7.6 Results

### 7.6.1 Pilot Trial

Most grains germinated, regardless of cultivar or sowing depth. Grains sown at 5.0 cm successfully reached the surface, however most grains sown at 10.0 and 15.0 cm failed to reach the surface. Spring Batten was the exception, exhibiting 60% successful emergence at 10 cm, but only a few plants overall emerged from

15cm. The lack of emergence of grains at sowing depths greater than 5.0 cm limited the sowing depth treatments in trial one to depths of 5.0 cm or less.

### 7.6.2 Trial One

The emergence time was fairly consistent across cultivars. Grains sown at 0.5 cm emerged around 45 °C days earlier than those sown at 5.0 cm. F-statistics were calculated by dropping fixed terms. These values indicated that there was strong evidence of a difference between cultivars ( $p < 0.001$ ); with Monad having the highest and Otane the lowest number of leaves. There was some evidence of a difference in minimum leaf number between sowing depths (around 0.25% of the FLN) ( $p = 0.063$ ), with four out of five cultivars having lower FLNs from the deeper sowing treatment. There was no evidence that this effect, if important, was different across the six cultivars ( $p = 0.688$ ). Back-transformed predicted values with back-transformed 95% confidence intervals are provided in Figure 18. Wheat plants past the flag leaf stage immediately prior to count FLN are shown in Figure 19.

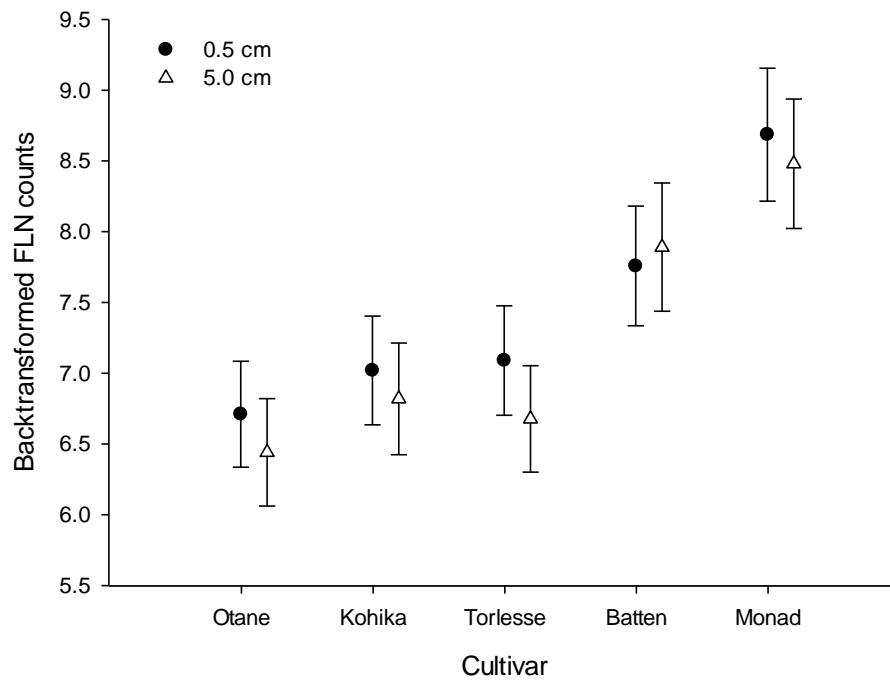


**Figure 18: Effect of Cultivar and Sow depth on back-transformed FLN counts.**  
**Bars represent back-transformed 95% confidence intervals.**



**Figure 19: Wheat plants in Trial One at the flag leaf stage.**

### 7.6.3 Trial Two

For primordia counts of germinated/emerged plants with a coleoptile measuring 0.7 – 2 cm, there were 4 primordia per plant for Petri dish germinated plants, and 5 per plant for 10cm deep sown plants, for both light and dark incubated treatments. There was no variability in organ counts within treatments at this stage of development. Assuming a soil temperature equal to the air temperature in the incubator of 22°C then the emergence time of ~3 days for Petri treatments would equate to  $TT$  of 66°Cd (degree days) and ~8-9 days for deep sown would be upto 198°Cd.

#### 7.6.4 Trial Three

There is strong evidence that the mean of the deep sown (both light 8.04 (7.70 - 8.42)<sup>2</sup> and dark 8.23 (7.90 - 8.66)) is significantly less ( $p=0.006$ ) than the Petri incubated 9.0 (8.60 - 9.43), and that once this difference is accounted for there is no evidence of a difference between dark and light incubated at 10cm sowing ( $p=0.412$ ). There was a difference of up to 132 °Cd in emergence (~2cm coleoptiles showing) time between Petri and deep sown treatments.

### 7.7 Discussion

Trial one indicated some evidence that increased sowing depth delayed emergence but also indicated that it led to a lower FLN across several spring wheat cultivars. However, the difference is slight, possibly due to the scale of the depth differential (only 3 days difference in emergence time which (assuming a mean temperature of 15 °C) is 45 °Cd later). The results of trial two indicated that, as expected, the number of primordia present at emergence was greater for the deep sown plants. However, the difference was not as great as was expected. However, trial three indicated that early exposure to light can lead to an increase in the FLN, and deeper sown plants committed to a lower number of leaves, even though the number of primordia at emergence was greater. These findings were the reverse to those hypothesised. Two mechanisms that may jointly explain the results are proposed.

---

<sup>2</sup>Backtransformed mean (95% confidence interval)

### 7.7.1 Differential Plastochron when *PP* Perception Delayed

In trial two, the results showed a *TT* of 66°Cd for the Petri dish treatment, and up to 198°Cd for the deep sown treatment. If the number of primordia in the seed at planting is 2-3 (shown as 2.0 in Figure 17 for mathematical convenience, but assumed to be 3 here), then the plastochron of 66°Cd for the first new primordia to develop seems reasonable. However, this then implies for the deep-sown treatment that the plastochron for the second new primordia to develop was ca 132°Cd. It seems likely that the linear development of primordia in response to *TT* prior to emergence as shown in Figure 17 is not accurate. This relationship is implicit in SIRIUS but is in fact an assumption based on work done by Brooking et al. (1995) (who investigated the relationship between primordia and leaf numbers *after* emergence). An alternative mechanism may be that at some point during primordia development, if the coleoptile has not yet emerged, the development of primordia slows and energy is focussed on getting the coleoptile to the surface. However, whilst this mechanism would explain the differential plastochron, it does not provide justification for the lower FLN observed in deep sown plants, as these do still have more primordia at emergence (although not as many more as might be expected if the plastochron were constant).

### 7.7.2 Differential *PP* Perception Response for Vernalisation Genes Vrn1, Vrn2, and Vrn3

A model recently put forward by Brown et al. (2013) may provide the insight required to explain these results. On a phenological basis, these authors predict FLN from the Haun stage at the time of terminal spikelet rather than PN at terminal spikelet.

Further, the results tally with molecular mechanisms as described by authors such as Trevaskis et al. (2007a) and Li et al. (2011). Brown et al. (2013) provided a molecular basis for phenological behaviours observed in near isogenic lines of wheat based on data described by Brooking and Jamieson (2002), and their model is also able to explain these results.

Spring wheat varieties are those that do not require vernalisation to flower. The mechanisms discussed and proposed in this Section are photoperiod responses for spring wheat varieties that are expected to occur regardless of exposure to vernalising temperatures. Our results support this, with trials two and three showing wide differentiation in results for plants incubated at 22 °C.

Vrn1, Vrn2 and Vrn3 are the key genes that control the time to anthesis for spring wheat varieties. Genetic variation and environmental signals control the rate at which these genes express proteins. The mechanisms describing how these genes interact are well described in the literature. Vrn1 is expressed in low concentrations in young plants and its transcription increases over time. In spring wheat, this occurs at the maximal rate regardless of temperature (Figure 20). The main function of the up regulation of Vrn1 in leaves in spring is to down regulate Vrn2 (Trevaskis et al. 2007a; Sasani et al. 2009; Diaz et al. 2012). The main role of Vrn2 is to repress the induction of Vrn3 in autumn, to prevent the induction of flowering before winter. Vrn2 is up regulated by long *PP* (Karsai et al. 2005; Dubcovsky et al. 2006; Trevaskis et al. 2007a; Sasani et al. 2009; Li et al. 2011; Kippes et al. 2014). Before vernalisation, Vrn3 transcript levels are maintained at low levels by Vrn2. During development, the up regulation of Vrn1 in the leaves results in the down regulation of Vrn2 and the release of Vrn3, which can further up regulate Vrn1 which ultimately results in the induction of flowering (Dubcovsky et al. 2006; Faure et al. 2007; Tanio and Kato 2007; Trevaskis et al.



2007b; Distelfeld et al. 2009b; Sasani et al. 2009; Guo et al. 2010; Kitagawa et al. 2012; Shaw et al. 2012).

Brown et al. (2013) combined phenological development model principles with the molecular responses described in the literature to represent the transferral from vegetative to reproductive development. Figure 20 provides a graphical representation of how molecular mechanisms relate to phenology in their integrated framework. Here, terminal spikelet does not occur until Vrn3 has been expressed at sufficiently high levels. Vrn2 is triggered at emergence by exposure to light, suppressing Vrn3 until Vrn1 has built up enough to suppress Vrn2, allowing Vrn3 to express and ultimately allow the plant to initiate terminal spikelet. Note also that as Vrn2 accumulates, the 'vernalisation target' also increases, increasing the final leaf number the plant achieves (even in spring varieties). The figure proposed by the Brown, Jamieson et al. (2013) has been modified in that Vrn1 expresses at its maximal rate from the time of imbibition, and Vrn4 is excluded as it is not relevant to spring wheat (Figure 20).

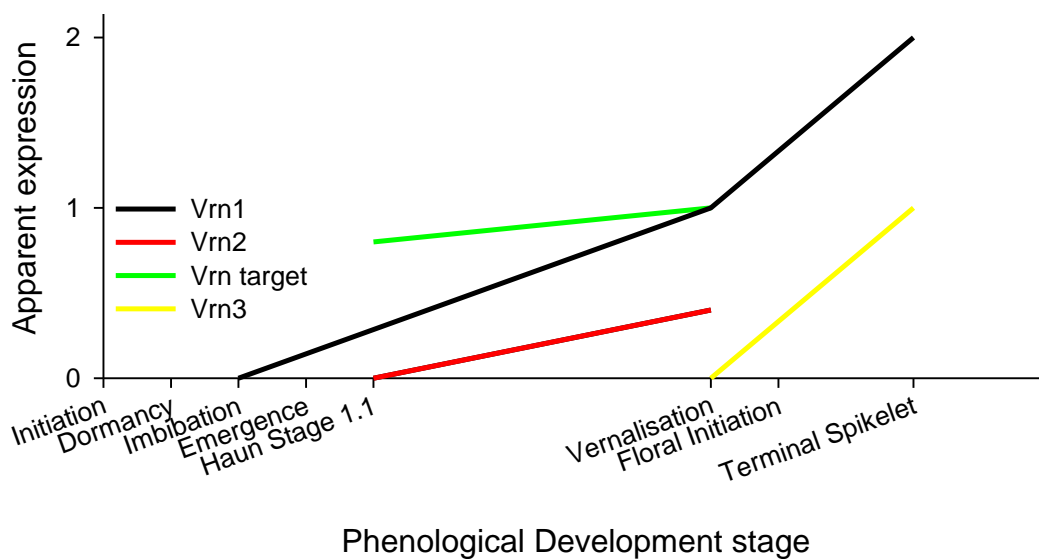


**Figure 20: Suggested interactions of Vrn1, Vrn2, and Vrn3 at different phases of phenological development modified from those proposed by Brown, Jamieson et al. (2013) for spring wheat.**

As shown in Figure 20, it is hypothesised that Vrn1 begins to express in low concentrations from the time of imbibition. As such, a later emerging crop will have already expressed more Vrn1 at the time of emergence, so will not only suppress Vrn2 earlier, but will also prevent Vrn2 from increasing the vernalisation target. This expected differential relative expression of Vrn1, Vrn2 and Vrn3 based on the time at which *PP* is perceived is shown for trial three late emergence (deep sown) and early emergence (Petri dish) imbibition treatments (Figure 21).

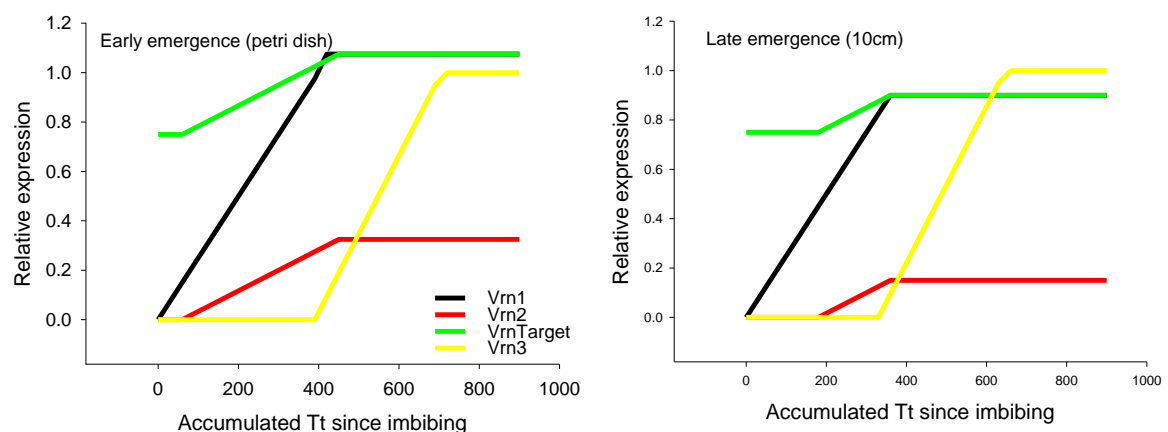


**Figure 21: Suggested differential relative expression of Vrn1, Vrn2, and Vrn3, including vernalisation target for early (Petri dish) and late (deep sown) *PP* perception after imbibition.**

## 7.8 Summary

The original hypothesis for this experimental work suggested constant development in response to *TT* for wheat plants during the phase between

imbibition and emergence. However, results did not support this hypothesis. Rather, results tallied with the molecular-phenological framework proposed by Brown, Jamieson et al. (2013). This model allowed differential *PP* perception response for vernalisation genes *Vrn1*, *Vrn2*, and *Vrn3*, explaining how later emerging plants with greater primordia numbers at emergence were able set a lower final leaf number than the earlier emerging plants. It also allowed for differences in plastochron when *PP* perception was delayed. It is not known whether these mechanisms interact. This Chapter highlighted the nature of crop models as constructs upon which researchers continue to develop mechanistic understanding of real-world systems. Better ability to account for this source of uncertainty has both research/development and practical implications.

Section II has illustrated how the scientific understanding encapsulated in a model must be properly described (Chapter Five) before potential sources of uncertainty (Chapters Six and Seven) can be identified. The next Section continues to work with SIRIUS first to illustrate the UE framework proposed in Section I, and then to implement approaches to quantify uncertainty, including the Bayesian approach first introduced in Chapter Two.

## Section III – Performance Statistics

In this final section, material provided in Sections I and II are combined to illustrate the UE framework for the case study model SIRIUS in Chapter Eight. Here, a traditional sensitivity analysis for spring and winter varieties of wheat is carried out and conclusions are compared and contrasted with those found by a recent paper by He et al. (2012). In Chapter Nine, a Bayesian hierarchical model fitted in a state-space framework is implemented to take advantage of data that updates through time. This approach allows quantification of input parameter, expert opinion, and observed data in a unified setting. It provides filtered estimates of a Poisson state variable (Leaf Number). These estimates are presented with the usual performance statistics that are available when fitting a Bayesian hierarchical model. Probabilistic sensitivity analysis of input parameters is carried out within this framework. In Chapter Ten, the flexibility of the framework is showcased in two ways. First, it is extended to estimate uncertainty for a latent dynamic state variable. Second, a probabilistic sensitivity analysis of structural uncertainty (state equations) is carried out. This last analysis reflects recent uncertainty research directions (Strong et al. 2012). *Quantification of uncertainty, and how it aids both biological and model understanding is the focus of this Section.*



# Chapter Eight: UE Framework and Sensitivity Analysis

## 8.1 Executive Summary

This Chapter shows the setting of SIRIUS in the UE framework proposed in Chapter Three. A sensitivity analysis for the spring wheat model is carried out, and results are compared and contrasted with those found by He et al. (2012).

## 8.2 Application of the UE Framework

Refer to Figure 3 in Chapter Three describing the seven steps in an UE, and apply them to our case study model SIRIUS.

### 8.2.1 Summary: Model Building, Verification and Validation

Model building, verification, and validation has been described for the published model SIRIUS. The model is reduced to include the developmental model for spring wheat only.

### 8.2.2 Identify Model Components

As described in full in Chapter 5, the model's state equations ME are used to predict the (observable) state variable leaf number ( $ln_t$ ) on day  $t$  based on calculations that simulate the rate of leaf development ( $phyllochron_t$ ), number of organs ( $primordia_t$ ), and the possible final number of leaves given daylength and developmental progress ( $flnt_t$ ,  $fln_t$ ).  $t = 1$  is the day the grain is sown and imbibes moisture, as this is assumed to be the stage at which its apical meristem germinates and becomes sensitive to temperature. SIRIUS simulates the plant's development based on mean daily environmental information. The simulations depend on input parameters  $\theta$  that describe cultivar specific characteristics and

responses to environmental signals, and observable environmental information  $E_t$  where  $TT$  = mean daily thermal time and  $PP$  = daily photoperiod. Each state variable excepting  $ln_t$ , is treated as an unobservable latent variable throughout the day-to-day simulation of the wheat plant development. At the completion of the vegetative development phase, the state variable  $fn_t$  is observable once the onset of spikelets is seen.

The state variables, input parameters with their prior distributions, and observed variables provide all the necessary components to begin state-space modelling. They are presented in matrix form in Table 9 (first introduced for the UE as Table 1). Recall the use of italics for all parameters and variables, the use of lower case for state variables and input parameters, and the use of upper case for observed variables. Calibration variables are upper case, but not italicised.

**Table 9: Step Two of Uncertainty Evaluation: Identify model components for the SIRIUS wheat computer simulation model.**

Input Parameter	Observation Variable		Structural Uncertainty		State Variable
	Calibration Variable	Environmental Variable	Model Form	State Equation	
$r = f(ME, \theta, E_v, C_v, \varepsilon)$	$r = f(ME, \theta, E_v, C_v, \varepsilon)$	$r = f(ME, \theta, E_v, C_v, \varepsilon)$	$r = f(ME, \theta, E_v, C_v, \varepsilon)$	$r = f(ME, \theta, E_v, C_v, \varepsilon)$	$Z_t$ - NA
<i>ps</i>	$LN_t$	$PP_t$	<i>the way in which model components interact at each time step</i>	$phyllochron_t$	<b><i>phyllochron_t</i></b>
<i>ppsats</i>		$TT_t$		$primordia_t$	<b><i>primordia_t</i></b>
<i>lmin</i>				$flnt_t$	<b><i>flnt_t</i></b>
<i>pn</i>				$fln_t$	<b><i>fln_t</i></b>
<i>pe</i>				$ln_t$	<b><i>ln_t</i></b>
<i>bp</i>					



**Table 10: Step Three of Uncertainty Evaluation: Curate available information about components of the SIRIUS wheat computer simulation model.**

Context	Notation	Data	Expert opinion	Other
Structural uncertainty	$r = f(\mathbf{ME}, \theta, \mathbf{E}_v, \mathbf{C}_v, \varepsilon)$		The developmental phase between imbibation and emergence may not be correctly specified.	Simulated Data for wheat grown in Southland consistently underestimates time of anthesis
Model Inputs	$r = f(\mathbf{ME}, \theta, \mathbf{Et}, \mathbf{Ct}, \varepsilon)$		Data from the literature (Jamieson et al. 2008) the rate of wheat development ( $bp$ ) is widely variable between cultivars. Expert opinion on range values for several cultivars: $bp$ 90-110; $lmin$ 5-9; $ps$ 0.01-0.7	unknown
Scaling, aggregation, sampling or aleatory sources of uncertainty	$r = f(\mathbf{ME}, \theta, \mathbf{Et}, \mathbf{Ct}, \varepsilon)$	Measured day of flag in southland crops for one cultivar. Measured observations of LN at weekly intervals for controlled climate conditions. Measured weather station data in Lincoln, Canterbury, New Zealand from 1960 - present	unknown	unknown

### 8.2.3 Curate Available Information

By filling in Table 3 from Chapter Three, we can summarise whatever data, expert knowledge, and other information is available for each of the computer simulation model components  $f$ ,  $ME$ ,  $\theta$ ,  $E_t$ , and  $C_t$  (Table 10).

### 8.2.4 Identify Principal Sources of Uncertainty

Sources of uncertainty can be identified given the information summarised in Tables 9 and 10. These include model structural error, incorrectly specified input parameters, bias in environmental data, and inherent stochasticity. For example, input parameters are not known exactly for any wheat cultivars, and they are not known at all for many wheat cultivars. Neither environmental nor wheat developmental data are observed perfectly. Finally, there is stochastic uncertainty in the real world system. This model does not take too long to run, however, so code uncertainty need not be of concern.

### 8.2.5 State Objectives of the UE

The objectives of the UE, based upon the structure of the computer simulation model and the available information summarised in the previous four sections could include one or more of the following:

- Explore structural uncertainty  $r = f(ME, \theta, E_t, C_t, \varepsilon)$ : Assess the size and direction of bias of model simulated values for  $fln_t$  for a new location, potentially to guide new research/calibration efforts.
- Explore input parameter uncertainty  $r = f(ME, \theta, E_t, C_t, \varepsilon)$ : Carry out a sensitivity analysis to assess whether the model is also (as the literature suggests the real world is) sensitive to changes in  $bp$ , or carry out a sensitivity analysis to assess whether the model is not (as personal

communications suggests the real world is not affected by) sensitive to changes in  $pe$ . This is carried out in the remainder of this Chapter.

- Explore environmental input data uncertainty  $r = f(\mathbf{ME}, \theta, \mathbf{E}_t, \mathbf{C}_t, \varepsilon)$ : Carry out a sensitivity analysis to assess the impact (in number of days of error in day of flag leaf estimation) of spatial bias in thermal time ( $TT$ ) input data.
- Explore calibration data uncertainty  $r = f(\mathbf{ME}, \theta, \mathbf{E}_t, \mathbf{C}_t, \varepsilon)$ : Fit a data assimilation model to explore not only whether the model ends up with accurate estimates of Flag leaf day, but also whether it correctly simulates the development of each leaf through time. This is done in Chapter Nine.

### 8.2.6 Sampling and Analysis of Simulation Data

The input parameter uncertainty will be explored in this chapter, and calibration data, input parameter, and structural uncertainty jointly in Chapters Nine and Ten.

## 8.3 Sensitivity Analysis of the Input Parameters

### 8.3.1 Steps for Analysis

There are four main steps required in performing a sensitivity analysis (Saltelli et al. 2000):

1. Assign pdf or range of variation for each input factor,
2. Generate an input vector/matrix through an appropriate design,
3. Evaluate (run) the model, for the input combinations included in the design thus creating an output distribution for the response of interest,
4. Analyse the influences or relative importance of each input factor on the output variables.

Step 1 requires expert elicitation as discussed in Chapter Two. Design concepts for Step 2 have been described in Chapter Four. Analysis (Step 4) was also discussed in Chapter Four. In this study will calculate the sensitivity ( $S_i$ ) and total sensitivity ( $T_i$ ) as follows: The sums of squares for each main factor in relation to total sums of squares from the ANOVA decompositions gave the first order sensitivity index ( $S_i$ ) for main factor effects; and the total sensitivity index ( $T_i$ ) was calculated by adding the interaction component to each main factor. In this analysis the indices are not normalised by the total sums of squares, and presented as percentages. The greater the value of  $T_i$ , the higher is the sensitivity of the output variable to a factor, including main effects and interactions. The larger the difference between  $T_i$  and  $S_i$ , the greater is the influence of interactions.

### 8.3.2 Case studies: Spring Varieties of Wheat

This analysis is implemented in GenStat v. 14. The techniques used for this sensitivity analysis will include EDA, ANOVA decomposition, tabulation of  $S_i$  and  $T_i$ , histograms, and box and whisker plots. Inputs that will be experimented on are 'varietal parameters'. These are cultivar specific responses or characteristics. A total of three varietal parameters are explored (Table 11):  $lmin$ ,  $bp$ , and  $ps$ .

### 8.3.3 Experimental Design

The design will be a complete factorial design over a selected range of years and sowing date combinations. The number of levels will vary based on the total number of 'treatments' for each case. Non-linearity in responses may be explored via experimental data and model outputs. Note that this does not allow for probabilistic information to be included. The factor levels of the design are shown in Table 12.

### 8.3.4 Expert Elicitation

Observed range values across several cultivars collected through experimentation are given in Table 11. This is a simple version of expert elicitation for a generic/default spring wheat variety which is expanded upon (including sources of information) in the next Chapter. This information is used to develop a plan for the computer simulation experiment. Daily weather information is available from 1960 until the present. This data is collected at NIWA's Broadfields Meteorological station in Canterbury, New Zealand. Latitude = -43.626, longitude = 172.47. Day is the date of sowing and is represented as Julian Day.

**Table 11: Range of varietal parameters in SIRIUS crop model.**

Varietal Term	Min	Max
<i>lmin</i>	5	9
<i>bp</i>	90	110
<i>ps</i>	0.01	0.7

### 8.3.5 Generate an input vector through an appropriate design

**Table 12: Input vector for theoretical spring varieties.**

Experimental Design theoretical spring variety				
Term	Levels			
	1	2	3	4
Year	1980	1990	2000	
Day	10	69	160	252
<i>lmin</i>	5	9		
<i>bp</i>	90	130		
<i>ps</i>	0.01	0.07		
Factorial	=3*4*2*2*2		96 observations	

### 8.3.6 Evaluate Model

The model outputs for input vectors given above for the spring wheat are given in Table 13.

**Table 13: Simulated fln counts for theoretical spring varieties.**

<i>lmin</i>	<i>base</i>	<i>ps</i>	1980	1980	1980	1980	1990	1990	1990	1990	2000	2000	2000	2000
			10	69	160	252	10	69	160	252	10	69	160	252
5	90	0.01	5.00	5.03	5.06	5.03	5.00	5.03	5.06	5.03	5.00	5.03	5.06	5.03
5	90	0.7	5.00	7.28	9.04	7.11	5.00	7.21	9.01	7.03	5.02	7.28	9.13	7.08
5	130	0.01	5.00	5.03	5.06	5.03	5.00	5.03	5.06	5.03	5.00	5.03	5.06	5.03
5	130	0.7	5.12	7.72	8.81	6.97	5.12	7.59	8.81	6.86	5.17	7.72	9.01	6.97
9	90	0.01	9.00	9.04	9.06	9.03	9.00	9.03	9.06	9.02	9.00	9.04	9.06	9.03
9	90	0.7	9.29	11.89	12.45	10.65	9.26	11.72	12.53	10.43	9.38	11.85	12.85	10.61
9	130	0.01	9.01	9.04	9.05	9.02	9.01	9.04	9.05	9.02	9.01	9.04	9.06	9.02
9	130	0.7	9.59	12.55	11.99	10.40	9.53	12.37	12.02	10.15	9.73	12.50	12.42	10.34

### 8.3.7 Analysis

Model outputs are analysed via variance decomposition as for ANOVA. Here, relative importance of each term can be assessed as the percentage of total variation explained by each main and interaction effect term. Alternatively (as shown in Table 14), the day and year of sowing can be fitted as a random effect in ANOVA. The sensitivity and total sensitivity indices  $S_i$  and  $T_i$  are calculated as described in Chapter Four and shown in Table 15. Results are described next.

### 8.3.8 Results

For the spring varieties we can draw the following inferences (Table 14, Table 15; Figures 22 & 24) (Mean temperatures for the 3 years under study are shown in Figure 23):

- Day provides a large source of variation,
- $lmin$  is the most influential at one order of magnitude less,
- $ps$  is also important.
- $bp$  is relatively uninfluential.
- If Day is treated as a fixed effect in the ANOVA decomposition, then we can see that the interaction between  $lmin$  and  $ps$  at different times of the year may be of interest:
- Figure 24 indicates that stronger daylength response ( $ps = 0.70$ ) has a differential effect on  $fn$ , and this effect is not exactly consistent with different  $lmin$  values.



**Table 14: ANOVA decomposition for theoretical spring varieties.**

Analysis of variance	d.f.	s.s.	F pr.
Source of variation			
Day & Year stratum	11	40.2246	
<i>bp</i>	1	0.0199	0.852
<i>lmin</i>	1	381.677	<.001
<i>ps</i>	1	104.318	<.001
<i>bp.lmin</i>	1	0	0.998
<i>bp.ps</i>	1	0.0186	0.856
<i>lmin.ps</i>	1	0.0037	0.936
<i>bp.lmin.ps</i>	1	0	0.999
Residual	77	43.4212	
Total	95	561.1378	

**Table 15: Variance decomposition for theoretical spring varieties;  $S_i$  and  $T_i$**

Term	$S_i$	$T_i$
<i>bp</i>	0.02	1.61
<i>lmin</i>	381.68	383.85
<i>ps</i>	104.32	144.88
Day	40.06	83.43
Year	0.09	0.39

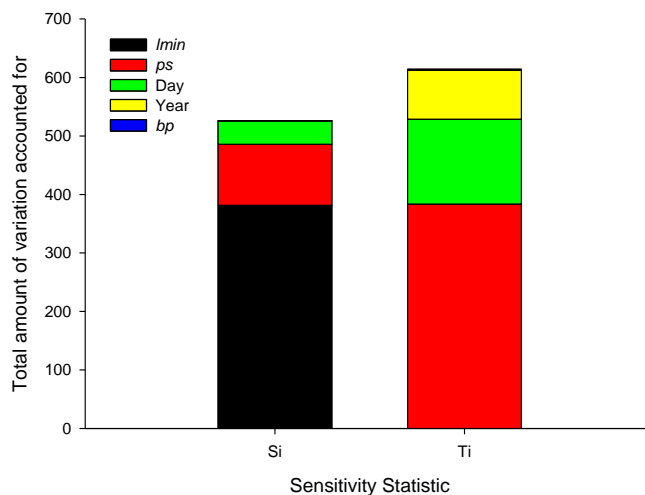


**Figure 22:  $S_i$  + remainder and  $T_i$  for theoretical spring varieties.**

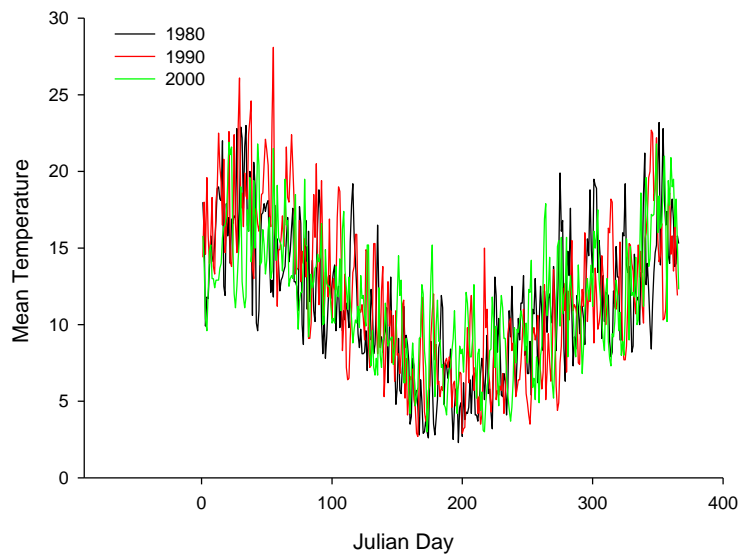


**Figure 23: Mean temperature for the three years under study.**

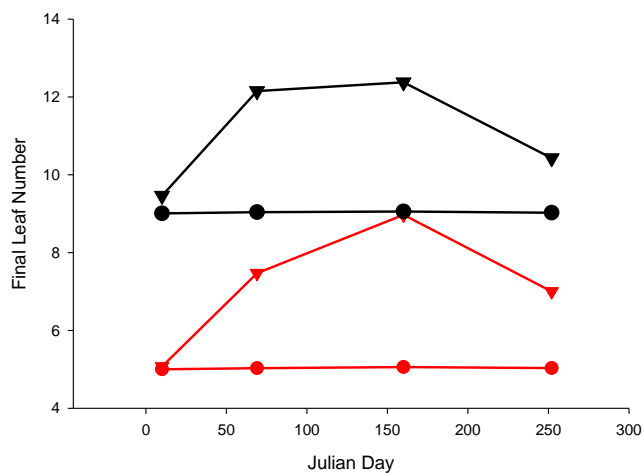


**Figure 24:  $f_{ln}$  (y-axis) for sowing day averaged over year (x-axis). Red lines represent  $lmin = 5$ , black lines represent  $lmin = 9$ . Triangle symbols represent  $ps = 0.70$ . Circle symbols represent  $ps = 0.01$ .**

### 8.3.9 Conclusion

The results of implementing the UE framework for SIRIUS allowed a clear description and understanding of the model under study. Objectives were set,

and inference made from analysis added insight into the behaviour of the model. These included the impact of variation in cultivar-specific input parameters such as *lmin* and *bp*. The next Chapter will continue to work with SIRIUS to provide estimates of uncertainty that account for as many sources of variability at the same time as possible.

# Chapter Nine: SIRIUS implemented as a State-Space model via MCMC

## 9.1 Executive Summary

Chapter Nine implements a Bayesian hierarchical data assimilation model (BHM) for SIRIUS. This model will allow us to provide credible intervals for state-space model estimates. Because this approach allows data to be used during the estimation process, the credible intervals include an element of aleatory uncertainty  $\epsilon$ . The effect of variations to the prior distributions placed on input parameters are explored, and results indicate that this approach allows real time estimation of crop responses to environmental conditions predictions to be pulled into line with observations that may not respond exactly as expected. It also allows predictions to be accompanied by performance statistics. There is a balance between prior belief (partially summarised by the state evolution model), and the observed data. As a research guide, it is an information-inclusive approach to help identify and quantify model parameter sensitivity. This approach also allows both calibration and sensitivity analysis of computer simulation model estimates that have been allowed to propagate through time, ensuring that the model correctly simulates not only the end result, but also the pathway to that result.

## 9.2 Introduction

The objective of this Chapter is to provide an estimate of the leaf number at time  $t$  based on all of the data available at that time, the state model, and expert prior knowledge of input parameters. As mentioned in Chapter Two, there is an inherently hierarchical structure to the concept of data assimilation. That Chapter shows how the state evolution model, observations, and input parameters are

unified to provide filtered estimates that can be used to explore model sensitivity, uncertainty, and predictability. Our data assimilation method aims to set the state evolution model in a probabilistic setting via Bayes rule. Here, the posterior at day  $t = 1$  becomes the prior at day  $t = 2$ . To recap the general form described in Chapter Two:

- The data model  $Q|Z,\theta$  is what is most likely given conditional dependency upon the state model in addition to the standard dependency upon the parameter model. An important feature of this framework is the lack of requirement for either linearity or normality in the data model.
- The state model  $Z|\theta$  (SIRIUS) is represented by a series of unobserved/hidden or latent variables that are inferred through mathematical equations that describe the underlying scientific process of interest and are conditionally dependent on the parameters. A first order Markov model in time is assumed.
- The parameter model  $\theta$  contains the parameters which are each described by a prior distribution usually represented by expert opinion or by independent 'non-informative' priors. The sequential estimation procedure additionally allows the prior at time  $t$  to be represented by the posterior pdf at time  $t-1$ .

## 9.3 Formulation of the Model via Bayes Theorem

### 9.3.1 SIRIUS in a State-space Framework

As summarised via the UE framework in Chapter Eight, the SIRIUS wheat development sub-model for spring wheat is a dynamic, deterministic computer simulation of the development of a wheat plant through time as realised by the number of fully extended leaves. It will henceforth be referred to as the state evolution model because of its discrete nature where on each day there are a

well-defined set of states by which each state variable may either remain in its current state or update according to environmental cues. State equations  $Z_t$  for the spring wheat model are as specified in 8.2.2.

### 9.3.2 Components of the State-space Model

The state variables, input parameters with their prior distributions, and observed variables provide all the necessary components to begin state-space modelling. They are presented in matrix form as follows.

#### 9.3.2.1 State Variables

$$\mathbf{Z}_t = \begin{pmatrix} \textit{phyllochron}_t \\ \textit{primordia}_t \\ \textit{flnt}_t \\ \textit{fln}_t \\ \textit{ln}_t \end{pmatrix}$$

#### 9.3.2.2 Input Parameters $\theta$ with Expert Priors

$$\boldsymbol{\theta} = \begin{pmatrix} \textit{ps} \\ \textit{ppsats} \\ \textit{lmin} \\ \textit{pn} \\ \textit{pe} \\ \textit{bp} \end{pmatrix}$$

#### 9.3.2.3 Observable Variables

$$\mathbf{D}_t = \begin{pmatrix} \mathbf{C}_t \\ \mathbf{E}_t \end{pmatrix}$$

Where

$$\mathbf{C}_t = (\mathbf{LN}_t)$$

$$\mathbf{E}_t = \begin{pmatrix} TT_t \\ PP_t \end{pmatrix}$$

### 9.3.3 Bayesian Filtering Processor for SIRIUS

The specific solution for the SIRIUS model (where  $t$  denotes a single day/time-step) is:

- Parameter Model

$$P(\boldsymbol{\theta})$$

- Environmental Data Model:

$$P(\mathbf{E}_t)$$

- Data Model:

$$P(\{\mathbf{C}_t : t = 1, \dots, t\} | \{\mathbf{Z}_t : t = 0, \dots, t\}, \boldsymbol{\theta})$$

- State Evolution Model:

$$P(\mathbf{Z}_0)P(\mathbf{Z}_t | \mathbf{Z}_{t-1} : t = 1, \dots, t)$$

- Filtering model

Forecast:

$$P(\mathbf{Z}_t | \mathbf{E}_{1:t-1}, \mathbf{C}_{1:t-1}, \boldsymbol{\theta}) = \int P(\mathbf{Z}_t | \mathbf{Z}_{t-1})P(\mathbf{Z}_{t-1} | \mathbf{E}_{1:t-1}, \mathbf{C}_{1:t-1}, \boldsymbol{\theta})d\mathbf{Z}_{t-1}$$

Filter:

$$P(\mathbf{Z}_t, \mathbf{E}_t, \boldsymbol{\theta} | \mathbf{C}_{1:t}) \propto P(\mathbf{C}_t | \mathbf{Z}_t, \mathbf{E}_t, \boldsymbol{\theta}) P(\mathbf{Z}_t | \mathbf{C}_{1:t-1}, \boldsymbol{\theta}, \mathbf{E}_{1:t-1}) P(\boldsymbol{\theta}) P(\mathbf{E}_t)$$

That is, the posterior distribution of the state variables is proportional to the likelihood (the data  $\mathbf{C}_t$  given all the other information on day  $t$ ), the state variables  $\mathbf{Z}_t$  on day  $t$  given all the other information on day  $t-1$ , the input parameters  $\boldsymbol{\theta}$  and the environmental data  $\mathbf{E}_t$ . These last two are not dependent upon each other, the data  $\mathbf{C}_{1:t}$  or the state variables  $\mathbf{Z}_{1:t}$ .

This filter does not work well on occasions when data is not present. Realistically, in the case of the spring model for example, the state evolution model updates on a daily basis, but data may enter only weekly. The model is therefore based on data interpolated using a simple polynomial regression.

## 9.4 Practical Implementation

### 9.4.1 Software

The recursive model was coded in GenStat v15 (VSN\_International 2013) which called WinBUGS (Gilks et al. 1996; Spiegelhalter et al. 2004) via the procedure BGXGENSTAT on each daily loop, extracting and saving the appropriate posterior statistics via the procedure BGIMPORT. These then enter the model on day  $t+1$  with the appropriate observed data. The code for this is shown in Appendix A3.

### 9.4.2 Nomenclature

A table of the names of all the variables and parameters used in the model and alternatives given software restrictions are given in Table 16.

**Table 16: Model component naming schemes.**



Type	Formal Name	WinBUGS Code Name
State Variable	$phyllochron_t$	phylln.t
State Variable	$primordia_t$	primn.t
State Variable	$fln_t$	flnt.t
State Variable	$fln_t$	fln.t
State Variable	$ln_t$	ln.t
State Variable	$fln_{t-1}$	fln.tmin1
State Variable	$ln_{t-1}$	ln.tmin1
Input Parameter	$ps$	ps
Input Parameter	$ppsats$	ppsats
Input Parameter	$lmin$	lmin
Input Parameter	$pn$	pn
Input Parameter	$pe$	pe
Input Parameter	$bp$	bp
Likelihood	$\mu.ln_t$	mu.ln.t
Recursive Hyperparameter	$\mu.ln_{t-1}$	fln.tmin1
Recursive Hyperparameter	$\mu.fln_{t-1}$	alpha.ln.tmin1
Data	$LN_k$	LN.t
Data	$PP_k$	PP.t
Data	$TT_k$	TT.t

### 9.4.3 Likelihood

The choice of likelihood can strongly impact behaviour of the model. The Poisson likelihood was selected as it is appropriate for count data.

### 9.4.4 Recursive Priors

Similarly posterior estimates for the means of  $ln_{t-1}$  and  $fln_{t-1}$  enter as prior distributions in the model. A Poisson distribution is assumed to appropriate for  $ln_{t-1}$  and a range of prior distributions for  $fln_{t-1}$  including Gamma, Poisson, and Normal distributions are tested. The method of moments was used to estimate appropriate statistics from the posterior distributions, where  $E[X] = \frac{\alpha}{\beta}$  for the Gamma distribution and  $E[X] = \lambda$  for the Poisson distribution.

#### 9.4.5 Elicitation of Prior Distribution for Input Parameters

Input parameters  $\theta$  represent cultivar specific characteristics and responses to environmental cues. These parameters do not evolve through time, nor are they updated by observation. They are the only terms in the model therefore that are constant through time and do not need to be denoted with the subscript  $t$ . Prior knowledge can be used to inform the form of input parameters into the model. Table 17 provides a summary of prior information for three varieties of spring wheat. These varieties were selected because observed LN count data through time is available for them. Otane is the variety with the most complete information, so is the focus of the analysis in this chapter.

The prior information for photoperiod response input parameters  $ps$  and  $ppsat$  are derived from Brooking et al. (1995) and are set as Normal (0.51, 0.01) and Normal (13.5, 0.01) respectively. The minimum leaf numbers are also derived from Brooking et al. (1995) and are set as a Gamma (7, 1). The input parameter for  $bp$  is not currently available in the literature for Otane, so was set to be Normal (110, 1) based on expert opinion (elicited as described in Chapter Two, H.E. Brown, E.D. Meenken, C.M. Triggs Auckland, 2013). The number of organs in the grain at germination and as a linear relationship with number of leaves is set at Poisson (4) and Poisson (2), respectively.

**Table 17: Prior information for three spring wheat cultivars<sup>1</sup>**

Cultivar	Conditions	Source	<i>lmin</i> /FLN	<i>bp</i>	<i>ps</i>	<i>pps</i>
Batten Spring	Inductive/many temps	1	7		0.78	15.5
Batten Spring	Field	1	7.7			
Batten Spring	Unknown	2	9.3			
Batten Spring	Inductive/Warm	3	8.8	110		
Batten Spring	Inductive/Warm	4	8.0			
Otane	Inductive/many temps	1	6.7		0.51	13.5
Otane	Field	1	7.1			
Otane	Field	2	8	110	0.25	
Otane	Inductive/Warm	2				
Otane	Inductive/Warm	3	6-7	120		
Otane	Inductive/Warm	4	6-7			
Rongotea	Inductive/many temps	1	7.1		0.68	15.9
Rongotea	Field	1	7.7			
Rongotea	Inductive/Warm	5		100		
Rongotea	Unknown	2				
Rongotea	Inductive/Warm	3	8.7	110		

<sup>1</sup> Data sources by number are:

1. Brooking et al. (1995)
2. Unpublished experimental work, Catherine Munro, Plant & Food Research
3. Unpublished experimental work, Sarah Sinton, Plant & Food Research
4. Experimental work, Chapter 6, Esther Meenken PhD thesis.
5. Jamieson et al. (1998)

#### 9.4.6 Assimilation Data: Spring Wheat Leaf Appearance Trial

This data arises from a historical Plant & Food Research trial planned and carried out by Hamish Brown and Sarah Sinton. On 6 March 2012, three replicates of six seeds of the wheat cultivar Otane along with several other cultivars were planted in 15cm diameter pots containing standard potting medium and placed in a sealed growth chamber. Pots were later thinned to four plants. The pots were grouped in large trays (about 15 to a tray) and these were arranged on a bench on either side of an access way in the growth chamber. Day length was set at 16 hours and lighting consisted of 400-watt mercury vapour and high pressure sodium bulbs. A logging temperature probe was placed at growing point level in each of four pots and distributed equally around the growth chamber. Temperature was recorded hourly. Mean temperature for the growing period was 22.6°C. A dehumidifier was used to reduce foliar disease risk and any insect incursion regularly sprayed with insecticide. Pots were manually watered.

On 17 occasions between 12 March and 14 September tips and ligules were counted on the main stem of each plant and as the plants grew and leaves died, a wire marker was used to keep track of leaf number. Any plants that did not conform to average growth (relative to other plants in the same pot) were abandoned; recurrent handling distorted growth in some plants. The date of final leaf appearance (flag leaf) booting, ear emergence, and flowering were also recorded. The daily number of leaves was interpolated from the observed data via a linear fit between observations. The observed response data  $C_t = LN_t$  represents this daily observed leaf number data for up to 8 plants per cultivar.

#### 9.4.7 Bayesian Network for SIRIUS

The state-space hierarchical framework can be visualised as in Figure 25.

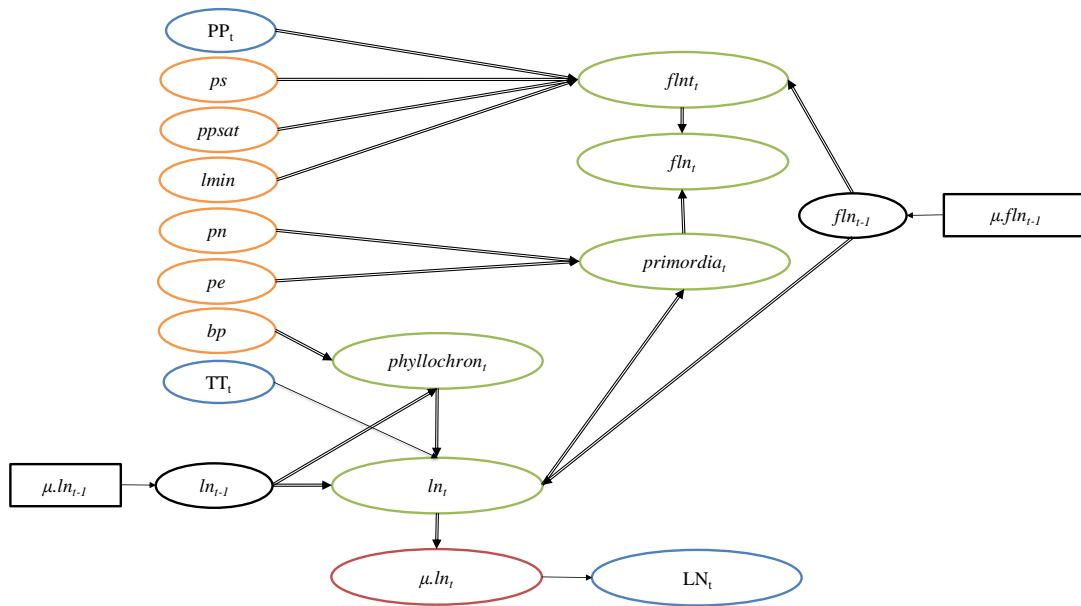


Figure 25: Bayesian graphical model; double edges link to logical nodes, single edges link to stochastic nodes, ovals denote variables and boxes denote constants. Here blue denotes observed data, green state variables, orange input parameters, and black recursive priors.

## 9.4.8 Bayesian Hierarchical Model for SIRIUS

The formal specification of the Bayesian model is shown in Figure 26.

$$\begin{aligned}LN_t &\sim \text{Poisson}(\mu.ln_t) \\ \log(\mu.ln_t) &= \log(ln_t) \\ ln_t &= f(E_t, Z_t, \mu.ln_{t-1}, fln_{t-1}, \theta) \\ ln_{t-1} &\sim \text{Poisson}(\mu.ln_{t-1}) \\ fln_{t-1} &\sim \text{Gamma}(\mu.fln_{t-1}, 1) \\ \theta &\sim \text{expert opinion} \\ E_t &= \text{observed variables} \\ Z_t &= \text{state equations}\end{aligned}$$

**Figure 26: Bayesian model for SIRIUS.**

## 9.4.9 WinBUGS details

### 9.4.9.1 Hierarchical Model Code for day $t$

The code for the model in Figure 26 is shown in Figure 27. This sits within the full GenState code that allows the recursive model to run automatically. The full code is given in Appendix A3.

```

model
{
for (i in 1:8){
LN.t[i] ~ dpois (mu.ln.t)
}
log (mu.ln.t) <- log (ln.t)

a[1] <- step (2 - (ln.ttmin1))
a[2] <- step ( 8 - (ln.ttmin1)) - step (2 - (ln.ttmin1))
a[3] <- min ((1 - ( a[1])), (1 - (a[2])))
phylln.t <- (a[1] * 0.75 * bp + a[2] * bp + a[3] * 1.3 * bp)

d[1] <- step ((( TT.t/phylln.tmin1) + ln.ttmin1) - fln.tmin1)
d[2] <- 1 - d[1]
ln.t <- d[1] * fln.ttmin1 + d[2] * ((TT.t/phylln.t) + ln.tmin1)

primn.t <- pn * ln.t + pe

b[1] <- step ((PP.t - ppsat))
b[2] <- 1 - b[1]
flnt.t <- lmin

c[1] <- step ((primn.t - (flnt.t + pe)))
c[2] <- 1 - c[1]
e[1] <- step((primn.t - flnt.t))
e[2] <- 1 - c[1]
fln.t <- c[1] * (e[1] * flnt.t + e[2] * primn.t) + c[2] * (fln.ttmin1)

bp ~ dnorm(110,1)
pe ~ dpois (4)
pn ~ dpois (2)
ppsat ~ dnorm (15.9, 0.01)
lmin ~ dgamma (7, 1)
ps ~ dnorm (0.625, 0.01)

ln.tmin1 ~ dpois (alpha.ln.tmin1)
ln.ttmin1 <- alpha.ln.tmin1
fln.ttmin1 ~ dgamma (fln.tmin1, 1)
}

```

**Figure 27: Hierarchical Model Code for day  $t$ .**



#### 9.4.9.2 Data File for Day $t = 45$

The data used for the model fitting are provided for day 45 in Figure 28.

```
list (  
  fln.tmin1      = 7.000  
  , TT.t        = 22.50  
  , PP.t        = 16.00  
  , alpha.ln.tmin1 = 6.608  
  , LN.t        = c(6, 7, 7, 6, 7, 7, 6, 6)  
)
```

**Figure 28: Data file for day  $t = 45$**

#### 9.4.9.3 Model Fitting Details

WinBUGS was set to initiate 3 chains, allowing for 1000 burn-ins and running 10,000 simulations on each day. Each model ran for 45 simulated days.

### 9.4.10 Bayesian Model Checking

#### 9.4.10.1 Effect of Observed Data

The impact of increasing the number of observations is explored for 1, 3, and 8 plants.

#### 9.4.10.2 Input Parameter Priors

We explored the effect of increasing and decreasing the estimated  $lmin$ , its precision, and its distribution. We explored the effect of increasing the decreasing the estimated  $bp$ , its precision, and how introducing it as a scalar input parameter rather than with a distribution affected results. The data were collected in photoperiod controlled chamber set at inductive conditions. To avoid experimenting with changing the priors to values that make little biological sense

we did not assess the effect changing photoperiod prior distributions for  $ps$  and  $ppsat$ . The literature and expert knowledge indicate that the uncertainty around the number of organs per grain and per leaf is subject to very little biological variability, so we did not explore these prior distributions beyond introducing them as scalar input parameters rather than with a distribution.

#### 9.4.10.3 $fln_{t-1}$ Priors

Three alternative prior models for the  $fln_{t-1}$  variable were tested. These were the Poisson, Normal and Gamma as shown in Table 18.

### 9.5 Results of UE

The results of the model fitting procedure carried out to explore the effect of changes in the prior on input parameters and the state equation  $fln$  are given in Table 18. Here the N, P and Gam outside the brackets indicate that the Normal, Poisson and Gamma distributions have been used as priors, respectively. Each of the other terms have been defined in Table 16. Changes in the number of observations used in modelling and results including estimated  $ln$  on day 45 and its predicted range are summarised in Table 19.

**Table 18: Prior distribution models for input parameters and state equations. Changes from baseline Model (b) are shown in **bold** in either Table 18 or Table 19.**

Model	$\theta$ prior distributions						Likelihood
	bp	pe	pn	lmin	mu.ln.t-1	fln.t-1	LN.t
a	$\sim N(110,1)$	$\sim P(4)$	$\sim P(2)$	$\sim \text{Gam}(7,1)$	$\sim P(\text{mu.ln.t-1})$	$\sim P(\text{fln.t-1})$	$\sim P(\text{mu.ln.t})$
b	$\sim N(110,1)$	$\sim P(4)$	$\sim P(2)$	$\sim \text{Gam}(7,1)$	$\sim P(\text{mu.ln.t-1})$	$\sim P(\text{fln.t-1})$	$\sim P(\text{mu.ln.t})$
c	$\sim N(110,1)$	$\sim P(4)$	$\sim P(2)$	$\sim \text{Gam}(7,1)$	$\sim P(\text{mu.ln.t-1})$	$\sim P(\text{fln.t-1})$	$\sim P(\text{mu.ln.t})$
d	$\sim N(110,1)$	$\sim P(4)$	$\sim P(2)$	<b><math>\sim \text{Gam}(6,1)</math></b>	$\sim P(\text{mu.ln.t-1})$	$\sim P(\text{fln.t-1})$	$\sim P(\text{mu.ln.t})$
e	$\sim N(110,1)$	$\sim P(4)$	$\sim P(2)$	<b><math>\sim \text{Gam}(8,1)</math></b>	$\sim P(\text{mu.ln.t-1})$	$\sim P(\text{fln.t-1})$	$\sim P(\text{mu.ln.t})$
f	$\sim N(110,1)$	$\sim P(4)$	$\sim P(2)$	<b><math>\sim \text{Gam}(10,1)</math></b>	$\sim P(\text{mu.ln.t-1})$	$\sim P(\text{fln.t-1})$	$\sim P(\text{mu.ln.t})$
g	$\sim N(110,1)$	$\sim P(4)$	$\sim P(2)$	<b><math>\sim \text{Gam}(7,.01)</math></b>	$\sim P(\text{mu.ln.t-1})$	$\sim P(\text{fln.t-1})$	$\sim P(\text{mu.ln.t})$
h	$\sim N(110,1)$	$\sim P(4)$	$\sim P(2)$	<b><math>\sim \text{Gam}(7,100)</math></b>	$\sim P(\text{mu.ln.t-1})$	$\sim P(\text{fln.t-1})$	$\sim P(\text{mu.ln.t})$
i	$\sim N(110,1)$	$\sim P(4)$	$\sim P(2)$	<b><math>\sim \text{Norm}(7,0.01)</math></b>	$\sim P(\text{mu.ln.t-1})$	$\sim P(\text{fln.t-1})$	$\sim P(\text{mu.ln.t})$
j	$\sim N(110,1)$	<b>4</b>	<b>2</b>	$\sim \text{Gam}(7,1)$	$\sim P(\text{mu.ln.t-1})$	$\sim P(\text{fln.t-1})$	$\sim P(\text{mu.ln.t})$
k	<b><math>\sim N(140,1)</math></b>	$\sim P(4)$	$\sim P(2)$	$\sim \text{Gam}(7,1)$	$\sim P(\text{mu.ln.t-1})$	$\sim P(\text{fln.t-1})$	$\sim P(\text{mu.ln.t})$
l	<b><math>\sim N(110,100)</math></b>	$\sim P(4)$	$\sim P(2)$	$\sim \text{Gam}(7,1)$	$\sim P(\text{mu.ln.t-1})$	$\sim P(\text{fln.t-1})$	$\sim P(\text{mu.ln.t})$
m	<b><math>\sim N(110,.1)</math></b>	$\sim P(4)$	$\sim P(2)$	$\sim \text{Gam}(7,1)$	$\sim P(\text{mu.ln.t-1})$	$\sim P(\text{fln.t-1})$	$\sim P(\text{mu.ln.t})$
n	<b>110</b>	$\sim P(4)$	$\sim P(2)$	$\sim \text{Gam}(7,1)$	$\sim P(\text{mu.ln.t-1})$	$\sim P(\text{fln.t-1})$	$\sim P(\text{mu.ln.t})$
o	<b><math>\sim N(90,1)</math></b>	$\sim P(4)$	$\sim P(2)$	$\sim \text{Gam}(7,1)$	$\sim P(\text{mu.ln.t-1})$	$\sim P(\text{fln.t-1})$	$\sim P(\text{mu.ln.t})$
p	<b><math>\sim N(90,1)</math></b>	$\sim P(4)$	$\sim P(2)$	$\sim \text{Gam}(7,1)$	$\sim P(\text{mu.ln.t-1})$	$\sim P(\text{fln.t-1})$	$\sim P(\text{mu.ln.t})$
q	$\sim N(110,1)$	$\sim P(4)$	$\sim P(2)$	<b><math>\sim \text{Gam}(9,1)</math></b>	$\sim P(\text{mu.ln.t-1})$	$\sim P(\text{fln.t-1})$	$\sim P(\text{mu.ln.t})$
r	$\sim N(110,1)$	$\sim P(4)$	$\sim P(2)$	<b><math>\sim \text{Gam}(9,1)</math></b>	$\sim P(\text{mu.ln.t-1})$	$\sim P(\text{fln.t-1})$	$\sim P(\text{mu.ln.t})$
s	$\sim N(110,1)$	$\sim P(4)$	$\sim P(2)$	$\sim \text{Gam}(7,1)$	$\sim P(\text{mu.ln.t-1})$	<b><math>\sim \text{Norm}(\text{fln.t-1},1)</math></b>	$\sim P(\text{mu.ln.t},1)$
t	$\sim N(110,1)$	$\sim P(4)$	$\sim P(2)$	$\sim \text{Gam}(7,1)$	$\sim P(\text{mu.ln.t-1})$	<b><math>\sim \text{Gam}(\text{fln.t-1},1)</math></b>	$\sim P(\text{mu.ln.t},1)$

Table 19: Number of observed data and filtered statistics for each model shown in Table 18. Changes from baseline Model (b) are shown in **bold** in Table 18 or 19.

Model	Leaf Numbers on Day 45							
	mean observed	variance observed	no observed included	process model ln	BHM LN ( $\mu$ )	range	BHM 2.5%	BHM 97.5%
a	6.00	-	<b>1</b>	7	6.6	7.3	3.4	10.6
b	6.67	0.33	3	7	6.9	5.1	4.5	9.6
c	6.50	0.29	<b>8</b>	7	6.6	3.3	5.1	8.4
d	6.67	0.33	3	6	6.9	5.2	4.5	9.7
e	6.67	0.33	3	8	6.9	5.2	4.5	9.7
f	6.67	0.33	3	<b>10</b>	7.2	5.3	4.7	10.0
g	6.67	0.33	3	8	6.8	5.3	4.5	9.7
h	6.67	0.33	3	8	6.8	5.1	4.5	9.6
i	6.67	0.33	3	8	6.9	5.1	4.5	9.6
j	6.67	0.33	3	7	6.8	5.1	4.5	9.6
k	6.67	0.33	3	7	6.9	5.2	4.5	9.7
l	6.67	0.33	3	7	6.9	5.2	4.5	9.6
m	6.67	0.33	3	7	6.9	5.0	4.5	9.6
n	6.67	0.33	3	7	6.8	5.1	4.5	9.6
o	6.67	0.33	<b>8</b>	7	6.6	3.4	5.0	8.4
p	6.67	0.33	3	7	6.8	5.1	4.5	9.6
q	6.67	0.33	<b>8</b>	9	6.7	3.4	5.1	8.5
r	6.67	0.33	3	9	7.0	5.3	4.6	9.9
s	6.5	0.33	<b>8</b>	9	6.54	3.4	4.98	8.34
t	6.5	0.33	<b>8</b>	9	6.58	3.3	5.03	8.35

### 9.5.1 Outcomes 1 – 8: Exploring Filtered Model Uncertainty

The results of the Bayesian Hierarchical Model (BHM) analysis is summarised in Table 19 lead to the following 10 conclusions.

1. Increasing the number of observations decreases the credible interval of prediction (Models a, b and c) (Figure 29).

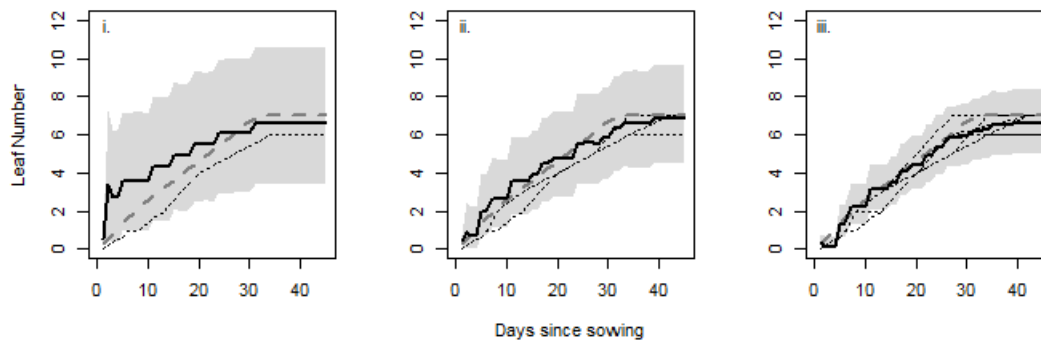


**Figure 29: Effect of number of observations on estimation and range of number of leaves through time for Otane. i. Model a, ii. Model b, and iii. Model c. Shading represents 95% credible intervals. Dashed line indicates the process model, solid line indicates the filtered estimate from the BHM, dotted lines indicate observed data.**

2. As the prior for  $lmin$  increases, the filtered estimate for leaf number also increases, but not linearly; the further from the data the prior forces the model the less weight it receives in the filtered estimate. This is accompanied by a slight increase in variation/range (Models d, e, and f) (Figure 30).

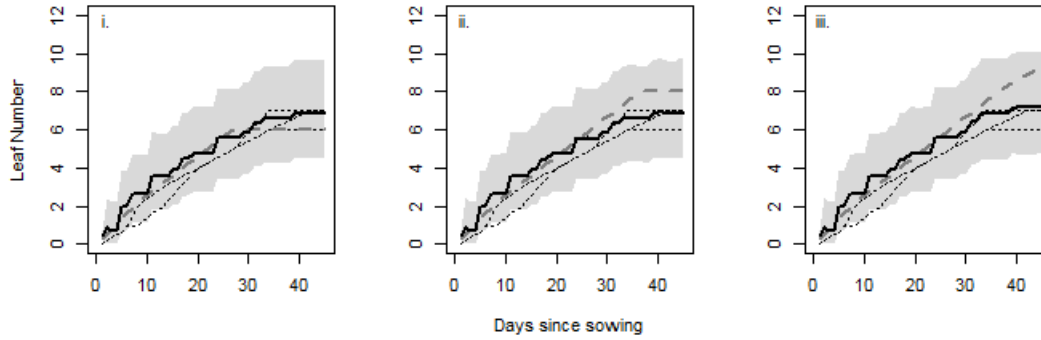


**Figure 30: Effect of adjusting prior for  $lmin$  on estimation and range of number of leaves through time for Otane. i. Model d, ii. Model e, and iii. Model f. Shading represents 95% credible intervals. Dashed line indicates the process model, solid line indicates the filtered estimate from the BHM, dotted lines indicate observed data.**

3. Decreasing the precision of the prior on the  $lmin$  very slightly increases the range of the filtered estimate for leaf number (Models e, g, and h) (shown only in Table 19).
4. Using a different but biologically meaningful prior distribution for  $lmin$  results in very little change to estimate or range (Models e and i) (shown only in Table 19).
5. Removing the prior distribution from the baseline number of grain and leaf primordia  $pn$  and  $pe$  does not affect the filtered leaf number estimate but very slightly decreases the range of the posterior (Models b and j) (shown only in Table 19).
6. As the prior value for  $bp$  changes, the filtered estimate for leaf number and the range around this estimate only varies slightly. However, an incorrect  $bp$  strongly affects the date at which the plant reaches its final leaf number, and whilst this is not the focus of this paper, the rate of development is also of biological interest (p, b and k) (Figure 31). Here, Model p (Figure

31i) with a  $bp$  of 90 grew slowly whilst Model k (Figure 31iii) with a  $bp$  of 140 grew too rapidly.

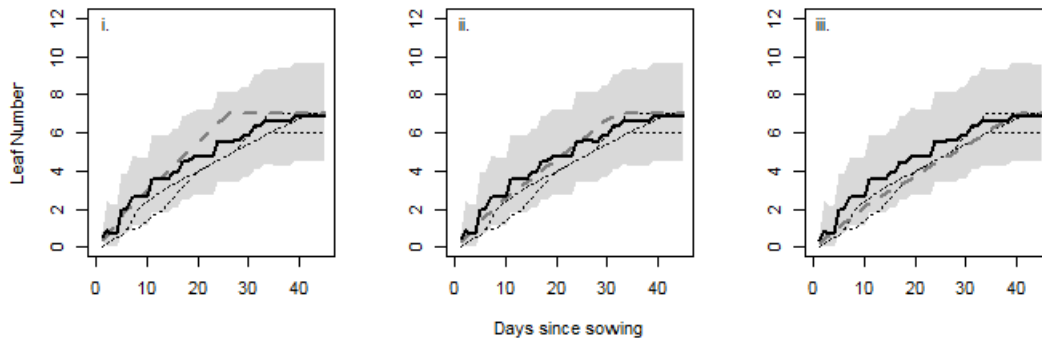


**Figure 31: Effect of  $bp$  on estimation and range of number of leaves through time for Otane. i. Model p, ii. Model b, and iii. Model k. Shading represents 95% credible intervals. Dashed line indicates the process model, solid line indicates the filtered estimate from the BHM, dotted lines indicate observed data.**

7. Decreasing the precision of the prior on  $bp$  slightly decreases the range of the filtered estimate for leaf number through time (Models b and i) (shown only in Table 19).
8. Removing the prior distribution around the  $bp$  does not affect the estimate but slightly increases the range (Models b, m, and n) (shown only in Table 19).

### 9.5.2 Outcomes 9-10: A Balance Between Expert Opinion, State Evolution Model and Data

Intuitively it may seem that reducing the credible intervals as much as possible is desirable, however, if the prior belief happens to be far away from the data, the state model predictions may be quite distant from the filtered prediction if the data is heavily weighted (e.g. there are many observations). I believe that the

credible intervals should ideally find a balance between data and prior belief. As such, the aim is to fit the state model with reasonable expert priors on the input parameters, but also only include as much data as required to update the forecasts without overwhelming them. However finding the correct balance is not necessarily straightforward, and will rely on a complete UE of the model.

9. If the  $bp$  is too low, the state model simulation of development is extremely close to the upper credible interval when there is a large amount of data (Models p and o) (Figure 32).

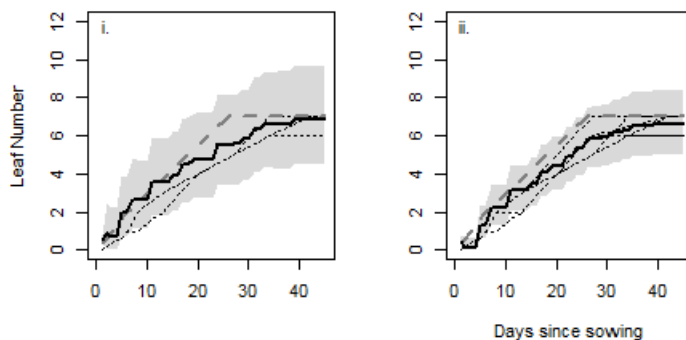


**Figure 32: Effect of low  $bp$  and # observations on estimation and range of number of leaves through time for Otane. i. Model p, and ii. Model o. Shading represents 95% credible intervals. Dashed line indicates the process model, solid line indicates the filtered estimate from the BHM, dotted lines indicate observed data.**

10. Similarly, if the prior belief for the  $lmin$  is far away from the current data set, the state model estimate of leaf number is outside the credible intervals when there is a large amount of data (Models r and q) (Figure 33).



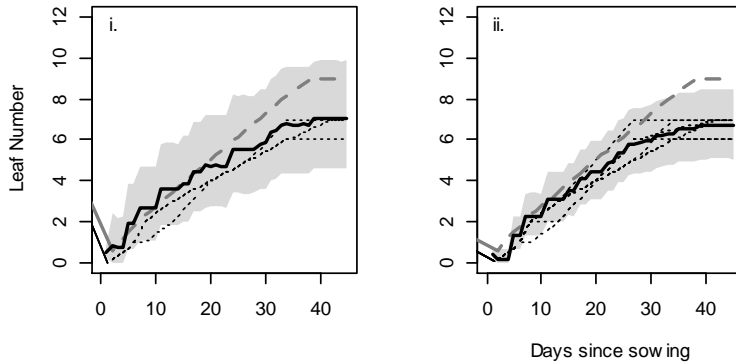


**Figure 33: Effect of high minimum leaf number and number of observations on estimation and range of number of leaves through time for Otane. i. Model  $r$ , and ii. Model  $q$ . Shading represents 95% credible intervals. Dashed line indicates the process model, solid line indicates the filtered estimate from the BHM, dotted lines indicate observed data.**

## 9.6 Diagnostics

As discussed in Chapter Five, MCMC sampling can be dangerous, and checking convergence of the model requires care. It is difficult to say conclusively that a chain (simulation) has converged, only to diagnose when it definitely hasn't. The following outputs can be used to diagnose when the chain definitely hasn't converged (Burn and Underwood 2007).

Stationarity is assessed by looking at the trace plots of the parameters. Irreducibility is also checked via traceplots. A formal assessment can be made via the Gelman and Rubin convergence statistic as modified by Brooks and Gelman (1998). Whether the chain converged to a distribution (not a point estimate) can be seen from the density. Finally, if values within a chain are very highly correlated, then convergence may take a very long time. To ensure the chain has converged the autocorrelation should converge to zero.

Diagnostics for the nodes  $ln_t$ ,  $phyllochron_t$ ,  $primordia_t$ ,  $fln_t$  can be seen in Figure 42, Figure 43, Figure 44, and Figure 45 in Appendix A5. The diagnostics provided include trace plots (Column One), posterior densities for each node (Column Two), Brooks–Gelman (B-G) plots (Column Three) and autocorrelations plots (Column Four). For efficient reporting, diagnostics are provided for 7 selected days:  $t = 1, 2, 5, 10, 20, 30,$  and  $50$ . These diagnostics are from the fitted Model t.

## 9.7 Alternative Formulations

As described in Chapter Five, there are other options to combine state-space model estimates with assimilated data. The Kalman Filter and the Particle Filter are two such options that were implemented during the early stages of the project. However, these models are not as suitable as the approach described in this chapter. The Kalman filter's requirements of normality and linearity are unlikely to be appropriate. The non-Bayesian nature of the particle filter is more restrictive than the Bayesian model. The Bayesian approach is preferred because of its flexibility.

## 9.8 Estimation of Uncertainty in a Latent Variable.

So far only the uncertainty for variables for which there is signal data has been discussed. Estimation uncertainty for an observable, dynamical state variable is a very useful tool; however, for SIRIUS and for other state-space agricultural models there may be other, latent (unobservable) variables which can also be evaluated with respect to uncertainty in their estimation. The approach provides a framework to investigate the behaviour of latent variables. Of particular biological interest is final leaf number ( $fln$ ). Some outputs from Model t (Table 19) are provided in the next Section to provide a starting point for the next stage of investigation: Uncertainty in a latent state variable (The topic of Chapter Ten).

The posterior densities for  $ln_t$  and  $fln_t$  where  $t = 1, 5, 10, 45$  are displayed row by row, from left to right, in Figure 34 and Figure 35. The spikes in the posterior densities of  $fln_t$  show that the discrete prior distribution has not been completely smoothed by the likelihood of the observed data. Whilst the posterior densities for  $ln$  update and changes through time, those for  $fln$  change very little. This is expected based upon the proper state equations for these variables. However, the credible intervals for the latent variable  $fln$  have a range of approximately 9.72, in comparison of 3.37 for the observable variable  $ln$ . That is, around 2.89 times as wide. This can be seen in Figure 36. Since  $fln$  and hence the expected data of flowering is also valuable information, methods to describe and reduce uncertainty around the latent state variable will be explored.

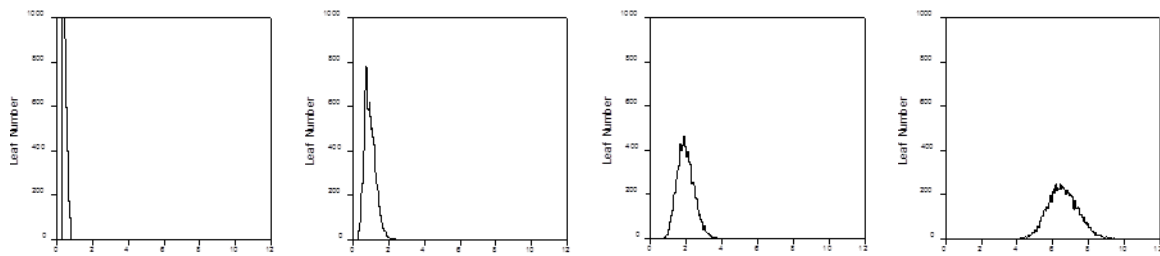


**Figure 34: Posterior density for  $ln_t$  where  $t = 1, 5, 10,$  and  $45$  from left to right based on model t.**

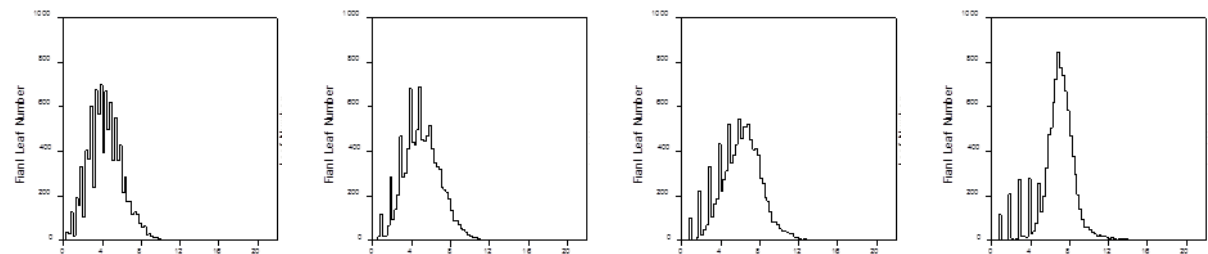


**Figure 35: Posterior density for  $fln_t$  where  $t = 1, 5, 10,$  and  $45$  from left to right based on model t.**

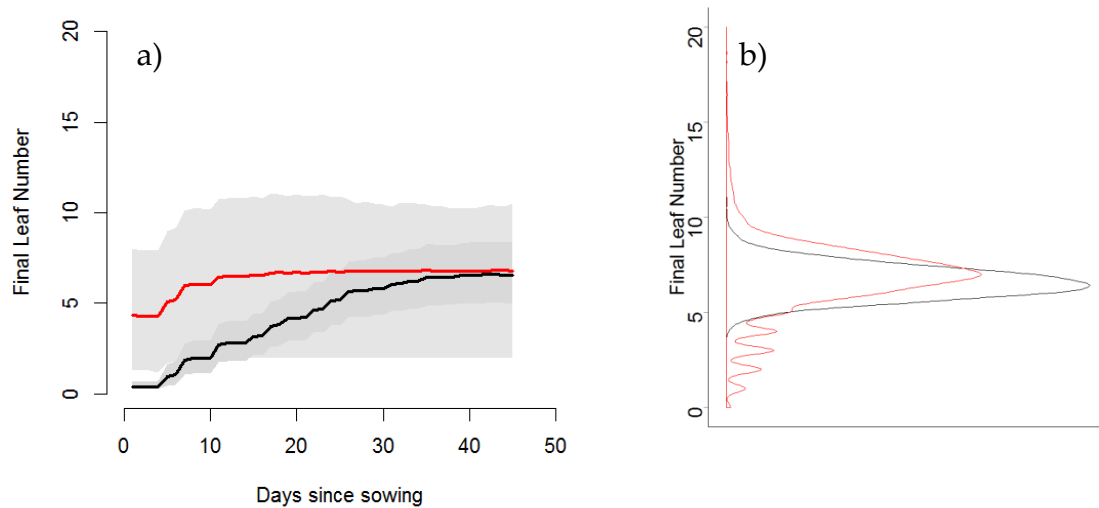


**Figure 36: a) Estimated values and credible intervals for  $ln_t$  (black line, dark grey range) and  $fln_t$  (red line, light grey range). b) Densities of  $ln$  and  $fln$  at  $t = 45$  based on 10,000 realisations.**

## 9.9 Summary

The successful implementation of a probabilistic Bayesian hierarchical model fitted with MCMC satisfied the primary objective of this research project. This model is the best paradigm to combine data, probability, expert opinion, and a state-space model (SIRIUS), seeking a balance between these contributors. Three important benefits of this approach are summarised. Firstly, often with dynamic agricultural computer simulation models it is not sufficient that a model is able to converge to the correct location; its behaviour during state evolution should also be a close approximation to reality. By allowing real time estimation of crop responses to environmental conditions predictions to be updated with observations, this approach can help add confidence that estimates are behaving in a close approximation to reality through time. Further, predictions are accompanied by performance statistics through time. Finally, whilst this approach can be used for prediction in real time, a greater value is probably in

calibration. As a research guide, it is an information-inclusive approach to help identify and quantify model parameter sensitivity. The combination of a state evolution model with data can help provide clues to the range in values that might be expected in novel climate scenarios using 'best guess' prior knowledge. This is in contrast to an ensemble approach which may give undesired weight to a combination of input parameters that are not biologically likely, a particular problem for unique New Zealand conditions. Important characteristics of the data assimilation model are detailed in this chapter, but some findings of particular interest include the following. First, incorporating more data rapidly reduces the credible bounds, indicating the observed rate of leaf development for the Otane wheat cultivar is fairly consistent. Second, the further from the data the prior forces the state model, the less weight it receives in the filtered estimate. This is accompanied by a slight increase in variation/range. Finally, if the prior belief for the  $l_{min}$  is far away from the current data set, the state model estimates of leaf number fall outside the credible intervals when there is a large amount of data. The implication is that when the deterministic model is far away from the observed data, the Bayesian model gives it very little weight in its filtered estimates. This is a consequence that must be considered relative to the UE objectives. In the next Chapter the strength and flexibility of this approach for exploring structural uncertainty is illustrated, and the uncertainty associated with estimating latent variables.

# Chapter Ten: Uncertainty Estimation for Latent State Variables

## 10.1 Executive Summary

Chapter Nine described how data could be used to derive information and insight about an observable variable. It focussed on using the Bayesian approach to fitting the state-space model. The ability to assess the effect of uncertainty in the specification of input parameters  $\theta$  was illustrated. Chapter Ten will build on the model to introduce and implement two other techniques for understanding and quantifying uncertainty in different aspects of computer simulation models.

First is the ability to improve estimation of uncertainty for a latent variable. The latent variable under study,  $fln_t$ , is important biologically both for model UE and prediction purposes. Early and accurate estimation of when flag leaf will occur in the field, based on real-time environmental and calibration data, will provide greater knowledge of when the crop will be ready for harvest. A mixture distribution approach is described and illustrated to improve the credible bounds of  $fln_t$  in the first part of this Chapter.

The second aspect is based on a recent topic in the UE literature that explores the uncertainty that enters model outputs due to incorrect specification of the state variables  $Z_t$  (Strong et al. 2012) via probabilistic sensitivity analysis (Oakley and O'Hagan 2004). Within the model framework already specified it is simple to explore the relative impact of allowing variation in structural equations through specification of a vague pdf for one or more of the elements of  $Z_t$ . Results indicate that most state equations are quite sensitive to this 'jittering' of other

state equations. Unsurprisingly, as the likelihood will alleviate state-equation uncertainty, estimation of  $ln_{45}$  is quite robust.

## 10.2 A Mixture Distribution to Reduce Uncertainty for a Latent Variable

### 10.2.1 Introduction

For many state-space agricultural models, including SIRIUS, there may also be unobservable (latent) variables which can be evaluated with respect to uncertainty in their estimation. The objective of this Chapter is to investigate approaches to better understand uncertainty of latent state variables. Where possible, uncertainty estimates for latent state variables will be improved. In the context of the case study model SIRIUS, the day at which we expect the final (flag) leaf to occur is of biological importance. An improved estimate of the uncertainty associated with  $fln_t$  then has value both for model UE assessment and for real-time model use.

The model implemented in Chapter Nine provides filtered estimates for  $ln_t$  by combining data and state equations. Since  $fln_t$  is a theoretical construct, there is no way in which  $fln_t$  can be observed until the final leaf emerges. A moment's thought, however, should suggest that the distributional characteristics of these two state variables are not independent at all times  $t$ . As such, associating, or mixing, the distributions of the state variables  $ln_t$  and  $fln_t$  to update the posterior distribution of  $fln_t$  is an approach that can make use of the observed LN data. This is described in detail in Section 10.2.2.1. A summary of indirect sources of information about the correlation between the state equations will be useful to help characterise the new, mixed pdf for  $fln_t$ . There are seven pieces of information:

1. The Bayes posterior estimate for  $ln_t$  and  $fln_t$  based on the state space model and the likelihood,
2. At time  $t=1,2,\dots,n$ ;  $ln_t$  is an updating, filtered estimate with moments estimated from the posterior distribution at time  $t - 1$ ,
3. At time  $t = 0$ ,  $fln_t \sim \text{UNIFORM}(lmin, lmax)$ ,
4. At time  $t = n$ ,  $P(fln_t) = P(ln_t)$ ,
5. The minimum and maximum possible numbers of leaves on a wheat plant are known and denoted  $lmin$  and  $lmax$ , respectively,
6. At all times  $t$ ,  $lmin \leq fln_t \leq lmax$ ,
7. For spring wheat,  $lmax$  will be lower than that of a winter wheat variety (dependent on sowing date and photoperiod).

The most obvious solution would be to take the uncertainty estimates directly from the model described in the previous Chapter (Figure 36a). Using the additional information above, a mixture distribution for  $fln_t$  will be obtained whilst ensuring that this mixture is as close as possible to our prior understanding whilst still within the bounds of the state-space model.

### 10.2.2 Method

The approach will consist of four tasks:

1. Using 1 and 2 above, begin as in the previous Chapter by simulating  $fln_t$  and  $ln_t$  recursively through time, calculating moments at time =  $t - 1$  and using these as prior moment estimators at time =  $t$ ,
2. Using (3 and 4 above), the densities of  $fln_1$  and  $fln_{45}$  are known, an algorithm is required to identify the appropriate rate of mixing at  $t=2\dots44$ ,
3. Estimate parameters from the resulting mixture distribution,



4. Values for the posterior estimates of  $fl_{n_t}$  are dependent on the prior distribution selected for this state variable. Using (5, 6, and 7 above) will help ensure an appropriate prior is chosen.

Additionally, the biological implications of improving uncertainty estimates for the state variable  $fl_{n_t}$  have been discussed. As a side-effect of this activity, at certain time points in the simulation additional information about the date of flag leaf become available. Specifically, a predicted date on which the final leaf is fully extended can be calculated early in the simulation process. A 5<sup>th</sup> task taking advantage of this information to predict 'date of final leaf' with uncertainty estimates is therefore of value:

5. Predict date of final leaf in real time early in the simulation process and compare to simulated date of final leaf late in the simulation process.

Step one was carried out in Chapter Nine. The remainder will be implemented next.

#### 10.2.2.1 Step 2: Generate the Mixture Distribution

One way to proceed is to update the covariance between  $fl_{n_t}$  and  $ln_t$  to reflect their convergence as time progresses and use this covariance to allow  $fl_{n_t}$ 's prior distribution to become more closely aligned to that of  $ln_t$  as the model proceeds through time. Throughout it is made up of the product of two distributions, but the relative weight, or contribution, of each distribution will change with the increasing covariance. That is, the relative contribution of the  $ln_t$  prior increases as  $t$  increases because it will be getting closer and closer to the true final leaf number. As time progresses it is useful to calculate an updating distribution to reflect the increasing unification of the two state variables. A straightforward way to achieve this is to utilise an equally-spaced approach to quantify the

increasing covariance between  $fln_t$  and  $ln_t$ . All that remains, therefore, is to specify the times  $t$  on which to begin mixing (this shall be specified as day  $\alpha$ ), and when to end mixing (this shall be specified as day  $\alpha + \tau$ ) and set  $P(fln_t) = P(ln_t)$ . Inspection of Figure 36 in the previous Chapter will help guide this.

In the model, the starting value for  $fln$  at time  $t = 1$  is set at some number, in this case  $lmin$ . The red line in Figure 36a in Chapter Nine shows that this value quickly updates to reach a constant value (in the model this is driven by the  $flnt$  state equation, calculating the target  $fln$  the plant will set), which  $ln$  then also eventually reaches. It seems unhelpful to begin mixing distributions before  $flnt$  has been set. Therefore, day  $\alpha$  is calculated as shown in algorithm 1, by searching for a point where estimated  $fln$  on consecutive days remains approximately constant. Here this is defined as variation of less than one twentieth of a leaf.

For day  $\alpha$  where  $\alpha = \text{day } 3, 4, \dots, n$

**Step 1:** Calculate the average value of the first three simulated values for  $fln$  i.e.

$$\overline{fln}_1 = \frac{fln_1 + fln_2 + fln_3}{3}$$

**Step 2:** Calculate the average value of the 2<sup>nd</sup>- 4<sup>th</sup> simulated values for  $fln$  i.e.

$$\overline{fln}_2 = \frac{fln_2 + fln_3 + fln_4}{3}$$

**Step 3:** Calculate the difference

$$fln_{dif} = \overline{fln}_1 - \overline{fln}_2 = \frac{1}{3}(fln_1 - fln_4)$$

**Step 4:** If the differences is  $> 0.05$  leaves<sup>1</sup>, then continue steps 1 – 3 for  $\overline{fln}_3, \overline{fln}_4, \dots, \overline{fln}_\alpha$  etcetera until the difference is  $\leq 0.05$  leaves, and the  $fln$  is within half a leaf of  $flntarget$ . Here the  $t = \alpha$  denotes the day on which our current simulation is up to. The parameter  $\alpha$  is then held constant, and denotes the day on which extra information is used to improve estimation of the final leaf number state equation:

### Algorithm 1: Algorithm to find day = $\alpha$ .

Next, to calculate when to stop, e.g. when  $t = \alpha + \tau$ . Step 1 in Algorithm 2 next makes the simplifying assumption that the rate of leaf development remains consistent. The estimated value of  $\alpha + \tau$  is then a *predicted* estimator of day of flag, the day on which the posterior distribution for  $fln$  becomes equal to that of  $ln$ . Using this number, for example if  $\alpha = 10$  and  $\alpha + \tau = 20$ , then on day 10 equilibrium in  $fln$  has been reached, and  $ln$  will reach this value in 10 days. Using an equally spaced approached, then on day 10 100% of the mixture

---

<sup>1</sup> e.g. if the estimated  $fln$  is relatively stationary

posterior is provided by the  $fln$  posterior. On day 11, 90% of the mixture posterior is provided by the  $fln$  posterior, and 10% by the  $ln$  posterior and so on. This is shown in Algorithm 2. Once  $\alpha$  and  $\tau$  have been calculated, the relative contribution of each distribution on each day is easily obtained as shown in Algorithm 2.

*On day  $t = \alpha$*

**Step 1:** Calculate the approximate number of days remaining (given a reasonable<sup>2</sup> average thermal time) to reach the leaf number indicated by the value of  $fln_{\alpha+3} = fln_t$ :

$$\text{Time}_{\text{days}} = \tau = \frac{\text{number of leaves remaining}}{\text{rate of development}} = \left( \frac{(2 - ln_t)}{\left( \frac{TT}{0.75 \times phyllochron_t} \right)} + 1 \times \frac{(fln_t - 2)}{\left( \frac{TT}{phyllochron_t} \right)} \right)$$

$$= \frac{(2 - ln_t)(0.75 \times phyllochron_t)}{TT} + 1 \times \frac{(fln_t - 2)(phyllochron_t)}{TT}$$

**Step 2:** Calculate  $v_1 = \frac{\tau - 1}{\tau}$ ,  $v_2 = \frac{\tau - 2}{\tau}$ , ...,  $v_\tau = \frac{\tau - 3}{\tau}$ . Define  $\bar{v} = 1 - v$

**Step 3:** Weight the proportion of value toward the posterior for  $fln_t, fln_{t+1}, \dots, fln_{t+Time\text{days}}$  and  $ln_t, ln_{t+1}, \dots, ln_{t+\tau}$  as follows:

Day  $\alpha$ :  $P(\text{revised}fln_t) = v_1 P(flnt) + \bar{v}_1 P(ln_t)$

Day  $\alpha + 1$ :  $P(\text{revised}fln_{t+1}) = v_2 P(flnt+1) + \bar{v}_2 P(ln_{t+1})$

Day  $\alpha + 2$ :  $P(\text{revised}fln_{t+2}) = v_3 P(flnt+2) + \bar{v}_3 P(ln_{t+2})$

Day  $\alpha + \tau$ :  $P(\text{revised}fln_{t+\tau}) = v_\tau P(flnt+\tau) + \bar{v}_\tau P(ln_{t+\tau})$

<sup>2</sup> Since the data used here comes from a controlled climate trial this is easy to ascertain in this example.

*At this stage the posterior distribution  $ln_t$  will be substituted for that of  $fln_t$  until the simulation is complete.*

**Step 5:** *calculate the revised estimate for the variance of  $fln_t$  using the method of moments estimator derived above, based on estimated weights  $\nu$  and  $\bar{\nu}$ .*

**Algorithm 2: Calculation of  $\alpha + \tau$  and generation of the mixture distribution.**

Here,  $\alpha + \tau$  is an estimate of the day of flag leaf;  $\nu$  and its complement are the relative proportions of the distributions of  $ln_t$  and  $fln_t$  respectively; and  $TT$  and  $phyllochron_t$  have been defined in Chapter Five.

10.2.2.2 Step 3: Estimation From the Mixture Distribution

Analytical derivation of the pdf of the product of two random variables is rarely possible. In a few cases can this be done explicitly. For example, the only product of two lognormal variates would also be lognormal. One solution in general is to compute an approximation, and one way to achieve this could be the method of moments (MoM). Under fairly general conditions the method of moments allows one to find estimators that are asymptotically normal, have mathematical expectation that differs from the true value of the parameter only by a quantity of order  $1/n$ , and standard deviation that deviates by a quantity of order  $1/\sqrt{n}$ . The estimators found by the MoM are not necessarily the best possible from the point of view that their variance is minimal. Using the mixing algorithm above, the moments can be estimated for the proposed mixture with the appropriate weights  $\nu$  and  $\bar{\nu}$ . Assuming the Central Limit Theorem this can be reduced to fitting a mixture of two Gaussians. However, one problem with this approach is that the mixture distribution is unlikely to be Gaussian, particularly early in the simulation process. This is partially because the two distributions are far from being homogeneous, and also that the Gaussian assumption is unlikely to be appropriate since the densities for  $ln_t$  and  $fln_t$  appear to be quite different (Figure

36b). For this reason, a simple (although slightly more work is required for coding) alternative approach as is discussed next is preferred.

An alternative approach could be to sort and take the appropriate intervals directly from this density function at the desired day  $t$ . Note that this approach also has weaknesses in the assumptions made in development, i.e., the normal distribution  $N(\ln_t, \text{flnvar}_t)$  that is used in the calculation of the mixture distribution is still not particularly close to reality. However, it does perform better than the MoM approach (results not shown) and is therefore preferred. The “approximation distribution” approach as shown next in Algorithm 3 (code shown in Appendix A4 will be adopted for this analysis of final leaf number simulation.

*On day  $t < \alpha$*

**Step 1:** *Set mixture distribution equal to the posterior distribution of  $\text{fln}_t$*

*On day  $\alpha \geq t < \tau + \alpha$*

**Step 1:** *Calculate mixture proportions  $v$  and  $\bar{v}$  as calculated by the mixing algorithm above.*

**Step 2:** *Save simulated values  $i$  of the node of  $\text{fln}_t$ , where  $i = 1, 2, \dots, 10000$*

**Step 3:** *Calculate mean and variance of the posterior distributions of  $\ln_t$ ,  $\text{fln}_t$*

**Step 4:** *Generate 10000 random samples from a  $N(\text{fln}_t, \text{lnvar}_t)$  distribution*

**Step 5:** *Mix the new distribution with that of  $\text{fln}_t$  at the rates set by  $v$  and  $\bar{v}$  by taking the first  $v$  and  $\bar{v}$  percent of values of the two distributions.*

**Step 6:** *Sort resultant variable and calculate desired credible intervals*

*On day  $t \geq \tau + \alpha$*

**Step 1:** Set mixture distribution equal to the posterior distribution of  $ln_t$

**Algorithm 3: Approximation algorithm.**

10.2.2.3 Step 4: Prior Distributions for  $fln_t$

This Section describes some options to update the recursive prior to reflect the information available.

**Gamma( $fln_{t-1}, 1$ )**

The first piece of information in the list above is the original Bayesian hierarchical model. An obvious first step is to assess the density of  $fln_t$  through the inherent mixing of distributions that results from fitting the model. Since this variable starts relatively high and adjusts to no higher than  $lmax$  and no lower than  $lmin$ , the Gamma distribution seems like a natural first option for the prior distribution. Here  $E[X] = \frac{\alpha}{\beta}$ , and  $Var[X] = \frac{\alpha}{\beta^2}$ . The parameters are set as  $\alpha = fln_{t-1}$  and  $\beta = 1$ . This prior is implemented (model t) in the previous Chapter.

**Poisson( $fln_{t-1}$ )**

However,  $fln_t$  is a count variable (even though it is not discrete in the model outputs) so a Poisson distribution may be appropriate. Here, of course  $E[X] = Var[X] = \lambda = fln_{t-1}$ . This prior is implemented (models a - r) in the previous Chapter.

**Normal ( $fln_{t-1}, 1$ )**

Setting the prior to be Normal may be useful. Here  $E[X] = \mu = \overline{fln_{t-1}}$ , and  $Var[X] = \sigma^2 = 1$ . This prior is implemented (model s) in the previous Chapter.

### **Vague Normal ( $fln_{t-1}, 100$ )**

The previous three distributions are quite informative prior distributions. Setting the prior to be Normal with a very wide variance may allow more information from the likelihood to impact on the precision estimates of  $fln_t$ . Here  $E[X] = \mu = \overline{fln}_{t-1}$ , and  $\text{Var}[X] = \sigma^2 = 100$ . (In WinBUGS the precision is used for the Normal distribution rather than the variance in the code, and is set to  $1/\sigma^2$ ).

### **Fully recursive Normal ( $fln_{t-1}, flnvar_{t-1}$ ) distribution**

Both of the two previous prior distributions did not include an independent variance parameter. Here  $E[X] = \mu = \overline{fln}_{t-1}$ , and  $\text{Var}[X] = \sigma^2 = \overline{flnvar}_{t-1}$ . As above, the precision is used rather than the variance in the code, and is set to  $1/\sigma^2$ .

### **Uniform (6, 18)**

If there is little prior information concerning variety or sowing date then it may be appropriate to set  $lmax$  at a conservative and high value. Then, when the mixing algorithm is applied to estimate improved credible intervals, there is the additional advantage of truncating the posterior for  $fln_t$  at a value that is biologically reasonable. This is in contrast with estimates for the previous 4 prior distributions which had credible ranges far below the biologically possible lower limit of 6 leaves. It is important to remember that here the posterior for  $fln_{t-1}$  no longer enters the model on day  $t$  so this aspect of the model is no longer directly recursive.

### **Uniform (6, 8)**

If prior knowledge concerning sowing date and/or photoperiod genetics and vernalisation genetics is available, it may be reasonable to set the uniform prior with more narrow limits.



#### 10.2.2.4 Step 5: Calculate Day of Final Leaf Early and Late in the Simulation

If being used in real time, a major biological goal of interest for SIRIUS is to estimate the date of final leaf (with uncertainty estimated) as soon as possible. Whilst the date of expected final leaf ( $\alpha + \tau$ ) is not a node that can be taken directly from the Bayesian fitting method, it is possible to estimate a density post-hoc based on the information that is available. There are two dates on which these credible intervals may be of particular note. First, the predicted day of flag as soon as it has reached equilibrium. And second the simulated day of flag. These are calculated as per the following Algorithm 4 (code shown in Appendix A4):

*Predicted density for day of flag leaf at time  $t = \alpha$*

**Step 1:** *Save simulated values for the node  $fln_t$*

**Step 2:** *Calculate estimated time  $\tau$  remaining until flag leaf as in mixing algorithm above, however rather than using the mean of node  $fln_t$ , calculate  $\tau$  for each simulated value:*

$$\tau_i = \frac{(2 - ln_t)(0.75 \bullet phyllochron_t)}{TT} + \frac{(fln_t - 2)(phyllochron_t)}{TT}$$

*Where  $i = 1, 2, \dots, 10000$*

**Step 3:** *Sort resultant variable  $\tau$  and calculate desired credible intervals*

*Smoothed density for day of flag leaf at time  $t = \alpha + \tau$*

**Step 1:** *Save simulated values for the node  $ln_t$*

**Step 2:** *Calculate estimated time  $\tau$  remaining until flag leaf as in mixing algorithm above, however rather than using the mean of node  $fln_t$ , calculate  $\tau$  for each simulated value:*

$$\tau_i = \frac{(2 - ln_t)(0.75 \bullet phyllochron_t)}{TT} + \frac{(ln_t - 2)(phyllochron_t)}{TT}$$

*Where  $i = 1, 2, \dots, 10000$*

**Step 3:** *Sort resultant variable  $\tau$  and calculate desired credible intervals*

**Algorithm 4: Algorithm to calculate  $\tau$ .**

### 10.2.3 Results and Discussion

Overall, it appears that the approach described above does work to improve the posterior pdf of  $fln_t$ . For example, Figure 37 displays the evolution of the mixture distribution for  $fln_t$ . It shows how the estimated distribution begins with a rather wide range which becomes more peaked and narrow as the distribution becomes closer to that of  $ln_t$ . This mixture distribution example is based on the model

fitted with the Gamma ( $f_{n_{t-1}}, 1$ ) prior for  $f_n$ . It seems likely that the spikes in the pdf arise due to the discrete nature of the prior distribution.

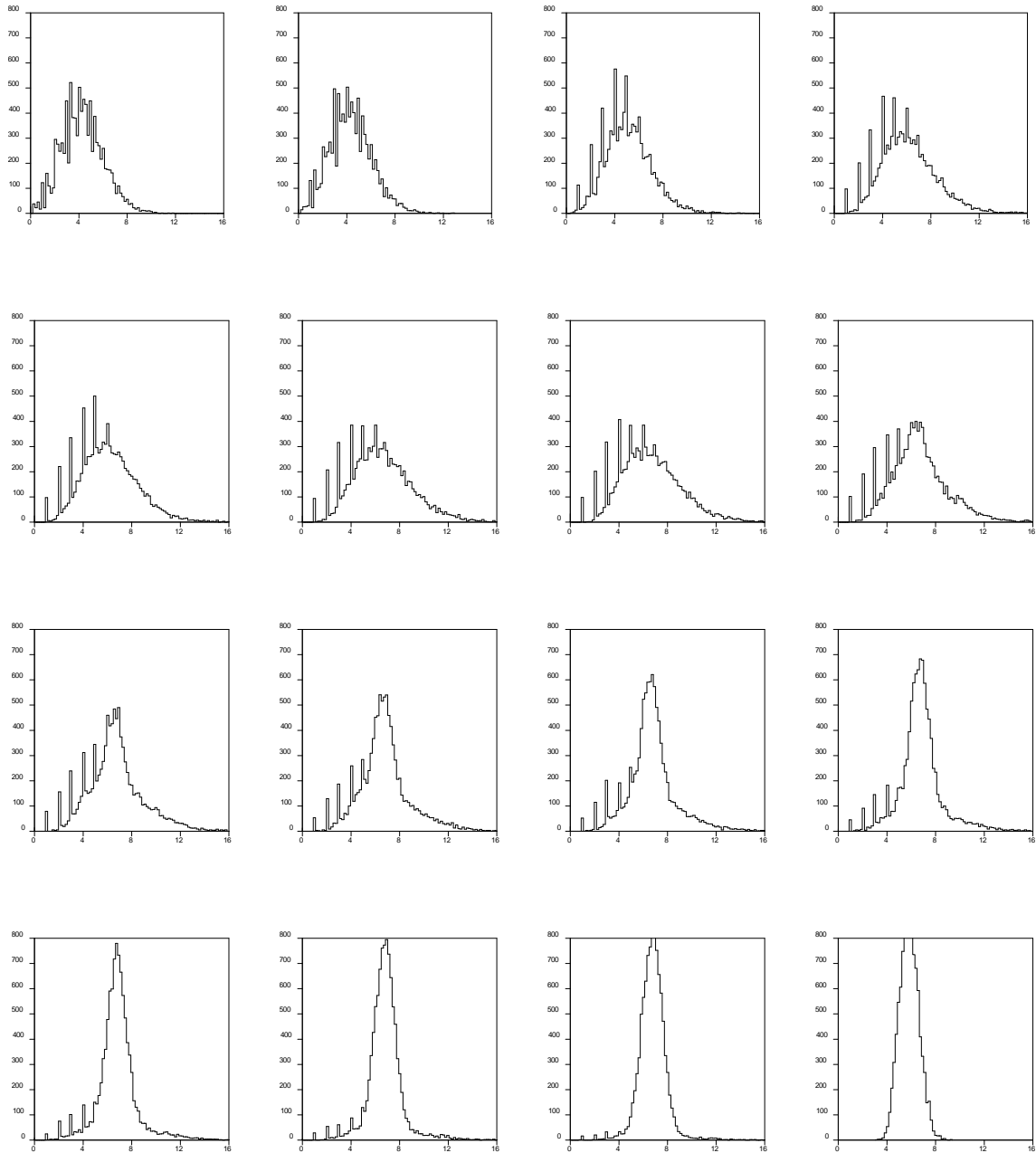


**Figure 37: Shape of Mixture density for  $f|n_t$  where  $t = 1, 3, \dots, 31$ . Frames ordered row 1, 1-4 from left to right, row 2, 5-8 from left to right and so on. Model with Gamma ( $f|n_{t-1}, 1$ ) prior for  $f|n_t$ .**

A close look at time  $t = 18$  (the day on which approximately 50% of the density is obtained from each of the two contributed densities) highlights the relationship between  $f|n_{18}$  and  $ln_{18}$ .

Figure 38 shows 1000 realisations of the Bayesian Hierarchical Model for  $fln_{18}$  and  $ln_{18}$  on the x and y axes, respectively. We can see that the distribution for  $fln_{18}$  is wider and more diffuse than that of  $ln_{18}$ .

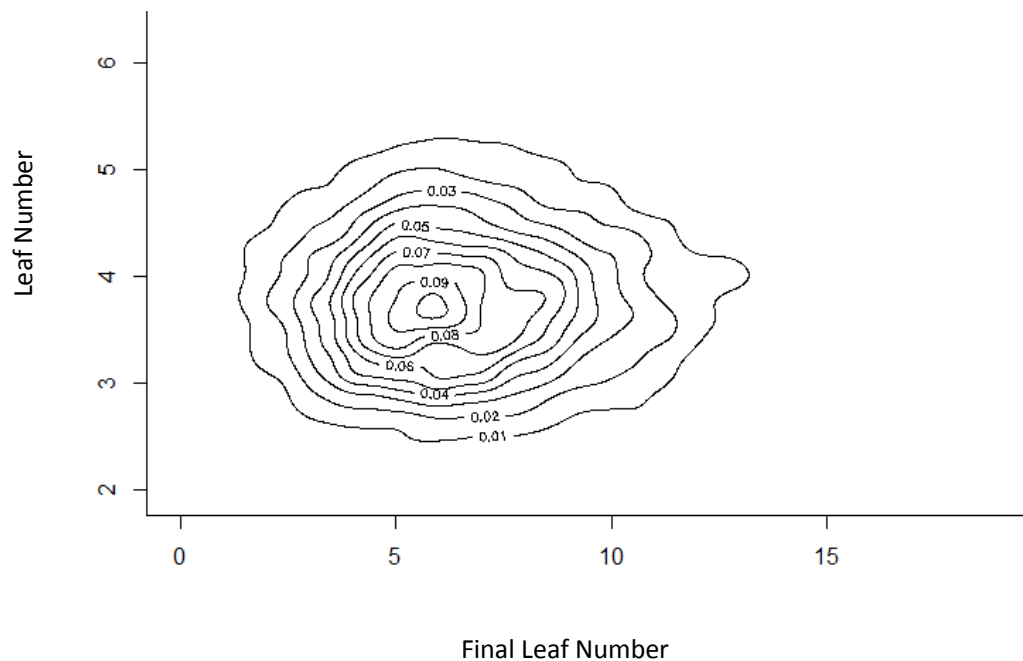
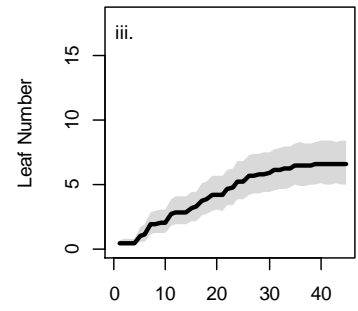
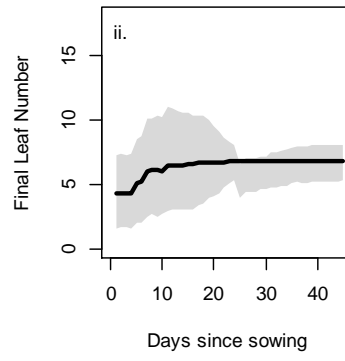
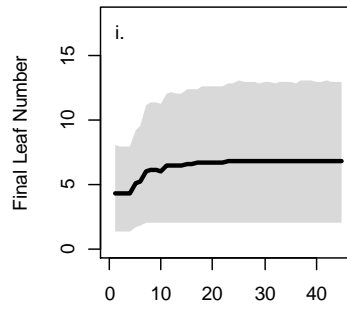


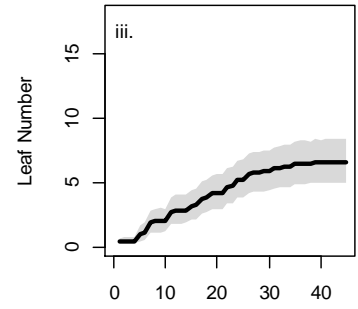
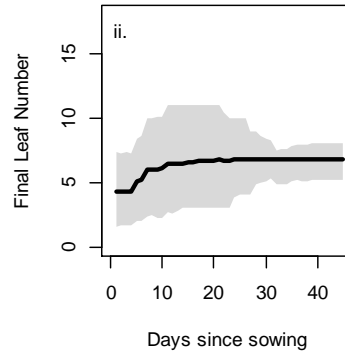
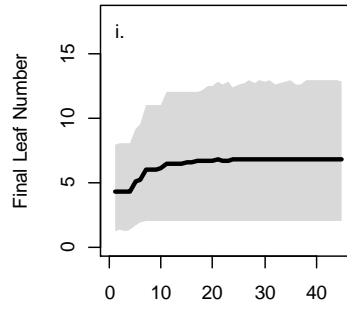
**Figure 38: Contour density plot of the model realisations for  $fln$  and  $ln$  on day 18. x-axis =  $fln_{18}$  and y-axis =  $ln_{18}$ .**

All results in Tables 20 - 24 in Section 10.2.2.3 are given for each of the 7 distributions proposed above.

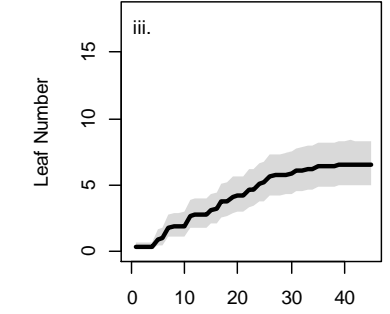
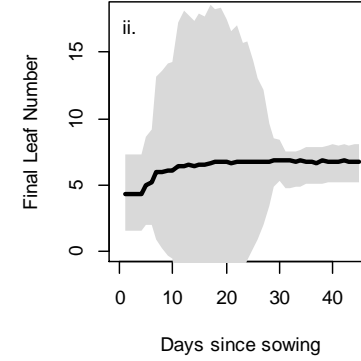
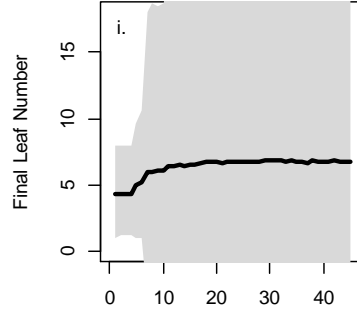
a) Gamma ( $f_{n_{t-1},1}$ )



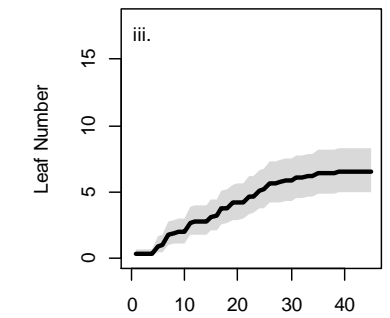
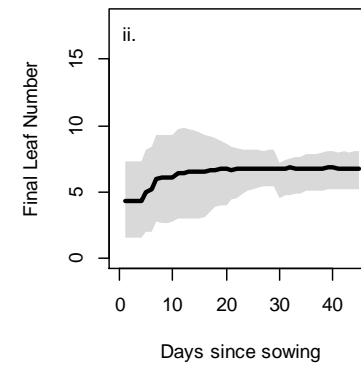
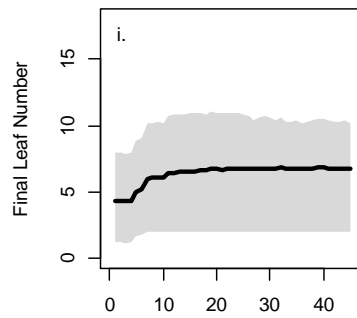
b) Pois ( $f_{n_{t-1}}$ )



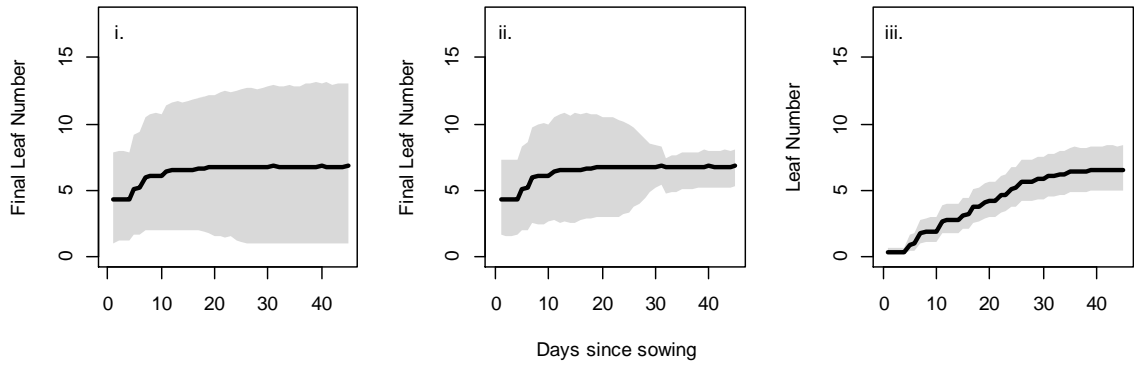
c) Normal ( $f_{n_{t-1},100}$ )



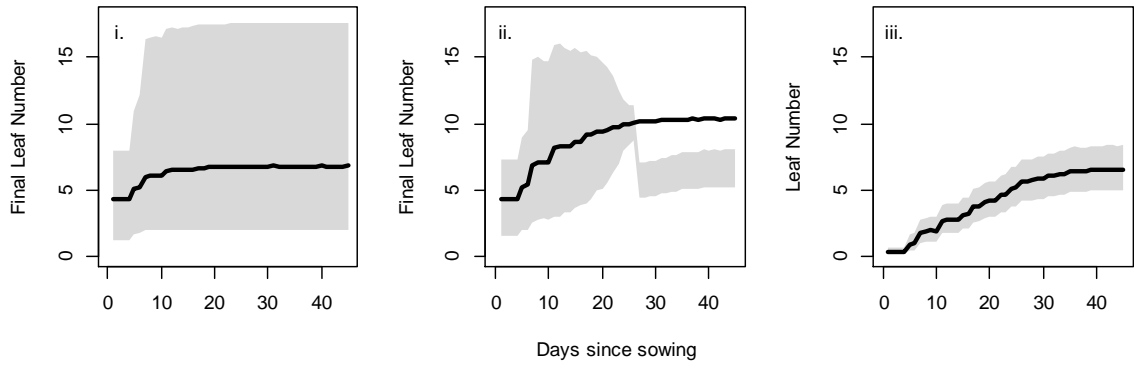
d) Normal ( $f_{n_{t-1},0.01}$ )



e) Normal ( $fln_{t-1}, fln_{var-t-1}$ )



f) Unif (6, 18)



g) Unif (6, 8)

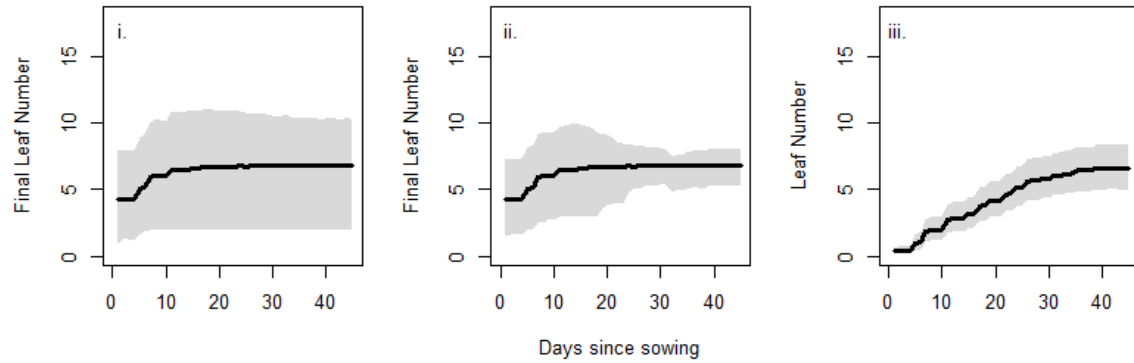


Figure 39: Estimated credible intervals for  $fln_t$  and  $ln_t$  based on several different prior distribution for  $fln_t$  for models *i.* without and *ii.* with incorporation of the mixing algorithm. Solid black line indicates the posterior estimate for  $fln_{t-1}$ , with light grey polygon indicating its credible intervals after mixture. In *iii.* the solid black line indicates posterior estimate for  $ln_t - 1$ , with light grey polygon indicating its credible intervals.

Table 20 shows the estimates of  $\alpha$  (day of equilibrium) and  $\tau$  (days remaining from equilibrium until Flag Leaf as calculated via Algorithm 1). This table shows that the values of  $\alpha$  and  $\tau$  are quite varied for the different distributions. This is because the rate at which different distributions approach equilibrium is not consistent (Figure 40i for each distribution). The posterior estimate for  $\alpha$ , the day on which  $f_{ln,t-1}$  reaches an equilibrium, is around day  $t = 11 - 15$  for each distribution excepting the winter uniform prior(6, 18).

**Table 20: alpha and tau estimates (calculated via Algorithms 1 and 2).**

Prior	Day of Equilibrium	Days remaining to Flag
	$\alpha$	$\tau$
Gamma ( $f_{ln_{k-1}}, 1$ )	11.0	13.8
Poisson ( $f_{ln_{k-1}}$ )	14.0	17.8
Normal ( $f_{ln_{k-1}}, 100$ )	13.0	18.0
Normal ( $f_{ln_{k-1}}, 1$ )	12.0	17.9
Normal ( $f_{ln_{k-1}}, f_{lnvar_{k-1}}$ )	14.0	17.7
Uniform (6,18)	7.0	19.3
Uniform (6,8)	15.0	16.8

Tables 21 and 22 show the credible intervals for the posterior density of  $f_{ln,t}$  at two time points ( $t = 13$  and  $35$ , respectively). The credible intervals are shown for each of the prior distributions described using the both original  $f_{ln}$  posterior and the mixture distribution posterior. These are calculated via Algorithm 3.

Figure 39ii for each distribution indicates an appreciable improvement in estimates for  $f_{ln}$  by the end of the simulation is afforded by inclusion of the mixing approach outlined above. Credible bounds for the estimated day of flag leaf were reduced by 23% on day 13 and by 68% on day 35 for the Normal ( $f_{ln_{t-1}}, 100$ ) prior distributions on  $f_{ln}$  at day 35. Credible bounds for  $f_{ln_{35}}$  were reduced



by 53% and 74% for the Gamma ( $f|n_{t-1},1$ ) and Poisson ( $f|n_{t-1}$ ) prior distributions respectively on  $f|n_t$  at day 35 when using the mixture distribution approach. Interestingly the credible bounds for these two distributions were wider for the mixture distribution on day 13. The credible intervals for Normal ( $f|n_{t-1},1$ ), Normal ( $f|n_{t-1}, f|nvar_{t-1}$ ), Uniform (6,18), and Uniform (6,8) prior distributions were not strongly affected on day 13, but were reduced on day 35. It is interesting to note the inappropriateness of the winter prior Uniform (6,18) for  $f|n_t$  where the state model estimate and the data are so divergent that the credible intervals do not even overlap the estimate after mixture.

**Table 21:  $f_{ln}$  statistics on day 13 of the simulation (calculated via Algorithm 3).**

Prior	Method	Predicted Credible Intervals for $f_{ln_{13}}$		Predictive Range
		Lower	Upper	
Gamma ( $f_{ln_{k-1}}, 1$ )	No mixture	6.3	12.1	5.8
Gamma ( $f_{ln_{k-1}}, 1$ )	mixture distribution	3.0	10.7	7.7
Poisson ( $f_{ln_{k-1}}$ )	No mixture	2.0	6.2	4.2
Poisson ( $f_{ln_{k-1}}$ )	mixture distribution	2.8	11.0	8.2
Normal ( $f_{ln_{k-1}}, 100$ )	No mixture	-7.6	21.6	29.2
Normal ( $f_{ln_{k-1}}, 100$ )	mixture distribution	-3.7	8.6	12.3
Normal ( $f_{ln_{k-1}}, 1$ )	No mixture	2.0	10.8	8.8
Normal ( $f_{ln_{k-1}}, 1$ )	mixture distribution	3.0	9.7	6.7
Normal ( $f_{ln_{k-1}}, f_{lnvar_{k-1}}$ )	No mixture	2.0	11.7	9.7
Normal ( $f_{ln_{k-1}}, f_{lnvar_{k-1}}$ )	mixture distribution	2.7	10.8	8.1
Uniform (6,18)	No mixture	2.0	17.2	15.2
Uniform (6,18)	mixture distribution	3.3	15.7	12.4
Uniform (6,8)	No mixture	2.0	10.8	8.8
Uniform (6,8)	mixture distribution	3.0	9.9	6.9

**Table 22:  $fln$  statistics on day 35 of the simulation (calculated via Algorithm 3).**

Prior	Method	Smoothed Credible Intervals for $fln_{35}$		Smoothed Range
		Lower	Upper	
Gamma ( $fln_{k-1}, 1$ )	No mixture	6.7	12.9	6.3
Gamma ( $fln_{k-1}, 1$ )	mixture distribution	4.9	7.8	2.9
Poisson ( $fln_{k-1}$ )	No mixture	2.0	12.9	10.9
Poisson ( $fln_{k-1}$ )	mixture distribution	5.1	7.8	2.8
Normal ( $fln_{k-1}, 100$ )	No mixture	-10.9	24.7	35.6
Normal ( $fln_{k-1}, 100$ )	mixture distribution	5.1	7.9	2.8
Normal ( $fln_{k-1}, 1$ )	No mixture	2.0	10.4	8.4
Normal ( $fln_{k-1}, 1$ )	mixture distribution	5.1	7.9	2.7
Normal ( $fln_{k-1}, flnvar_{k-1}$ )	No mixture	1.0	12.9	11.9
Normal ( $fln_{k-1}, flnvar_{k-1}$ )	mixture distribution	5.1	7.9	2.8
Uniform (6,18)	No mixture	2.0	17.5	15.5
Uniform (6,18)	mixture distribution	5.1	7.9	2.8
Uniform (6,8)	No mixture	2.0	10.4	8.4
Uniform (6,8)	mixture distribution	5.1	7.9	2.8

Table 23 shows the predicted and smoothed predicted day of flag as calculated from the density via Algorithm 4. Figure 40 shows the density for  $\tau$  based on several prior distributions for  $fln_t$  for (left) predicted at  $day = \tau + \alpha$  and (right) smoothed at  $day = 35$ . The estimated value of  $\tau$  is an important parameter since the value of  $\tau + \alpha$  is an early estimate of the day of Flag leaf. The estimate of the date of final leaf according to the data is 36.13 (34.04, 38.21)<sup>3</sup> based on 8 observations. However, the predicted day of final leaf (on  $t = 13$ ) is lower than this. However, the credible intervals at this time are fairly wide for all prior distributions. The smoothed estimate is closer to the data, with credible intervals that overlap the data range (if not the data itself). This reflects the findings in the previous Chapter which indicates that the filtered estimates are of  $ln_t$  at the end

<sup>3</sup> 95% Confidence Interval

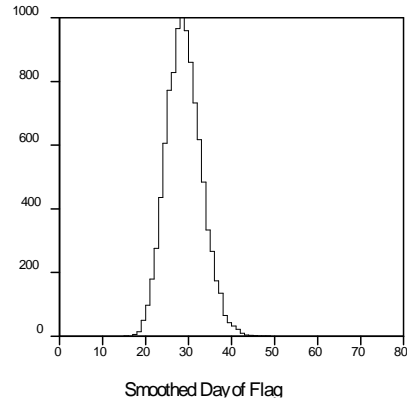
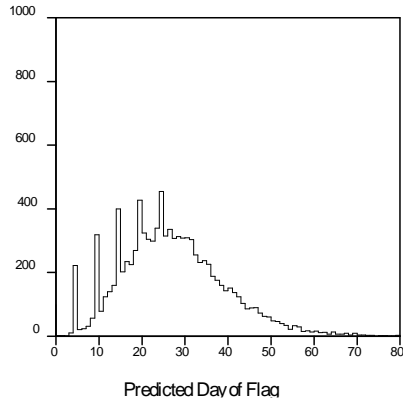
are slightly lower than the mean of the data for this data set. The densities for  $\tau$  shown in Figure 41i show the higher uncertainty before the seven pieces of extra information are included updating, smoothing, and narrowing the density in Figure 40ii.

**Table 23: Credible intervals for predicted and smoothed Day of Flag (calculated via Algorithm 4).**

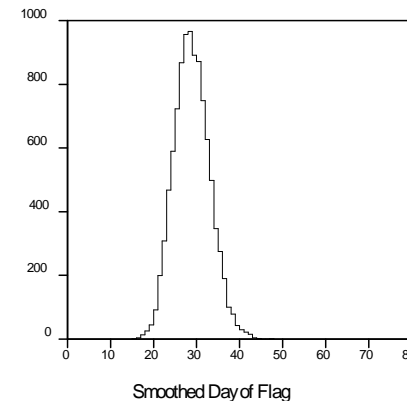
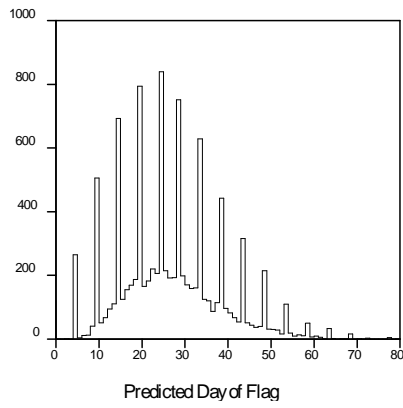
Prior	Predicted Day of Flag	Predicted Credible Intervals of Day of Flag (at $t = \alpha$ )		Smoothed Day of Flag	Smoothed Credible Intervals of Day of Flag (at $t = \alpha + \tau$ )	
		Lower	Upper		Lower	Upper
Gamma ( $fln_{t-1}, 1$ )	26.8	11.8	42.9	28.9	23.9	34.3
Poisson ( $fln_{t-1}$ )	26.4	10.4	43.6	28.9	23.7	34.2
Normal ( $fln_{t-1}, 100$ )	25.6	-1.3	57.9	29.0	23.9	34.4
Normal ( $fln_{t-1}, 1$ )	24.6	11.9	35.2	29.0	23.8	34.4
Normal ( $fln_{t-1}, flnvar_{t-1}$ )	26.3	10.4	42.1	29.0	23.8	34.4
Uniform (6,18)	26.3	12.7	44.6	29.0	23.9	34.3
Uniform (6,8)	24.3	11.6	34.5	29.0	23.7	34.4



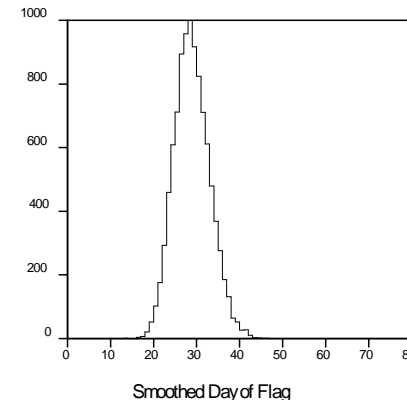
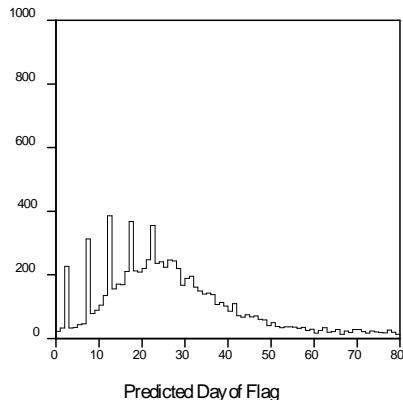
a) Gamma ( $f_{t-1}, 1$ )



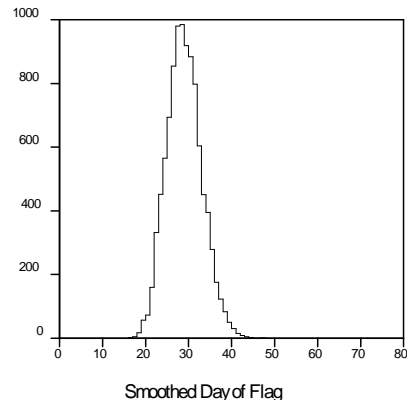
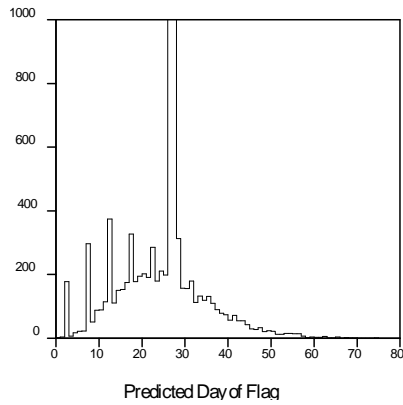
b) Pois ( $f_{t-1}$ )



c) Normal ( $f_{t-1}, 100$ )



d) Normal ( $f_{t-1}, 0.01$ )



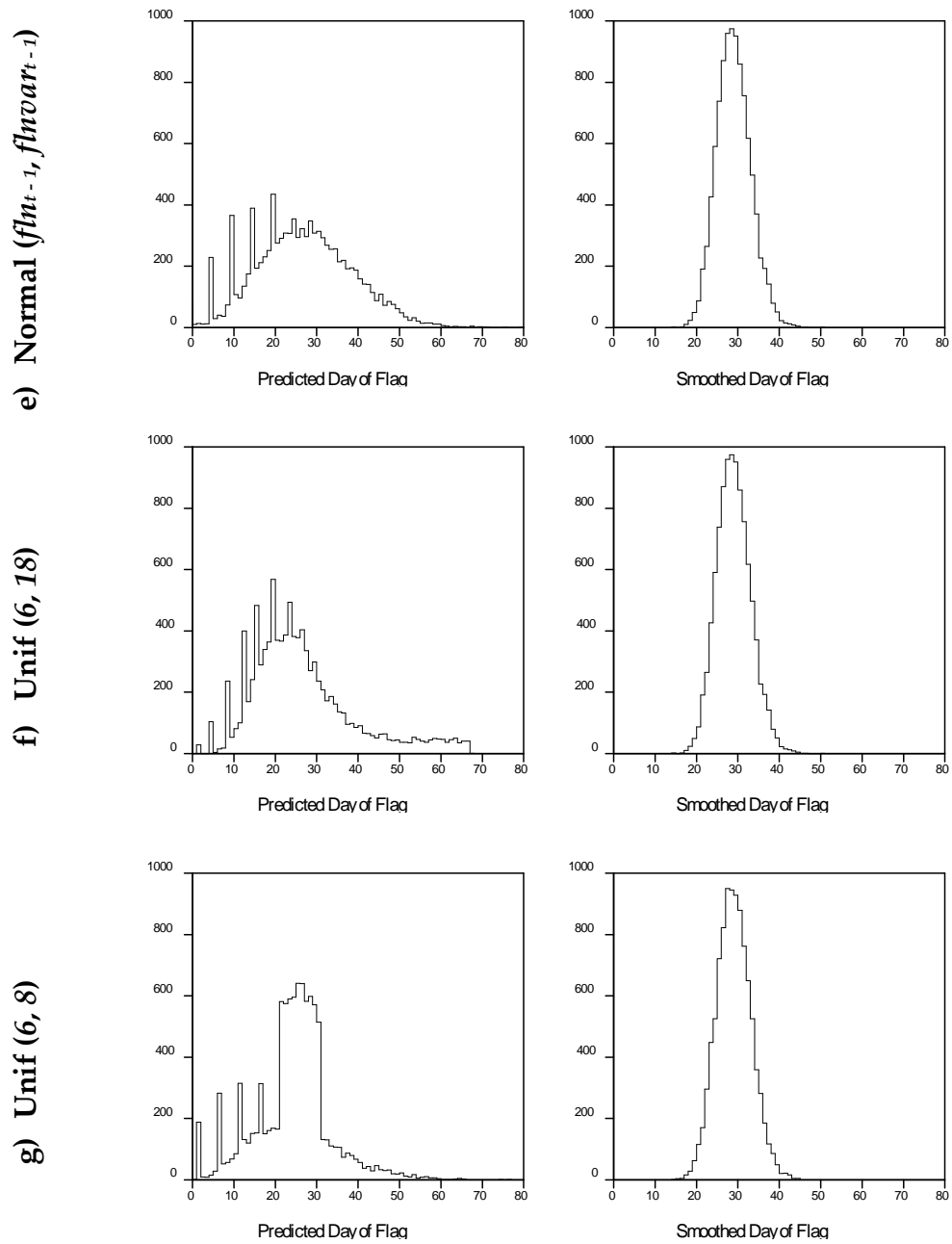


Figure 40: Density for  $\tau$  based on several prior distributions for  $fln_t$  for (left) predicted at  $day = \alpha$  and (right) smoothed at  $day = t = 35$ .

Overall, the Gamma, Poisson, and fully recursive Normal distributions are probably more reliable prior choices as they allow both direct inclusion of information from  $fn_{t-1}$ , in the state model filtered estimation process, and are biologically sensible choices Figure 39 (i and ii) (a, b, and e). The issue seen in Figure 39 i (f) with the Uniform (6, 18) prior distribution would be unable to occur with a recursive prior. Further, the estimates for  $ln_t$  are not negatively impacted by switching between these three prior distributions Figure 39iii (a, b, and e). The uninformative Normal and winter uniform distributions are poor choices leading to extremely wide credible intervals for  $fn_t$  Figure 39 i (c and f). Similar conclusions apply to the ability of the model to predict date of final leaf, Figure 40 and 21.

## 10.3 Sensitivity Analysis of Latent State Equations

### 10.3.1 Method

This Section is based on the work of Strong et al. (2012). Here we aim to allow a probabilistic sensitivity analysis of the state equations of the model. Structural uncertainty is defined as uncertainty in the outputs of the model  $f(\bullet)$  due to inaccurate or incomplete specification of the real world process in the state-equations and their interactions. Within the model framework already specified it is possible to explore the relative impact of allowing variation in structural equations  $Z_t$ . This is simply achieved through specification of a vague pdf for one or more of  $Z_t$ . For example, in the model code the **highlighted** code could be **replaced by** in Figure 41 below:



```

'model',\
'{' ,\
'for(i in 1:8){',\
'LN.k[i] ~ dpois(mu.ln.k)',\
'}',\
',\
'log(mu.ln.k) <-log(ln.k)',\
',\
'a[1] <- step((2 - (ln.kkmin1)))',\
'a[2] <- step((8 - (ln.kkmin1))) - step((2 - (ln.kkmin1)))',\
'a[3] <- min((1 - (a[1])),(1 - (a[2])))',\
'phylln.k <- (a[1]*0.75*bp + a[2]*bp + a[3]*1.3*bp)',\
'phylln.kk <- (a[1]*0.75*bp + a[2]*bp + a[3]*1.3*bp)',\
'phylln.k ~ dnorm (phylln.kk,0.001)\
',\
'd[1] <- step(((TT.k/phylln.kmin1) + ln.kkmin1) - fln.kmin1)',\
'd[2] <- 1 - d[1]',\
'ln.k <- d[1] * fln.kkmin1 + d[2] * ((TT.k/phylln.k) + ln.kmin1)',\
',\
'primn.k <- pn *ln.k + pe',\
',\
'b[1] <- step ((PP.k - ppsat))'\
,\
'b[2] <- 1 - b[1]',\
'flnt.k <- lmin',\
',\
'c[1] <- step ((primn.k - (flnt.k + pe)))',\
'c[2] <- 1 - c[1]',\
'e[1] <- step((primn.k - flnt.k))',\
'e[2] <- 1 - e[1]',\
'fln.k <- c[2] * (e[1] * flnt.k + e[2] * primn.k) + c[1] * (fln.kkmin1)',\
',\
'bp ~dnorm (110,1)',\
'pe ~dpois (4)',\
'pn ~dpois (2)',\
'ppsat ~dnorm (15.9 ,0.01)',\
'lmin ~dgamma (7,1)',\
'ps ~dnorm (0.625,0.01)',\
',\
'ln.kmin1 ~ dpois(alpha.ln.kmin1)',\
'ln.kkmin1 <- alpha.ln.kmin1',\
'fln.kkmin1 ~ dgamma(flnt.kmin1,1)',\
'})'

```

**Figure 41: Jittering model code.**

### 10.3.2 Results

The impact of allowing the ‘jittering’ of the ‘sub-functions’ (as they are called by Strong et al. (2012)) can then be assessed as shown in Table 24 below. In this table there are 4 models: Model 1 is the baseline, model 2 is the baseline with additional variation for the *primordia<sub>t</sub>* state equation, model 3 is the baseline with additional variation for the *phyllochron<sub>t</sub>* state equation, and model 4 is the baseline with additional variation for the *flnt<sub>t</sub>* state equation. Table 24 provides the estimate and 95% credible intervals for each state equation node arising from model **t** as described in Table 18 & Table 19 in Chapter Nine. Five UE outcomes are presented next:

1. For the *flnt<sub>45</sub>* node, the credible intervals for models 2 and 4 are much wider than that of the baseline. The mean estimate for model 4 is ~30% greater than that of the baseline. It appears that jittering the phyllochron base equation does not strongly affect the *fln<sub>45</sub>* node (e.g. *fln<sub>45</sub>* is not sensitive to changes in *flnt<sub>45</sub>*, but it is sensitive to changes in *primordia* and *flnt<sub>45</sub>*,
2. *flnt<sub>45</sub>* is only sensitive to changes in the state equation *flnt<sub>45</sub>*,
3. *ln<sub>45</sub>* is not sensitive to changes in any of the state equations. This may be due to the presence of data to pull predictions into line,
4. *phyllochron<sub>45</sub>* is only sensitive to changes in the state equation *phyllochron*,
5. *Primordia<sub>45</sub>* is only sensitive to changes in the state equation *primordia*.

**Table 24: Results of jittering analysis.**

Model	$Z_t$ jittered	$Y_t$	mean	2.50%	97.50%
1	model t	$fln_t$	6.83	2.00	12.96
2	$primordia_t$	$fln_t$	5.39	-8.58	12.82
3	$phyllochron_t$	$fln_t$	6.76	2.00	12.83
4	$flnt_t$	$fln_t$	10.14	2.00	20.28
<hr/>					
1	model t	$flnt_t$	6.99	2.82	13.07
2	$primordia_t$	$flnt_t$	6.98	2.80	13.02
3	$phyllochron_t$	$flnt_t$	7.03	2.82	13.09
4	$flnt_t$	$flnt_t$	7.11	-13.08	27.76
<hr/>					
1	model t	$ln_t$	6.58	5.02	8.35
2	$primordia_t$	$ln_t$	6.58	5.01	8.36
3	$phyllochron_t$	$ln_t$	6.58	5.02	8.34
4	$flnt_t$	$ln_t$	6.59	4.98	8.36
<hr/>					
1	model t	$phyllochron_t$	110	108.00	112.00
2	$primordia_t$	$phyllochron_t$	110	108.00	112.00
3	$phyllochron_t$	$phyllochron_t$	110	103.50	116.80
4	$flnt_t$	$phyllochron_t$	110	108.00	111.90
<hr/>					
1	Int+flnt	$primordia_t$	17.29	2.00	39.84
2	$primordia_t$	$primordia_t$	17.32	-8.58	46.18
3	$phyllochron_t$	$primordia_t$	17.22	2.00	39.79
4	$flnt_t$	$primordia_t$	17.21	2.00	39.53

## 10.4 Summary

The heterogeneity of densities for  $ln_t$  and  $flnt_t$  for the MoM approach would be expected to result in wider credible intervals early in simulation. For this reason, this methodology was rejected in favour of the approach that, directly sampled from an approximate mixture distribution of  $ln_{13}$  to  $ln_{35}$ . This approach depends on sampling from the simulated data to follow a prior mixture distribution and so depends on the normal distribution  $N(ln_t, flnvar_t)$  that is used in the calculation of the mixture distribution mixture distribution being appropriate. However, this

approach allowed greater precision of predicted day of flag at an earlier date for some prior distributions, and at the day of flag for most prior distributions for  $fln$ .

These results indicate that selecting the Gamma, Poisson, and fully recursive Normal distributions as prior distribution for  $fln$  are probably more reliable prior choices as they allow direct inclusion moments from  $fln_{t-1}$ , in the state model filtered estimation process. The credible intervals in the case without mixture do fall below the current estimator of  $ln_t$  which is not biologically sensible, and this is a problem with the original model given in the previous Chapter. The Uniform distributions are naturally able to avoid this issue with careful selection of parameters; however they do not allow the same flexibility in recursively fitting today's prior as yesterday's posterior. The approximate mixture distribution solutions both solve this problem, whilst also providing sensible estimates for  $\tau$ . Finally, probabilistic sensitivity analysis of the state equations indicated that although  $ln_{45}$  is not sensitive to jittering in any of the other state equations,  $fln_{45}$  is sensitive to changes in  $primordia_{45}$  and  $flnt_{45}$ .

This Chapter has provided predicted and smoothed estimates for day of flag, an important biological indicator for wheat development computer simulation models. It has also explored the sensitivity of estimates to structural uncertainty. Combined with the benefits described in the summary of the previous chapter, the solutions put forward in this Chapter provides insight for model UE; whether it is calibration, sensitivity analysis or prediction. The illustration of the UE framework and UE techniques discussed in Section III highlight the value and flexibility of both the framework and the Bayesian data assimilation approach to quantifying multiple sources of uncertainty. These outcomes should provide a valuable contribution to the crop modelling community, particularly in New Zealand.



## Section IV - Conclusions

### Chapter Eleven: Conclusions

#### 11.1 Introduction

Deterministic, dynamic farm systems models built in computer code have played an important role in agronomic and agricultural research for over four decades. They are built via a process of hypothesising mechanisms for observed responses in the real world, empirically testing the hypotheses, and combining them to construct computer simulation models. This process results in a valuable research tool that provides insight into how a system responds and how individual mechanisms interact (Jamieson and Ewert 1999). Such models have value in many situations, particularly where access to observational data may be difficult or impossible to obtain. They can be used to simulate an experiment prior to carrying it out, or to make scientific judgements about phenomena that cannot currently be studied experimentally (Trucano et al. 2006). Farm management, environmental policy, development and research into climate change are three domains where such information can save money and other resources, or provide insight that would be otherwise impossible to obtain (Rosenzweig et al. 2013; Teixeira et al. 2015).

However, the complex combination of multiple mechanisms with simulations can make it difficult to evaluate the many potential sources of uncertainty in simulated output data (Rotter et al. 2011). The use of complex computer simulation models is ubiquitous in almost all domains of scientific discovery, so unsurprisingly managing uncertainty in complex models is also very topical. However, the large number of methodological options for model uncertainty

evaluation (UE) can make it difficult to select the appropriate technique when undertaking an analysis.

The objective of this research project is therefore to explore the *definition, sources, quantification, and management* of uncertainty as it occurs in bio-physical agricultural computer simulation models. One important aim is to provide recommendations from a formalised statistical viewpoint on management of uncertainty for a relatively small pool crop modelling community in New Zealand who work with farm systems models that describe temperate, island-based environmental conditions. An equally important goal is to identify and implement ways in which to provide computer simulation predictions complete with uncertainty bounds. Whilst sensitivity analysis is usually the most obvious pathway to achieve this, I ideally wanted to quantify the aleatory source of uncertainty,  $\epsilon$ . Further, although multi-model ensemble techniques to assess uncertainty (particularly structural uncertainty) have been of particular interest to agricultural model researchers in continental regions with a large pool of researchers such as Europe, in New Zealand this approach may be less practical. My focus therefore was to improve understanding of uncertainty in a single model. This also facilitates learning about the ability of the model to simulate the system under study.

This concluding Chapter will describe what has been done to achieve objectives and tie-together results from each aspect of my work. It will address how this work has added value, limitations, and future directions in modelling UE.

## 11.2 What Was Done

The first aspect of achieving my objective is to cohesively describe and assess information around model uncertainty that is already in the public domain. As stated above, this is a very topical research subject in many areas of scientific

discovery, including agriculture (Boote et al. 1996; Sinclair and Seligman 2000; Jamieson et al. 2007; Cooper et al. 2009; Hochman et al. 2009; Bezlepkina et al. 2010; Teixeira et al. 2011; Teixeira et al. 2013; Holzworth et al. 2014). However, not all fields of research face the same problems in terms of principal types and sources of uncertainty. For this reason, it is unlikely that all techniques will have equal value for all applications. The decision as to which techniques are of greatest value is therefore dependent on all the *other* information that is available. As such, there is a need for a clear UE framework that formally promotes careful and systematic curating of information, diagnosis of important sources of uncertainty, and identification of UE objectives. I have built upon similar themes in the literature (Refsgaard et al. 2007; Uusitalo et al. 2015) to create such a framework, set in a formal state-space structure (Gordon et al. 1993; Cressie and Wikle 2011). The state-space structure is of value because it provides a pathway for a clear, objective allocation of each source of uncertainty in a time-step model early in the analysis process. The UE framework links qualitative and quantitative analysis through a review of classical and modern techniques for generating and analysing data from computer simulation models, with the appropriate techniques identified on the basis of available information, primary sources of information, and the objective of the analysis. Examples include sensitivity analysis (Saltelli et al. 2000), data assimilation (Kalnay 2003), or multi-model ensembles (Wallach et al. 2014). It is important to note that this UE framework should not be seen as a static construct. Details are likely to require refinement as the field moves forward.

Besides being tools for research into novel situations, crop models act as constructs upon which researchers continue to develop mechanistic understanding of real world systems. An example of this is a recent paper by Brown et al. (2012b), who used the crop model APSIM (Holzworth et al. 2014) to



characterise the developmental phenotype of different wheat varieties. An important aspect of UE is therefore to identify biological processes that are not accurately represented in the model. In this thesis, the wheat development model SIRIUS was carefully described following He et al. (2012) and used as a case study throughout sections II and III. When the SIRIUS model was built, it was based upon historical, *phenological* characterisations (such as used by the model AFRCWHEAT (Porter 1993)) of the joint processes of growth and development of wheat in response to the presence of temperature and daylight. The SIRIUS model built upon and fine-tuned these characterisations to create a new paradigm of model that is based on *physiological* mechanisms that well describe observed experimental data. Models are still evolving, with recent work beginning to additionally incorporate *genetic* information to help describe differing physiological responses under different conditions and for different cultivars (Brown et al. 2013)<sup>1</sup>. One biological process that was identified as not being experimentally confirmed during model building of either SIRIUS or the new genetic/physiological model is the development of the wheat plant prior to emergence and exposure to daylight. SIRIUS has modelled development of the plant between sowing and emergence as a constant relationship between organ numbers and accumulated thermal time. Given this, we hypothesised that deeper sown seeds will take longer to reach the surface, will have greater numbers of organs at primordia, and will therefore develop more leaves before becoming reproductive. However, results from our experimental work did not support this hypothesis. Rather, later exposure to daylight resulted in fewer leaves in spring varieties. These outcomes do however fit well into the new genetic/physiological model (Brown et al. 2013). An alternative mechanism based on the vernalisation

---

<sup>1</sup> This model has not been implemented in code at this time.

genes Vrn1 – Vrn3 (Trevaskis et al. 2007a) was proposed as follows. Vrn1 begins to express in low concentrations from the time of imbibition. As such, a later emerging crop will have already expressed more Vrn1 at the time of emergence, so will not only suppress Vrn2 earlier, but will also prevent Vrn2 from increasing the vernalisation target. This expected differential relative expression of Vrn1, Vrn2, and Vrn3 based on the time at which Pp is perceived directly relates to final leaf number, and hence the time at which the plant becomes reproductive. This provides a mechanism to explain why plants that are down at greater depth will have a lower final leaf number even though the number of primordia at the time of light perception was higher. This work represents a reduction in *structural* uncertainty that can at a future date be incorporated in a computer simulation model.

The final contribution of this dissertation centres on the final stage in the seven-step UE framework – analysis of simulated data. Specifically, to provide credible intervals that incorporate an indication of *aleatory* uncertainty (as well as input parameter and structural uncertainty). A probabilistic Bayesian hierarchical model fitted with MCMC (Gelman et al. 2006) is the best paradigm to date to combine data, probability, expert opinion, and a state-space model to achieve this objective (Cressie and Wikle 2011). It is a general form of data assimilation that recursively updates state predictions based on whatever data is available to provide the best estimate possible. It also incorporates expert opinion on input parameters as identified in the UE framework, pooling them with observed data to provide credible intervals of wheat development through time. This approach maximises available information in a cohesive way to provide a unified estimate of model output uncertainty. One important biological finding from the Bayesian data assimilation model was the conclusion that collecting cultivar intensive data to provide accurate input parameter data for the phyllochron (*bp*) of different

wheat cultivars will have a strong impact on the ability of SIRIUS to make accurate predictions. This approach also has several beneficial side effects. One is that exploring uncertainty related to the scientific understanding (structural uncertainty) of one or more of the processes within the deterministic model can be easily achieved by incorporating prior distributions. A second side effect of particular relevance for SIRIUS relates to the ability to estimate credible bounds of latent variables using available prior information. For SIRIUS, accurately predicting the final leaf number is of particular interest, however it is impossible to observe prior to the date of flag leaf. I was able to estimate and reduce credible bounds for the estimated data of final leaf number both early and late in the simulation process using additional information.

### 11.3 The Pathway

The combination of considering previous research, historical and sensitivity analysis, and data assimilation modelling has resulted in the focus of the project around the UE framework. Holding all the different details, types/sources of uncertainty, information, and model components together was extremely challenging without some form over-arching framework in which to curate and store information. There are many excellent resources that discuss and describe the different types of uncertainty (Sacks et al. 1989; Arulampalam et al. 2002; Kurowicka and Cooke 2006; Saltelli et al. 2006; O'Hagan 2008; Oberkampf and Roy 2010; Montanari 2011; Wallach et al. 2014). Others describe the conceptualisation of time-step models in a state-space structure (Gordon et al. 1993; Spiegelhalter and Best 2002; Cressie and Wikle 2011). Others again put forward plans and frameworks for UE (Refsgaard et al. 2006; Refsgaard et al. 2007; Uusitalo et al. 2015). However, as far as I could ascertain, none combined the three aspects to explicitly describe and allocate each type of uncertainty within a state-space structure and then curate available information *prior* to

diagnosing principal sources of uncertainty and setting or adjusting analysis objectives in the light of actions. This framework, particularly the compartmentalisation of types and sources of uncertainty, is an exciting outcome of this project.

## 11.4 Key Outcomes - UE Framework

Planning and design of experiments to allow inference is one of the major tools of empirical science (Hacking 1975), and although the analysis of computer simulation models is less familiar, many of the same principles apply. The UE framework encapsulates how experimental planning can and should be carried out for computer simulation models. Use of the UE framework by crop modellers commencing upon an uncertainty evaluation of a model will help save time and resources, and add confidence in conclusions by ensuring that available information is not overlooked, but rather is utilised as well as possible. This will ensure that minimal time will be spent back-tracking and re-doing simulations.

The value added by a thorough UE of a model can have very real implications. First, it ensures that all available information is collected, stored, and considered holistically. Second, it forces the analyst to identify and consider all possible sources of uncertainty. Third, it allows objectives to be framed after all sources of uncertainty have been summarised, ensuring clarity in what will be achieved prior to expenditure of time and resources. Fourth, it is based on a Design of Experiments foundation by which to conceptualise the response surface of the model. This should provide justification to end-users that the simulated data is representative to the best of the analyst's knowledge and the model's capability. Fifth, and finally, it provides a reference source of up-to-date analysis techniques, offering assurance that there is not some 'better' option out there that would be more fit-for-purpose.

Exploration of deterministic model uncertainty is a relatively new scientific activity and is still evolving rapidly. Formalised guidelines describing what UE should encapsulate will provide confidence at each stage of the model's life, from building, to assessment; and through to extension for research, management and policy applications.

## 11.5 Key Outcomes - Bayesian Data Assimilation

Unlike sensitivity analysis tools, Bayesian data assimilation techniques are not commonly used in the agricultural domain, although there are exceptions to this rule. Whilst sensitivity analysis is an excellent tool for *understanding* a model, and usually straightforward to implement, the ability to incorporate and pool most types and sources of uncertainty that is offered by the Bayesian data assimilation approach provides a far more complete summary of uncertainty. As such, it can provide unparalleled insight into and confidence in model predictions. At the current stage of technology, whenever this approach is practicable, it should be considered to be the 'gold standard' approach.

## 11.6 Further Work and Limitations of the Research

Results of the data assimilation modelling of SIRIUS indicated that the impact of incorrect specification of *bp* had a relatively large impact on model predictions. Experimental work to characterise this input parameter for more wheat cultivars is underway as part of a separate project within PFR.

Future work may include updating a computer simulation model to incorporate the genetic/physiological drivers of wheat development described above. Part of this could be to incorporate the new hypothesised mechanism for wheat development from the time of imbibition, rather than from emergence as is currently implemented in SIRIUS.

As the primary outcome of this project is the UE framework, exploring/confirming the generalisability of this approach is likely to represent an important component of my post-doctoral work.

None of the work in this thesis addresses the impact of spatial scaling/aggregation on model output uncertainty; whether via calibration or sensitivity analysis. This is an area at which upcoming research projects are aimed.

Although the value of the recursive Bayesian model is great, a clear limitation with this approach is that it does require appropriate, time-step data, and may become increasingly difficult to implement with increasing model complexity. Further, a certain level of specialised knowledge around the elicitation of expert opinion and implementation of Bayesian modelling is required.

## 11.7 Conclusion

This dissertation has built on a diverse body of research concerning uncertainty in deterministic models from across a wide range of research domains. In the context of a single, bio-physical agricultural model, the complex combination of information relating to such models has been given a concrete foundation upon which to build a robust analysis. The ability to *define, compartmentalise, quantify, and manage* uncertainty sits naturally within this framework. Given the strong foundation, the analysis aspect of the framework is itself flexible enough to take advantage of available information to holistically resolve research objectives. This should provide modellers and end-users with confidence that the analysis of the model is fit-for-purpose. Finally, the ability to incorporate many types of uncertainty to provide point estimates with pooled credible bounds started out as the highest priority for this research project. The Bayesian hierarchical modelling paradigm, whilst not without its limitations, is the best technique to date to

achieve this goal, and the successful implementation of this model is the highlight of this project.

# Appendices

## A1: GenStat Code for Photoperiod response analysis as described in Chapter Six

```
"Tuesday 6 December 2011
Historical data analysis
'The flowering time model; parameterisation and uncertainty'"

"'The influence of daylength on final leaf number in spring wheat'
I.R. Brooking et al, Field Crops Research, 1995"

"This paper describes a new way of considering the daylength response in
wheat: that the plant responds to environmental drivers such as
photoperiod as its leaf and spikelet primordia develop. It goes on to
suggest a daily updating procedure that responds to environmental
drivers. This procedure was slightly adjusted in the latest version of
SIRIUS by Pete Jamieson and Mikhail Semenov."

"Data set:
+ 6 sowdates (2.6; 24.7; 18.9; 25.11; 21.2; 5.5)

+ 11 wheat cultivars with range of vern and pp responses
  - only 4 were used in paper, Otane, Rongotea, Batten, CRSW6, because
    they are spring wheat varieties.
  - this was tested by recording LNfinal for plants grown in the dark
    for 0,2,4,6 weeks at 6 degrees then transferred to inductive
    conditions. There was no evidence of a difference in LNfinal;
    confirming correct specification of vernalisation requirement.

+ randomised split plot design, with SD as main and cult as split

+ at 10-15 day intervals, 5 plants were sampled/pot and Haun stage and #
prim were counted

+ at final sampling event LNfinal was counted.

+++ hence, two data sets to investigate; developmental data and final
leaf number data +++

all data stored in Phen89Ians.xls
some developmental data information in IRBRONG.xls by Pete.

unfortunately block and plot information is missing for developmental
data.

need to use field layout data if Ian can find it. would need this to
properly merge developmental data with FLN data,
but it is only present for FLN data set, which means that we can only
get the mean haun stages, prim #'s, etc.
this is a concern because it defeats the purpose of this historical
analysis; which is to better understand these uncertainties.
there are 6 obs for each treat, which would indicate 2 values/plot, but
this is odd because the paper says they sampled 5 plants
```



per plot, so would expect either 3 or 15 obs/treat....talked to ian, he says its a mistake in the paper; there were only 2 sampled during course of the trial; and 5 at the FLN count.

To deal with the above problem; and based on the assumption that data is recorded in replicate order, main plots and split plots are randomly allocated within these.

This assumes uniformity within reps and main plots - i.e. the fact that they are not in the right place within a rep/main plot (but are in the reps and main plots with the right individuals/other plots) is ok.

1a and 2a deleted from FLN set; they are subsets for some reason Ian doesn't remember.

"

"

Analyses/Objectives:

plot (LNfinal) against (daylength at haun stage 1.5) determines when plants responded to daylength to fix LNfinal

plot (LNfinal) against (daylength at initiation of final leaf primordium (FLP))

plot (LNfinal) against (daylength at 2 haun stages after initiation of FLP)

plot (LNfinal) against (daylength at mean daylength between FLP and terminal spikelet)

Linear regression of LN final against each of 4 above daylength measures.

"

```
sload 'Final Leaf Number.gsh'
\restrict data set to include only relevant cultivars; 1,3,5,11
sload 'Final Leaf Number rest.gsh'
```

```
sload 'Developmental.gsh'
\restrict data set to include only relevant cultivars; 1,3,5,11
sload 'Developmental rest.gsh'
```

```
\merge the two data sets together
sload 'mergedMeanrestDevelopmentandFLN.gsh'
```

```
\begin analysis
\first need to calculate relevant daylength data.
\remember the 4 required daylengths defined above.
```

```
\the next step after dl data is calculated is to graph the hysteresis graphs
\ and then run regressions to reproduce R2.
```

```
"*****calculations to find daylength for hysteresis graphs*****"
```

```

*****calculate inflexion leaf
# and date - this is when FLP occurs*****
"to calculate daylength at inflexion leaf (this is the leaf where FLP is
initiated). "

"first need to calculate haun stage information at sowdate, rather than
starting at the first sampling
  tabu[class=SplitE]DAS;min=tdaslow "restrict the data to the first
sampling occasion"
  calc tdaslow=mvre(tdatelow;0) "not sure what else"
  fact Days_after_sowing;newl(SplitE;0) "is going on here"
"

"convert SD into a julian number"
  calc DoY=ndayinyear(sowdate_var)"converts the date of inflexion to a
julian number of the year"

"calculate inflexion leaf for each SplitE. Inflexion leaf is calculated
at LN-4(#grain prim)/2(Plastochron/Phyllochron)"
  tabu[class=SplitE](((Final_Leaf_Number)-4)/2);mean=MFLN
  vari infl_leaf;newl(SplitE;!(#MFLN))
  prin infl_leaf

"now need to calculate a date variable which adds DAS to sowdate"

  vari []date;drepresentation='dd/mm/yy'
  calc date=sowdate_var+DAS

"find largest Haun_stage in list that is smaller than infl_leaf; find
smallest Haun_stage in list that is larger than infl_leaf.
also need to find the date at these Haun stages"
  tabu[class=SplitE]mvin(Haun_stage;Haun_stage.ge.infl_leaf);max=tlow
"mvin inserts missing values greater than infl. then table calcs max of
remaining "
  tabu[class=SplitE]mvin(Haun_stage;Haun_stage.lt.infl_leaf);min=tup
"same as above, but calcs min of those greater than infl."
  calc tlow=mvre(tlow;0)"if infl_leaf occurs prior to first
sampling, then vlow is forced to zero"
  vari leaflow,leafup;newl(SplitE;!(#tlow),!(#tup))

"find the date of leafflow and leafup"
  tabl []dlow;drepresentation='dd/mm/yy'
  tabl []dup;drepresentation='dd/mm/yy'

  tabu[class=SplitE]mvin(date;Haun_stage.ge.leaflow);max=dlow "mvin
inserts missing values gt than leaf low. then table calcs max of
remaining "
  tabu[class=SplitE]mvin(date;Haun_stage.lt.infl_leaf);min=dup
  vari
datelow,dateup;newl(SplitE;!(#dlow),!(#dup));drepresentation='dd/mm/yy'
  calc datelow=mvre(datelow;sowdate_var)"if leafflow was forced to zero,
the dlow should equal sowdate."

"now calculate date of inflexion(date of initiation of final leaf
primordium (FLP), this is done by using the two sampling dates BEFORE
and AFTER the estimated date of inflexion as above,

```

and finding the ratio of the difference between Inflexion Leaf and leafflow, and leafup and leafflow, this value is multiplied by the # of days between sampling dates associated between leafup and leafflow. continue to calculate julian day in year, and the daylength on the date of inflexion"

```

    vari date_infl;(((infl_leaf-leafflow)/(leafup-leafflow))*(dateup-
datelow))+datelow;drep='dd/mm/yy'
    calc DAY=ndayinyear(date_infl)"converts the date of inflexion to
a julian number of the year"
    daylength [lat=-43]dayn=DAY;daylength=dayl_infl "calculates
daylength on the day of inflexion"

```

"now calculate the dates and daylengths for the other haun stages used in the paper"

\(LNfinal) against (daylength at 1 haun stage after initiation of FLP)

"find largest Haun\_stage in list that is smaller than infl\_leaf+ 1; find smallest Haun\_stage in list that is larger than infl\_leaf + 1. also need to find the date at these Haun stages then find the date of leafflow and leafup and then calculate date of inflexion(date of initiation of final leaf primordium (FLP), this is done by using the two sampling dates BEFORE and AFTER the estimated date of inflexion as above, and finding the ratio of the difference between Inflexion Leaf and leafflow, and leafup and leafflow, this value is multiplied by the # of days between sampling dates associated between leafup and leafflow. continue to calculate julian day in year, and the daylength on the date of inflexion"

```

    tabu[class=SplitE]mvin(Haun_stage;Haun_stage.gt.((infl_leaf)+1));max=
tlow "mvin inserts missing values greater than infl. then table calcs max
of remaining "
    tabu[class=SplitE]mvin(Haun_stage;Haun_stage.lt.((infl_leaf)+1));min=
tup "same as above, but calcs min of those greater than infl."
    calc tlow=mvre(tlow;0)"if infl_leaf occurs prior to first
sampling, then vlow is forced to zero"
    vari leafflow,leafup;newl(SplitE,! (#tlow),! (#tup))
    tabl []dlow;drepresentation='dd/mm/yy'
    tabl []dup;drepresentation='dd/mm/yy'

```

prin tlow

```

    tabu[class=SplitE]mvin(date;Haun_stage.ge.leafflow);max=dlow "mvin
inserts missing values gt than leaf low. then table calcs max of
remaining "
    tabu[class=SplitE]mvin(date;Haun_stage.lt.infl_leaf);min=dup
    vari
    datelow,dateup;newl(SplitE,! (#dlow),! (#dup));drepresentation='dd/mm/yy'
    calc datelow=mvre(datelow;sowdate_var)"if leafflow was forced to zero,
the dlow should equal sowdate."

```

```

    vari date_infl_1;(((infl_leaf+1)-leafflow)/(leafup-leafflow))*(dateup-
datelow))+datelow;drep='dd/mm/yy'

```

```

    calc DAY_1=ndayinyear(date_infl_1)"converts the date of inflexion to
a julian number of the year"
    daylength [lat=-43]dayn=DAY_1;daylength=dayl_infl_1 "calculates
daylength on the day of inflexion"

```

```

"(LNfinal) against (daylength at 2 haun stages after initiation of FLP)
find largest Haun_stage in list that is smaller than infl_leaf+ 2; find
smallest Haun_stage in list that is larger than infl_leaf + 2.
also need to find the date at these Haun stages then find the date of
leafflow and leafup and then calculate date of inflexion(date of
initiation of final leaf primordium (FLP), this is done by using the two
sampling dates BEFORE and AFTER the estimated date of inflexion as
above,
and finding the ratio of the difference between Inflexion Leaf and
leafflow, and leafup and leafflow,this value is multiplied by the # of
days
between sampling dates associated between leafup and leafflow. continue
to calculate julian day in year, and the daylength on the date of
inflexion"

```

```

    tabu[class=SplitE]mvin(Haun_stage;Haun_stage.ge.((infl_leaf)+2));max=
tlow "mvin inserts missing values greater than infl. then table calcs max
of remaining "
    tabu[class=SplitE]mvin(Haun_stage;Haun_stage.lt.((infl_leaf)+2));min=
tup "same as above, but calcs min of those greater than infl."
    calc tlow=mvre(tlow;0)"if infl_leaf occurs prior to first sampling,
then vlow is forced to zero"
    vari leafflow,leafup;newl(SplitE;!(#tlow),!(#tup))

```

```

    tabl []dlow;drepresentation='dd/mm/yy'
    tabl []dup;drepresentation='dd/mm/yy'

```

```

    tabu[class=SplitE]mvin(date;Haun_stage.ge.leafflow);max=dlow "mvin
inserts missing values gt than leaf low. then table calcs max of
remaining "
    tabu[class=SplitE]mvin(date;Haun_stage.lt.((infl_leaf)+2));min=dup
    vari
    datelow,dateup;newl(SplitE;!(#dlow),!(#dup));drepresentation='dd/mm/yy'
    calc datelow=mvre(datelow;sowdate_var)"if leafflow was forced to zero,
the dlow should equal sowdate."

```

```

    vari date_infl_2;((((infl_leaf+2)-leafflow)/(leafup-leafflow))*(dateup-
datelow))+datelow;drep='dd/mm/yy'
    calc DAY_2=ndayinyear(date_infl_2)"converts the date of inflexion to
a julian number of the year"
    daylength [lat=-43]dayn=DAY_2;daylength=dayl_infl_2 "calculates
daylength on the day of inflexion"
    fspr dayl_infl_2

```

```

"(LNfinal) against (daylength at 3 haun stages after initiation of FLP)
find largest Haun_stage in list that is smaller than infl_leaf+ 3; find
smallest Haun_stage in list that is larger than infl_leaf + 3.
also need to find the date at these Haun stages then find the date of
leafflow and leafup and then calculate date of inflexion(date of
initiation of final leaf primordium (FLP), this is done by using the two

```

sampling dates BEFORE and AFTER the estimated date of inflexion as above,  
 and finding the ratio of the difference between Inflexion Leaf and leafflow, and leafup and leafflow, this value is multiplied by the # of days  
 between sampling dates associated between leafup and leafflow. continue to calculate julian day in year, and the daylength on the date of inflexion"

```

tabu[class=SplitE]mvin(Haun_stage;Haun_stage.ge.((infl_leaf)+3));max=
tlow "mvin inserts missing values greater than infl. then table calcs max
of remaining "
tabu[class=SplitE]mvin(Haun_stage;Haun_stage.lt.((infl_leaf)+3));min=
tup "same as above, but calcs min of those greater than infl."
calc tlow=mvre(tlow;0)"if infl_leaf occurs prior to first sampling,
then vlow is forced to zero"
vari leafflow,leafup;newl(SplitE;!(#tlow),!(#tup))
tabl []dlow;drepresentation='dd/mm/yy'
tabl []dup;drepresentation='dd/mm/yy'

```

```

tabu[class=SplitE]mvin(date;Haun_stage.ge.leafflow);max=dlow "mvin
inserts missing values gt than leaf low. then table calcs max of
remaining "
tabu[class=SplitE]mvin(date;Haun_stage.lt.((infl_leaf)+3));min=dup
vari
datelow,dateup;newl(SplitE;!(#dlow),!(#dup));drepresentation='dd/mm/yy'
calc datelow=mvre(datelow;sowdate_var)"if leafflow was forced to zero,
the dlow should equal sowdate."

```

```

vari date_infl_3;((((infl_leaf+3)-leafflow)/(leafup-leafflow))*(dateup-
datelow))+datelow;drep='dd/mm/yy'
calc DAY_3=ndayinyear(date_infl_3)"converts the date of inflexion to a
julian number of the year"
daylength [lat=-403]dayn=DAY_3;daylength=dayl_infl_3 "calculates
daylength on the day of inflexion"

```

"(LNfinal) against (daylength at 4 haun stages after initiation of FLP)  
 find largest Haun\_stage in list that is smaller than infl\_leaf+ 4; find  
 smallest Haun\_stage in list that is larger than infl\_leaf + 4.  
 also need to find the date at these Haun stages then find the date of  
 leafflow and leafup and then calculate date of inflexion(date of  
 initiation of final leaf primordium (FLP), this is done by using the two  
 sampling dates BEFORE and AFTER the estimated date of inflexion as  
 above,  
 and finding the ratio of the difference between Inflexion Leaf and  
 leafflow, and leafup and leafflow, this value is multiplied by the # of  
 days  
 between sampling dates associated between leafup and leafflow. continue  
 to calculate julian day in year, and the daylength on the date of  
 inflexion"

\Figure 1: Relationships between FLN in Otane wheat and daylength at a)  
 emergence, b) haun stage 1.5, c) final leaf primordium (FLP), d) FLP+2,  
 c) FLP + 3, e) FLP +

```

    tabu[class=SplitE]mvin(Haun_stage;Haun_stage.ge.((infl_leaf)+4));max=
tlow "mvin inserts missing values greater than infl. then table calcs max
of remaining "
    tabu[class=SplitE]mvin(Haun_stage;Haun_stage.lt.((infl_leaf)+4));min=
tup "mvin inserts missing values less than infl, then calcs min of those
remaining i.e. those greater than infl."
    calc tlow=mvre(tlow;0)"if infl_leaf occurs prior to first sampling,
then vlow is forced to zero"
    \calc tup=mvre(tup;Final_Leaf_Number)"if infl_leaf + 4 occurs at a
number that is greater than FLN, then that Haun stage does not occur,
and hence this calculation is not possible"
                                "so where did the value at the
first sd for crsw6 come from for the graph???"
    vari leaflow,leafup;newl(SplitE;!(#tlow),!(#tup))
    tabl []dlow;drepresentation='dd/mm/yy'
    tabl []dup;drepresentation='dd/mm/yy'

    tabu[class=SplitE]mvin(date;Haun_stage.ge.leaflow);max=dlow "mvin
inserts missing values gt than leaf low. then table calcs max of
remaining "
    tabu[class=SplitE]mvin(date;Haun_stage.lt.(infl_leaf)+4);min=dup
    vari
datelow,dateup;newl(SplitE;!(#dlow),!(#dup));drepresentation='dd/mm/yy'
    calc datelow=mvre(datelow;sowdate_var)"if leaflow was forced to zero,
the dlow should equal sowdate."

    vari date_infl_4;((((infl_leaf+4)-leaflow)/(leafup-leaflow))*(dateup-
datelow))+datelow;drep='dd/mm/yy'
    calc DAY_4=ndayinyear(date_infl_4)"converts the date of inflexion to
a julian number of the year"
    daylength [lat=-43]dayn=DAY_4;daylength=dayl_infl_4 "calculates
daylength on the day of inflexion"
    fspre dayl_infl_4
    prin Days_after_sowing,infl_leaf,Haun_stage

*****Haun stage
1.5*****
*****"
\to calculate Haun 1.5 - this is "visible tips" = (Haun + 1)
"to do this need to find the two dates surrounding that where haun stage
was < 1.5 (unless we have the exact dat it was measured)
and then find the ratio of the difference between 1.5-low/high-low
multiplied by high date - low date and all added to low date.
much of this is very similar to the inflexion leaf calculations"

"find largest Haun_stage in list that is smaller than Haun 1.5; find
smallest Haun_stage in list that is larger than Haun 1.5.
also need to find the date at these Haun stages"
    tabu[class=SplitE]mvin(Haun_stage;Haun_stage.ge.(1.5));max=hlow "mvin
inserts missing values greater than haun 1.5. then table calcs max of
remaining "
    tabu[class=SplitE]mvin(Haun_stage;Haun_stage.lt.(1.5));min=hup "same
as above, but calcs min of those greater than haun 1.5."
    calc hlow=mvre(hlow;0)"if haun 1.5 occurs prior to first sampling,
then vlow is forced to zero"
    vari haunlow,haunup;newl(SplitE;!(#hlow),!(#hup))

```

```

tabl []dhlow;drepresentation='dd/mm/yy'
tabl []dhup;drepresentation='dd/mm/yy'

tabu[class=SplitE]mvin(date;Haun_stage.ge.haunlow);max=dhlow "mvin
inserts missing values gt than leafhaunlow. then table calcs max of
remaining "
tabu[class=SplitE]mvin(date;Haun_stage.lt.haunup);min=dhup
vari
datehaunlow,datehaunup;newl(SplitE;!(#dhlow),!(#dhup));drepresentation='
dd/mm/yy'
calc datehaunlow=mvre(datehaunlow;sowdate_var)"if leafhaunlow was
forced to zero, the dlow should equal sowdate."

vari datehaun1_5;(((1.5-haunlow)/(haunup-haunlow))*(datehaunup-
datehaunlow))+datehaunlow;drep='dd/mm/yy'
calc DAY=ndayinyear(datehaun1_5)"converts the date of inflexion to a
julian number of the year"
daylength [lat=-43]dayn=DAY;daylength=dayhaun1_5 "calculates
daylength on the day of haun 1.5"

!*****
*****!
\plot (LNfinal) against (daylength at mean daylength between FLP and
terminal spikelet) "15.1.2013 this appears to have been redone below the
graphs!!"

"Pete said that ts is set on the day that the FL primordia is initiated.
so just need to use the
same approach as before to find daylength on that day. - no messing
about with acc tt!"
splot 'mergedMEANrestDevelopmentalandFLN.gsh'

"find largest primordia number in list that is smaller than FLN ; find
smallest primordia number in list that is larger than FLN.
also need to find the date at these primordia numbers. no longer need to
worry about finding the mean between ts and fln, since in
petes 2007 paper he showed that the fln and ts actually do occur and the
same time; which means i can just use the daylength when fln
was initiated; ie when prmorida number = FLN"
tabu[class=SplitE]mvin(primordia_number;primordia_number.ge.(Final_Le
af_Number));max=primlow "mvin inserts missing values greater than FLN.
then table calcs max of remaining "
tabu[class=SplitE]mvin(primordia_number;primordia_number.lt.(Final_Le
af_Number));min=primup "same as above, but calcs min of those greater
than FLN."
vari primorlow,primorup;newl(SplitE;!(#primlow),!(#primup))

tabl []dpflow;drepresentation='dd/mm/yy'
tabl []dpup;drepresentation='dd/mm/yy'

tabu[class=SplitE]mvin(date;primordia_number.ge.primorlow);max=dpflow
"mvin inserts missing values gt than leafhaunlow. then table calcs max of
remaining "
tabu[class=SplitE]mvin(date;primordia_number.lt.primorup);min=dpup

```

```

    vari
dateprimlow,dateprimup;newl(SplitE,! (#dpow),! (#dpup));drepresentation='
dd/mm/yy'

    vari dateprimFLN;(((Final_Leaf_Number-primorlow)/(primorup-
primorlow))*(dateprimup-dateprimlow))+dateprimlow;drep='dd/mm/yy'
    calc DAY=ndayinyear(dateprimFLN)"converts the date of inflexion to a
julian number of the year"
    daylength [lat=-43]dayn=DAY;daylength=dayprimFLN "calculates
daylength on the day of ts/FLP; which are the same thing"

prin primlow,primup,Genotype
prin dayprimFLN,Genotype

"output all vars in the section into the original spreadsheet; use this
from now on. will need to calculate some summarys for some things of
course."
    fspre dayl_infl,dayl_infl_1,dayl_infl_2,dayhaun1_5,dayprimFLN,
dayl_infl_3,dayl_infl_4

"Section Two graphing"

!*****now to
graph the hysteresis graphs*****
\things to graph \not sure these are all right unfortunatley; better do
sum checkin

\dayl_infl
\dayl_infl_1
\dayl_infl_2
\dayl_infl_3
\dayl_infl_4
\dayhaun1_5
\dayl_emerge
\dayprimFLN

spload 'mean for hysteresis grpahs summary daylengh vs FLN data.gsh'

poin data;
!p(dayl_emerge,dayhaun1_5,dayl_infl,dayl_infl_2,dayl_infl_4,dayprimFLN)
"all"
poin data; !p(dayhaun1_5,dayl_infl,dayl_infl_2) "Rongotea, Batten and
Otane"
poin data; !p(dayhaun1_5,dayl_infl,dayl_infl_2,dayl_infl_4)"CRSW6"

text t; !t('Photoperiod (PP) at Haun stage 1.5', 'PP at Final Leaf
Primordium (FLP)', 'PP at FLP + 2', 'PP at FLP + 4' )
prin t
calc ns=nval(data)
\getat [id]data[];id[1...ns]
poin id; !p(#t)
prin id[]
getat [att=lab]Genotype;gen
poin gtitle;!p(#gen[])
pen [RESET=yes] 1; SYM=1; METH=line; JOIN=given; LIFESTYLE=1; THICK=1
pen[Reset=y]1;meth=p

```



```

for [index=j;ntimes=3]
  ffram [row=2;col=2;clearwindow=0;xmlower=.1;ymlower=0.08]
  text scr; 'clear'

  for [index=i; ntimes=ns]v=data[]
    restr v,Final_Leaf_Number;Genotype.eq.j
    prin v,Final_Leaf_Number
    XAXIS [RESET=yes] WINDOW=i; TITLE=id[i]
    YAXIS [RESET=yes]"low=7;up=13; "WINDOW=i; TITLE='Final Leaf Number'
    if i.eq.1
      DGRAPH [WINDOW=i;title=gtitle[j];keyw=0;screen=#scr]
X=v;Y=Final_Leaf_Number
    else
      DGRAPH [WINDOW=i;title=*;keyw=0;screen=#scr] X=v;Y=Final_Leaf_Number
    endif
    text scr; 'keep'
  endif

endif

"do variable at a time so that can add both mean and scatter data, for
final figures in thesis 30 June 2015"
poin data; !p(dayhaun1_5,dayl_infl,dayl_infl_2,dayl_infl_4)

"Otane"
\code for both sets
poin data; !p(dayhaun1_5,dayl_infl,dayl_infl_2,dayl_infl_4)
text t; !t('Photoperiod (PP) at Haun stage 1.5', 'PP at Final Leaf
Primordium (FLP)', 'PP at FLP + 2', 'PP at FLP + 4' )
prin t
calc ns=nval(data)
\getat [id]data[];id[1...ns]
poin id; !p(#t)
prin id[]
ffram [row=2;col=2;clearwindow=0;xmlower=.1;ymlower=0.08]

\do data first
spload 'mergedMEANrestDevelopmentalFLN.gsh.gsh'text scr; 'clear'
text scr; 'clear'
pen[Reset=y]1;meth=p;csym='red'

for [index=i; ntimes=ns]v=data[]
  restr v,Final_Leaf_Number;Genotype.eq.1
  prin v,Final_Leaf_Number,Genotype
  XAXIS [RESET=yes] WINDOW=i; TITLE=id[i]
  YAXIS [RESET=yes]"low=7;up=13; "WINDOW=i; TITLE='Final Leaf Number'
  DGRAPH [WINDOW=i;title=*;keyw=0;screen=#scr] X=v;Y=Final_Leaf_Number
  text scr; 'keep'
endif

"then means"
spload 'mean for hysteresis grpahs summary daylengh vs FLN data.gsh'
text scr; 'keep'
pen [RESET=yes] 1; SYM=1; METH=line; JOIN=given; LINESSTYLE=1; THICK=1

for [index=i; ntimes=ns]v=data[]
  restr v,Final_Leaf_Number;Genotype.eq.1

```

```

    prin v,Final_Leaf_Number,Genotype
    XAXIS [RESET=yes] WINDOW=i; TITLE=id[i];action='hide'
    YAXIS [RESET=yes]"low=7;up=13; "WINDOW=i; TITLE='Final Leaf
Number';action='hide'
    DGRAPH [WINDOW=i;title=*;keyw=0;screen=#scr] X=v;Y=Final_Leaf_Number
    text scr; 'keep'
    endf

"Rongotea"
\code for both sets
poin data; !p(dayhaun1_5,dayl_infl,dayl_infl_2,dayl_infl_4)
text t; !t('Photoperiod (PP) at Haun stage 1.5', 'PP at Final Leaf
Primordium (FLP)', 'PP at FLP + 2', 'PP at FLP + 4' )
prin t
calc ns=nval(data)
\getat [id]data[];id[1...ns]
poin id; !p(#t)
prin id[]
ffram [row=2;col=2;clearwindow=0;xmlower=.1;ymlower=0.08]

\do data first
supload 'mergedMEANrestDevelopmentalFLN.gsh.gsh'text scr; 'clear'
text scr; 'clear'
pen[Reset=y]1;meth=p;csym='red'

for [index=i; ntimes=ns]v=data[]
    restr v,Final_Leaf_Number;Genotype.eq.2
    prin v,Final_Leaf_Number,Genotype
    XAXIS [RESET=yes] WINDOW=i; TITLE=id[i]
    YAXIS [RESET=yes]"low=7;up=13; "WINDOW=i; TITLE='Final Leaf Number'
    DGRAPH [WINDOW=i;title=*;keyw=0;screen=#scr] X=v;Y=Final_Leaf_Number
    text scr; 'keep'
    endf

"then means"
supload 'mean for hysteresis grpahs summary daylengh vs FLN data.gsh'
text scr; 'keep'
pen [RESET=yes] 1; SYM=1; METH=line; JOIN=given; LIFESTYLE=1; THICK=1

for [index=i; ntimes=ns]v=data[]
    restr v,Final_Leaf_Number;Genotype.eq.2
    prin v,Final_Leaf_Number,Genotype
    XAXIS [RESET=yes] WINDOW=i; TITLE=id[i];action='hide'
    YAXIS [RESET=yes]"low=7;up=13; "WINDOW=i; TITLE='Final Leaf
Number';action='hide'
    DGRAPH [WINDOW=i;title=*;keyw=0;screen=#scr] X=v;Y=Final_Leaf_Number
    text scr; 'keep'
    endf

"Batten"
\code for both sets
poin data; !p(dayhaun1_5,dayl_infl,dayl_infl_2,dayl_infl_4)
text t; !t('Photoperiod (PP) at Haun stage 1.5', 'PP at Final Leaf
Primordium (FLP)', 'PP at FLP + 2', 'PP at FLP + 4' )
prin t
calc ns=nval(data)

```

```

\getat [id]data[];id[1...ns]
poin id; !p(#t)
prin id[]
ffram [row=2;col=2;clearwindow=0;xmlower=.1;ymlower=0.08]

\do data first
spload 'mergedMEANrestDevelopmentalFLN.gsh.gsh'text scr; 'clear'
text scr; 'clear'
pen[Reset=y]1;meth=p;csym='red'

for [index=i; ntimes=ns]v=data[]
  restr v,Final_Leaf_Number;Genotype.eq.3
  prin v,Final_Leaf_Number,Genotype
  XAXIS [RESET=yes] WINDOW=i; TITLE=id[i]
  YAXIS [RESET=yes]"low=7;up=13; "WINDOW=i; TITLE='Final Leaf Number'
  DGRAPH [WINDOW=i;title=*;keyw=0;screen=#scr] X=v;Y=Final_Leaf_Number
  text scr; 'keep'
endf

"then means"
spload 'mean for hysteresis grpahs summary daylengh vs FLN data.gsh'
text scr; 'keep'
pen [RESET=yes] 1; SYM=1; METH=line; JOIN=given; LINESTYLE=1; THICK=1

for [index=i; ntimes=ns]v=data[]
  restr v,Final_Leaf_Number;Genotype.eq.3
  prin v,Final_Leaf_Number,Genotype
  XAXIS [RESET=yes] WINDOW=i; TITLE=id[i];action='hide'
  YAXIS [RESET=yes]"low=7;up=13; "WINDOW=i; TITLE='Final Leaf
Number';action='hide'
  DGRAPH [WINDOW=i;title=*;keyw=0;screen=#scr] X=v;Y=Final_Leaf_Number
  text scr; 'keep'
endf

"CRSW6"
\code for both sets
poin data; !p(dayhaun1_5,dayl_infl,dayl_infl_2,dayl_infl_4)
text t; !t('Photoperiod (PP) at Haun stage 1.5', 'PP at Final Leaf
Primordium (FLP)', 'PP at FLP + 2', 'PP at FLP + 4' )
prin t
calc ns=nval(data)
\getat [id]data[];id[1...ns]
poin id; !p(#t)
prin id[]
ffram [row=2;col=2;clearwindow=0;xmlower=.1;ymlower=0.08]

\do data first
spload 'mergedMEANrestDevelopmentalFLN.gsh.gsh'text scr; 'clear'
text scr; 'clear'
pen[Reset=y]1;meth=p;csym='red'

for [index=i; ntimes=ns]v=data[]
  restr v,Final_Leaf_Number;Genotype.eq.4
  prin v,Final_Leaf_Number,Genotype
  XAXIS [RESET=yes] WINDOW=i; TITLE=id[i]
  YAXIS [RESET=yes]"low=7;up=13; "WINDOW=i; TITLE='Final Leaf Number'
  DGRAPH [WINDOW=i;title=*;keyw=0;screen=#scr] X=v;Y=Final_Leaf_Number

```

```

    text scr; 'keep'
  endif

  "then means"
  splot 'mean for hysteresis grpahs summary daylengh vs FLN data.gsh'
  text scr; 'keep'
  pen [RESET=yes] 1; SYM=1; METH=line; JOIN=given; LINESSTYLE=1; THICK=1

  for [index=i; ntimes=ns]v=data[]
    restr v,Final_Leaf_Number;Genotype.eq.4
    prin v,Final_Leaf_Number,Genotype
    XAXIS [RESET=yes] WINDOW=i; TITLE=id[i];action='hide'
    YAXIS [RESET=yes]"low=7;up=13; "WINDOW=i; TITLE='Final Leaf
Number';action='hide'
    DGRAPH [WINDOW=i;title=*;keyw=0;screen=#scr] X=v;Y=Final_Leaf_Number
    text scr; 'keep'
  endif

  '*****regressions*****'
  "this is where the statistical thing should come in more; is regression
the best thing, are the r2 values
really what they appeared to be, is there another way to compare
competing models? "

  splot 'summary daylength vs FLN data.gsh'

  poin data; !p(dayhaun1_5,dayl_infl,dayl_infl_2,dayl_infl_4)
  calc ns=nval(data)
  getat [id]data[];id[1...ns]
  getat [att=lab]Genotype;gen
  poin gtitle;!p(#gen[])

  for [index=j;ntimes=4]
    ffram [row=3;col=2;clearwindow=0]
    text scr; 'clear'
    for [index=i; ntimes=ns]v=data[]
      restr v,Final_Leaf_Number;Genotype.eq.j
      corr [prin=*]series=v,Final_Leaf_Number
      MODEL Final_Leaf_Number
      FIT [PRINT=model,summary,est; CONSTANT=estimate; FPROB=yes;
TPROB=yes]v
      XAXIS [RESET=yes] WINDOW=i; TITLE=id[i][1]
      YAXIS [RESET=yes] WINDOW=3; TITLE='Fitted Model'
      \RCHECK [RMETHOD=deviance] residual; composite
      if i.eq.1
        RGRAPH [window=i;CIPLLOT=yes;title=gtitle[j];screen=#scr]
      else
        RGRAPH [window=i;CIPLLOT=yes;title='';screen=#scr]
      endif
      text scr; 'keep'
    endif
  endif

```

```

"mean ts prim and fl prim daylength "

!*****
*****!
\plot (LNfinal) against (daylength at mean daylength between FLP and
terminal spikelet)

"*****daylength at emergence
*****"
\find daylength at emergence. this is 150 degree days after sowing. use
palmy temperature data set (namely soil temp not air temp)

spload 'palmy daily temp data.gsh'

\code to calculate cumulative soil temperature from each sowing
date...we have daily temperatures.
  calc n=nval(SD)
  vari [nval=n]st
  vari [nval=n]cumSTemp
  for [ntimes=6;index=i]
    restr st,cumSTemp,Soiltemp;SD.ge.i
    calc st=cumulate(Soiltemp)
    calc cumSTemp=(mvin(st;SD.gt.i))
    restr cumSTemp
  endf
  prin cumSTemp

"since we have every day covered, we know that the plant should have
emerged dyrubg the smallest day that is larger than 150 on a cumulative
scale since sowing. .
find largest tt in list that is smaller than 150; find smallest tt in
list that is larger than 150, then calculate Day at 150 dd"
  tabu[class=SD]mvin(Day;cumSTemp.lt.150);min=demhigh "find min value
gt 150 dd"

spload 'mergedMEANrestDevelopmentalandFLN.gsh'

  vari DAY_emerge;newl(SD;!(#demhigh))
  daylength [lat=-43]dayn=DAY_emerge;daylength=day_emerge
"calculates daylength on the day of haun 1.5"
  prin day_emerge
  fact [lev=6;val=day_emerge]d_em
\this matches the palmy daily temp data set; now need to merge it into
the larger data set - did this by hand rather than coding

"*****work out ts and hence mean
ts/infl dl*****"

spload 'mergedMEANrestDevelopmentalandFLN.gsh'

getat [att=lab]Genotype;gen
poin gtitle;!p(#gen[])

calc prim=primordia_number-Final_Leaf_Number
for [index=j;ntimes=4]
  restr
sowdate_f,Spikelet_Number,primordia_number,RepE,prim,spikelet_primordia;
Genotype.eq.j

```

```

TRELLIS [GROUPS=sowdate_f; PENGROUP=RepE;
FIRSTPICTURE=top;title=gtitle[j];xtitle='Days after
sowing';ytitle='Spikelet_Number'] \
  Y=Spikelet_Number,prim,spikelet_primordia; X=DAS;\
  METHOD=Point
endif

"restrict primordia number to only those that become leaves; this is
around when the rate of prim developmentincreases.
this rate can be used to calculate when the terminal spikelet prordia
was initiated. the final values used are those starting
at the first spikelet primordia and finishing at one primordia before
terminal primordia. this can be used to find plastochron and
hence find when final primordia was initiated."
calc prim=primordia_number-Final_Leaf_Number "makes leaf primordia
negative"
calc spikelet_prim=mvin(primordia_number;prim.lt.0) "gets rid or
primordia that became leaves"
tabu
[class=SplitE]mvin(spikelet_prim;primordia_number.eq.0);max=max_prim
"calculates the max prim number should be equal to Spikelet Number"
VARI max_PRIM;newl(SplitE;!(#max_prim)) "turns above values into variate
to match rest of data"
tabu
[class=SplitE]mvin(DAS;primordia_number.ne.max_PRIM);min=max_prim_DAS
"calculates the first day on which the final primordia was seen"
VARI max_prim_das;newl(SplitE;!(#max_prim_DAS))"turns above into variate
to match rest of data"
calc primforgraphs=mvin(spikelet_prim;spikelet_prim.eq.max_PRIM) "makes
a new primordia variate only containing spikelet primordia"
calc primforgraph=mvin(primforgraphs;DAS.gt.max_prim_das) "and stoppping
on the second to last primordia observed"

fspre primforgraph \primforgraph added to big data sheet. bad data
(primordia at subsequent data less than previously) deleted by hand at
units 157,245,319,416 and 514.

"calculate accumulated tt for the DAS we are observing data."
supload 'palmy daily temp data.gsh'

\code to calculate cumulative soil temperature from each sowing
date...we have daily tempertures.
calc n=nval(SD)
vari [nval=n]at
vari [nval=n]cumATemp
for [ntimes=6;index=i]
  restr at,cumATemp,Airtemp;SD.ge.i
  calc at=cumulate(Airtemp)
  calc cumATemp=(mvin(at;SD.gt.i))
  restr cumATemp
endif
fspre cumATemp \ add this to palmy daily temp data.gsh

"merge this with big data set. to do this, will just need to match SD
with sowdate_f, and Day with a Julian day variable in the
big data set (mergedMEANrestDevelopmentalandFLN.gsh). calculate this
first."

```

```

    calc DoY=ndayinyear(sowdate_var)"converts the date of inflexion to a
julian number of the year"
    calc DoYSDplusDAS=DoY+DAS "calculates sampling days for each sd and
sampling observation"
    calc DoYdasminus=DoYdas-365 "Julian day if observation rolls
over into next year; 1990"
    calc DoYSDplusDAS=mvin (DoYSDplusDAS;DoYSDplusDAS.gt.365)"puts
missing values where > 365; ie has rolled over "
    calc DoYSDplusDAS=mvre (DoYSDplusDAS;DoYdasminus) "puts the julian
day of the observation in to the variate"

    fspre DoY,DAS,DoYSDplusDAS \add DoYplusDAS to big spreadsheet by
hand

\now merge, by hand.

```

```

splot 'mergedMEANrestDevelopmentalandFLN.gsh'

```

```

"graph new value to see rate of plastochron development"
getat [att=lab]Genotype;gen
poin gtitle;!p(#gen[])

```

```

\against day
for [index=j;ntimes=4]
    restr primforgraph,cumATemp;Genotype.eq.j
    TRELLIS [GROUPS=sowdate_f; PENGROUP=RepE;
FIRSTPICTURE=top;title=gtitle[j];xtitle='Days after
sowing';ytitle='Primordia Number'] \
    Y=primforgraph; X=cumATemp;\
    METHOD=point
endf

```

```

\against accumulated tt
for [index=j;ntimes=4]
    restr primforgraph,cumATemp;Genotype.eq.j
    TRELLIS [GROUPS=sowdate_f; PENGROUP=RepE;
FIRSTPICTURE=top;title=gtitle[j];xtitle='Days after
sowing';ytitle='Primordia Number'] \
    Y=primforgraph; X=cumATemp;\
    METHOD=point
endf

```

```

"run regresssions to get slope parameter separately "
for [index=j;ntimes=4]
    ffram [row=3;col=2;clearwindow=0]
    text scr; 'clear'
    for [index=i; ntimes=6]
        restr primforgraph,cumATemp,Genotype,sowdate_f;
        restr
primforgraph,cumATemp,Genotype,sowdate_f;(Genotype.eq.j).AND.(sowdate_f.
eq.i)
        MODEL primforgraph
        FIT [PRINT=model,summary,estimates; CONSTANT=estimate; FPROB=yes;
TPROB=yes]cumATemp
        rkeep [est=est[j]][i]
        if i.eq.5
            XAXIS [RESET=yes] WINDOW=i; low=200;up=800;title='acc thermal time'

```

```

else
  XAXIS [RESET=yes] WINDOW=i; low=200;up=800
endif
if i.eq.3
  YAXIS [RESET=yes] WINDOW=i ;low=0;up=50;TITLE='Primordia Number -
only spikelet primordia shown'
else
  YAXIS [RESET=yes] WINDOW=i ;low=0;up=50
endif
\RCHECK [RMETHOD=deviance] residual; composite
if i.eq.1
  RGRAPH [window=i;CIPLLOT=yes;title=gttitle[j];screen=#scr]
else
  RGRAPH [window=i;CIPLLOT=yes;title='';screen=#scr]
endif
text scr; 'keep'
endf
endf

"is there evdience that these slopes are singificantly different for
each sd and geno combination - yes strong evdience for all
interactioons.
r2 for this model is 94.2%"
MODEL primforgraph
FIT [PRINT=model,summary,estimates,acc; CONSTANT=estimate; FPROB=yes;
TPROB=yes]cumATemp*sowdate_f*Genotype
rgra
rcheck

prin est[][] "take these put them into excel; match them with
appropriate genotype+sd. return and merge with big data sheet."

```



## A2: Genstat code for Leaf Appearance in response to temperature as described in Chapter Six

"8.2.2012 'Prediction of leaf appearance in wheat: a question of temperature'. two data sets were used in this paper.

the first was from palmy, done in 1984, on avalon wheat

the second was from Lincoln, I think done in the same year, on rongotea wheat

"

'Figure 1.'

"the only thing using the avalon data set which is nicely replicated. no stats don in the paper though; just the figure."

```
spload 'avaolon tips and air tt.gsh'
```

```
poin data; !p(dacc_air_temp,acc_soil_temp)
calc ns=nval(data)
getat [id]data[];id[1...ns]
getat [att=lab]Genotype;gen
poin gtitle;!p(#gen[])
pen [RESET=yes] 1; SYM=1; METH=line; JOIN=given; LINESYLE=1; THICK=1
```

```
for [index=j;ntimes=ns]
  ffram [row=3;col=1;clearwindow=0]
  text scr; 'clear'
  for [index=i; ntimes=2]v=data[]
    restr v,Final_Leaf_Number;Genotype.eq.j
    prin v,Final_Leaf_Number
    XAXIS [RESET=yes] WINDOW=i; TITLE=id[i][1]
    YAXIS [RESET=yes] WINDOW=i; TITLE='Final Leaf Number'
    if i.eq.1
      DGRAPH [WINDOW=i;title=gtitle[j];keyw=0;screen=#scr]
      X=v;Y=Final_Leaf_Number
    else
      DGRAPH [WINDOW=i;title=*;keyw=0;screen=#scr] X=v;Y=Final_Leaf_Number
    endif
    text scr; 'keep'
  endf
endf
```

'Figure 2'

"used the spreadsheet 'COMPAR.GSH' for the data; the TDATE.wq1 files didn't appear to hold replicated data either unfortunately,

"note that the length of data is only measured for 8 times in the COMPAR data set, but 10 times in the TDATE data sets.  
 I just inserted relevant sampling numbers in sheet below, but these may not be correctly associated... seems odd  
 that observed leav numbers go from 1,2,3,...12 so evenly... but figures seem to match the paper graphs"

```
spload 'data for fig 2.gsh'
```

```
  calc DoY=ndayinyear(Date)"converts the date of inflexion to a julian
number of the year"
  calc SowDoY=ndayinyear(Sowdatev)
  calc daysfromsowing=DoY-SowDoY \this is fine since no sampling
occured in 85.
```

```
prin DoY,SowDoY,daysfromsowing,Sowdate
```

```
  getat [att=lab]Sowdate;sd
  poin stitle;!p(#sd[])
  pen      [RESET=yes]      number=1,2,3,4,5;      SYM=2,0,0,0,0;
METH=point,line,line,line,line;  JOIN=ascending;  LIFESTYLE=0,2,1,3,4;
THICK=1
```

```
ffram [row=3;col=2;clearwindow=0]
```

```
text scr; 'clear'
```

```
for [index=i; ntimes=4]
```

```
  restr
```

```
measured,Air,Soil_air,dphidt,Miglietta,daysfromsowing;Sowdate.eq.i
```

```
  XAXIS [RESET=yes] WINDOW=i; TITLE='Days from sowing';lo=0;up=180
```

```
  YAXIS [RESET=yes] WINDOW=i; TITLE='Leaf Number' ;lo=0;up=12
```

```
  DGRAPH [WINDOW=i;title=stitle[i];keyw=6;screen=#scr] \
```

```
    X=daysfromsowing;Y=measured,Air,Soil_air,dphidt,Miglietta
```

```
  text scr; 'keep'
```

```
  restr measured,Air,Soil_air,dphidt,Miglietta,daysfromsowing
```

```
endf
```

```
'Table one.'
```

"now need to remember how they calculate their rmsds and maybe do another type of statistical comparison  
 (eg like regression with groups)"

```
"modellers calculation of rmsd is (ob-pre)*squared"
```

```
spload 'data for fig 2.gsh'
```

```
poin data; !p(Air,Soil_air,dphidt,Miglietta)
```

```
calc ns=nval(data)
```

```
getat [id]data[];id[1...ns]
```

```
text vars;!t(Air,Soil_air,dphidt,Miglietta)
```

```
fact [lab=vars]Vars
```

```
getat [att=lab]Sowdate;sd
```

```
poin stitle;!p(#sd[])
```

```
for [index=j;ntimes=4]
```

```
  restr v,measured;Sowdate.eq.j
```

```

for [index=i;ntimes=ns]v=data[]
  calc rmsd[i][j]=sqrt(mean((measured-v)*(measured-v)))
endf
restr v,measured;
endf

table [class=Vars,Sowdate]RMSD;!(#rmsd[][]))
fspre RMSD

'better thing to doo....??? look at again when finished doing other
tables and figures'

"regression to test whether model one is singificantly better than the
others? aic? r2?"

for [index=j;ntimes=4]
  for [index=i;ntimes=ns]v=data[]
    restr v,measured;Sowdate.eq.j
    model measured
    fit [prin=summary]v
  endf
  restr v,measured;
endf

'Table 2'
"this looks at comparing when to switch from soil to canopy temperature,
and chooses the haun stage
of switch which has the best rmsd value. so is there another way to
assess this?"

'Figure 3'
"distance of obseved-predicted against observed"
splot 'data for fig 2.gsh'

poin data; !p(Air,Soil_air,dphidt,Miglietta)
for [index=i;ntimes=4]v=data[]
  calc md[i]=mean(measured-v)
endf
vari mean_bias;newl(Sowdate;!(#md))

poin data; !p(Air,Soil_air,dphidt,Miglietta)
calc ns=nval(data)
getat [id]data[];id[1...ns]
ffram [row=3;col=2;clearwindow=0]
pen [RESET=yes] number=1,2,3,4,5; SYM=2,5,6,7,10;
smsym=1,1,1,1,3;METH=line,line,line,line,point; JOIN=ascending;
LINESTYLE=1,2,3,4,0; THICK=3,3,3,3,5

text scr; 'clear'
for [index=i;ntimes=ns]v=data[]
  calc dif=measured-v
  XAXIS [RESET=yes] WINDOW=i; TITLE='Observed';
  YAXIS [RESET=yes] WINDOW=i; TITLE='Observed - Predicted' ;lo=-3;up=1.5
  DGRAPH [WINDOW=i;title=id[i][1];keyw=6;screen=#scr] pen=i;\
    X=measured;y=dif;pen=Sowdate
  text scr; 'keep'

```

```

    restr mdif,measured;Sowdate.eq.i "restricting by sowdate, even though
its a model thing; weird but should work."
    dgra [window=i;title=*;keyw=*;scr=#scr]pen=5;x=measured;y=mdif
    restr mean_bias,measured
endf

'Table 3' "rmsds of mean bias errors for each model and month. have to
ADD the mean bias to the predicted to calculate,
because they are inherently negative. i.e. we subtract the absolute
value of the mean bias error."
poin data; !p(Air,Soil_air,dphidt,Miglietta)
for [index=i;ntimes=4]v=data[]
    calc md[i]=mean(measured-v)
endf
vari (v-mean_bias);newl(Sowdate;!(#md))

poin data; !p(Air,Soil_air,dphidt,Miglietta)
text vars;!t(Air,Soil_air,dphidt,Miglietta)
fact [lab=vars]Vars

for [index=i;ntimes=4]v=data[]
    for [index=j;ntimes=4]
        restr v,measured,mean_bias
        restr v, measured,mean_bias;Sowdate.eq.j
        calc rmsdunbias[i][j]=sqrt(mean((measured-(v+mean_bias))*(measured-
(v+mean_bias))))
        calc rmsd[i][j]=sqrt(mean((measured-v)*(measured-v)))
    endf
endf

table [class=Vars,Sowdate]RMSD;!(#rmsdunbias[][]))

fspre RMSD

```

### A3: Genstat wrap-around code for Bayesian Data Assimilation model described in Chapter Nine.

```

"Including winbugs data and model code June 2014"

"Load dynamic data for assimilation"

SPLOAD 'Otane plants.gsh'

"Set sowing date. Since assimilating controlled climate chamber data
this does not need to reference any weather files and so can begin as 1"
Scalar DAY; 1

"Starting values for data, TT and PP constant since we are simulating
controlled climate chamber data"
scalar TT;22.5
scalar PP;16
scalar alphalnkmn1;0 "model calls yesterdays' value for ln; so need to
set and save this as a constant for the first day "
scalar flnkmn1; 9 "model calls yesterdays' value for fln; so need to
set and save this as a constant for the first day"
scalar phyllnkmn1; 97.5

"load leaf count data and set up text file for WinBugs"
subset [DayNo.eq.DAY] tips;LN
calc nv=nval(LN)-1
text tcomma; !t(#nv(', '))
open 'simplifiedata3.txt';ch=2; f=o; wid=200
print [ch=2;sq=y;ip=*; miss='NA'] 'list('

& 'phylln.kmn1=',phyllnkmn1; fie=1,*; j=1; "scalars"
& 'fln.kmn1=',flnkmn1; fie=1,*; j=1; "scalars"
& 'TT.k=',TT; fie=1,*; j=1; "scalars"
& 'PP.k=',PP; fie=1,*; j=1; "scalars"
& ',alpha.ln.kmn1=',alphalnkmn1; fie=1,*; j=1; "scalars"
& ',LN.k=c('; fie=1; j=1
& LN,tcomma;fie=*,1; j=1;dec=0
& ') '
& ') '
close 2; file=o

"Data names (data for WinBUGS to use)"
TEXT dnames;
VALUES=!t('LN.k','TT.k','PP.k','alpha.ln.kmn1','beta.ln.kmn1','ln.kmn
1')

" Specify WinBUGS model."
TEXT tmodel; VALUES=!t(\
'model',\
'{' ,\
'for(i in 1:8){',\
'LN.k[i]~dpois(mu.ln.k)',\
'}',\
',\
',\
'log(mu.ln.k)<-log(ln.k)
',\

```

```

'a[1]<-step((2-(ln.kkmin1)))',\
'a[2]<-step((8-(ln.kkmin1))-step((2-(ln.kkmin1))))',\
'a[3]<-min((1-(a[1])),(1-(a[2])))',\
'phylln.k<-(a[1]*0.75*bp+a[2]*bp+a[3]*1.3*bp)',\
',\
',\
'd[1]<-step(((TT.k/phylln.kmin1)+ln.kkmin1)-fln.kmin1)',\
'd[2]<-1-d[1]',\
'ln.k<- d[1]*fln.kkmin1+d[2]*((TT.k/phylln.k)+ln.kmin1)',\
',\
',\
'primn.k<-pn*ln.k+pe',\
',\
',\
'b[1]<-step((PP.k-ppsats))',\
'b[2]<-1-b[1]',\
'flnt.k<-lmin',\
',\
',\
'c[1]<-step((primn.k-(flnt.k+pe)))',\
'c[2]<-1-c[1]',\
'e[1]<-step((primn.k-flnt.k))',\
'e[2]<-1-c[1]',\
'fln.k<-c[1]*(e[1]*flnt.k+e[2]*primn.k)+c[2]*(fln.kkmin1)',\
',\
',\
'bp~dnorm(110,1)',\
'pe~dpois(4)',\
'pn~dpois(2)',\
'ppsats~dnorm(15.9,0.01)',\
'lmin~dgamma(7,1)',\
'ps~dnorm(0.625,0.01)',\
',\
',\
'ln.kmin1~dpois(alpha.ln.kmin1)',\
'ln.kkmin1<-alpha.ln.kmin1',\ "for some state equations require
posterior point estimate rather than distribution, i.e. to use the
'step' function in WinBUGS"
'fln.kkmin1~dgamma(flnt.kmin1,1)',\
}')'

"Write the WinBUGS model to a file"
OPEN 'simplemodel2.txt'; CHAN=2; FILE=output
PRINT [CHANNEL=2; IPRINT=*; SQUASH=yes] tmodel; JUST=left
CLOSE 2; FILETYPE=output

"automatic monitoring of nodes"
text monnames;
!t('fln.k','lambda.ln.k','mu.ln.k','phylln.k','flnt.k','primn.k','ln.k',
'tau.ln.k')

"set up for loop to run recursive model over k = 45 days. "
for [index=k;ntimes=60]
  prin flnkmin1
  prin DAY
  prin LN
  "call WinBUGS"
  BGxGenstat [prin=node;modelfile='simplemodel2.txt';\
    data='simpledata3.txt';idatanames=dnames; "wpath= 'C:/Program Files
(x86)/winbugs14/WinBUGS14';"viewbugs=y;"mon=monnames;nsamples=10000;ncha
ins
=3;coda=y]"init=*;"simulations=sim[1]

"retrieve posterior values"
BGIMPORT [INDEXFILE='WBGCODAIndex.txt';\

```

```

        OUTPREFIX='WBGCODA'; PNames=tNames; NOUT=1] sim[]

"plot diagnostics"
BGPLOT [PRINT=summary; PLOT=trace,density,auto,gelm;
ARRANGEMENT=multiple] sim[]

"calculate and save posterior predictions for fln and ln. we are using
the method of moments to estimates the parameters from the posterior
distribution of ln from the previous run of the model
hence using the gamma distribution as the prior for fln mu =
alpha/beta; sigma2=alpha/beta2, and poisson for ln so just mu=mean."

calc alphaLnkmin1=mean(sim[1][5])
calc lambdaLnk=mean(sim[1][3])
calc flnkmin1=mean(sim[1][1])
calc phyllnkmin1=mean(sim[1][6])
PRIN alphaLnkmin1,lambdaLnk,flnkmin1
vari [nval=2;val=7,flnkmin1]sc
calc flnkmin1=max(sc)
prin flnkmin1

"update day"
CALCULATE DAY=DAY+1

"update Data file, i.e. load updated assimilation data and todays
posterior will enter the next loop of the model as tomorrows prior"
subset [DayNo.eq.DAY] tips;LN
calc nv=nval(LN)-1
text tcomma; !t(#nv(', '))
open 'simplifiedata3.txt';ch=2; f=o; wid=200
print [ch=2;sq=y;ip=*; miss='NA'] 'list('

& 'phylln.kmin1=',phyllnkmin1; fie=1,*; j=1; "scalars"
& 'fln.kmin1=',flnkmin1; fie=1,*; j=1; "scalars"
& 'TT.k=',TT; fie=1,*; j=1; "scalars"
& ',PP.k=',PP; fie=1,*; j=1; "scalars"
& ',alpha.ln.kmin1=',alphaLnkmin1; fie=1,*; j=1; "scalars"
& ',LN.k=c('; fie=1; j=1 "not sure if initial comma is needed"
& LN,tcomma;fie=*,1; j=1;dec=0
& ') '
& ') '
close 2; file=o
ENDFOR

```

## A4: GenStat Code for mixing algorithms described in Chapter Ten

\ code uses k to denote time rather than t as in the text.

### A4.1: Mixing algorithm plus MoM estimation

```
\December 2014
\results not shown in text
\this codes sits within the dynamic for loop and will run every day of
the simulation.
\calculations for revised, pooled fln certainty estimation. MoM approach
assumes two Gaussian Distributions which is probably inappropriate
  \obtain dynamic estimates
  calc flnmean[k]=mean(sim[1][1])"calculates the first moment of the
fln posterior"
  calc flnvar[k]=variance(sim[1][1])"calculate the second moment of
the fln"
  calc lnmean[k]=mean(sim[1][5])"calculates the first moment of the
mu.ln posterior"
  calc lnvar[k]=variance(sim[1][5])"calculate the second moment of the
mu.ln"
  calc flntmean[k]=mean(sim[1][2])
  calc kmin1 = k-1
  calc kmin2 = k-2

\calculate test value for alpha (equilibrium)
if k.ge.3
  calc flnk[k]=(flnmean[k]+flnmean[kmin1]+flnmean[kmin2])/3
else
  calc flnk[k]=1
endif

\Calculate alpha, day of equilibrium (correct working for tau now)
if k.gt.3
  calc flndif[k] = flnk[kmin1]-flnk[k]
  prin flndif[k]
  if a.ne.1000
    calc a=a
  elseif flndif[k].le.0.05.AND.flnmean[k].lt.(flntmean[k]+.5) "i.e. fln
is within half a leaf of flntarget"
    calc a = k
  endif
  prin a
endif

\now do the calcuations for the revised fln variance estimator
if t.ne.1000
  calc t=t
elseif a.ne.1000
  calc t = ((2-lnmean[k])*(phyllnkmin1)/TT)+((flnmean[k]-
lnmean[k])*(phyllnkmin1/.75))/TT
endif
print t
```



```

\create an indicator variable for working with simulated chains of
data
  vari [nval=10000;val=1...10000]indicator

\calculate how far through the process we are in terms of mixture up
until day of flag (a + tau)
\and thence calculate the relative proportions for mixing
  calc count = k-a
  prin count
  calc v = (t-count)/t
  calc vcomp = 1-(t-count)/t
  prin v, vcomp

\calculate revised flnvar based on progress through simulations

  if a.eq.1000
    calc revisedflnvar[k]=flnvar[k]
  elsif k.gt.(a+t)
    calc revisedflnvar[k]=lnvar[k]
  else
    calc
revisedflnvar[k]=v*((flnmean[k])**2+flnvar[k])+vcomp*((lnmean[k])**2+lnv
ar[k])-(v*flnmean[k]+vcomp*lnmean[k])**2
  endif

```

## A4.2: Sampling from approximate mixture distribution

```

\this codes sits within the dynamic for loop and will run every day of
the simulation.
\generate a random distribution to mimic variance of ln, but with mean
for fln
\has to be normal otherwise cant do it.
\this will enable us to graph what the mixture distriubtion might look
like through the simulation process

```

```

  GRANDOM [DISTRIBUTION=Normal; NVALUES=10000; SEED=0; MEAN=flnmean[k];
VARIANCE=lnvar[k]] lnisfln

```

```

\estimate mixture distribution for algorithm 1
  if a.eq.1000
    calc mixtureflndensity[k]=sim[1][1]
  elsif k.gt.(a+t)
    calc mixtureflndensity[k]=sim[1][5]
  else
    calc ffln = sim[1][1]
    calc lln=lnisfln
    if v.eq.1
      calc vv=v*10000-1
      calc vvcomp=vcomp*10000+1
    else
      calc vv=v*10000
      calc vvcomp=vcomp*10000+1
    endif
  dele [redef=y]indicator
  vari [nval=10000;val=1...10000]indicator
  subset [condition=indicator.le.vv]ffln;fffln
  subset [condition=indicator.le.vvcomp]lln;llln

```

```

dele [redef=y]mixtureflndensity[]
stack []mixtureflndensity[k];fffln;llln
endif

```

### A4.3: Calculations for *tau*

\this codes sits within the dynamic for loop and will run every day of the simulation.

\ approach to calculate **predicted** intervals for tau based on distribution of fln

```

if k.eq.a
  calc fln[k]=sim[1][1]
  for [index=i;ntimes=10000]
    subset [condition=indicator.eq.i]fln[k];flni
    calc tt[i]=(((2-lnmean[k])*phyllnkmin1)/TT)+((flni-
lnmean[k])*(phyllnkmin1/.75))/TT)+a
  endf
  vari [nval=10000;val=tt[]]tpred
  ffram [row=2;col=2;xmlower=.085;ymlower=0.085]
  pen 1; colour='White'
  yaxis [reset='y']window=3;title='Frequency';low=0;up=1000
  xaxis[]window=3; low=0;up=80;mark=*; title='Predicted Day of Flag'
  DHISTOGRAM
[window=3;k=*;scr='clear';binwidth=1;outline=perimeter]tpred;pen=1
  \calculate credible intervals
  sort tpred
  subset [condition=indicator.eq.1000]tpred;tpredlow
  subset [condition=indicator.eq.9000]tpred;tpredup
  dele [redef=y]tt[]
endif

```

\calculate the **smoothed** credible intervals once it has reached flag; i.e. at day 35.

```

if k.eq.35
  calc lnn=sim[1][5]
  for [index=i;ntimes=10000]
    subset [condition=indicator.eq.i]lnn;lni
    calc tt[i]=(((2)*(.75*phyllnkmin1))/TT)+((lni-2)*phyllnkmin1)/TT)
  endf
  vari [nval=10000;val=tt[]]tsmooth
  ffram [row=2;col=2;xmlower=.085;ymlower=0.085]
  pen 1; colour='White'
  yaxis [reset='y']window=3;title='Frequency';low=0;up=1000
  xaxis[]window=3; low=0;up=80;mark=*; title='Smoothed Day of Flag'
  DHISTOGRAM
[window=3;k=*;scr='clear';binwidth=1;outline=perimeter]tsmooth;pen=1
  \calculate credible intervals
  sort tsmooth
  subset [condition=indicator.eq.1000]tsmooth;tsmoothlow
  subset [condition=indicator.eq.9000]tsmooth;tsmoothup
  dele [redef=y]tt[]
endif

```

## A5: Diagnostics for Model c described in Chapter Nine

### A5.1: $\mu.\ln_t$

As for LN, in the first few simulations (i.e days 1 and 2) the trace plots appear to be a little inconsistent between chains, however the G-B plots do not indicate a problem. From day 5 onwards the trace plots for each chain looks consistent.

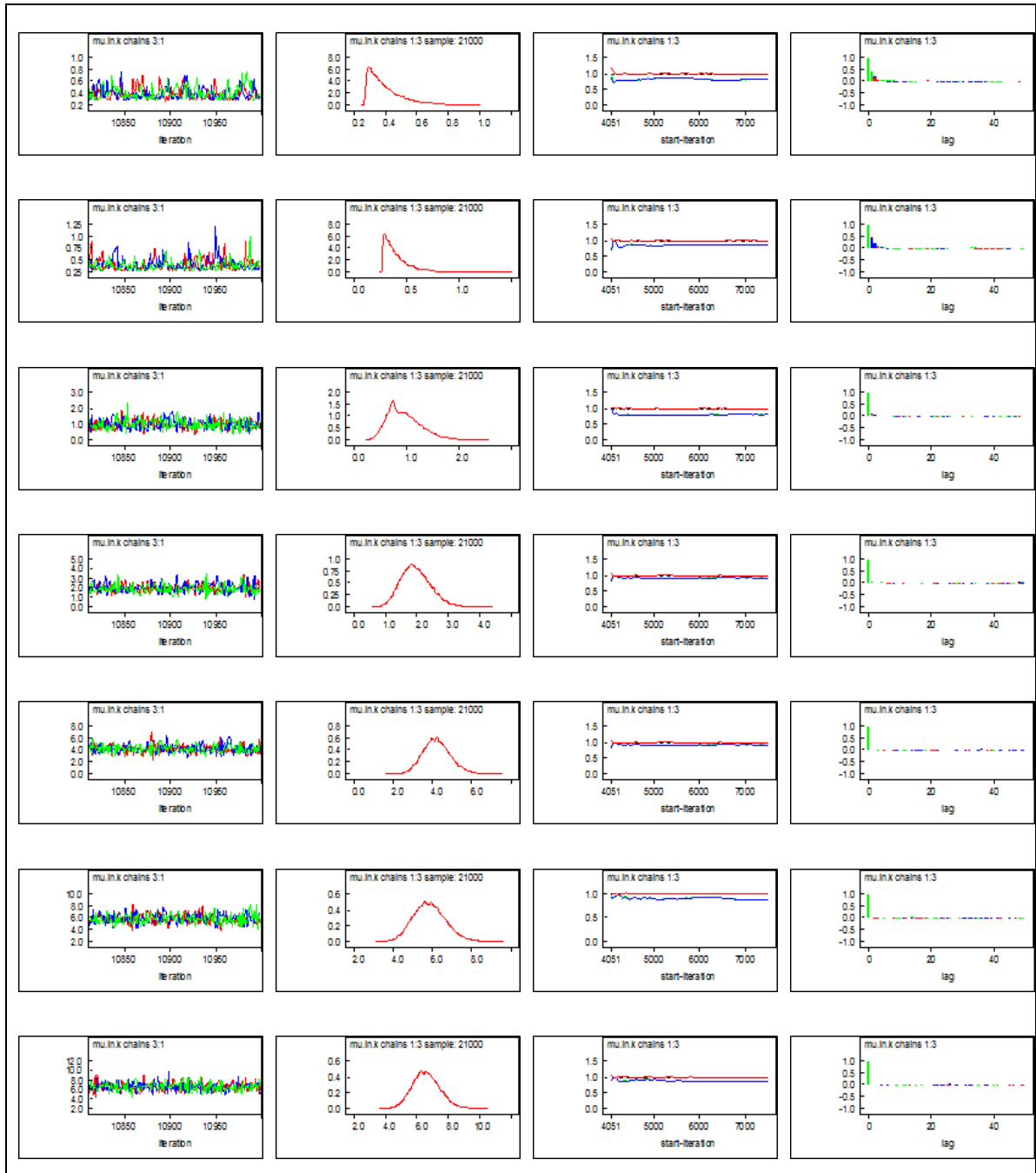


Figure 42: Diagnostics for  $\mu.ln.k_t$  where  $t = 1, 2, 5, 10, 30$  and  $50$

### A5.2: phyllochron<sub>t</sub>

The trace plots looks unusual, however the density, G-B and autocorrelation plots all seem acceptable.

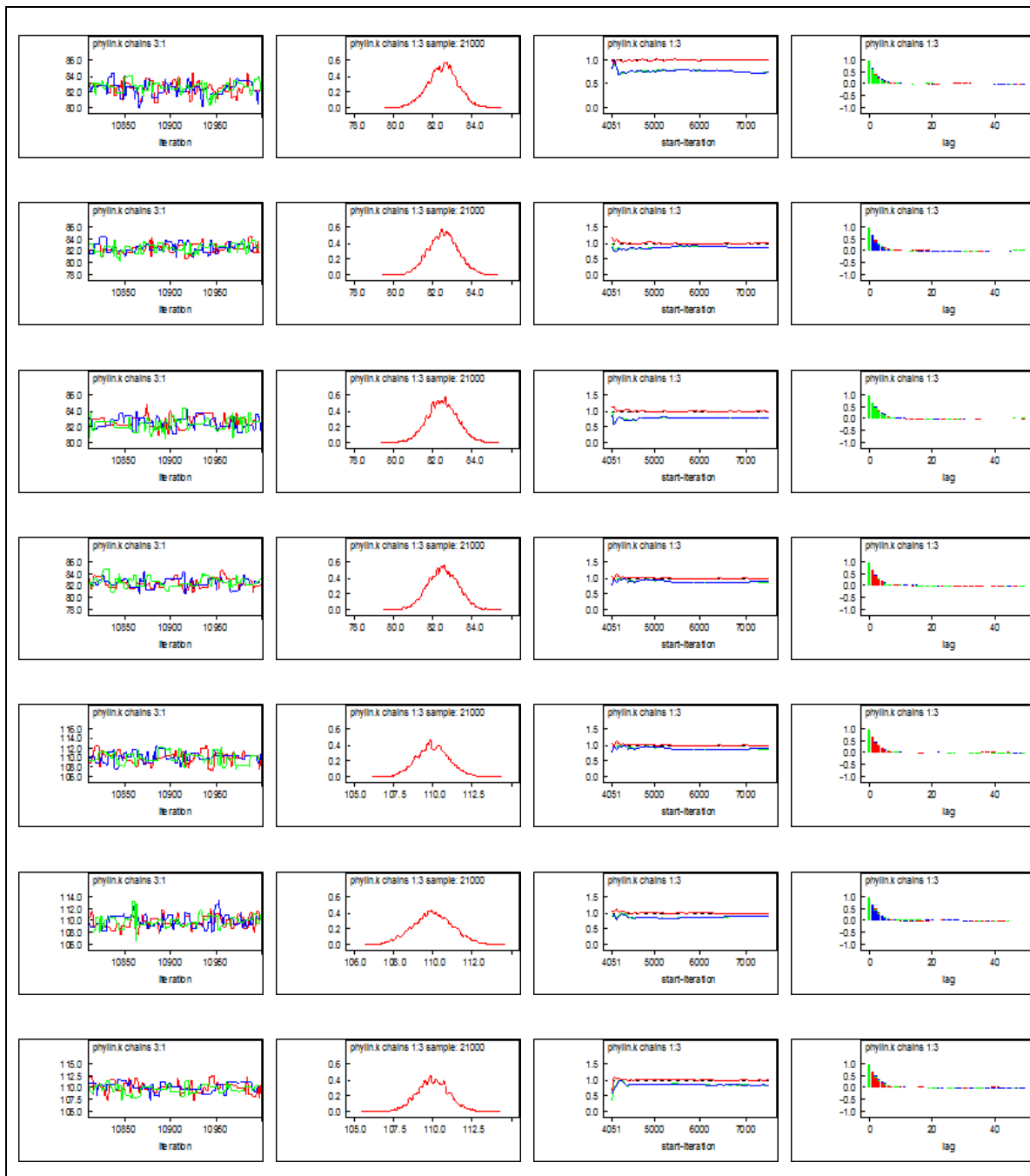


Figure 43: Diagnostics for  $phyllochron_t$  where  $t = 1, 2, 5, 10, 30$  and  $50$

### A5.3: $primordia_t$

The  $primordia_t$  parameter appears to be well behaved.

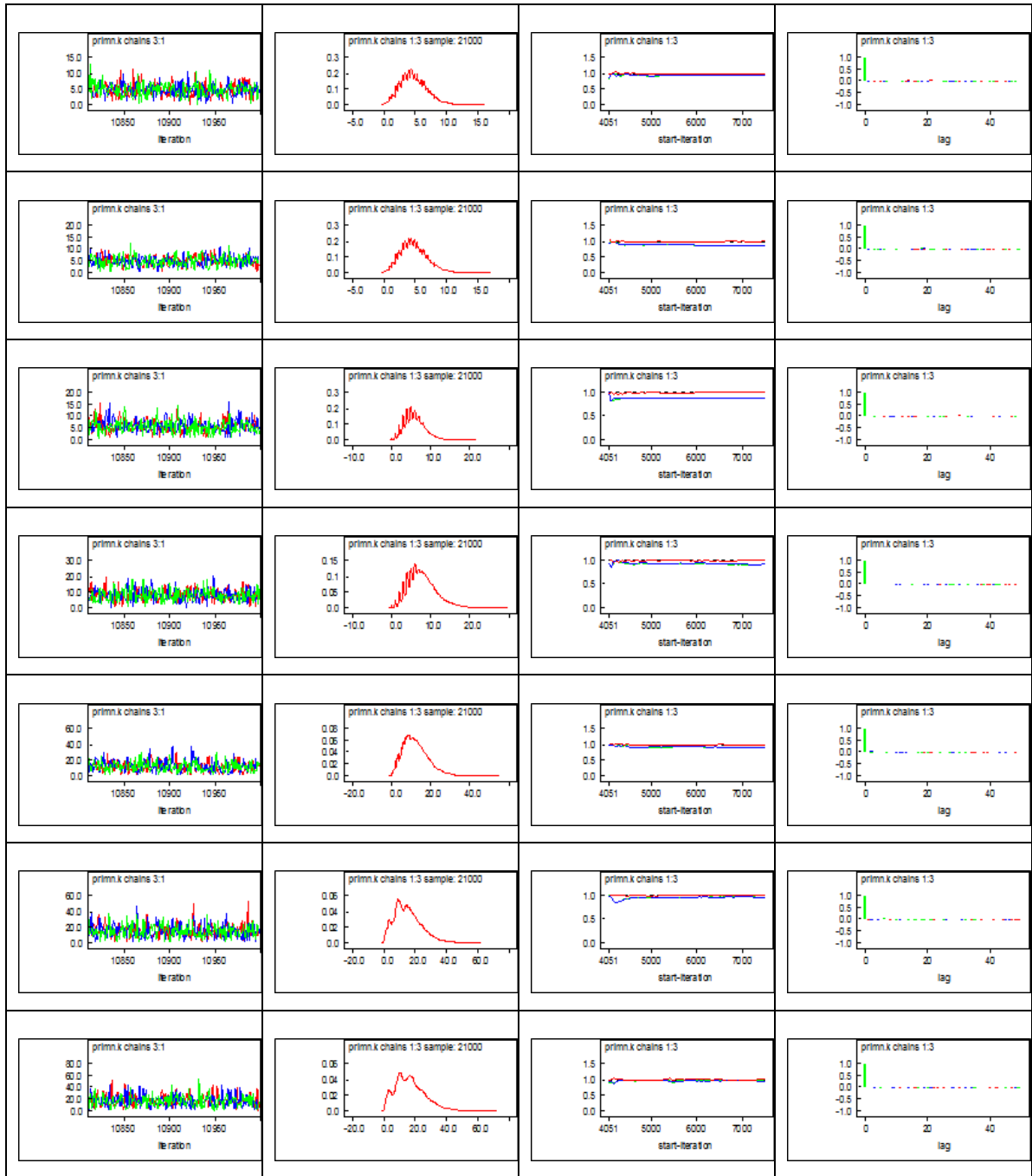


Figure 44: Diagnostics for  $\text{primordia}_t$  where  $t = 1, 2, 5, 10, 30$  and  $50$

A5.4:  $\text{fln}_t$

The  $\text{fln}_t$  parameter appears to be well behaved.

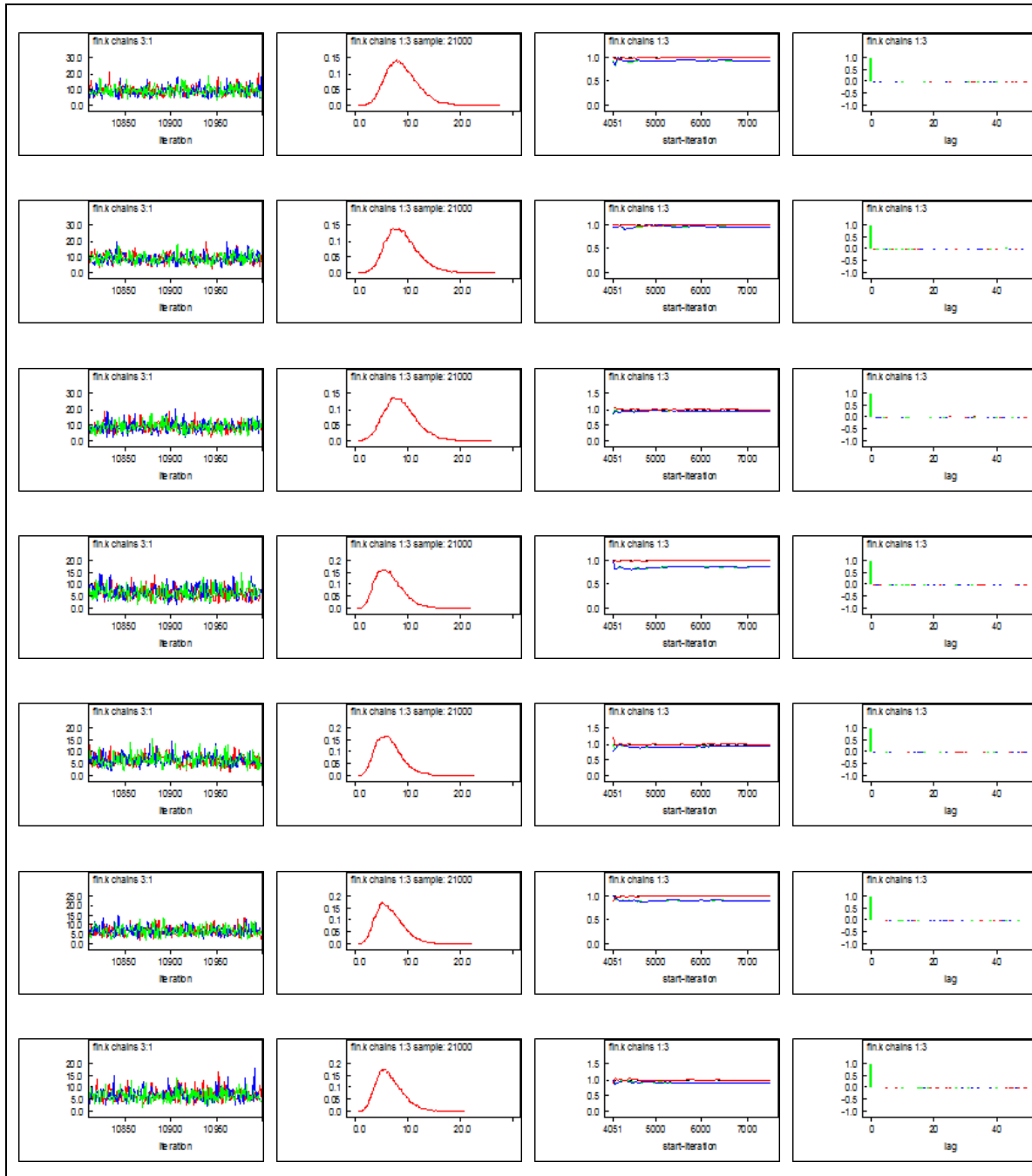


Figure 45: Diagnostics for  $f_{ln_t}$  where  $t = 1, 2, 5, 10, 30$  and  $50$

A6: Conference Posters

A6.1: Australasian Applied Statistics Conference, Queenstown, New Zealand, 2012



A6.2 International Biometrics Conference, Florence, Italy, 2014 and  
Uncertainty in Complex Models Conference, Sheffield, UK, 2014

# Bibliography

- Ahrens J.F., Loomis W.E. 1963. Floral induction and development in winter wheat. *Crop Science* 3:463-466
- Aitken Y. 1961. Flower initiation in relation to maturity in crop plants. I. Internode lengthening in relation to grazing oat varieties. *Australian Journal of Agricultural Research* 12:389-396
- Archer G., Saltelli A., Sobol I. 1997. Sensitivity measures, ANOVA-like techniques and the use of bootstrap. *Journal of Statistical Computation and Simulation* 58:99-120
- Arulampalam M.S., Maskell S., Gordon N., Clapp T. 2002. A tutorial on particle filters for online nonlinear/non-Gaussian Bayesian tracking. *IEE Transactions on Signal Processing*, 50
- Asseng S., Ewert F., Rosenzweig C., Jones J., Hatfield J., Ruane A., Boote K., Thorburn P., Rötter R., Cammarano D. 2013. Uncertainty in simulating wheat yields under climate change. *Nature Climate Change* 3:827-832
- Baker C.K., Gallagher J.N. 1983a. The development of winter-wheat in the field. 1. Relation between apical development and plant morphology within and between seasons. *Journal of Agricultural Science* 101:327-335
- Baker C.K., Gallagher J.N. 1983b. The development of winter-wheat in the field. 2. The control of primordium initiation rate by temperature and photoperiod. *Journal of Agricultural Science* 101:337-344
- Baker C.K., Gallagher J.N., Monteith J.L. 1980. Daylength change and leaf appearance in winter wheat. *Plant, Cell & Environment* 3:285-287. doi:10.1111/1365-3040.ep11581834
- Bassu S., Brisson N., Durand J.L., Boote K., Lizaso J., Jones J.W., Rosenzweig C., Ruane A.C., Adam M., Baron C. 2014. How do various maize crop models vary in their responses to climate change factors? *Global Change Biology* 20:2301-2320
- Bayarri M., Berger J., Steinberg D.M. 2009. Special issue on computer modeling. *Technometrics* 51:353-353

- Becker W., Rowson J., Oakley J.E., Yoxall A., Manson G., Worden K. 2011. Bayesian sensitivity analysis of a model of the aortic valve. *Journal of Biomechanics* 44:1499-1506. doi:10.1016/j.jbiomech.2011.03.008
- Berliner L.M. 1996. Hierarchical Bayesian time series models. In *Maximum Entropy and Bayesian Methods*, eds. K. Hanson, R. Silver, 15-22. Springer Netherlands.
- Bernardo J., Smith A. 1994. Bayesian Theory. Chichester, UK: John Wiley & Sons.
- Beven K. 2006. On undermining the science? *Hydrological Processes* 20:3141-3146. doi:10.1002/hyp.6396
- Beven K., Binley A. 1992. The future of distributed models: Model calibration and uncertainty prediction. *Hydrological Processes* 6:279-298. doi:10.1002/hyp.3360060305
- Beven K., Freer J. 2001. Equifinality, data assimilation, and uncertainty estimation in mechanistic modelling of complex environmental systems using the GLUE methodology. *Journal of Hydrology* 249:11-29. doi:10.1016/s0022-1694(01)00421-8
- Bezlepkina I., Adenäeur M., Kuiper M., Janssen S., Knapen R., Kanellopoulos A., Brouwer F., Wien J., Wolf J., van Ittersum M. 2010. Using the SEAMLESS integrated framework for ex-ante assessment of trade policies. In *Towards Effective Food Chains: Models and Applications*. Wageningen, NL: Wageningen Academic Publishers
- Bhattacharya S. 2007. A simulation approach to Bayesian emulation of complex dynamic computer models. *Bayesian Analysis* 2:783-815
- Bindi M., Porter J.R., Miglietta F. 1995. Comparison of models to calculate leaf number in wheat. *European Journal of Agronomy* 4:15-25
- Blasone R.S., Vrugt J.A., Madsen H., Rosbjerg D., Robinson B.A., Zyvoloski G.A. 2008. Generalized likelihood uncertainty estimation (GLUE) using adaptive Markov Chain Monte Carlo sampling. *Advances in Water Resources* 31:630-648. doi:10.1016/j.advwatres.2007.12.003
- Blazkova S., Beven K. 2009. A limits of acceptability approach to model evaluation and uncertainty estimation in flood frequency estimation by continuous simulation: Skalka catchment, Czech Republic. *Water Resources Research* 45:W00B16. doi:10.1029/2007wr006726

- Boone M.Y.L., Rickman R.W., Whisler F.D. 1990. Leaf appearance rates of two winter wheat cultivars under high carbon dioxide conditions. *Agronomy Journal* 82:718-724
- Boote K.J., Jones J.W., Pickering N.B. 1996. Potential uses and limitations of crop models. *Agronomy Journal* 88:704-716
- Box G.E.P. 1976. Science and statistics. *Journal of the American Statistical Association* 71:791-799
- Brooking I.R. 1996. Temperature response of vernalization in wheat: A developmental analysis. *Annals of Botany* 78:507-512
- Brooking I.R., Jamieson P.D. 2002. Temperature and photoperiod response of vernalization in near-isogenic lines of wheat. *Field Crops Research* 79:21-38
- Brooking I.R., Jamieson P.D., Porter J.R. 1995. The influence of daylength on final leaf number in spring wheat. *Field Crops Research* 41:155-165
- Brooks S.P., Gelman A. 1998. General methods for monitoring convergence of iterative simulations. *Journal of Computational and Graphical Statistics* 7:434-455
- Brown H., Munro C., Huth N., Meenken E. 2012a. Using a crop model to characterise the developmental phenotype of different wheat varieties. *Sage* 11:5
- Brown H.E., Jamieson P.D., Brooking I.R., Moot D.J., Huth N.I. 2013. Integration of molecular and physiological models to explain time of anthesis in wheat. *Annals of Botany* 112:1683-1703. doi:10.1093/aob/mct224
- Brown H.E., Munro C., Huth N., Meenken E.D. 2012b. Using a crop model to characterise the developmental phenotype of different wheat varieties. Paper presented at the *Proceedings of the 16th Australian Agronomy Conference*, Armidale, Australia, 14-18 October 2012.
- Bulygina N., Gupta H. 2009. Estimating the uncertain mathematical structure of a water balance model via Bayesian data assimilation. *Water Resour. Res.* 45:W00B13. doi:10.1029/2007wr006749
- Burn B., Underwood F. 2007. *Practical Bayesian Data Analysis*. Reading, UK: University of Reading.
- Cacuci D.G., Ionescu-Bujer M., Navon I.M. 2005. *Sensitivity and Uncertainty Analysis*. Boca Raton, USA: Chapman & Hall.

- Candy J.V. 2009. Bayesian Signal Processing: Classical, Modern and Particle Filtering Methods. New Jersey, USA: John Wiley and Sons.
- Cao W., Moss D.N. 1991. Phyllochron change in winter wheat with planting date and environmental changes. *Agronomy Journal* 83:396-401
- Carlin B.P., Louis T.A. 2000. Bayes and Empirical Bayes Methods for Data Analysis. New York, USA: Chapman & Hall.
- Carson J.S. 2002. Model verification and validation. In *Proceedings of the Winter Simulation Conference.*, San Diego, USA, 8-11 December 2002. IEEE, 52-58.
- Chatfield C., Collins A.J. 1980. Introduction to Multivariate Analysis. New York, USA: Chapman and Hall.
- Chourd P. 1960. Vernalization and its relations to dormancy. *Annual Review of Plant Physiology* 11
- Chujo H. 1966a. Difference in vernalization effect in wheat under various temperatures. *Journal of the Crop Science Society of Japan* 35:177-186
- Cichota R., Snow V.O., Kelliher F.M. 2013. Sensitivity analysis to investigate the factors controlling the effectiveness of a nitrification inhibitor in the soil. Paper presented at the *Proceedings of the 20th International Congress on Modelling and Simulation*, Adelaide, Australia, 1-6 December 2013.
- Claeskens G., Hjort N.L. 2008. Model Selection and Model Averaging. Cambridge, UK: Cambridge University Press.
- Clark M.P., Slater A.G., Rupp D.E., Woods R.A., Vrugt J.A., Gupta H.V., Wagener T., Hay L.E. 2008. Framework for Understanding Structural Errors (FUSE): A modular framework to diagnose differences between hydrological models. *Water Resources Research* 44:W00B02. doi:10.1029/2007wr006735
- Clifford D., Pagendam D., Baldock D., Cressie N., Farquaharson R., Farrell M., Macdonald L., Murray L. 2013. Bayesian hierarchical modeling of soil carbon dynamics. Paper presented at the *Proceedings of the 20th International Congress on Modelling and Simulation*, Adelaide, Australia, 1-6 December 2013.
- Cochran W.G., Cox G.M. 1957. Experimental Designs, 6th edn. Ames, USA: John Wiley & Sons.

- Collinson S.T., Ellis R.H., Summerfield R.J., Roberts E.H. 1992. Durations of photoperiod-sensitive and photoperiod-insensitive phases of development to flowering in four cultivars of rice (*Oryza sativa* L.). *Annals of Botany* 70:339-346
- Conti S., O'Hagan A. 2010. Bayesian emulation of complex multi-output and dynamic computer models. *Journal of Statistical Planning and Inference* 140:640-651. doi:10.1016/j.jspi.2009.08.006
- Cooper J.P. 1956. Developmental analysis of populations in the cereals and herbage grasses. 1. Methods and techniques. *Journal Agricultural Science* 47:262-279
- Cooper M., van Eeuwijk F.A., Hammer G.L., Podlich D.W., Messina C. 2009. Modeling QTL for complex traits: Detection and context for plant breeding. *Current Opinion in Plant Biology* 12:231-240
- Cressie N., Wikle C.K. 2011. *Statistics for Spatio-Temporal Data*. Hoboken, USA: John Wiley & Sons.
- Cripps E., O'Hagan A., Quaife T. 2013. Quantifying uncertainty in remotely sensed land cover maps. *Stochastic Environmental Research and Risk Assessment* 27:1239-1251. doi:10.1007/s00477-012-0660-3
- Cussans G.W., Raudonius S., Brain P., Cumberworth S. 1996. Effects of depth of seed burial and soil aggregate size on seedling emergence of *Alopecurus myosuroides*, *Galium aparine*, *Stellaria media* and wheat. *Weed Research* 36:133-141. doi:10.1111/j.1365-3180.1996.tb01809.x
- Da Veiga S., Wahl F., Gamboa F. 2009. Local polynomial estimation for sensitivity analysis on models with correlated inputs. *Technometrics* 51:452-463
- Delecolle R., Hay R.K.M., Guerif M., Pluchard P., Varletgrancher C. 1989. A method of describing the progress of apical development in wheat, based on the time-course of organogenesis. *Field Crops Research* 21:147-160
- Diaz A., Zikhali M., Turner A.S., Isaac P., Lauri D.A. 2012. Copy number variation affecting the photoperiod-B1 and vernalization-A1 genes is associated with altered flowering time in wheat (*Triticum aestivum*) *Plos One* 7:1-11
- Distelfeld A., Li C., Dubcovsky J. 2009a. Regulation of flowering in temperate cereals. *Current Opinion in Plant Biology* 12:178-184. doi:<http://dx.doi.org/10.1016/j.pbi.2008.12.010>

- Distelfeld A., Tranquilli G., Li C., Yan L., Dubcovsky J. 2009b. Genetic and molecular characterization of the VRN2 loci in tetraploid wheat. *Plant Physiology* 149:245-257. doi:10.1104/pp.108.129353
- Draper D. 1995. Assessment and propagation of model uncertainty. *Journal of the Royal Statistical Society. Series B (Methodological)* 57:45-97
- Draper N.R., Smith H. 1981. Applied Regression Analysis 2nd edn. New York, USA: Wiley.
- Dubcovsky J., Loukoianov A., Fu D., Valarik M., Sanchez A., Yan L. 2006. Effect of photoperiod on the regulation of wheat vernalization genes VRN1 and VRN2. *Plant Molecular Biology* 60:469-480. doi:10.1007/s11103-005-4814-2
- Eagles H.A., Cane K., Kuchel H., Hollamby G.J., Vallance N., Eastwood R.F., Gororo N.N., Martin P.J. 2010. Photoperiod and vernalization gene effects in southern Australian wheat. *Crop and Pasture Science* 61:721-730. doi:<http://dx.doi.org/10.1071/CP10121>
- Ellis R.H., Collinson S.T., Hudson D., Patefield W.M. 1992. The analysis of reciprocal transfer experiments to estimate the durations of photoperiod-sensitive and photoperiod-insensitive phases of plant development: An example in soya bean. *Annals of Botany* 70:87-92
- Evensen G. 2007. Data Assimilation: The Ensemble Kalman Filter. Berlin, GE: Springer.
- Ewert F., van Ittersum M.K., Bezlepkina I., Therond O., Andersen E., Belhouchette H., Bockstaller C., Brouwer F., Heckeley T., Janssen S. 2009. A methodology for enhanced flexibility of integrated assessment in agriculture. *Environmental Science & Policy* 12:546-561
- Faure S., Higgins J., Turner A., Laurie D.A. 2007. The flowering locus T-like gene family in barley (*Hordeum vulgare*). *Genetics* 176:599-609. doi:10.1534/genetics.106.069500
- Fisher R.A. 1926. The arrangement of field experiments. *Journal of the Ministry of Agriculture* 33:503-513
- Fowler A. 2012. Data Assimilation tutorial on the Kalman filter. University of Reading. <https://earth.esa.int/documents/973910/1002056/DA2.pdf/9cd3c6c8-7d89-400d-8c9c-df33259f47c2>. Accessed 16 October 2015.

- Fricker T.E., Oakley J.E., Sims N.D., Worden K. 2011. Probabilistic uncertainty analysis of an FRF of a structure using a Gaussian process emulator. *Mechanical Systems and Signal Processing* 25:2962-2975.  
doi:10.1016/j.ymssp.2011.06.013
- Gal G., Makler-Pick V., Shachar N. 2014. Dealing with uncertainty in ecosystem model scenarios: Application of the single-model ensemble approach. *Environmental Modelling & Software* 61:360-370.  
doi:<http://dx.doi.org/10.1016/j.envsoft.2014.05.015>
- Gauch H.G., Hwang J., Fick G.W. 2003. Model evaluation by comparison of model-based predictions and measured values. *Agronomy Journal* 95:1442-1446
- Gelman A., Carlin J.B., Stern H.S., Dunson D.B., Vehtari A., Rubin D.B. 2006. Bayesian Data Analysis, Third Edition edn. Boca Raton, USA: Chapman & Hall.
- Gharib Shirangi M. 2014. History matching production data and uncertainty assessment with an efficient TSVD parameterization algorithm. *Journal of Petroleum Science and Engineering* 113:54-71.  
doi:<http://dx.doi.org/10.1016/j.petrol.2013.11.025>
- Gilks W.R., Richardson S., Spiegelhalter D.J. 1996. Introducing Markov Chain Monte Carlo. In *Markov Chain Monte Carlo in Practice*, 1-19. Boca Raton, USA: Chapman & Hall.
- Giorlami. 1997. EPSRC grant proposal. In.
- Goldringer I., Prouin C., Rousset M., Galic N., Bonnin I. 2006. Rapid differentiation of experimental populations of wheat for heading time in response to local climatic conditions. *Annals of Botany* 98:805-817
- Goldstein M., Rougier J.C. 2009. Reified Bayesian modelling and inference for the physical systems. *Journal of Statistical Planning and Inference*
- González-Rodríguez P., Kindelan M., Moscoso M., Dorn O. 2005. History matching problem in reservoir engineering using the propagation-backpropagation method. *Inverse Problems* 21:565
- Gonze D. 2012. Linear Difference Equations. Université Libre de Bruxelles. <http://homepages.ulb.ac.be/~dgonze/TEACHING/difference.pdf>. Accessed 16 October 2015.



- Gordon N.J., Salmond D.J., Smith A.F.M. 1993. Novel approach to nonlinear/non-Gaussian Bayesian state estimation. *Radar and Signal Processing, IEE Proceedings F* 140:107-113
- Gott M.B. 1957. Vernalization of green plants of a winter wheat. *Nature* 180:714-715
- Gott M.B., Gregory F.G., Purvis O.N. 1955. Studies in vernalization of cereals XIII. Photoperiodic control of stages in flowering between initiation and ear formation in vernalized and unvernallized 'Petkus' rye. *Annals of Botany* 56:501-511
- Greene B. 2005. *The Fabric of the Cosmos*. New York, USA: Vintage Books.
- Griffiths F.E.W., R.F. L., Bennett M.D. 1985. The effects of vernalization on the growth of the wheat shoot apex. *Annals of Botany* 17:417-432
- Guo Z., Song Y., Zhou R., Ren Z., Jia J. 2010. Discovery, evaluation and distribution of haplotypes of the wheat Ppd-D1 gene. *New Phytologist* 185:841-851. doi:10.1111/j.1469-8137.2009.03099.x
- Gupta H.V., Clark M.P., Vrugt J.A., Abramowitz G., Ye M. 2012. Towards a comprehensive assessment of model structural adequacy. *Water Resources Research* 48:W08301. doi:10.1029/2011wr011044
- Hacking I. 1975. *The Emergence of Probability*, 2nd edn. Cambridge, UK: Cambridge University Press.
- Hall J.W., Manning L.J., Hankin R.K.S. 2011. Bayesian calibration of a flood inundation model using spatial data. *Water Resources Research* 47:10.1029/2009wr008541. doi:10.1029/2009wr008541
- Halloran G.M. 1975. Genotype differences in photoperiodic sensitivity and vernalization response in wheat. *Annals of Botany* 39:845-851
- Hammer G.L., Kropff M.J., Sinclair T.R., Porter J.R. 2002. Future contributions of crop modelling - from heuristics and supporting decision making to understanding genetic regulation and aiding crop improvement. *European Journal of Agronomy* 18:15-31
- Hansel H. 1953. Vernalization of winter rye by negative temperatures and the influence of vernalization upon the lamina length of the first and second leaf in winter rye, spring barley, and winter barley. *Annals of Botany* 17:417-432
- Harding S., Payne R.W. 2011. *A Guide to Multivariate Analysis in GenStat*, GenStat Release 14 edn. Rothamsted, UK: VSN International Ltd.

- Harshbarger B., Davis L.L. 1952. Latinized rectangular lattices. *Biometrics* 8:73-84
- Haun J.R. 1973. Visual quantification of wheat development. *Agronomy Journal* 65:116-119
- Hawking S.W. 1988. A brief History of Time. New York: Bantam Books.
- Hay R., Porter J. 2006. The Physiology of Crop Yield, 314 edn. Oxford, UK: Blackwell Publishing.
- Hay R.K.M. 1999. Physiological control of growth and yield in wheat: Analysis and synthesis. In *Crop Yield. Physiology and Processes*, eds. D.L. Smith, C. Hamel, 1-38. Hong Kong: Springer
- Hay R.K.M., Kemp D.R. 1990. Primordium initiation at the stem apex as the primary event controlling plant development: Preliminary evidence from wheat for the regulation of leaf development. *Plant Cell and Environment* 13:1005-1008
- Hay R.K.M., Kemp D.R. 1992. The prediction of leaf canopy expansion in the leek from a simple model-dependent on primordial development. *Annals of Applied Biology* 120:537-545
- Hay R.K.M., Kirby E.J.M. 1991. Convergence and synchrony - a review of the coordination of development in wheat. *Australian Journal of Agricultural Research* 42:661-700
- He J., Le Gouis J., Stratonovitch P., Allard V., Gaju O., Heumez E., Orford S., Griffiths S., Snape J.W., Foulkes M.J., Semenov M.A., Martre P. 2012. Simulation of environmental and genotypic variations of final leaf number and anthesis date for wheat. *European Journal of Agronomy* 42:22-33. doi:10.1016/j.eja.2011.11.002
- Helton J.C. 1997. Uncertainty and sensitivity analysis in the presence of stochastic and subjective uncertainty. *Journal of Statistical Computation and Simulation* 57:3-76. doi:10.1080/00949659708811803
- Helton J.C., Davis F.J. 2000. Sampling-based methods. In *Sensitivity Analysis*, eds. A. Saltelli, K. Chan, E.M. Scott. Chichester, UK: John Wiley & Sons.
- Higdon D. 2007. A primer on space-time modeling from a Bayesian perspective. In *Statistical Methods for Spatio Temporal Systems*. Boca Raton, USA: Chapman & Hall/CRC.
- Hillborn R., Mangel M. 1997. The Ecological Detective. Confronting Models with Data. Princeton, USA: Princeton University Press.

- Hochman Z., Van Rees H., Carberry P., Hunt J., McCown R., Gartmann A., Holzworth D., Van Rees S., Dalgliesh N., Long W. 2009. Re-inventing model-based decision support with Australian dryland farmers. 4. Yield Prophet® helps farmers monitor and manage crops in a variable climate. *Crop and Pasture Science* 60:1057-1070
- Holzkämper A., Klein T., Seppelt R., Fuhrer J. 2015. Assessing the propagation of uncertainties in multi-objective optimization for agro-ecosystem adaptation to climate change. *Environmental Modelling & Software* 66:27-35. doi:<http://dx.doi.org/10.1016/j.envsoft.2014.12.012>
- Holzworth D.P., Huth N.I., deVoil P.G., Zurcher E.J., Herrmann N.I., McLean G., Chenu K., van Oosterom E.J., Snow V., Murphy C., Moore A.D., Brown H., Whish J.P.M., Verrall S., Fainges J., Bell L.W., Peake A.S., Poulton P.L., Hochman Z., Thorburn P.J., Gaydon D.S., Dalgliesh N.P., Rodriguez D., Cox H., Chapman S., Doherty A., Teixeira E., Sharp J., Cichota R., Vogeler I., Li F.Y., Wang E., Hammer G.L., Robertson M.J., Dimes J.P., Whitbread A.M., Hunt J., van Rees H., McClelland T., Carberry P.S., Hargreaves J.N.G., MacLeod N., McDonald C., Harsdorf J., Wedgwood S., Keating B.A. 2014. APSIM – Evolution towards a new generation of agricultural systems simulation. *Environmental Modelling & Software* 62:327-350. doi:<http://dx.doi.org/10.1016/j.envsoft.2014.07.009>
- Hora S.C., Iman R.L. 1986. A comparison of maximus/bounding and the Bayes/Monte Carlo for fault tree uncertainty analysis. In: Albuquerque, USA: Sandia National Laboratory.
- Hsu K.-l., Moradkhani H., Sorooshian S. 2009. A sequential Bayesian approach for hydrologic model selection and prediction. *Water Resource Research* 45:W00B12. doi:10.1029/2008wr006824
- Iman R.L., Davenport J.M. 1982. Rank correlation plots for use with correlated input variables. *Communications in Statistics - Simulation and Computation* 11:335-360. doi:10.1080/03610918208812266
- Innis G.S., Noy-Meir I., Godron M., Van Dyne G.M. 1980. Total-system simulation models. In *Grasslands, Systems Analysis and Management*, eds. A.I. Breymer, G.M. Van Dyne. Cambridge, UK: Cambridge University Press.
- Iwaki K., Haruna S., Niwa T., Kato K. 2001. Adaptation and ecological differentiation in wheat with special reference to geographical variation of growth habit and Brn genotype. *Plant Breeding/Zeitschrift fuer Pflanzenzuchtung* 120:107-114

- Jacques J., Lavergne C., Devictor N. 2006. Sensitivity analysis in presence of model uncertainty and correlated inputs. *Reliability Engineering & System Safety* 91:1126-1134. doi:DOI: 10.1016/j.res.2005.11.047
- Jamieson P., Brooking I., Zyskowski R., Munro C. 2008. The vexatious problem of the variation of the phyllochron in wheat. *Field Crops Research* 108:163-168. doi:10.1016/j.fcr.2008.04.011
- Jamieson P.D., Brooking I.R., Porter J.R. 1995a. How temperature and daylength determine flowering time in spring wheat - A discussion. *Agronomy Society of New Zealand - Proceedings, Twenty-Fifth Annual Conference 1995/96* 25:23-27
- Jamieson P.D., Brooking I.R., Porter J.R. 1996. A new model of spring wheat phenological response to temperature and daylength. Paper presented at the *Proceedings of the 8th Australian Agronomy Conference*, Toowoomba, Australia, 30 January-2 Februar.
- Jamieson P.D., Brooking I.R., Porter J.R., Wilson D.R. 1995b. Prediction of leaf appearance in wheat - A question of temperature. *Field Crops Research* 41:35-44
- Jamieson P.D., Brooking I.R., Semenov M.A., McMaster G.S., White J.W., Porter J.R. 2007. Reconciling alternative models of phenological development in winter wheat. *Field Crops Research* 103:36-41. doi:10.1016/j.fcr.2007.04.009
- Jamieson P.D., Brooking I.R., Semenov M.A., Porter J.R. 1998b. Making sense of wheat development: A critique of methodology. *Field Crops Research* 55:117-127
- Jamieson P.D., Ewert F. 1999. The role of roots in controlling soil water extraction during drought: an analysis by simulation. *Field Crops Research* 60:267-280. doi:10.1016/s0378-4290(98)00144-0
- Jamieson P.D., Munro C.A. 1999. A simple method for the phenological evaluation of new cereal cultivars. *Agronomy New Zealand* 29:63-68
- Jamieson P.D., Semenov M.A., Brooking I.R., Francis G.S. 1998a. Sirius: A mechanistic model of wheat response to environmental variation. *European Journal of Agronomy* 8:161-179
- Johnson J.S., Gosling J.P., Kennedy M.C. 2011. Gaussian process emulation for second-order Monte Carlo simulations. *Journal of Statistical Planning and Inference* 141:1838-1848. doi:10.1016/j.jspi.2010.11.034

- Jong R.D., Best K.F. 1979. The effect of soil water potential, temperature and seeding depth on seedling emergence of wheat. *Canadian Journal of Soil Science* 59:259-264. doi:10.4141/cjss79-029
- Juston J., Andrén O., Kätterer T., Jansson P.-E. 2010. Uncertainty analyses for calibrating a soil carbon balance model to agricultural field trial data in Sweden and Kenya. *Ecological Modelling* 221:1880-1888. doi:10.1016/j.ecolmodel.2010.04.019
- Kadane J.B., Lazar N.A. 2004. Methods and criteria for model selection. *Journal of the American Statistical Association* 99:279-290
- Kalnay E. 2003. Atmospheric Modeling, Data Assimilation, and Predictability. Cambridge, UK: Cambridge University Press.
- Karsai I., Szűcs P., Mészáros K., Filichkina T., Hayes P.M., Skinner J.S., Láng L., Bedő Z. 2005. The VRN-H2 locus is a major determinant of flowering time in a facultative × winter growth habit barley (*Hordeum vulgare* L.) mapping population. *Theoretical and Applied Genetics* 110:1458-1466. doi:10.1007/s00122-005-1979-7
- Katz R.W. 2002. Techniques for estimating uncertainty in climate change scenarios and impact studies. *Climate Research* 20:167-185
- Kavetski D., Franks S.W., Kuczera G. 2002. Confronting input uncertainty in environmental modelling. In *Calibration of watershed models*, eds. Q. Duan, H.V. Gupta, S. Sorooshian, A.N. Rousseau, R. Turcotte, 49-68. Washington, USA: American Geophysical Union.
- Kavetski D., Kuczera G., Franks S.W. 2006. Bayesian analysis of input uncertainty in hydrological modeling: 2. Application. *Water Resources Research* 42:10.1029/2005WR004376. doi:10.1029/2005WR004376
- Kennedy M.C., Anderson C.W., Conti S., O'Hagan A. 2006. Case studies in Gaussian process modelling of computer codes. *Reliability Engineering & System Safety* 91:1301-1309. doi:DOI: 10.1016/j.ress.2005.11.028
- Kennedy M.C., O'Hagan A. 2001. Bayesian calibration of computer models. *Journal of the Royal Statistical Society: Series B (Statistical Methodology)* 63:425-464. doi:10.1111/1467-9868.00294
- Kiniry J.R., Ritchie J.T., Musser R.L., Flint E.P., Iwig W.C. 1983. The photoperiod sensitive interval in maize. *Agronomy Journal* 75:687-690
- Kippes N., Zhu J., Chen A., Vanzetti L., Lukaszewski A., Nishida H., Kato K., Dvorak J., Dubcovsky J. 2014. Fine mapping and epistatic interactions of

- the vernalization gene VRN-D4 in hexaploid wheat. *Molecular Genetics and Genomics* 289:47-62. doi:10.1007/s00438-013-0788-y
- Kirby E.J.M. 1974. Ear development in spring wheat. *Journal Agricultural Science* 82:437-447
- Kirby E.J.M. 1990. Coordination of leaf emergence and leaf and spikelet primordium initiation in wheat. *Field Crops Research* 25:253-264
- Kirby E.J.M. 1992. A field-study of the number of main shoot leaves in wheat in relation to vernalization and photoperiod. *Journal of Agricultural Science* 118:271-278
- Kirby E.J.M. 1993. Effect of sowing depth on seedling emergence, growth and development in barley and wheat. *Field Crops Research* 35:101-111. doi:[http://dx.doi.org/10.1016/0378-4290\(93\)90143-B](http://dx.doi.org/10.1016/0378-4290(93)90143-B)
- Kirby E.J.M., Appleyard M. 1981. Cereal Development Guide. In. Stoneleigh, UK: Cereal Unit, National Agricultural Centre,.
- Kirby E.J.M., Porter J.R., Day W., Adam J.S., Appleyard M., Ayling S., Baker C.K., Belford R.K., Biscoe P.V., Chapman A., Fuller M.P., Hampson J., Hay R.K.M., Matthews S., Thompson W.J., Weir A.H., Willington V.B.A., Wood D.W. 1987. An analysis of primordium initiation in Avalon winter-wheat crops with different sowing dates and at 9 sites in England and Scotland. *Journal of Agricultural Science* 109:123-134
- Kitagawa S., Shimada S., Murai K. 2012. Effect of *Ppd-1* on the expression of flowering-time genes in vegetative and reproductive growth stages of wheat. *Genes & Genetic Systems* 87:161-168. doi:10.1266/ggs.87.161
- Kobayashi K., Salam M.U. 2000. Comparing simulated and measured values using mean squared deviation and its components. *Agronomy Journal* 92:345-352
- Koehler J.R., Owen A.B. (eds). 1996. Computer Experiments, 13. Handbook of Statistics, 13: Design and Analysis of Experiments. Elsevier, Amsterdam, NL
- Krzanowski. 2000. Principles of Multivariate Analysis: A User's Perspective, Revised edn. Oxford, UK: Oxford University Press.
- Kuczera G., Kavetski D., Franks S., Thyer M. 2006. Towards a Bayesian total error analysis of conceptual rainfall-runoff models: Characterising model error using storm-dependent parameters. *Journal of Hydrology* 331:161-177

- Künsch H.R. 2013. Particle filters. *Bernoulli* 19:1391-1403
- Kurowicka D., Cooke R. 2006. Uncertainty Analysis. Chichester, UK: John Wiley & Sons.
- Law C.N., Worland A.J. 1997. Genetic analysis of some flowering time and adaptive traits in wheat. *New Phytologist* 5:19-28
- Lee Y., Nelder J.A., Pawitan Y. 2006. Generalized Linear Models with Random Effects, 1 edn. Boca Raton, USA: Chapman & Hall.
- Levitt J. 1948. Frost Killing and Hardiness of Plants. A Critical Review. Minneapolis, USA: Burgess Publishing Company.
- Levy J., Peterson M.L. 1972. Responses of spring wheats to vernalization and photoperiod. *Crop Science* 12:487-490.  
doi:10.2135/cropsci1972.0011183X001200040029x
- Lewis J.M., Lakshmivarahan S., Dhall S.K. 2006. Dynamic Data Assimilation: A Least Squares Approach. Cambridge, UK: Cambridge University Press.
- Li C., Distelfeld A., Comis A., Dubcovsky J. 2011. Wheat flowering repressor VRN2 and promoter CO2 compete for interactions with NUCLEAR FACTOR-Y complexes. *The Plant Journal* 67:763-773.  
doi:10.1111/j.1365-313X.2011.04630.x
- Liang Y.L., Richards R.A. 1994. Coleoptile tiller development is associated with fast early vigour in wheat. *Euphytica* 80:119-124.  
doi:10.1007/bf00039306
- Lorenz E.N., Emanuel K.A. 1998. Optimal sites for supplementary weather observations: Simulation with a small model. *Journal of the Atmospheric Sciences* 55:399-414
- Mahdi L., Bell C.J., Ryan J. 1998. Establishment and yield of wheat (*Triticum turgidum* L.) after early sowing at various depths in a semi-arid Mediterranean environment. *Field Crops Research* 58:187-196.  
doi:[http://dx.doi.org/10.1016/S0378-4290\(98\)00094-X](http://dx.doi.org/10.1016/S0378-4290(98)00094-X)
- Martre P., He J., Le Gouis J., Semenov M.A. 2015. In silico system analysis of physiological traits determining grain yield and protein concentration for wheat as influenced by climate and crop management. *Journal of Experimental Botany*:erv049
- McFarland J.M. 2008. Uncertainty Analysis for Computer Simulations Through Validation and Calibration. Vanderbilt University, Nashville, USA.

- McKay M.D. 1995. Evaluating prediction uncertainty. In. Washington, USA: Nuclear Regulatory Commission, Division of Systems Technology.
- McKay M.D., Morrison J.D. 1997. Structural model uncertainty in stochastic simulation. In. Los Alamos, USA: Los Alamos National Laboratory.
- Mead R. 1988. *The Design of Experiments*. Cambridge, UK: Cambridge University Press.
- Miglietta F. 1989. Effect of photoperiod and temperature on leaf initiation rates in wheat (*Triticum spp.*). *Field Crops Research* 21:121-130. doi:10.1016/0378-4290(89)90048-8
- Miglietta F. 1991a. Simulation of wheat ontogenesis. I. Appearance of main stem leaves in the field. *Climate Research* 2:145-150
- Miglietta F. 1991b. Simulation of wheat ontogenesis. II. Predicting dates of ear emergence and main stem final leaf number. *Climate Research* 1:151-160
- Montanari A. 2007. What do we mean by ‘uncertainty’? The need for a consistent wording about uncertainty assessment in hydrology. *Hydrological Processes* 21:841-845. doi:10.1002/hyp.6623
- Montanari A. 2011. Uncertainty of Hydrological Predictions. In *Treatise on Water Science*, ed P. Wilderer, 459-478. Oxford, UK: Elsevier.
- Montanari A., Grossi G. 2008. Estimating the uncertainty of hydrological forecasts: A statistical approach. *Water Resources Research* 44:W00B08. doi:10.1029/2008wr006897
- Montanari A., Shoemaker C.A., van de Giesen N. 2009. Introduction to special section on Uncertainty Assessment in Surface and Subsurface Hydrology: An overview of issues and challenges. *Water Resources Research* 45:W00B00. doi:10.1029/2009wr008471
- Monteith J.L. 1996. The quest for balance in crop modeling. *Agronomy Journal* 88:695-697
- Montgomery J.M., Hollenbach F.M., Ward M.D. 2012. Improving predictions using ensemble Bayesian model averaging. *Political Analysis* 20:271-291. doi:10.1093/pan/mps002
- Murray L.M. 2013. Bayesian state-space modelling on high-performance hardware using LibBi. *arXiv preprint arXiv:1306.3277*



- Neyman J. 1957. "Inductive behaviour" as a basic concept of philosophy of science. *Revue Internationale de Statistique* 25:7-22
- O'Hagan A. 2006. Bayesian analysis of computer code outputs: A tutorial. *Reliability Engineering & System Safety* 91:1290-1300. doi:DOI: 10.1016/j.ress.2005.11.025
- O'Hagan A. 2008. Managing uncertainty in complex models. <http://mucm.group.shef.ac.uk/index.html>. Accessed 10 April 2010.
- O'Hagan A. 2012. Probabilistic uncertainty specification: Overview, elaboration techniques and their application to a mechanistic model of carbon flux. *Environmental Modelling & Software* 36:35-48. doi:10.1016/j.envsoft.2011.03.003
- O'Hagan A., Kennedy M.C., Oakley J.E. 1999. Uncertainty analysis and other inference tools for complex computer codes. In *Bayesian Statistics 6*, eds. J.M. Bernardo, J.O. Berger, A.P. Dawid, A.F.M. Smith, 503-524. Oxford, UK: Oxford University Press.
- O'Hagan A., McCabe C., Akehurst R., Brennan A., Briggs A., Claxton K., Fenwick E., Fryback D., Sculpher M., Spiegelhalter D., Willan A. 2005. Incorporation of uncertainty in health economic modelling studies. *Pharmacoeconomics* 23:529-536
- O'Hagan A., Oakley J.E. 2004. Probability is perfect, but we can't elicit it perfectly. *Reliability Engineering & System Safety* 85:239-248. doi:10.1016/j.ress.2004.03.014
- O'Hagan A., Stevens J.W., Montmartin J. 2001. Bayesian cost-effectiveness analysis from clinical trial data. *Statistics in Medicine* 20:733-753. doi:10.1002/sim.861
- Oakley J., O'Hagan A. 2002. Bayesian inference for the uncertainty distribution of computer model outputs. *Biometrika* 89:769-784
- Oakley J.E., O'Hagan A. 2004. Probabilistic sensitivity analysis of complex models: a Bayesian approach. *Journal of the Royal Statistical Society: Series B (Statistical Methodology)* 66:751-769
- Oberkampf W.L., Roy C.J. 2010. *Verification and Validation in Scientific Computing*. Cambridge, UK: Cambridge University Press.
- Oreskes N., Shrader-Frechette K., Belitz K. 1994. Verification, validation and confirmation of numerical models in the earth sciences. *Science* 263

- Pappenberger F. 2006. Ignorance is bliss: Or seven reasons not to use uncertainty analysis. *Water Resources Research* 42.  
doi:10.1029/2005wr004820
- Passioura J.B. 1996. Simulation models: Science, snake oil, education, or engineering? *Agronomy Journal* 88:690-694
- Pease C.M., Bull J.J. 1992. Is science logical? *Bioscience* 42:293-298
- Photiades I., Hadjichristodoulou A. 1984. Sowing date, sowing depth, seed rate and row spacing of wheat and barley under dryland conditions. *Field Crops Research* 9:151-162. doi:[http://dx.doi.org/10.1016/0378-4290\(84\)90021-2](http://dx.doi.org/10.1016/0378-4290(84)90021-2)
- Popper K.R. 1959. *The Logic of Scientific Discovery*. New York, USA: Harper and Row.
- Popper K.R. 1972. *Objective Knowledge*. Oxford, UK: Clarendon Press.
- Porter J.R. 1993. AFRCWHEAT2: A model of the growth and development of wheat incorporating responses to water and nitrogen. *European Journal of Agronomy* 2:69-82
- Porter J.R., Bragg P.L., Rayner J.H., Weir A.H., Landsberg J.J. 1982. The ARC winter wheat simulation model - principles and progress. *Monograph, British Plant Growth Regulator Group*:97-108
- Porter J.R., Gawith M. 1999. Temperatures and the growth and development of a wheat: a review. *European Journal of Agronomy* 10:23-36
- Porter J.R., Jamieson P.D., Wilson D.R. 1993. Comparison of the wheat simulation models AFRCWHEAT2, CERES-Wheat and SWHEAT for non-limiting conditions of crop growth. *Field Crops Research* 33:131-157. doi:Doi: 10.1016/0378-4290(93)90098-8
- Portier C.J. 2001. Linking toxicology and epidemiology: the role of mechanistic modelling. *Statistics in Medicine* 20:1387-1393
- Prieur C. 2014. Recent inference approaches for Sobol' sensitivity indices. In *Proceedings of Uncertainty in Computer Models Conference*, Sheffield, UK.
- Raftery A.E., Gneiting T., Balabdaoui F., Polakowski M. 2005. Using Bayesian model averaging to calibrate forecast ensembles. *Monthly Weather Review* 133:1155-1174

- Rebetzke G.J., Richards R.A., Fettell N.A., Long M., Condon A.G., Forrester R.I., Botwright T.L. 2007. Genotypic increases in coleoptile length improves stand establishment, vigour and grain yield of deep-sown wheat. *Field Crops Research* 100:10-23.  
doi:<http://dx.doi.org/10.1016/j.fcr.2006.05.001>
- Refsgaard J.C., van der Sluijs J.P., Brown J., van der Keur P. 2006. A framework for dealing with uncertainty due to model structure error. *Advances in Water Resources* 29:1586-1597.  
doi:<http://dx.doi.org/10.1016/j.advwatres.2005.11.013>
- Refsgaard J.C., van der Sluijs J.P., Højberg A.L., Vanrolleghem P.A. 2007. Uncertainty in the environmental modelling process – A framework and guidance. *Environmental Modelling & Software* 22:1543-1556.  
doi:<http://dx.doi.org/10.1016/j.envsoft.2007.02.004>
- Reinink K., Jorritsma I., Darwinkel A. 1986. Adaptation of the AFRC wheat phenology model for Dutch conditions. *Netherlands Journal of Agricultural Science* 34:1-13
- Renard B., Kavetski D., Kuczera G., Thyer M., Franks S.W. 2010. Understanding predictive uncertainty in hydrologic modeling: The challenge of identifying input and structural errors. *Water Resources Research* 46
- Rings J., Vrugt J.A., Schoups G., Huisman J.A., Vereecken H. 2012. Bayesian model averaging using particle filtering and Gaussian mixture modeling: Theory, concepts, and simulation experiments. *Water Resources Research* 48:W05520. doi:10.1029/2011wr011607
- Robertson M.J., Brooking I.R., Ritchie J.T. 1996. Temperature response of vernalization in wheat: Modelling the effect on the final number of mainstem leaves. *Annals of Botany* 78:371-381
- Rosenzweig C., Jones J., Hatfield J., Ruane A., Boote K., Thorburn P., Antle J., Nelson G., Porter C., Janssen S. 2013. The agricultural model intercomparison and improvement project (AgMIP): Protocols and pilot studies. *Agricultural and Forest Meteorology* 170:166-182
- Rotter R.P., Carter T.R., Olesen J.E. 2011. Crop-climate models need an overhaul. *Nature Climate Change* 1:175-177
- Rougier J. 2008. Efficient emulators for multivariate deterministic functions. *Journal of Computational and Graphical Statistics* 17:827-843
- Rougier J., Guillas S., Maute A., Richmond A.D. 2009. Expert knowledge and multivariate emulation: The Thermosphere-Ionosphere

- Electrodynamics General Circulation Model (TIE-GCM). *Technometrics* 51:414-424. doi:10.1198/tech.2009.07123
- Rougier J.C. 1996. Probabilistic inference for future climate using an ensemble of climate model evaluations. *Climatic Change* 81:247-267
- Sacks J., Welch W.J., Toby J.M., Wynn H.P. 1989. Design and analysis of computer experiments. *Statistical Science* 4:409-423
- Saltelli A., Chan K., Scott E.M. (eds). 2000. Sensitivity Analysis. Wiley, New York, USA
- Saltelli A., Ratto M., Tarantola S., Campolongo F. 2006. Sensitivity analysis practices: Strategies for model-based inference. *Reliability Engineering & System Safety* 91:1109-1125. doi:DOI: 10.1016/j.res.2005.11.014
- Santner T., Williams B., Notz W. (eds). 2003. The Design and Analysis of Computer Experiments. Springer Verlag, New York, USA
- Sargent R.G. 2005. Verification and validation of simulation models. In *Proceedings of the 37th Winter Simulation Conference*, Orlando, USA. 130-143.
- Sasani S., Hemming M.N., Oliver S.N., Greenup A., Tavakkol-Afshari R., Mahfoozi S., Poustini K., Sharifi H.-R., Dennis E.S., Peacock W.J., Trevaskis B. 2009. The influence of vernalization and daylength on expression of flowering-time genes in the shoot apex and leaves of barley (*Hordeum vulgare*). *Journal of Experimental Botany* 60:2169-2178. doi:10.1093/jxb/erp098
- Schall R. 1991. Estimation in generalized linear models with random effects. *Biometrika* 78:719-727
- Schoups G., Vrugt J.A. 2010. A formal likelihood function for parameter and predictive inference of hydrologic models with correlated, heteroscedastic, and non-Gaussian errors. *Water Resources Research* 46:W10531. doi:10.1029/2009wr008933
- Sharma D.L., D'Antuono M.F. 2011. Predicting flowering dates in wheat with a new statistical phenology model. *Agronomy Journal* 103:221-229
- Shaw L.M., Turner A.S., Laurie D.A. 2012. The impact of photoperiod insensitive Ppd-1a mutations on the photoperiod pathway across the three genomes of hexaploid wheat (*Triticum aestivum*). *The Plant Journal* 71:71-84. doi:10.1111/j.1365-313X.2012.04971.x

- Simpson J., Weiner E. 1989. Oxford English Dictionary. In. Oxford, UK: Oxford University Press.
- Sinclair T.R., Muchow R.C. 2001. System analysis of plant traits to increase grain yield on limited water supplies. *Agronomy Journal* 93:263-270
- Sinclair T.R., Seligman N. 2000. Criteria for publishing papers on crop modeling. *Field Crops Research* 68:165-172. doi:10.1016/s0378-4290(00)00105-2
- Sinclair T.R., Seligman N.G. 1996. Crop modeling: From infancy to maturity. *Agronomy Journal* 88:698-704
- Skinner B.F. 1956. A case history in scientific method. *American Psychologist* 11:221-233
- Slafer G.A., Rawson H.M. 1994b. Does temperature affect final numbers of primordia in wheat? *Field Crops Research* 39:111-117. doi:10.1016/0378-4290(94)90013-2
- Slafer G.A., Rawson H.M. 1995. Photoperiod\*temperature interactions in contrasting wheat genotypes: Time to heading and final leaf number. *Field Crops Research* 44:73-83
- Slafer G.A., Rawson H.M. 1997. Phyllochron in wheat as affected by photoperiod under two temperature regimes. *Australian Journal of Plant Physiology* 24:151-158
- Smith P., Smith J.U., Powlson D.S., McGill W.B., Arah J.R.M., Chertov O.G., Coleman K., Franko U., Frolking S., Jenkinson D.S., Jensen L.S., Kelly R.H., Klein-Gunnewiek H., Komarov A.S., Li C., Molina J.A.E., Mueller T., Parton W.J., Thornley J.H.M., Whitmore A.P. 1997. A comparison of the performance of nine soil organic matter models using datasets from seven long-term experiments. *Geoderma* 81:153-225
- Snape J.W., Butterworth K., Whitechurch E., Worland A.J. 2001. Waiting for fine times: Genetics of flowering time in wheat. *Euphytica* 119:185-190
- Spiegelhalter D.J., Best N.G. 2002. Bayesian approaches to multiple sources of evidence and uncertainty in complex cost-effectiveness modelling. *Statistics in Medicine* 22:3687-3709. doi:10.1002/sim.1586
- Spiegelhalter D.J., Thomas A., Best N.G., Lund D. 2004. WinBUGS Version 2.0 Users Manual. In. Cambridge, UK: MRC Biostatistics Unit.
- Stanfill B., Clifford D., Thorburn P. 2014. An efficient sensitivity analysis method for spatio-temporal data from an agricultural systems

- simulator. In *Proceedings of the Australasian Applied Statistic Conference*, Kangaroo Island, AU, 1-5 December.
- Stedinger J.R., Vogel R.M., Lee S.U., Batchelder R. 2008. Appraisal of the generalized likelihood uncertainty estimation (GLUE) method. *Water Resources Research* 44:W00B06. doi:10.1029/2008wr006822
- Stevens J.W., O'Hagan A., Miller P. 2003. Case study in the Bayesian analysis of a cost-effectiveness trial in the evaluation of health care technologies: Depression. *Pharmaceutical Statistics* 2:51-68. doi:10.1002/pst.43
- Stigler S.M. 1986. *The History of Statistics: The Measurement of Uncertainty Before 1900* Cambridge, UK: Harvard University Press.
- Streamsim Technologies I. 1999-2014. History matching using evolutionary algorithms. <http://www.streamsim.com/>. Accessed June 2014
- Strogatz S. 2014. *Nonlinear dynamics and chaos*. Youtube.com. [https://www.youtube.com/playlist?list=PLbN57C5Zdl6j\\_qJA-pARJnKsmROzPnO9V](https://www.youtube.com/playlist?list=PLbN57C5Zdl6j_qJA-pARJnKsmROzPnO9V). Accessed October 16 2015.
- Strong M. 2012. *Managing Structural Uncertainty in Health Economic Decision Models*. University of Sheffield, Sheffield, UK.
- Strong M., Oakley J.E. 2014. When is a model good enough? Deriving the expected value of model improvement via specifying internal model discrepancies. *SIAM/ASA Journal on Uncertainty Quantification* 2:106-125. doi:doi:10.1137/120889563
- Strong M., Oakley J.E., Chilcott J. 2012. Managing structural uncertainty in health economic decision models: A discrepancy approach. *Journal of the Royal Statistical Society: Series C (Applied Statistics)* 61:25-45
- Syme J.R. 1973. Quantitative control of flowering time in wheat cultivars by vernalization and photoperiod sensitivities. *Australian Journal of Agricultural Research* 24:657-665. doi:10.1071/ar9730657
- Tanio M., Kato K. 2007. Development of near-isogenic lines for photoperiod-insensitive genes, *Ppd-B1* and *Ppd-D1* Carried by the Japanese wheat cultivars and their effect on apical development. *Breeding Science* 57:65-72. doi:10.1270/jsbbs.57.65
- Teixeira E., Brown H., Sharp J., Meenken E., Ewert F. 2015. Evaluating methods to simulate crop rotations for climate change impact assessments - a case study on the Canterbury plains of New Zealand. *Environmental Modelling & Software* 72:304-313

- Teixeira E., Fischer G., van Velthuis H., van Dingenen R., Dentener F., Mills G., Walter C., Ewert F. 2011. Limited potential of crop management for mitigating surface ozone impacts on global food supply. *Atmospheric Environment* 45:2569-2576
- Teixeira E.I., Fischer G., van Velthuis H., Walter C., Ewert F. 2013. Global hot-spots of heat stress on agricultural crops due to climate change. *Agricultural and Forest Meteorology* 170:206-215
- Teixeira E.I., Moot D.J., Brown H.E. 2009. Modelling seasonality of dry matter partitioning and root maintenance respiration in lucerne (*Medicago sativa* L.) crops. *Crop and Pasture Science* 60:778-784
- Thacker N.A., Lacey A.J. 1996. Tutorial: The Kalman Filter. In. Manchester, UK: Imagin Science and Biomedical Engineering Division, Medical School, University of Manchester.
- Thyer M., Renard B., Kavetski D., Kuczera G., Franks S.W., Srikanthan S. 2009. Critical evaluation of parameter consistency and predictive uncertainty in hydrological modeling: A case study using Bayesian total error analysis. *Water Resources Research* 45
- Tottman D.R. 1987. Growth stage identification key, cereals. Bracknell, UK: British Crop Protection Council.
- Trevaskis B., Hemming M.N., Dennis E.S., Peacock W.J. 2007a. The molecular basis of vernalization-induced flowering in cereals. *Trends in Plant Science* 12:352-357.  
doi:<http://dx.doi.org/10.1016/j.tplants.2007.06.010>
- Trevaskis B., Tadege M., Hemming M.N., Peacock W.J., Dennis E.S., Sheldon C. 2007b. Short vegetative phase-like MADS-box genes inhibit floral meristem identity in barley. *Plant Physiology* 143:225-235.  
doi:10.1104/pp.106.090860
- Trucano T.G., Swiler L.P., Igusa T., Oberkampf W.L., Pilch M. 2006. Calibration, validation, and sensitivity analysis: What's what. *Reliability Engineering & System Safety* 91:1331-1357. doi:DOI: 10.1016/j.ress.2005.11.031
- Uusitalo L., Lehikoinen A., Helle I., Myrberg K. 2015. An overview of methods to evaluate uncertainty of deterministic models in decision support. *Environmental Modelling & Software* 63:24-31.  
doi:<http://dx.doi.org/10.1016/j.envsoft.2014.09.017>
- van Beem J., Mohler V., Lukman R., van Ginkel M., William M., Crossa J., Worland A.J. 2005. Analysis of genetic factors influencing the

- developmental rate of globally important CIMMYT wheat cultivars. *Crop Science* 45:2113-2119. doi:10.2135/cropsci2004.0665
- Van Ittersum M.K., Ewert F., Heckelei T., Wery J., Olsson J.A., Andersen E., Bezlepkina I., Brouwer F., Donatelli M., Flichman G. 2008. Integrated assessment of agricultural systems–A component-based framework for the European Union (SEAMLESS). *Agricultural Systems* 96:150-165
- Vincour M.G., Ritchie J.T. 2001. Maize leaf development biases caused by air-apex temperature differences. *Agronomy Journal* 93:767-772
- Vrugt J., Braak C.F., Gupta H., Robinson B. 2009a. Equifinality of formal (DREAM) and informal (GLUE) Bayesian approaches in hydrologic modeling? *Stochastic Environmental Research and Risk Assessment* 23:1011-1026. doi:10.1007/s00477-008-0274-y
- Vrugt J.A., Gupta H.V., Bouten W., Sorooshian S. 2003. A Shuffled Complex Evolution Metropolis algorithm for optimization and uncertainty assessment of hydrologic model parameters. *Water Resources Research* 39:1201. doi:10.1029/2002wr001642
- Vrugt J.A., ter Braak C.J.F., Clark M.P., Hyman J.M., Robinson B.A. 2008. Treatment of input uncertainty in hydrologic modeling: Doing hydrology backward with Markov chain Monte Carlo simulation. *Water Resources Research* 44:W00B09. doi:10.1029/2007wr006720
- Vrugt J.A., ter Braak C.J.F., Diks C.G.H., Robinson B.A., Hyman J.M., Higdon D. 2009b. Accelerating Markov Chain Monte Carlo simulation by differential evolution with self-adaptive randomized subspace sampling. In *International Journal of Nonlinear Sciences and Numerical Simulation*.
- VSN\_International. 2013. GenStat for Windows 14th Edition. In, 15.2.0.8821 edn. Hemel Hempstead, UK: VSN International.
- Wallach D., Makowski D., Jones J.W., Francois B. (eds). 2014. Working with Dynamic Crop Models. Second Edition edn. Elsevier, Amsterdam, NL
- Wegman E.J. 1990. Hyperdimensional data analysis using parallel coordinates. *Journal of the American Statistical Association* 85:664-675
- Weir A.H., Bragg P.L., Porter J.R., Rayner J.H. 1984. A winter-wheat crop simulation model without or nutrient limitations. *Journal of Agricultural Science* 102:371-382



- Welch W.J., Buck R.J., Sacks J., Wynn H.P., Mitchell T.J., Morris M.D. 1992. Screening, predicting, and computer experiments. *Technometrics* 34:15-25. doi:10.1080/00401706.1992.10485229
- Wilkinson R.D., Vrettas M., Cornford D., Oakley J.E. 2011. Quantifying simulator discrepancy in discrete-time dynamical simulators. *Journal of Agricultural Biological and Environmental Statistics* 16:554-570. doi:10.1007/s13253-011-0077-3
- Williams B.K., Nichols J.D., Conroy M.J. 2002. Analysis and Management of Animal Populations - Modelling, Estimation and Decision making. San Diego, USA: Academic.
- Wullschleger S.D., Lynch J.P., Bernstson G.M. 1994. Modeling the belowground response of plants and soil biota to edaphic and climate change: What can we expect to gain? *Plant and Soil* 165:149-160
- Yang F., Han L., Yan J., Xia X., Zhang Y., Qu Y., Wang Z., He Z., Yang F.P., Han L.M., Yan J., Xia X.C., Zhang Y., Qu Y.Y., Wang Z.W., He Z.H. 2011. Distribution of allelic variation for genes of vernalization and photoperiod among wheat cultivars from 23 countries. *Acta Agronomica Sinica* 37:1917-1925